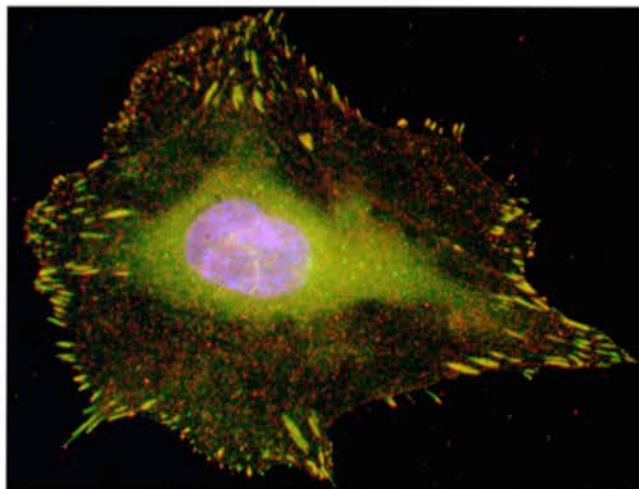
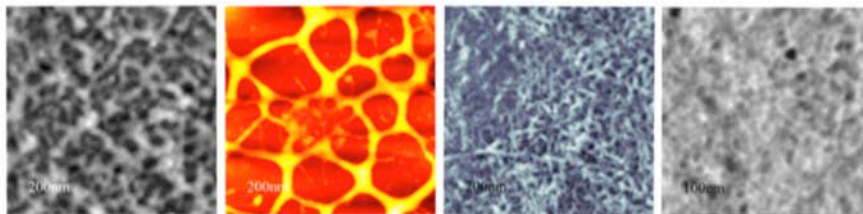


ADVERTIMENT. La consulta d'aquesta tesi queda condicionada a l'acceptació de les següents condicions d'ús: La difusió d'aquesta tesi per mitjà del servei TDX (www.tesisenxarxa.net) ha estat autoritzada pels titulars dels drets de propietat intel·lectual únicament per a usos privats emmarcats en activitats d'investigació i docència. No s'autoritza la seva reproducció amb finalitats de lucre ni la seva difusió i posada a disposició des d'un lloc aliè al servei TDX. No s'autoritza la presentació del seu contingut en una finestra o marc aliè a TDX (framing). Aquesta reserva de drets afecta tant al resum de presentació de la tesi com als seus continguts. En la utilització o cita de parts de la tesi és obligat indicar el nom de la persona autora.

ADVERTENCIA. La consulta de esta tesis queda condicionada a la aceptación de las siguientes condiciones de uso: La difusión de esta tesis por medio del servicio TDR (www.tesisenred.net) ha sido autorizada por los titulares de los derechos de propiedad intelectual únicamente para usos privados enmarcados en actividades de investigación y docencia. No se autoriza su reproducción con finalidades de lucro ni su difusión y puesta a disposición desde un sitio ajeno al servicio TDR. No se autoriza la presentación de su contenido en una ventana o marco ajeno a TDR (framing). Esta reserva de derechos afecta tanto al resumen de presentación de la tesis como a sus contenidos. En la utilización o cita de partes de la tesis es obligado indicar el nombre de la persona autora.

WARNING. On having consulted this thesis you're accepting the following use conditions: Spreading this thesis by the TDX (www.tesisenxarxa.net) service has been authorized by the titular of the intellectual property rights only for private uses placed in investigation and teaching activities. Reproduction with lucrative aims is not authorized neither its spreading and availability from a site foreign to the TDX service. Introducing its content in a window or frame foreign to the TDX service is not authorized (framing). This rights affect to the presentation summary of the thesis as well as to its contents. In the using or citation of parts of the thesis it's obliged to indicate the name of the author

DYNAMIC BEHAVIOR OF TYPE IV COLLAGEN AT CELL-BIOMATERIAL INTERFACE



PhD Thesis
Nuno Miranda Coelho

DYNAMIC BEHAVIOR OF TYPE IV COLLAGEN AT CELL-BIOMATERIAL INTERFACE

Author: Nuno Miranda Coelho

Director: Prof. George Altankov

UPC tutor: Prof. Josep A. Planell

Programa de doctorat en Enginyeria Biomèdica
Departament de Ciència dels Materials i Enginyeria Metal·lúrgica
Universitat Politècnica de Catalunya, Barcelona, España

Barcelona, April 2012

Tesi presentada per obtenir el títol de Doctor per la Universitat Politècnica de Catalunya (UPC).



UNIVERSITAT POLITÈCNICA
DE CATALUNYA



Institute for bioengineering
of Catalonia

Director

UPC tutor

Author

.....
(Prof. George Altankov)

.....
(Prof. Josep A. Planell)

.....
(Nuno Miranda Coelho)

Vol. 1

ACTA DE QUALIFICACIÓ DE LA TESI DOCTORAL

MODEL ACTA TD

Dades de l'autor de la tesi

DNI / NIE / Passaport -

Nom i cognoms - Nuno Miranda Coelho

Reunit el tribunal integrat pels sota signants per jutjar la tesi doctoral:

Acorda atorgar la qualificació de:

No apte

Apte

Apte Cum Laude

El President

El Secretari

.....
(nom i cognoms)

.....
(nom i cognoms)

El vocal

El vocal

El vocal

.....
(nom i cognoms)

.....
(nom i cognoms)

.....
(nom i cognoms)

Lloc i data

Abstract

The initial molecular events that take place at biomaterials interface mimic to a certain extent the natural interaction of cells with the extracellular matrix (ECM). In this thesis we describe the fate of adsorbed type IV collagen (Col IV) - the main structural component of the basement membrane (BM) - as an important target in vascular tissue engineering. We studied the adsorption kinetic of Col IV on different model surfaces varying in wettability, chemistry and charge, and followed how it alters the molecular organization of the adsorbed protein layer. We strived to learn how it will affect the subsequent cellular interaction. AFM studies revealed specific substratum-dependent adsorption pattern of Col IV ranging from single molecular deposition to fine meshwork formation at high coating concentrations, which is characteristic for hydrophilic and NH_2 functionalized substrates. Conversely, the formation of a complex networks consisting of molecular aggregates were found on hydrophobic and COOH modified surfaces. Complex structures were found also when a family of model substrates with tailored density of OH , CH_3 and NH_2 functions were used. Human umbilical endothelial cells (HUVEC) and fibroblasts were employed to study the biological response on these substrata. We found that fibroblast not only interact with adsorbed Col IV but also tend to reorganize it in fibril like pattern, which is strongly dependent on the materials surface properties. Following the trend of adsorption $\text{NH}_2 > \text{CH}_3 > \text{COOH} > \text{OH}$ the reorganization pattern of Col IV improve with lowering the amount of protein. However, the cells interact better with hydrophilic and NH_2 surfaces, thus acting independently on the amount of adsorbed Col IV. This trend was confirmed by the quantitative measurements of cell adhesion and spreading, as well as, the expression of p-FAK, α_1 and α_2 integrins – all reflecting the proper functioning of cell adhesion machinery. This is the first study that addresses the relationship between microscopic observation for remodeling of surface associated Col IV and it's dynamic behavior in nano scale. We found that cells remodel Col IV in two ways: by mechanical reorganization and via proteolytic degradation. We identify the role of FN in the reorganization process and the involvement of MMP2 and MMP9 in the pericellular degradation activity of both HUVEC and fibroblasts. The later was further quantified via FITC labeled Col IV release and zymography. We found that in hydrophobic environment the degradation activity can override the Col IV organization process, which corroborates with the altered cell morphology, abrogated cell adhesion machinery and altered capability of HUVEC to form capillary-like structures. Taken together these results support our view that the ability of cells to remodel surface associated proteins affects strongly the biological performance of a biomaterial. They also show that the appropriate chemical functionalization (NH_2 , OH), combined with Col IV pre-adsorption, comprises a prospective biomimetic modification that might provide insights for the improved endothelization of cardiovascular implants.

Acknowledgements

Finally it is time to show my gratitude to all the people who made this thesis possible. For me this thesis is the result of many professional and personal experiences therefore many people contributed to it even without knowing. I believe that at the end all of you made me a better student, a better researcher, a better colleague, a better friend and therefore I would like to thank you all.

First and foremost I offer my sincerest gratitude to my supervisor, Prof. George Altankov, without him this thesis would not have been completed or written. Thank you for teaching me how to do science, how to write and how to think and work independently. It was an honor for me to be your first student in this new stage in your carrier and I thank you for allowed me to participate in the start up of your laboratory. Finally I would like thank you for all your friendly advices.

I am grateful to Professor Josep Planell (my university tutor and the director of my host institute). He made available his support in a number of ways by advising me in the best way each time I request a little bit of his time.

If there is a person who could be my co-director and really helped improving the quality of my thesis is Prof. Manuel Salmerón-Sánchez. It was an honor for me to participate in this productive collaboration with his group, all the time I passed in his group in Valencia he made it worth while providing me all the conditions to perform the planed experiments. Thank you for your availability and your valuable advises.

I owe my deepest gratitude to Dr. Richard Hampson for his advices during my final undergraduate project. Although we worked together in a company your advices helped me a lot to decide to do a PhD in an academic laboratory.

Se há uma pessoa responsável pelo meu interesse em ciência é o Prof. António Jacinto. Primo obrigado pela oportunidade de ter o primeiro contacto com a ciência no teu laboratório durante o meu curso, por todos os teus conselhos e pela tua amizade. Para mim és um modelo a seguir.

Al término de esta etapa de mi vida, quiero expresar mis agradecimientos al Prof. Jordi Domingo y al Prof. Ricardo Pérez por su amabilidad y por la forma en que nos han recibido a mi y al grupo en el departamento y cómo hicieron posible mi trabajo en éste.

Quiero expresar un agradecimiento sentido a la Dra. Soledad Alcántara por su disponibilidad para ayudarme a resolver muchas de las adversidades que encontré en la parte experimental de la tesis. Agradezco todo sus consejos para la elaboración de la tesis así como todas las discusiones de carácter científico que hemos tenido durante estos años.

Agradezco también la disponibilidad y los consejos dados por el Prof. Raimon Jané y la Prof. Maria Pau Ginebra por guiarme durante los cursos de doctorado y durante los trámites de la elaboración de la tesis.

Quiero agradecer al Prof. Jordi Alcaraz todos los conocimientos y consejos transmitidos en su asignatura de bioingeniería molecular así como durante todos estos años de tesis.

I am indebted to many of my group colleagues to support me. Dencho, Joro, and Kami, thank you for your generosity and availability to help me. You are very good persons, also great friends, I will never forget what you did for me. I would like to thank also Johan for helping me with my first experiments in PCB.

A todo el grupo de Bellvitge: Os debo mucho. Juntamente con mi grupo antes descrito, habéis sido parte de mi familia en Barcelona y creo que eso ya dice mucho. Vanesa, “la mami”, gracias por compartir tu experiencia y por estar siempre disponible para escucharme y aconsejarme. Albert, eres muy grande, tienes una disciplina de trabajo increíble y trabajar a tu lado y a tu ritmo me ha dado muchos resultados, gracias por estar siempre disponible sea como colega o como amigo. Martotti, hemos ido mano a mano desde el principio, gracias por tu amistad, por tus ideas, por tu música, y principalmente por ser así, tan tú. Zaida, tienes una energía alucinante, mucho potencial y tu positivismo me ha ayudado mucho a tirar adelante. Gracias por tu disponibilidad para ayudar (western-blot!!!! Y mucho mas), por tu alegría y por tu amistad. Greti te ha costado comunicarte con el grupo pero, a la que te dejaste conocer, ha sido una alegría. Gracias por ayudarme con la parte molecular de la tesis y por tu amistad. Aina gracias por tu alegría, amistad y felicidad, me ayudaron mucho a reír en la fase final de redacción de mi tesis cuando todo era oscuro.

Tengo que agradecer también a María Isabel, tu experiencia me ayudo mucho. Nuestras conversaciones me ayudaron a pensar y solucionar fallos en mi trabajo. Gracias también por creer en mí y por estar ahí cuando lo necesitaba.

Gracias también a Mercè por estar siempre animando y a los demás, a Natalia, a Santi, a Lucrecia, a Ariadna y a Silvia por las vibraciones positivas que me pasaron durante la redacción de la tesis y durante todo el tiempo que estuvimos juntos en Bellvitge.

Muchas gracias a Cristina, del grupo de Valencia, por todos los esfuerzos hechos para que mis estancias allí fueran aun más productivas. Gracias también a Pachi, Marco, Virginia, Pepe y todos los demás del centro por la forma como me han recibido.

Tengo que agradecer también a Titziano mi compañero de congresos, mi amigo. Todas nuestras conversaciones de ciencia y no ciencia han sido de gran provecho.

Gracias a todos los jefes de grupo, post-docs, estudiantes y personal administrativo del IBEC con quien he compartido experiencias al largo de estos años.

Agradezco también a todos los otros que pasaron por el laboratorio de Bellvitge, los que subían a comer, los de la 4ª planta, los del futbol de los martes, los de las caipiriñas party, todos me han hecho ser una mejor persona.

Quiero también expresar mi agradecimiento a los serveis científico-tècnics del campus de Bellvitge, principalmente a Benjamín, por transmitirme todos sus conocimientos de microscopia, por ser un buen amigo y por organizar los partidos de futbol que dan alegría a los martes.

Quiero igualmente expresar mi agradecimiento a la plataforma de Nanotecnología del PCB por los servicios que han puesto a mi disposición. Gracias a Xavi por tu asistencia con el AFM. Finalmente quería agradecer también a Manolo y José Luis de los servicios de microscopia de la Universidad Politécnica de Valencia por su ayuda técnica con el AFM.

Se há pessoas a quem quero dedicar esta tese é aos meus país Graça e Miguel. Obrigado por acreditarem em mim mesmo quando eu próprio não acreditava. Tudo o que sou hoje é o resultado do vosso amor e da educação que me deram por isso vos digo “Parabéns” esta tese também é vossa. Esta tese também é tua Pedro sem o teu apoio nunca a teria feito, perguntarás porque? Porque também o teu esforço me serviu de exemplo e inspiração e porque ambos dependemos do bem estar do outro, estando perto ou estando longe estamos sempre juntos e a olhar para a frente.

A quien jamás encontraré la forma de agradecer su apoyo, comprensión, confianza, amistad y amor es a Blanca. Espero que una forma de hacerlo sea diciendo que este logro mío también es tuyo y es un triunfo que quiero compartirlo contigo siempre. Deseo que sea el primero de muchos juntos.

Não me posso esquecer de toda a demais família Miranda e Coelho que apesar de longe esteve sempre perto e me reconfortou em cada momento que estivemos juntos, obrigado. Há sempre uns que se superam e tenho que mencionar, é verdade Mickas, meu irmão mais velho, estiveste sempre ai para o que eu precisava com um energia inesgotável para me apoiar e ainda por cima tens a coragem de tentar entender os meus artigos, obrigado por tudo. Joana e Filipe a vossa visita aqui foi mais importante do que vocês imaginam deu-me uma força fundamental para acabar a parte experimental da minha tese, foram 5 dias incríveis obrigado.

Además de mi familia portuguesa tengo también una familia catalana. Gracias Mary, Ignacio, Carmina, Merche, Mir, Nacho, Inés, Candela y Romeo por hacerme sentir uno más en casa.

Quero agradecer também a todos os meus amigos que sempre estiveram comigo mesmo estando longe. Obrigado Sonares, Cabral, Beny e Xico, mas também Mary, Joana, Ines, Krepes, Madalena, Leonor, Jeco e tantos mais que crescemos juntos. Somos o que vivemos e crescer todos juntos teve um papel importantíssimo em quem sou hoje.

Quero também agradecer a minha família portuguesa em Barcelona, fomos muitos, hoje somos menos, mas a amizade que nos uniu continua estejamos onde estivermos. Vocês fizeram-me sentir em casa obrigado Gonçalo, Didas, Ines, Barros, Alveti, veruka, Joana, Matilde, Martas, Xica, Duarte, Mariana, Kiko, Maria, Iko e tantos mais que foram sendo a minha família portuguesa em Barcelona.

Finalmente pero no por ser los menos importantes quería agradecer a todos los amigos que me ha dado mi vida en Barcelona. Me habéis hecho sentir uno más del grupo y eso te hace sentir muy bien y se ha plasmado positivamente en este trabajo. Gracias Anita y Alexis por todo vuestro apoyo, me habéis ayudado mucho de verdad. Gracias a “las niñas” de Blanca y también gracias a “los de Cadaqués”, sois los mejores.

Table of Contents

Abstract	V
Acknowledgements	VI
Table of Contents	1
List of Figures and Tables	5
Abbreviations	9
Chapter 1 - State of the Art	11
1. Biomaterials, tissue engineering and regenerative medicine	11
1.1 Introduction	11
1.2 Host response to biomaterials	12
1.3 Definition of biomaterial	12
<i>1.3.1 First generation of “bioinert” biomaterials</i>	13
<i>1.3.2 Second generation of “bioactive” and “biodegradable” biomaterials</i>	13
<i>1.3.3 Third generation of “cell – activating” biomaterials</i>	14
1.4 Tissue engineering and regenerative medicine	14
<i>1.4.1 Biomaterials for tissue engineering and regenerative medicine</i>	17
2. Extracellular Matrix	19
2.1 Rough Extracellular	20
2.2 Basement membrane structure and function	21
<i>2.2.1 Type IV Collagen – structure and function</i>	23
<i>2.2.2 Type IV Collagen interaction with cells</i>	24
<i>2.2.3 Laminin – structure and function</i>	26
<i>2.2.4 Laminin interaction with cells</i>	28
2.3 Extracellular matrix remodeling	28
3. Cell-Biomaterials Interaction	31
3.1 Cell adhesion	31
3.2 Integrin receptors	32
3.3 Focal adhesion contacts	33
<i>3.3.1 Fibrillar adhesions</i>	35
<i>3.3.2 Three-dimensional matrix adhesions</i>	35
3.4 Dynamics of cell adhesion	36
4. Protein behavior at interfaces	39
4.1 Protein adsorption and biocompatibility	39
4.2 Effect of external parameters in protein adsorption	39
<i>4.2.1 Temperature effect on protein adsorption</i>	40

4.2.2	<i>Effect Ionic strength on protein adsorption</i>	40
4.2.3	<i>Effect of pH on protein adsorption</i>	40
4.2.4	<i>Effect of buffer composition on protein adsorption</i>	41
4.2.5	<i>“Vroman” effect</i>	41
4.3	Measurement of protein adsorption	41
5.	Engineering of Cell - Biomaterial Interface	45
5.1	Control of protein adsorption	45
5.1.1	<i>Effect of intrinsic properties of the proteins on adsorption</i>	45
5.1.2	<i>Effect of surface properties on protein adsorption</i>	46
5.1.3	<i>Protein adsorption orientation</i>	47
5.1.4	<i>Conformational changes</i>	47
5.1.5	<i>Protein assembly at solid surface</i>	48
5.1.6	<i>Lateral interactions between adsorbed proteins</i>	48
5.2	Self-assembled monolayers as model biomaterials surfaces	49
5.2.1	<i>Self-assembled monolayers</i>	49
5.2.2	<i>Silane based self assembled monolayers</i>	49
5.2.3	<i>Self-assembled monolayers of alkanethiolates on gold</i>	50
5.2.4	<i>Bio-specific motifs presented by self-assembled monolayers</i>	51
5.3	Control of material surface properties	51
5.3.1	<i>Most important methods for surfaces characterization</i>	51
5.3.2	<i>Contact angle goniometry</i>	51
5.3.3	<i>X-ray photoelectron spectroscopy</i>	52
5.3.4	<i>Fourier-transform infrared spectroscopy</i>	52
5.3.5	<i>Atomic force microscopy</i>	52
5.4	Control of cell behavior-Applying SAMs to study cell-materials interaction	53
5.4.1	<i>Influence of terminal end groups on cellular responses</i>	53
5.4.2	<i>Hydrophilic (-OH) surface</i>	53
5.4.3	<i>Negatively charged (-COOH) surface</i>	54
5.4.5	<i>Positively charged (-NH₂) surface</i>	54
5.4.6	<i>Hydrophobic (-CH₃) surface</i>	54
5.4.7	<i>Surfaces with mixed functionalities</i>	55
5.4.8	<i>Cellular interaction with surfaces varying in wettability</i>	55
5.4.9	<i>Cellular interaction with surfaces varying in charge</i>	56
5.4.10	<i>Cellular interaction with surfaces varying in topography</i>	56
5.5	Substratum effects on focal adhesion formation and integrin signaling	57
5.6	Control of matrix remodeling	57

<i>5.6.1 Remodeling of ECM proteins at cell-biomaterial interface</i>	57
<i>5.6.2 Development of early matrix</i>	58
<i>5.6.3 Development of late matrix</i>	58
<i>5.6.4 proteolytic remodeling of surface associated ECM</i>	59
6. Aim and Specific Objectives	61
6.1 Aim	61
6.2 Specific Objectives	61
Chapter 2 - Material and Methods	63
Chapter 3 - Results	75
1. Different Assembly of Type IV Collagen on Hydrophilic and Hydrophobic Substrata Alters Endothelial Cells Interaction	75
1.1 Preface 1	75
1.2 Original Publication 1	77
1.2 Supplementary results 1	89
2. Arrangement of Type IV Collagen and Laminin on Substrates with Controlled Density of –OH Groups	91
2.1 Preface 2	91
2.2 Original Publication 2	93
2.2 Supplementary results 2	107
3. Arrangement of Type IV Collagen on NH₂ and COOH Functionalized Surfaces	109
3.1 Preface 3	109
3.2 Original Publication 3	111
4. Fibroblasts Remodeling Type IV Collagen at Biomaterials interface depends on Fibronectin and Substratum Chemistry	121
4.1 Preface 4	121
4.2 Submitted manuscript	123
4.3 Supplementary results 3	149
5. Remodeling of Type IV Collagen by Endothelial Cells	153
5.1 Preface 5	153
5.2 Supplementary Results 4	155
Chapter 4 - Discussion	167
Chapter 5 - Conclusion	183
References	185

List of Figures and Tables

Chapter 1 - Introduction	11
Figure 1.1 - Main tissue engineering strategy.	15
Figure 1.2 - The main strategies of regenerative medicine.	17
Figure 2.1 - Reciprocal molecular interactions between cells and ECM.	20
Figure 2.2 - Basement membrane - schematic representation in various tissues.	21
Figure 2.3 - Basement membrane assembly.	22
Figure 2.4 - Types of Col IV molecules association.	23
Figure 2.5 - Integrin binding sites within Col IV molecules.	25
Figure 2.6 - Diversity of laminin structure.	27
Figure 2.7 - Schematic structure of MMPs.	29
Figure 3.1 - Integrin receptors superfamily.	32
Figure 3.2 - Integrin activation cascade.	33
Figure 3.3 - Dynamic cross-talk between cells and ECM.	37
Figure 4.1 - Illustration of the final state of a protein layer adsorbed from a single protein solution.	42
Table 1 - Summary of techniques used to study protein adsorption behavior.	43
Figure 5.1 - Soft versus hard protein adsorption on hydrophilic surfaces.	45
Figure 5.2 - General self assembled monolayers structure and formation.	49
Figure 5.3 - Models for SAMs of alkanethiolates on gold and alkylsiloxanes on hydroxylated surfaces.	50
Figure 5.4 - AFM's operation mode.	53
Chapter 2 - Material and Methods	63
Figure 1 - The parallel flow chamber.	70
Chapter 3 -Results	75
1. Different Assembly of Type IV Collagen on Hydrophilic and Hydrophobic Substrata Alters Endothelial Cells Interaction	75
Table 1. Values for advancing and receding WCA of model hydrophilic and hydrophobic surfaces.	79
Table 2. Average roughness and height of the model surfaces characterized by AFM.	80
Fig. 1. Adsorption profile of FITC-Col IV on model hydrophilic and hydrophobic ODS surfaces.	80
Fig. 2. AFM images of adsorbed native collagen type IV to hydrophilic and hydrophobic surfaces.	80
Fig. 3. Fraction of substrate covered by the protein as a function of the concentration of the initial solution.	81
Fig. 4. AFM images of adsorbed native collagen type IV to hydrophilic and hydrophobic surfaces at adsorption concentration 50 µg/ml for 30 minutes.	81
Fig. 5. Overall morphology of HUVEC adhering on native Col IV coated hydrophilic and hydrophobic ODS surfaces.	81
Fig. 6. Quantification of cell adhesion expressed as number of cells per cm ² and the average spreading area measured in µm ² to hydrophilic and hydrophobic Col IV coated surfaces.	82
Fig. 7. Development of focal adhesions contacts and actin stress fibers of HUVEC seeded on Col IV coated hydrophilic and hydrophobic ODS surfaces.	82
Fig. 8. Expression of alpha 1 and alpha 2 integrins in HUVEC adhering on hydrophilic and hydrophobic ODS surfaces coated with Col IV.	83
1.2 Supplementary results 1	89

Figure 1 - AFM images of Col IV adsorbed onto hydrophilic and hydrophobic surfaces.	89
Figure 2 - AFM images of FITC-Col IV adsorbed onto model hydrophilic (glass) and hydrophobic (ODS) surfaces.	89
2. Arrangement of Type IV Collagen and Laminin on Substrates with Controlled Density of –OH Groups	91
Table 1. Equilibrium Water Content and Water Contact Angle for the Different Substrates with Increasing Fraction of –OH Groups.	95
FIG. 1. Phase AFM images of adsorbed Col IV on substrates with increasing fraction of –OH groups.	96
Table 2. Total Volume Occupied by the Protein on a 1 μm^2 Area of the Substrate as Calculated from AFM Data After Adsorption of Col IV, Lam, or Col IV + Lam.	97
FIG. 2. Overall morphology of HUVEC adhering on Col IV-coated substrates with increasing –OH density.	98
FIG. 3. Phase AFM images of adsorbed Lam on substrates with increasing fraction of –OH groups.	99
FIG. 4. Overall morphology of HUVEC adhering to Lam-coated substrates with increasing –OH density.	100
FIG. 5. Overall morphology of HUVEC adhering on plain substrates with increasing OH density, and different control samples.	101
FIG. 6. Phase AFM images of sequentially adsorbed Col IV and Lam on substrates with increasing fraction of –OH groups.	102
FIG. 7. Overall morphology of HUVEC adhering to sequentially adsorbed Col IV and Lam on substrates with increasing –OH density.	103
2.2 Supplementary results	107
Figure 1 - Overall morphology of HUVEC adhering to Col IV-coated substrates with increasing density of –OH groups.	107
Figure 2 - Expression of alpha 1 and alpha 2 integrins in HUVEC adhering to the same Col IV coated model surfaces with increasing density of OH groups.	108
3. Arrangement of Type IV Collagen on NH₂ and COOH Functionalized Surfaces	109
Table I. Water contact angles of NH ₂ and COOH surfaces before and after coating with Col IV.	114
Figure 1. Adsorption profile of FITC-Col IV on model NH ₂ and COOH SAMs.	114
Figure 2. AFM images of adsorbed native collagen type IV to model NH ₂ and COOH surfaces.	115
Figure 3. Overall cell morphology of HUVEC adhering on native Col IV coated NH ₂ and COOH surfaces.	116
Figure 4. Expression of alpha 1 and alpha 2 integrins in HUVEC adhering on NH ₂ and COOH samples coated with Col IV.	116
Figure 5. Recruitment of the signaling molecule p-FAK in the focal adhesion complexes in HUVEC seeded on Col IV coated NH ₂ and COOH samples.	117
4. Fibroblasts Remodeling of Type IV Collagen at Biomaterials Interface - effect of - Fibronectin and Substratum Chemistry	121
Figure 1 - Human fibroblasts cultured for 5 hours on native or FITC-conjugated Col IV.	128
Figure 2 - Co-localization between remodeled Col IV and secreted or exogenously added fibronectin.	129
Figure 3 - Water contact angles of model surfaces measured before and after coating with Col IV.	129
Figure 4 - Adsorption and desorption of FITC-Col IV on different model surfaces.	130
Figure 5 - Overall morphology of human fibroblasts adhering on Col IV coated model materials for 2h in serum free conditions.	131
Figure 6 - Expression of alpha 1 and alpha 2 integrins in fibroblasts adhering on Col IV coated model surfaces.	132
Figure 7 - Recruitment of the signaling molecule p-FAK in the focal adhesion complexes.	133

Figure 8 - Fibroblast remodeling of native Col IV on different model surfaces after 5 hours.	134
Figure 9 - Fibroblast remodeling of native Col IV on different model surfaces after 24 hours.	134
Figure 10 - Fibroblast remodeling of FITC-Col IV on different model surfaces for 5.	135
4.2 Supplementary results 3	149
Figure 1 - Relation between the volumetric flow and the shear stress applied in the wall of the chamber.	149
Figure 2 - Reynolds number as function of the wall shear stress.	149
Figure 3 - Entrance length as function of the wall shear stress.	150
Figure 4 - Detachment of human fibroblast from hydrophilic glass and hydrophobic ODS as function of the shear stress applied (n=5).	150
5. Remodeling of Type IV Collagen by Endothelial Cells	153
Figure 1 - Recruitment of the signaling molecule p-FAK in the focal adhesion complexes in HUVEC seeded on Col IV coated OH, CH ₃ , NH ₂ , and COOH surfaces.	155
Figure 2 - Western-blot of cellular extracts of HUVEC adhering to the same Col IV coated model surfaces for 2h. Detection of MMP2 and vinculin expression.	156
Figure 3 - HUVEC remodeling of adsorbed Col IV on different model surfaces after 5 h and 24 h corroborated with FN secretion.	157
Figure 4 - Zymography of the conditioned medium of HUVEC cultured for 24 h on Col IV coated model materials.	158
Figure 5 - FITC-Col IV remodeling by HUVEC on different model surfaces for 5 (A-D) and 24 (M-P) hours.	158
Figure 6 - Release of FITC in the supernatant after culturing HUVEC on FITC-Col IV coated model surfaces for 5 (A) and 24 (B) hours.	159
Figure 7 - HUVEC were cultured on Col IV coated model materials for 2h and then the samples were overlaid with BME-2%FITC-Col IV and further cultured for 5 and 24 hours.	160
Figure 8 - FITC-Col IV adsorption on model mixed SAMs presenting different portions of NH ₂ and CH ₃ chemistries.	161
Figure 9 - Overall morphology of HUVEC adhering for two hours in serum free medium to plane and Col IV coated mixed SAMs.	162
Figure 10 - Development of focal adhesion contacts viewed by vinculin and actin stress fibers viewed by FITC phalloidin of HUVEC seeded on Col IV coated mixed SAMs for 2h.	163
Figure 11 - Expression of alpha 1 (A to E) and alpha 2 (F to J) integrins in HUVEC adhering on the same mixed SAMs coated with Col IV.	163
Figure 12 - Remodeling of adsorbed native Col IV by HUVEC on different mixed SAMs for 5 and 24 hours viewed simultaneously with secreted FN.	164
Figure 13 - (A) Zymography of the conditioned medium of HUVEC cultured for 24 h on Col IV coated mixed SAMs.	165
Figure 14 - HUVEC remodeling of adsorbed FITC-Col IV on different model surfaces of mixed SAMs after 5 and 24 hours.	166
Figure 15 - Release of FITC in the supernatant after HUVEC culturing on FITC-Col IV coated mixed SAMs for 5 and 24 hours.	166

Abbreviations

3D - three dimensions
AFM - atomic force microscopy
 β -Lg - β -lactoglobulin
BM - basement membrane
BME - basement membrane extract
CB3 - cyanogen bromide-derived fragment
Col I - type I collagen
Col III - type III collagen
Col IV - type IV collagen
DMEM - Dulbecco's Modified Eagle's Medium
EA - ethyl acrylate
ECM - extracellular matrix
ELISA - enzyme like immunosorbent assay
ESCs - embryonic stem cells
FA - focal adhesions
FAK - focal adhesion kinase
FBG - fibrinogen
FBGC - foreign body giant cells
FBS - fetal bovine serum
FDA - food and drug administration
FDA – fluorescein diacetate
FGF - fibroblast growth factor
FITC - fluorescein isothiocyanate
FN - fibronectin
FTIR - Fourier transform infrared spectroscopy
HEA - hydroxy ethyl acrylate
HPSPGs - heparan-sulphate proteoglycans
HUVEC - human umbilical vein endothelial cells
IGF - insulin growth factors
IgG - immunoglobulin G
ILK - integrin linked kinase
iPSCs - induced pluripotent stem cells
JNK - jun kinase
L4 - globular domains laminin 4
LAM - laminin

l_e - entrance length
LE - epidermal-growth factor like domains
LF - laminin four domain
LN - N-terminal domain
MAPK - mitogen activated protein kinase
MMPs - matrix metalloproteinases
ODS - trichloro-(octadecyl)-silane
PBS - phosphate buffer saline
pI - isoelectric point
PKC - protein kinase C
QCM - quartz crystal microbalance
 Re - Reynolds number
RGD - arginine-glycine-aspartic acid
SAMs - self-assembled monolayers
Ti - titanium
TIRF - total internal reflection fluorescence
tPA - tissue plasminogen activator
uPA - urokinase plasminogen activator
uPaR - urokinase plasminogen activator receptor
VN - vitronectin
WCA[°] - water contact angle
XPS - x-ray photoelectron spectroscopy

Chapter 1 - State of the Art

1. Biomaterials, tissue engineering and regenerative medicine

1.1 Introduction

The fate of a biomaterial once implanted in the body is strongly dependent on various parameters such as its localization within tissues, its size, shape, surface chemistry, porosity and many others (Hubbell 1995; Anderson 2001). Even the age and the health condition of the host should be taken into account. Upon contact with tissues a cascade of events will take place at the biomaterials interface initiated by the interaction with the surrounding physiological environment which is rather aggressive and contains many bioactive molecules like proteins, polysaccharides and enzymes (Remes and Williams 1992; Tang et al. 1998; Williams 2008). These events will determine the fate of the implant, so the complex interplay that exists between the surface properties of a material and the physiological environment is crucial for understanding the phenomena of biocompatibility. For example, the wettability of a material is a result of its surface energy, but it also relates to the electrical charge distribution and specific chemistry, and this will affect its biological activity. At the same time topography alters the distribution of electrical charges, which in turn is a consequence of crystallinity (Anderson 2001; Planell et al. 2010). The combination of all these surface properties will affect the adsorption of plasma proteins that may expose recognition sequences for cell adhesion receptors. As a result the cells will attach and form cell adhesion contacts that will establish the communication of the material surface with the cell interior - processes that will strongly affect its tissue compatibility (Anderson 2001; Hench and Thompson 2010; Planell et al. 2010). Conversely, the lowered protein adsorption of some material surfaces might be a prerequisite for their good blood compatibility, because of the less contact activation of the coagulation cascade.

There are two main strategies of using biomaterials, the first one focuses on the repair and substitution of a damaged tissue with an implanted device or prostheses that aims to recover the tissue or organ function in a short period of time (Hench and Thompson 2010). This strategy is applicable in urgent situations, for example of traumatological injuries and pathologies that require immediate treatment, and where the regeneration of the tissue or organ will not be possible. The biomaterials used for such purposes already require additional biological properties such as for example biodegradability – the material should disappear from the body when it accomplishes its function (Hench 1980; Hench and Thompson 2010). The other strategy focuses on the tissues and organs regeneration (Hench and Polak 2002) representing the next generation of biomaterials that are applied to support the healing process and to promote the organization of the new tissue (Hubbell 1995; Hench and Polak 2002). In the next section, we will briefly describe

the hierarchic generations of biomaterials focusing on their tissue engineering application, which is relevant to the scientific content of the thesis.

1.2 Host response to biomaterials

When we describe biocompatibility we should first consider the biological response that any foreign material induces upon contact with the body. The first event that occurs on the surface of a biomaterial is the adsorption of proteins, which are uniformly available in the biological fluids. The attachment of phagocytic cells also occur, in most cases because of the so called opsonization of the materials surface that is a consequence of the adsorption of plasma proteins, such as activated C3b component of the complement system, IgG and others, that “label” the biomaterial as a foreign body (Tang et al. 1998). This induces inflammation that is in fact a biological response to the foreign material and persists as long as the material is there. Inflammation induces chemotaxis of inflammatory cells and recruitment of cytokines in order to phagocyte the material marked as foreign starting with the migration of neutrophils and monocytes/macrophages to the injury site. The sustained recruitment of numerous macrophages leads to the formation of multinucleated giant cells, known also as foreign body giant cells (FBGC). This process is followed by the recruitment of fibroblasts that quickly became the main cell population while macrophages may inactivate their attack mechanism (Hunt 2004). Fibroblasts are responsible for secreting extracellular matrix (ECM) proteins mainly type I, and III collagen and form a capsule that will isolate the material from the host tissue (Tang et al. 1998; Hunt 2004). The body response to a foreign material is therefore the serious obstacle in the physiological performance of a biomaterial since the direct contact and integration is fundamental for its proper function. For that reason, to study how biomaterial surface affect these processes is an important issue comprising a strategy to avoid chronic inflammation and promote implant integration (Remes and Williams 1992; Tang and Eaton 1999).

1.3 Definition of biomaterial

“A biomaterial is a substance that has been engineered to take a form which, alone or as part of a complex system, is used to direct the course of any therapeutic or diagnostic procedure in human or veterinary medicine” (Williams 2009).

The development of biomaterials is based on the continuous adding of required properties connected with avoiding undesirable effects such as foreign body reaction, stress shielding, as well as the evolution of concepts for biocompatibility involving biodegradability, bioactivity, etc. The biomaterials can be conditionally divided in 3 generations: first, comprising the “bioinert” materials; the second, consisting of “bioactive” and also “biodegradable” materials, and the third, including the materials designed to stimulate specific cellular responses at the molecular level

(Hench and Polak 2002). All these three generations of biomaterials are still in use and the appearance of new trends does not imply the exclusion of the preceding ones.

1.3.1 First generation of “bioinert” biomaterials

Initially the combination of the proper physical properties with a minimal toxic response of the host to match the functionality of the substituted tissue was the main concern. For that reason, the first generation of biomaterials is based on “inert materials” that present the proper physical and chemical properties (Hench 1980; Hench and Thompson 2010). This first generation includes materials used in several industrial applications, such as chemistry, food, transport, and energy, among others that are treated to have higher levels of purity in order to eliminate release of by-products and minimize corrosion. Some examples include: stainless steels; Co-Cr-alloys; Titanium (Ti) and Ti alloys; oxidic ceramics (that cannot oxidize); and fully polymerized thermoplastic and thermo stable polymers (Planell et al. 2010).

1.3.2 Second generation of “bioactive” and “biodegradable” biomaterials

Although the host response to inert materials is usually low it does not avoid the fibrous capsule formation (Williams 2008). The capsule completely blocks the interaction between the biomaterial surface and the host tissue. With the aim to overcome the formation of this fibrous layer and promote the interaction of material and tissue, appeared the second generation of biomaterials. Accordingly, first, the biomaterial should promote specific biological response, and second, it should be able to degrade progressively as the new tissue regenerates (Hench and Thompson 2010). These biomaterials are therefore called bioactive and biodegradable (Williams 2009; Hench and Thompson 2010; Planell et al. 2010). More than one definition of bioactive material exists, one, reports the boundary between tissues and materials and is dependent on the capacity of a material to elicit a specific biological response at its interface (Hench and Andersson 1993), other, considers the capacity of the material to modulate and support distinct biological events (Black 2006). Bioactive materials are, for example, the calcium phosphate ceramics because *in vivo* calcium phosphate induces the formation of a physiological active hydroxyapatite layer that improves the interaction of the material surface and bone tissue (Planell et al. 2010). The other types of biomaterials are the biodegradable biomaterials that consist of materials that have a controlled chemical breakdown and resorption time in the host. This strategy considers that the material should be degraded while the host tissue is regenerating (Hench 1980). These materials comprise natural and synthetic polymers that have been extensively used in orthopedic applications such as bone substitution, repair of fractures, as sutures, rods, screws, pins and plates (Ciccone et al. 2001); others - for cardiovascular and nervous regeneration (Huang and Huang 2006).

1.3.3 Third generation of “cell – activating” biomaterials

The third generation of biomaterials aims to stimulate specific cellular responses at the molecular level (Hench and Polak 2002). During the last decades various polymer systems that elicit specific interactions with integrins and thereby direct cell adhesion, proliferation, differentiation and ECM production have been developed. They are based on distinct molecular modifications mainly on bioresorbable polymer systems. In order to activate genes that stimulate regeneration of living tissues a third-generation bioactive glasses and hierarchical porous foams are also being designed (Hench and Thompson 2010). The new molecularly tailored biomaterials use two alternative routes, the tissue engineering and the *in situ* tissue regeneration. The final aim is the repair or replacement of a tissue that last as long as the patient adapt to the physiological environment (Langer and Vacanti 1993; Griffith and Naughton 2002; Hench and Thompson 2010). The *in situ* tissue engineering approach aims to stimulate tissue repair with biomaterials in form of powders, solutions or doped micro- or nano-particles. The release of chemicals in form of ionic dissolution products, or macromolecular growth factors, at controlled rates that activate the cells in contact with the stimuli can be obtained by a proper formulation of bioactive materials. Along with the biochemical and biomechanical gradients that are present the cells produce additional growth factors, which in turn stimulate multiple generations of growing cells to self-assemble into the required tissues *in situ* (Hench and Polak 2002). The genetic control of the tissue repair process is an additional approach that might be offered in the regenerative medicine (Griffith and Naughton 2002; Atala 2004; Hench and Thompson 2010).

It exists also an additional group of biomaterials reported as “smart” or “intelligent” biomaterials (Anderson et al. 2004; Furth et al. 2007). These are materials that can change their properties upon variation in the biological environment; exemplified by temperature and pH responsible polymers, shape memory biomaterials, etc., (Anderson et al. 2004; Furth et al. 2007) which are out of the topic of this thesis.

1.4 Tissue engineering and regenerative medicine

Initially tissue engineering was equalized with the third generation of biomaterials, however with growing in scope and importance it is now considered as an independent field. Although it covers a broad range of applications, the practical definition is associated with applications that repair or replace portions, or whole tissues (e.g., bone, cartilage, blood vessels, bladder, skin, etc). Tissue engineering aims to replace damage tissues with molecularly modified scaffolds that are previously colonized or not with cells. In fact, this is an attempt to mimic the natural occurring tissues (Langer and Vacanti 1993; Atala 2004). Ideally, a host tissue that includes a viable blood supply should replace the scaffold. The improvement or replacement of a biological function is addressed using a combination of cells, engineering and material processing technologies,

providing suitable biochemical and physico-chemical factors (Langer and Vacanti 1993; Hubbell 1995; Atala 2004). Tissue engineering strategies generally include: (i) implantation of freshly isolated cultured cells; (ii) implantation of tissues that were previously assembled *in vitro* using cells and scaffolds; and (iii) *in situ* tissue engineering (Langer and Vacanti 1993; Hubbell 1995; Griffith and Naughton 2002; Atala 2004). In fact, these strategies overlap the strategies of the 3rd generation biomaterials. The implantation of isolated or cultured cells uses individual cells or small aggregates from the patient or donor, to inject to the damage tissue directly or to combine with a biodegradable scaffold *in vitro* and then implant in the damage area. For the implantation of tissues assembled *in vitro*, a complete 3D tissue is growth *in vitro* using a scaffold and cells from the patient or donor in an appropriate bioreactor and once the tissue reaches maturity is implanted (Figure 1.1).

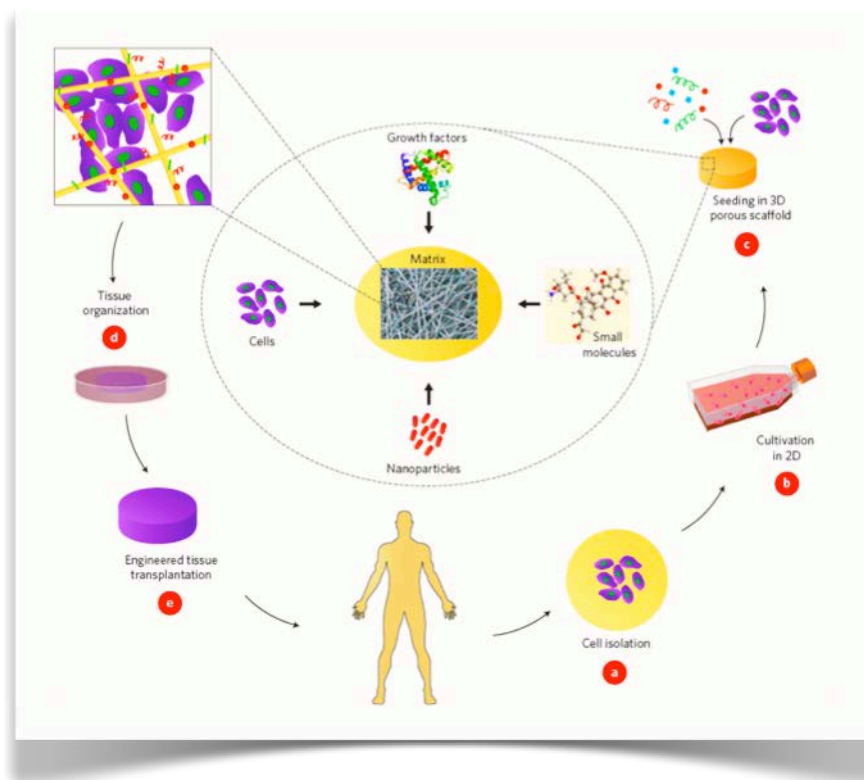


Figure 1.1 – Main tissue engineering strategy: a) Isolation of cells from the patient; (b) Isolated cells are expanded *in vitro*; (c) Cell seeding in a porous scaffold together with growth factors, small molecules, and micro-and/or nanoparticles. The mechanical support and the shape of the implant are determined by the scaffold and the porosity that enable high mass transfer and waste removal; (d) The organization of the scaffold into a functioning tissue might be obtained by cultivation of the cell constructs in bioreactor; (e) The construct is finally transplanted in the defect to restore function (Dvir et al. 2011).

The *in situ* tissue engineering promotes the regeneration of tissues using a scaffold that is implanted directly into the injury site and stimulates the body's own cells to promote local tissue repair (Langer and Vacanti 1993; Hubbell 2003; Atala 2004; Dvir et al. 2011). The body's natural

ability to regenerate determines the use of acellular scaffolds. The production of acellular scaffolds comprises two approaches: the use of synthetic scaffolds, or the removal of the cellular components from natural ECM via mechanical and/or chemical manipulation. When using scaffolds colonized with cells various sources of donor cells can be used: heterologous (other species), allogeneic (same species, different individual), or autologous (from the same) (Atala 2004; Dvir et al. 2011).

The *regenerative medicine* often overlaps in its meaning with tissue engineering, but it should not be considered as identical approach. Regenerative medicine is an emerging interdisciplinary field of research and clinical applications that is focused on the repair of human body. It involves replacement or regeneration of cells, tissues or organs aiming to restore impaired function resulting from any cause, including congenital defects, trauma and aging. It uses a combination of several technological approaches that moves it beyond traditional transplantation and replacement therapies. These approaches may include, but are not limited to, the use of soluble molecules, gene therapy, stem cell transplantation, tissue engineering and reprogramming of cell and tissue types (Greenwood et al. 2006; Mason and Dunnill 2007). The implication of human cells is central focus of the regenerative medicine. The cell types include mainly stem cells, somatic, adult or embryo-derived. A big focus is given lately to the fact that pluripotent cells can be obtained by reprogramming adult cells (Yu et al. 2007) - a fact that may help avoiding the ethical problems of using embryo-derived stem cells. In the moment most of the treatments involving embryo-derived cells are based in pure cell therapies, but it is very probable that in future stem cells therapies will need a temporary support or scaffold that will improve cell survival. It is important to emphasize also the growing linkage between gene therapy and regenerative medicine. In this case the cell therapy focus on to place genes in cells, check if the outcome is safe and then implant the cells in the patient (Atala 2004; Cohen and Melton 2011). An example is the use of such genetic approach to immortalize fetal neuronal cells thus making them cell line for the potential treatment of strokes (Donato et al. 2007).

The proper definition of the word regeneration elucidates the main focus of the area, it is described as “the process in humans whereby lost specialized tissue is replaced by proliferation of undamaged specialized cells” (Mason and Dunnill 2007). However, this process is quite limited in humans and restricted to just a few tissues, such as liver and bone. Understanding the definition of repair is also important in order to distinguish it from regeneration. Repair is the replacement of a lost tissue by granulation tissue that matures to form a scar tissue (Yannas 2001; Mason and Dunnill 2007). In this respect the organ regeneration is distinct from organ repair as an endpoint of a healing process following injury. Repair is an adaptation to the loss of normal organ mass and leads to restoration of the interrupted continuity by synthesis of scar tissue without restoration

of the normal tissue. In contrast, regeneration restores the interrupted continuity by synthesis of the missing organ mass at the original anatomical site. Thus, regeneration restores the normal structure and function of the organ while the repair does not (Yannas 2001; Mason and Dunnill 2007).

The Figure 1.2 schematizes the regeneration medicine strategies employing different stem cells sources from the proper patient. Pluripotent embryonic stem cells (ESCs) can be obtained and differentiated *in vitro* to a desired cell state by directing their differentiation (right). Other way is the use of primary cells derived from the patient to generate a desired cell type (iPS) directly by reprogramming the primary cells (left). The obtained cells by either of the methods can be studied *in vitro* (bottom) or used for transplantation into patients (top).

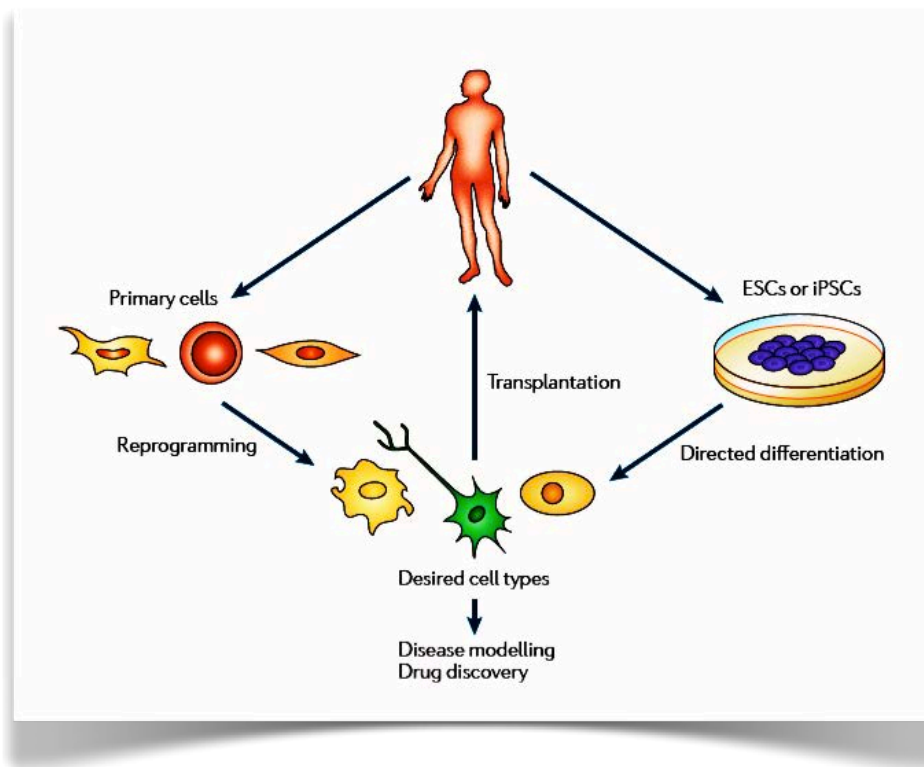


Figure 1.2 - The main strategies of regenerative medicine. This figure describes the two main strategies for generating patient-specific cells of a desired type. Patient-derived (induced pluripotent stem cells - iPSCs) or non-patient-derived (either embryonic stem cells - ESCs or iPSCs) are the two types of pluripotent cells to be used for regenerative medicine (Cohen and Melton 2011).

1.4.1 Biomaterials for tissue engineering and regenerative medicine

The biomaterials used for tissue engineering and regenerative medicine are generally scaffolds, e.g. materials from the 3rd generation of biomaterials, designed to mimic the ECM and to host the cells. They are very important since they provide the designable biophysical and biochemical milieus that direct cellular behavior and function (Lutolf and Hubbell 2005). One clear concept is

that all biomaterials used for tissue engineering shall induce ingrowth of desirable cell types coming from the host organism. Thus, the engineered scaffolds or devices must provide sufficient mechanical support to maintain a space for new tissue to form or serve as a barrier to undesirable interactions. Furthermore, the scaffolds are intended to degrade slowly after implantation in the patient and be replaced by new tissue (Place et al. 2009). The use of synthetic or natural materials is a fundamental question. Synthetic materials (e.g., organic polymers) can be easily processed into various structures and can be produced cheaply and reproducibly; they provide also possibility to tightly control various surface properties such as the mechanical strength, hydrophobicity and degradation rate. While natural materials (e.g., collagen, fibrinogen etc.) often exhibit a limited range of physical properties and can be difficult to isolate and process, but they do have specific biologic activity. In addition, these molecules generally do not elicit unfavorable host tissue responses, a condition which indicates that a material is biocompatible. Some synthetic polymers however, in contrast, can elicit long-term inflammatory response from the host tissue (Mooney and Langer 2000).

Naturally derived ECM systems (for example Matrigel, collagen and fibrin gels, etc.) have been used to study in three dimensions (3D) the organization and the multicellular complexity of tissues to better understand the function of ECM within tissues and organs. Tissue engineering and regenerative medicine strategies substantially improved with learning this processes (Dutta and Dutta 2010). Nowadays cell matrices are used to induce regeneration and remodeling *in vivo* promoting proper cells infiltration. Once implanted, these matrices act as carriers for the transplanted cells that are subsequently grafted into tissue defects (Hubbell 2003). As example, we have tissue sealants and skin substitutes like fibrin and collagen matrices that are FDA-approved and are widely used for chronic wounds treatment, healing burns, etc. (Currie et al. 2001; Patino et al. 2002). The creation of artificial materials with similar biological function however is another attractive option. For that reason one of the main strategies in tissue engineering and regenerative medicine is to develop synthetic or natural biomaterials that mimic the complexity of the natural ECM (Griffith and Naughton 2002; Lutolf and Hubbell 2005).

2. Extracellular Matrix

The ECM is a complex network of polysaccharides and proteins secreted by the cells. It serves as a structural element in tissues by influencing their development and physiology (Alberts et al. 2002). As the principal extracellular component of all tissues and organs, the ECM provides the scaffold that gives physical support to cells and regulates intercellular biochemical and biomechanical signaling. As a result, it is determinant in most cellular processes including adhesion, migration, apoptosis, proliferation, and differentiation (DuFort et al. 2011). The main molecular components of the ECM include: (i) the insoluble hydrated macromolecules (fibrillar proteins like collagens, elastin, laminin and fibronectin), (ii) the hydrophilic proteoglycans with large glycosaminoglycan side chains; (iii) the soluble macromolecules (growth factors, chemokines and cytokines) and (iv) the adhesive proteins associated with the surface of neighboring cells (Figure 2.1) (Lutolf and Hubbell 2005). At the molecular level, the ECM is capable of binding, integrating and controlling the presentation of growth factors and other ligands to the cells (Hynes 2009). Cells are constantly rearranging and reordering their surroundings by mechanical translocation and/or by enzymatic cleavage, and these features should also be considered (Mager et al. 2011). The ECM organization is not static, the opposite, it is very dynamic since its composition and distribution varies between different tissues and also during stages of development. Actually the great diversity of ECM composition is the main reason for the wide range of forms and functions, ranging from solid structures found in bones and teeth to the elastic and pliable matrix found in cartilage and tendons. Disruptions and perturbations to ECM result in loss of cell and tissue homeostasis and lead to a number of diseases, including cancer (Lutolf and Hubbell 2005; Daley et al. 2008; Mager et al. 2011).

Nowadays the design of biomaterials for tissue engineering must take into account this bidirectional signaling events in order to maintain cell viability and obtain control on cell behavior (Lutolf and Hubbell 2005; Place et al. 2009). The ECMs varies in composition and spatial organization of collagens, elastins, proteoglycans and adhesive molecules between tissues in the body in order to maintain specific tissue morphologies, organ specific shape and function, and to supply specific instructive cues. Therefore, the desired scaffold for an engineered tissue should take into account the existing strong knowledge on the ECM organization and the diverse cell-ECM interactions (Lutolf and Hubbell 2005; Place et al. 2009; Dvir et al. 2011). ECM varies also on its structure and functional organization; the rough ECM of the connective tissues is less specialized in comparison to the organ-specific matrix represented by the basement membranes.

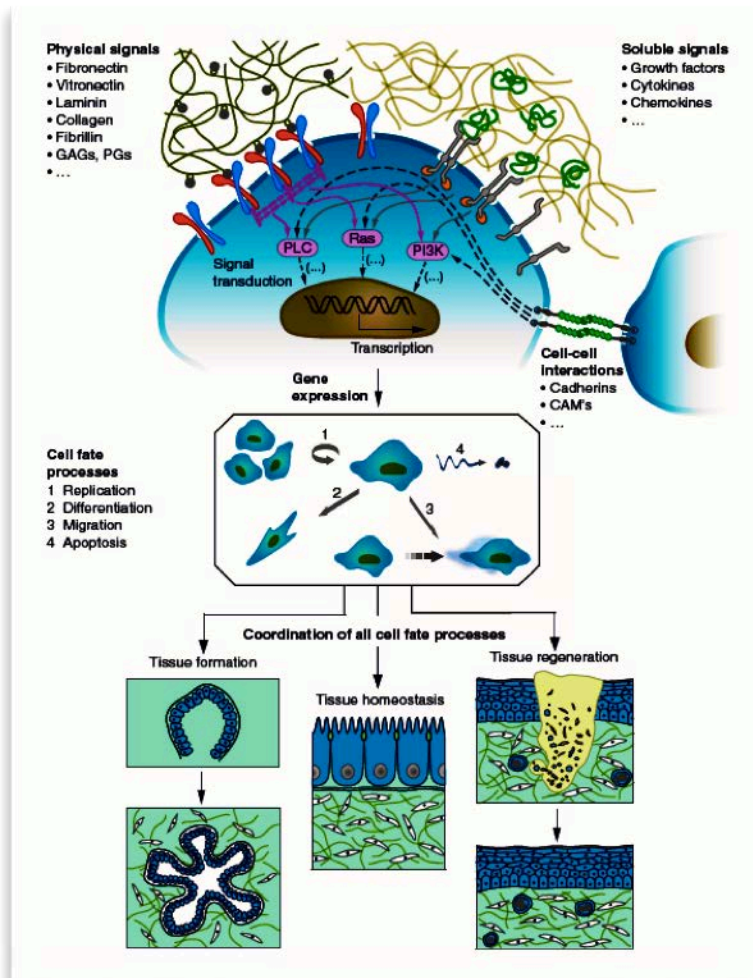


Figure 2.1 - Reciprocal molecular interactions between cells and ECM. These tight relations regulates the behavior of individual cells and the dynamic state of multicellular tissues (Lutolf and Hubbell 2005).

2.1 Rough Extracellular Matrix

The rough ECM is the tissue where the portion of ECM occupies a greater volume than the cellular component. It is a type of connective tissue that includes areolar (loose) connective tissue, reticular tissue, and adipose tissue (Alberts et al. 2002). It also surrounds the blood vessels and nerves. It is the most common type of connective tissue in vertebrates and their main functions is to hold organs in place and attach epithelial tissue to other underlying tissues. Reticular cells, namely fibroblasts, are widely dispersed in this tissue; they are irregular branching cells that secrete strong fibrous proteins and proteoglycans. A gel-like substance primarily made of collagen and elastic fibers generally separates the fibroblasts. There are distinct hierarchy in the organization of the ECM, and the rough ECM is the most disordered part, but it supports the basement membrane (BM) (described separately below) which is the highly organized ECM and therefore they are involved in a continuous interplay (Alberts et al. 2002; Lutolf and Hubbell 2005).

2.2 Basement membrane structure and function

The basement membrane (BM) represents the most specialized form of ECM that is always in contact with cells. The main BM functions are to provide structural support for cells, to divide tissues into compartments, as well as, to regulate the cellular behavior (Paulsson 1992; Kalluri 2003; Yurchenco 2011). The BM is a sheet-like structure composed of large insoluble molecules that come together via a process known as “self-assembly” (Yurchenco et al. 1986), but it can be also driven by cell-surface anchors and receptors (Yurchenco 1990; Kalluri 2003). The BM constituents are produced by the residing cells (Paulsson 1992), or delivered by the circulation. Type IV collagen (Col IV), laminin (LAM), heparan-sulphate proteoglycans (HPSPGs) and nidogen/entactin are the main structural components of BM. Other components, known to be minor part of BM’s, include agrin, SPARS/BM-40/osteopontin, fibulins, type XV collagen and type XVIII collagen (Yurchenco 1990; Paulsson 1992; Kalluri 2003). Although the complexity of its structure and similar appearance, the BM is tissue specific, which means that BMs have unique structure depending on the tissue of origin. Understanding how the cellular microenvironment specifies functionality to different tissues can arise from understanding the potential differences in the composition and structure of BMs in different organs (Kalluri 2003). An important link to the present study is the vascular BM, making up the structure and the functionality of blood vessels and capillary. The vascular BM is lined from one side by endothelial cells (e.g. in the inner part) and from outside by specialized smooth-muscle cells – pericytes (Figure 2.2).

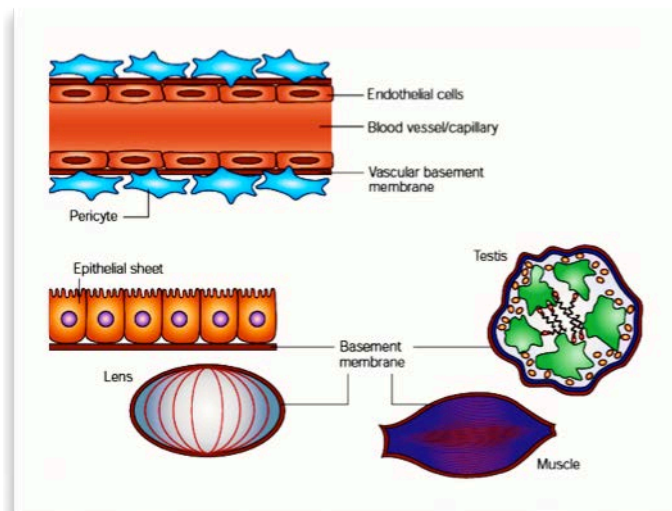


Figure 2.2 - Basement membrane - schematic representation in various tissues. Particularly the vascular BMs is lined by endothelial cells in the inner part and from outside by specialized smooth-muscle cells – pericytes. The BM underlies also the epithelial cell sheets found for example in the testis or surround the muscles and lens of the eye (Kalluri, 2003).

The main structural components of the BM have the capacity to self-assemble and form the sheet-like structure via specific binding sites (Yurchenco and Furthmayr 1984; Yurchenco 1990; Yurchenco 2011). The fact that the BMs cannot be formed by minor constituents led to the discovery that Col IV and LAM form independent scaffolds that interact with each other via nidogen/entactin cross-linking to initiate BM assembly (Yurchenco and Furthmayr 1984; Timpl and Brown 1996). Recent studies revealed that although LAM initiate the assembly of the BM the Col IV acts as a natural scaffold (Kalluri 2003; Yurchenco 2011). LAM polymerizes on the cell surface with the participation of cell-surface molecules such as β_1 integrins and dystroglycan (Cognato and Yurchenco 2000). The deposition of LAM polymers on the cell surface is associated with the deposition of Col IV on the extracellular environment. Cells deposit LAM polymers on top of Col IV scaffold (Cognato and Yurchenco 2000) and nidogen/entactin do the bridging and thus forming the BM-like structure (Timpl and Brown 1996; Kalluri 2003; Yurchenco 2011). The fully functional BM is generated by the interaction of other BM constituents with specific binding sites in the previously formed LAM-Col IV scaffold (Figure 2.3).

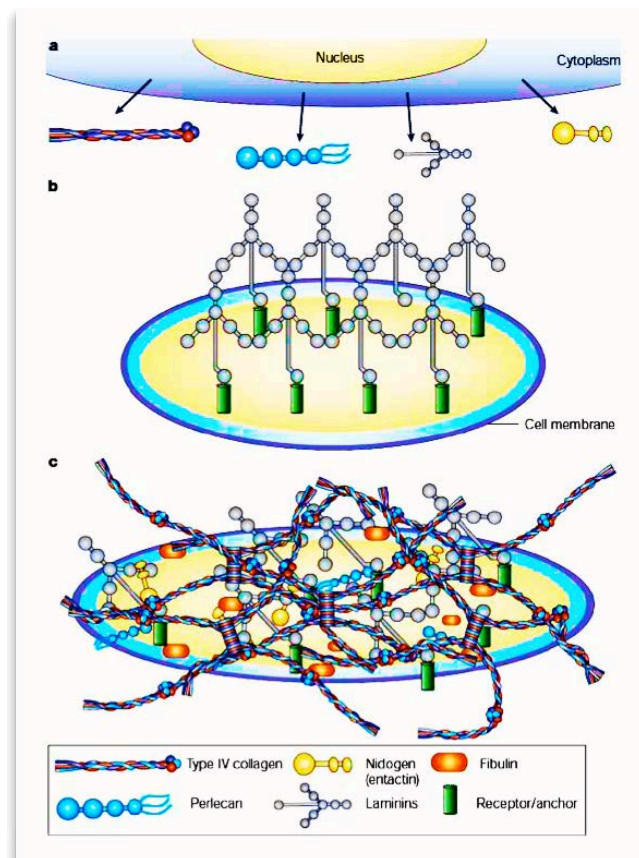


Figure 2.3 - Basement membrane assembly. a) The BM components are pre-assembled inside the cell into functional units. b) The BM formation is initiated by laminin polymerization at the basolateral surface of the cells after anchoring to cell surface receptors such as integrins and dystroglycans. c) The formed laminin polymer is deposited on the Col IV network. The nidogen/entactin further crosslink the Lam polymer to the Col IV network (Kalluri 2003).

2.2.1 Type IV Collagen – structure and function

Type IV collagen (Col IV) is the most specific and abundant collagenous glycoprotein of the basement membranes (Timpl and Brown 1996). It is a heterotrimer, consisting of three alpha (IV) chains, which are a combination of six monomers, $\alpha 1(\text{IV})$ to $\alpha 6(\text{IV})$ (Yurchenco and Furthmayr 1984). Despite the number of different chains they interact and assemble with high specificity to give rise to only three distinct heterotrimers of $\alpha 1\alpha 1\alpha 2$, $\alpha 3\alpha 4\alpha 5$, and $\alpha 5\alpha 5\alpha 6$ (LeBleu et al. 2007), each ~ 400nm long (Kühn 1995). The so called “classical” chains include $\alpha 1(\text{IV})$ and $\alpha 2(\text{IV})$ which were the first to be described and are present in the BM of all tissues, while the other four chains have restricted tissue distribution during development (LeBleu et al. 2007). Col IV molecules are composed by a short non-helical amino-terminal domain called 7S, a long Gly-X-Y repeat triple-helical domain with numerous small interruptions and a highly conserved globular carboxyl-terminal, or NC1 domain (see Figure 2.4).

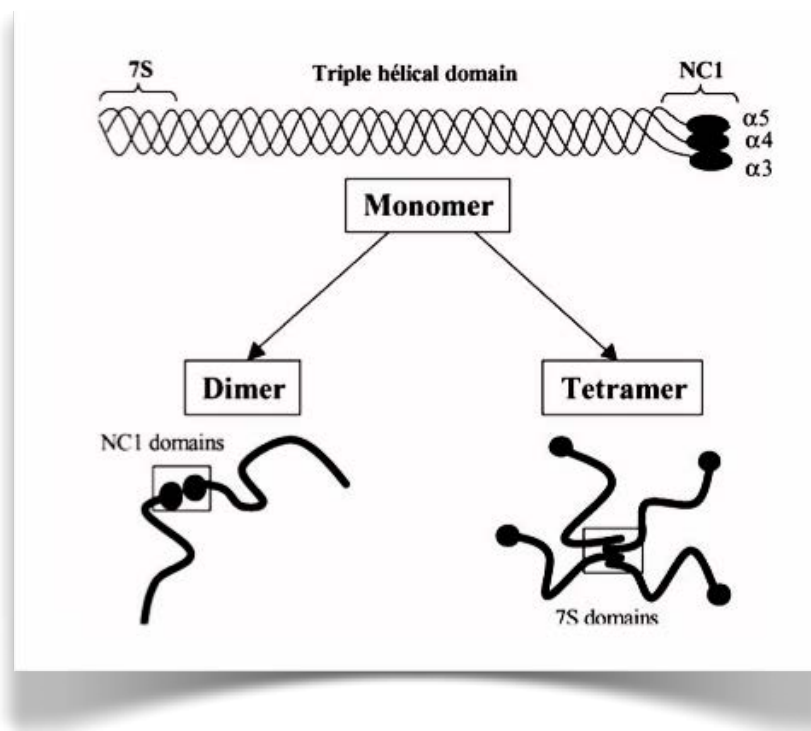


Figure 2.4 - Types of Col IV molecules association. Schematic draw of Col IV heterotrimer multimerization in two main types, dimers and tetramers, that self-assemble through 7S or NC1 domains, respectively.

The tertiary structure of Col IV is formed by specific interaction of three NC1 domains (NC1-trimers), followed by supercoiling of the triple-helical collagenous domains which proceeds toward the N-terminal 7S domains (Yurchenco and Furthmayr 1984; Timpl and Brown 1996). Col IV is termed network-forming collagen because of its capacity to self-assemble into organized networks (Yurchenco and Furthmayr 1984; Khoshnoodi et al. 2008). This property is what makes it different from the fibrillar collagens (Khoshnoodi et al. 2008). Col IV further self

assemble to form networks by 7S amino-terminal interactions, thus forming tetramers (Figure 2.4) (Yurchenco and Furthmayr 1984), while NC1 domain interactions form dimers (Figure 2.4) (Tsilibary and Charonis 1986). The subsequent lateral interactions (disulfide bonding) giving rise to a semi-hexagonal network (see Figure 2.3) observed both *in vitro* (Yurchenco and Furthmayr 1984) and *in vivo* (Yurchenco and Ruben 1987).

2.2.2 Type IV Collagen interaction with cells

Col IV is extremely important component of the basement membrane since it provides a scaffold for the assembly and mechanical stability of cell adhesion sites, thus determining the migration, survival, proliferation and differentiation of anchoring cells *in vivo* (Yurchenco and Furthmayr 1984). Cell culture studies have shown that collagen IV is the binding substrate for a large number of cell types, including platelets (Santoro 1986), hepatocytes (Rubin et al. 1981), keratinocytes (Murray et al. 1979), endothelial (Cheng and Kramer 1989), mesangial (Setty et al. 1998), pancreatic (Kaido et al. 2004), and tumor cells, such as breast and prostate carcinomas (Abecassis et al. 1987), melanoma (Chelberg et al. 1989), fibrosarcoma and glioma (Aumailley and Timpl 1986).

Multiple binding sites mediate cell attachment to Col IV suggesting involvement of several adhesion recognition sites within both triple-helical and NC1 domains (Chelberg et al. 1989). As for many other ECM components, the major cell surface receptors for Col IV are the integrins. Several studies have shown that cell adhesion to collagen IV is arginine-glycine-aspartic acid (RGD) -independent. Although multiple RGD sequences exist within the triple-helical region of several Col IV α -chains (Herbst et al. 1988) these RGD sequences are not accessible to integrins due to their triple-helical nature. However, since reduction of disulfide bonds followed by heat-denaturation dramatically decreases cell binding and spreading, the adhesion to Col IV is considered to be predominantly dependent on triple-helical state of Col IV (Aumailley and Timpl 1986; Santoro 1986). The major collagen receptors include the β_1 subgroup of integrins, namely $\alpha_1\beta_1$ and $\alpha_2\beta_1$ (Aumailley and Gayraud 1998; Leitinger and Hohenester 2007). All collagens, including Col IV and Col I, are recognized by those two receptors, however, with distinct specificity. Integrin $\alpha_1\beta_1$ has a higher affinity for Col IV, while $\alpha_2\beta_1$ binds stronger to Col I (Khoshnoodi et al. 2008). A dramatic decrease in adhesion and migration of fibroblasts and smooth muscle cells to collagen IV substrate was found after deletion of $\alpha_1\beta_1$ integrin (Gardner et al. 1996), while the importance of $\alpha_2\beta_1$ integrin was demonstrated by the decrease of adhesion and morphogenesis after block $\alpha_2\beta_1$ expression using antisense mRNA (Keely et al. 1995). The $\alpha_2\beta_1$ integrin also plays an important role in platelet adhesion to collagens and in the homeostasis in the blood vessel wall (Khoshnoodi et al. 2008). The $\alpha_2\beta_1$ integrin was shown to recognize a binding site composed of a short sequence of GFOGER peptide (Knight et al. 1998). The

sequence is entirely dependent on the native triple-helical conformation and represents a high-affinity binding site in both Col I and IV. Moreover, this sequence is present in $\alpha 1$ chain of the cyanogen bromide-derived (CB3 (IV)) fragment (385–390), where it might represent one of the two binding sites for $\alpha_2\beta_1$ integrin (Figure 2.5) (Knight et al. 1998; Khoshnoodi et al. 2008).

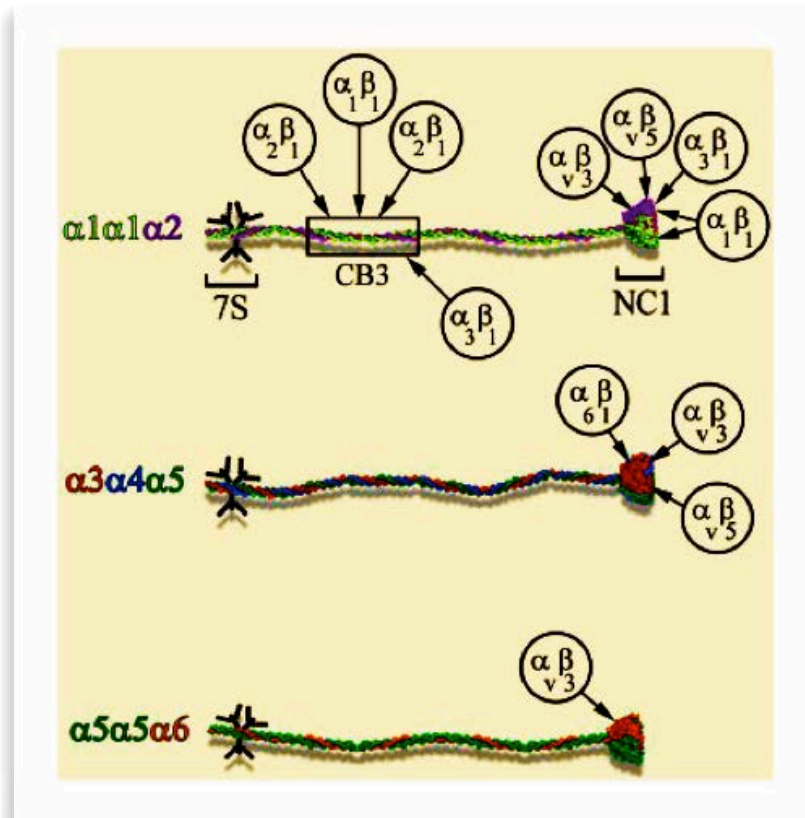


Figure 2.5 - Integrin binding sites within Col IV molecules. The scheme represents three different Col IV heterotrimers showing the location of integrin-binding sites within each molecule. NC1 domain binding sites, and cyanogen bromide-derived fragment (CB3) binding sites are indicated (Khoshnoodi et al. 2008).

Other integrins may also participate in cell binding in addition to $\alpha_1\beta_1$ and $\alpha_2\beta_1$. Cell adhesion to Col IV mediated by $\alpha_3\beta_1$ integrin was shown for small lung carcinoma cell line expressing low levels of other β_1 integrins (Bredin et al. 1998). However, since integrin-specific antibody failed to block the adhesion of various cells and over-expression of $\alpha_3\beta_1$ does not increase adhesion to the Col IV (Nishiuchi et al. 2003) the role of $\alpha_3\beta_1$ as a Col IV receptor remains controversial (Elices et al. 1991). Recently, binding of two new integrins, $\alpha_{10}\beta_1$ and $\alpha_{11}\beta_1$, to Col IV have been reported (Tiger et al. 2001; Tulla et al. 2001). The α_{11} I domain binds stronger to collagen I through the same GFOGER motif as $\alpha_2\beta_1$ integrin, while binding of α_{10} is more specific for Col IV similar to α_1 I domain (Tulla et al. 2001). Nevertheless, the structure of the binding sites for the later two integrins on Col IV remains unknown. Expression of $\alpha_{10}\beta_1$ and $\alpha_{11}\beta_1$ is spatially and

temporally restricted to chondrocytes and fetal muscle cells, suggesting their specific role in development (Khoshnoodi et al. 2008).

Thermal denaturation or proteolytic degradation can also result in the exposure of novel binding sites on collagen molecules, as it was described for Col I and later for Col IV, demonstrating an increased affinity to fibronectin (Aumailley and Timpl 1986). For this reason it was proposed that cell adhesion to denatured collagen could be mediated by fibronectin- $\alpha_5\beta_1$ integrin bridge (Tuckwell et al. 1994). Nevertheless, this and other results suggest that degradation and proteolytic remodeling of BMs might expose cryptic sites within Col IV molecule with altered integrin specificity and biological functions. Recently, it was identified $\alpha_v\beta_3$ and $\alpha_v\beta_5$ integrins as endothelial receptors for $\alpha 3$ NC1 domain by affinity chromatography, which was further confirmed by the binding of purified integrins *in vitro* (Pedchenko et al. 2004). So far, specific integrin binding sites have been characterized only for $\alpha 3$ NC1 domain. Thus, collagen acts as ligand for distinct integrins through several binding sites that may mediate their anti-angiogenic and anti-tumor activities. Additional, yet uncharacterized binding sites have been reported by several groups suggesting also the interaction of cells with 7S domain of Col IV (Khoshnoodi et al. 2008).

2.2.3 Laminin – structure and function

The other main constituent of the BM is LAM - a heterotrimeric protein that normally presents a cruciform-shaped morphology, although rod-like or Y-shaped LAM morphologies may also occur (Miner and Yurchenco 2004). LAM is composed by one α , one β , and one γ chain and in vertebrates there are, five α , three β , and three γ chains that represent distinct gene products and can assemble into at least 15 LAM proteins (Miner and Yurchenco 2004). According to LAM chain composition the trimers are also named and Figure 2.6 show the most widely studied isoform, laminin-111, that is composed by one $\alpha 1$, one $\beta 1$, and one $\gamma 1$ chains (Durbeej 2010; Yurchenco 2011). All LAM chains share a common domain structure with a number of globular and rod-like domains. A globular laminin N-terminal domain (LN), globular domains laminin 4 (L4) and laminin four (LF) separated by rod-like spacer formed by epidermal-growth factor like (LE) domains compose the short arms of laminin-111 (Miner and Yurchenco 2004).

The LAM reach their final heterotrimeric form by assembly inside the cell, but further extracellular proteolytic processing may also occur (Timpl and Brown 1996). The long arm of LAM is formed by all three chains, giving a α -helical coiled coil domain and a C-terminal end, which is composed of five homologous globular domains (LG domains, each of approximately 20 kDa) that are unique to the α chain (see Figure 2.6a) (Durbeej 2010). The size of the cross-shaped LAM molecule was estimated to range between 70–100 nm, however, it depends on the

conformation of the molecule because the maximal dimensions of the completely extended cruciform molecule is 125 nm long, 72 nm wide, and 2.2 nm thick (Chen et al. 1998).

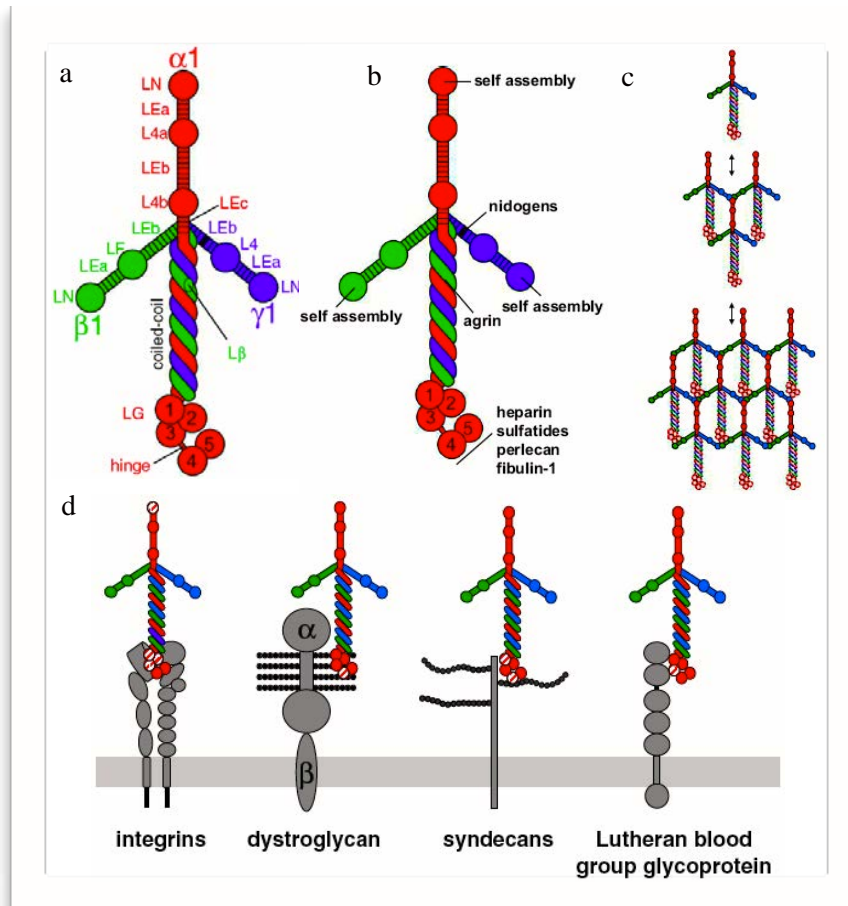


Figure 2.6 - Diversity of laminin structure. a) Overall structure of LAM; b) Biologically active domains within LAM molecules; c) LAM assembly model; and d) Major cell receptors responsible for binding to LAMs and their presumed mode of recognition. Adapted from (Durbeej 2010).

The ability to polymerize is associated with LAMs short arms. The three-arm interaction model describes the production of a lattice-type supramolecular network by the interaction of the three N-terminal short arms in a calcium dependent bounding (Figure 2.6b). In addition to polymerize LAM molecules are incorporated in BM by interactions with other ECM proteins such as Col IV, nidogen and fibulin, or other LAMs (Yurchenco et al. 1986; Timpl and Brown 1996; Colognato and Yurchenco 2000).

Several LAM domains have key biological activities, ranging from self-assembly, binding to other matrix proteins and specific recognition by cell surface receptors, which have been mapped and are shown in Figure 2.6b (Durbeej 2010). The LAMs play a prominent role in providing

structure to the ECM and anchorage for cells to the basement membrane. Thus, the main role of LAMs is to link the BM to the cells through interactions with cell surface receptors that influence cell signaling and behavior, in addition to providing a structural role (Van Agtmael and Bruckner-Tuderman 2010). LAM is crucial for the assemble of the basement membrane since in the absence of LAM, or the presence in a truncated form where the cell-adhesive LG domains are absent, the basement membrane do not assemble (Miner and Yurchenco 2004). Mutations in LAM molecules or the use of block antibodies results in a group of diseases known as epidermolysis bullosa (JEB), and muscular dystrophy. LAM was also shown to be critical to neural development by promoting cell survival and migration, neurite outgrowth and synapse formation (Colognato and Yurchenco 2000; Perris and Perissinotto 2000; Testaz and Duband 2001). For that reason LAM coatings have been extensively used to promote nerve cell adhesion and growth on different substrates for tissue engineering applications (Yu et al. 2008).

2.2.4 Laminin interaction with cells

Both integrins and non-integrin molecules are the major LAM cellular receptors (Mecham 1991). LAMs can be recognized at least by eight integrins ($\alpha_1\beta_1$, $\alpha_2\beta_2$, $\alpha_3\beta_1$, $\alpha_6\beta_1$, $\alpha_6\beta_4$, $\alpha_7\beta_1$, $\alpha_9\beta_1$, $\alpha_v\beta_3$) that recognize sequences mainly in the α LG domains 1-3 and in α LN domains (Figure 2.6a, and d). However, integrin binding was also associated to the C-terminals of β_1 , β_2 , γ_1 and γ_2 chains (but not γ_3) (Belkin and Stepp 2000; Taniguchi et al. 2009; Durbeej 2010). Once LAM bounds to its proper ligand, the intracellular cytoplasmic portion of integrin can activate focal adhesion kinases (FAK), small rho GTPases and mitogen-activated protein kinase (MAPK) pathways to effect cellular activities (Tzu and Marinkovich 2008). Dystroglycan, syndecans, and Lutheran blood group glycoprotein are the non-integrin receptors for LAMs (Figure 2.6c). Dystroglycan have high affinity for LAM α_1 and α_2 chains but moderate or low affinity for other α chains. It was demonstrated that syndecans consist of four members that all bind synthetic peptides mainly from the LG4 domain. The other non-integrin receptor, the Lutheran glycoprotein, binds only to LAM containing α_5 chain (Mecham 1991; Colognato and Yurchenco 2000; Durbeej 2010; Yurchenco 2011).

2.3 Extracellular matrix remodeling

The process of ECM remodeling is critical during development and tissue repair. ECM remodeling is also associated with several pathological conditions, such as hypertension, restenosis following angioplasty, heart failure, fibrosis and cancer which points on its important role in already formed tissues. ECM remodeling comprises three main processes: ECM synthesis, arrangement and degradation. The balance between these processes will determine the loss or net accumulation of ECM (Ala-aho and Kahari 2005; Berk et al. 2007; Daley et al. 2008; Wynn 2008; Shi et al. 2010). Different ECM proteins, and their combination can have different effects

on the phenotype of cells, affecting important processes such as cell survival, growth, differentiation, and migration (Sechler and Schwarzbauer 1998; Wynn 2008). Furthermore, the products of ECM proteolysis can accumulate *in vivo* and contribute to the changes in cell behavior because they can have distinct properties from the intact parental protein (Giannelli et al. 1997; Weathington et al. 2006). Therefore, mechanisms that control ECM fragments accumulation are very important for regulating a variety of cell processes.

The major enzymes that degrade ECM and cell surface associated proteins are matrix metalloproteinases (MMPs) (Page-McCaw et al. 2007). As shown on Figure 2.7, MMPs are a family (24 members) of zinc dependent endopeptidases, which together with adamalysin-related membrane proteinases that contains disintegrin and metalloproteinase domains (ADAMs or MDCs), such as thrombin, tissue plasminogen activator (tPA), urokinase (uPA) and plasmin, are involved in the degradation of ECM proteins. MMPs are either secreted or anchored to the cell membrane by a transmembrane domain or by their ability to bind directly uPA receptor (uPaR) and integrin $\alpha_v\beta_3$ (Buck et al. 1992; Page-McCaw et al. 2007).

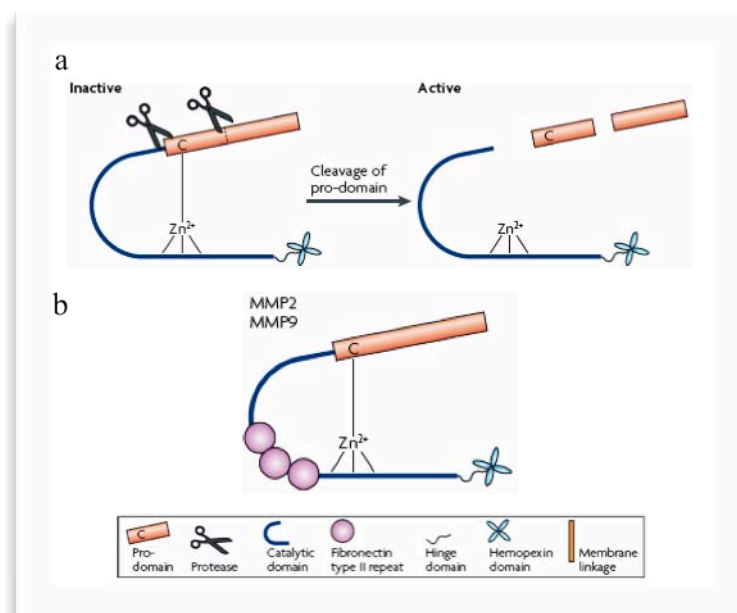


Figure 2.7 - Schematic structure of MMPs. a) MMPs are secreted as pro-proteins. The combination of a cleavage in the pro-domain and the interaction between the pro-domain and catalytic domain results in the removal of the pro-domain and consequent activation of the MMP. Structurally MMPs share a conserved domain structure of pro-domain, catalytic domain, hinge region and hemopexin domain. b) MMP2 and MMP9 are also known as collagenases and represent the main MMPs that degrade Col IV. Apart from the other basic MMPs they have three-fibronectin type II repeats in their catalytic domains. Adapted from (Page-McCaw et al. 2007).

Initially, MMPs were thought to function mainly as enzymes that degrade structural components of the ECM. In addition however, MMP proteolysis can create space for cells to migrate, can produce specific substrate-cleavage fragments with different biological activity, can regulate tissue architecture through effect on the ECM and intercellular junctions, and can activate, deactivate or modify the activity of signaling molecules both directly and indirectly (Page-McCaw et al. 2007). MMPs can cleave ECM proteins and change their cellular functions because this cleavage of ECM components generates fragments that have different biological activities from their precursors. For example, the exposure of cryptic sites that promotes migration results from the cleavage of laminin-5 or Col IV (Egeblad and Werb 2002). MMP1 degrades type I collagen and this process is necessary for epithelial cell migration and wound healing (Page-McCaw et al. 2007). The degradation of ECM molecules can also result in the release of ECM-bound growth factors, including insulin growth factors (IGF) and FGF (fibroblast growth factor) (Egeblad and Werb 2002; Page-McCaw et al. 2007).

3. Cell-Biomaterials Interaction

Understanding the cellular events that take place at the biomaterials interface is fundamental for biology and medicine and is a key for understanding the phenomena of biocompatibility (Williams 2008). Nowadays it is clear that biomaterials for tissue engineering should promote cell adhesion for the successful incorporation of implants and the proper colonization of scaffolds (Griffith and Naughton 2002; Sipe 2002). Cell-biomaterials interaction can be divided on early and late. Early events concern the recognition of the signals, incorporated in the material or coming from the soluble adhesive proteins that rapidly adsorb to the biomaterial surface followed by the generation of proper biological signals that are transmitted to cell interior. Later events need a continuous exchange of biological signals with the biomaterial surface that support cell functionality promoting proliferation and their proper differentiation (Griffith and Naughton 2002; Sipe 2002; Place et al. 2009). The initial cell-biomaterial interaction mimics to a certain extent the natural communication of cells with the ECM. However, cells cannot interact directly with the biomaterials surface, they rather recognize the adsorbed soluble matrix proteins that like fibronectin are available in most biological fluids (Hynes 2002). The most important soluble adhesive proteins include fibronectin (FN), vitronectin (VN), and fibrinogen (FBN). Therefore, according to the classical ligand receptor theory (Grinnell 1986) the initial cell-biomaterial interaction is a multi-step process initiated by the adsorption of proteins from the surrounding medium, followed by cell adhesion, spreading and polarization (Grinnell 1986; Altankov et al. 2010).

3.1 Cell adhesion

Cell adhesion is a fundamental process that is extremely important for cells functionality and proper arrangement of tissues. Cells adhere through several cell adhesion mechanisms that involve their connections to the internal cytoskeleton, which determine the overall architecture of the tissue. Therefore, cell adhesion system is considered as basic mechanisms that help to translate genetic information into the complex three-dimensional patterns of cells in tissues (Gumbiner 1996; Yamada and Geiger 1997; Geiger and Yamada 2011). The three general classes of proteins that form the multi-protein adhesive complexes are the cell adhesion receptors, the ECM proteins and the cytoplasmic plaque/peripheral membrane protein complex (Gumbiner 1996). The cell adhesion receptors are usually transmembrane glycoproteins that mediate binding interactions at the extracellular surface and determine the specificity of cell-cell and cell-ECM recognition. Cell adhesion receptors include members of integrin, cadherin, immunoglobulin, selectin, and proteoglycan (e.g., syndecans) superfamilies (Aplin et al. 1998; Hynes 2009). Conversely, the ECM proteins are large glycoproteins that assemble into fibrils or other complex

Figure 3.2 describes the three states of integrin extracellular domain: (a) When integrins are unbound to their ligand they are in a bent conformation (inactive) and the transmembrane and cytoplasmic regions are closely associated (Figure 3.2a); (b) Once integrins recognize a specific ligand they are activated by talins and kindlins, and extend their extracellular domain (Figure 3.2b); (c) Activated integrins cluster (Figure 3.2c) to provide intracellular signals and form tight focal adhesions (FA) that are very important for actin cytoskeleton assembly and the activation of further downstream signals that control various cellular functions (Takada et al. 2007; Srichai and Zent 2010).

Integrins play a central role in development, organization, maintenance and repair of various tissues by providing anchorage and triggering signals that direct cell survival, migration, cell cycle progression and expression of differentiated phenotypes (Danen and Sonnenberg 2003). Abnormalities in integrin adhesive interactions are often associated with pathological states, including blood clotting and wound healing defects as well as malignant tumors formation (Wehrle-Haller and Imhof 2003).

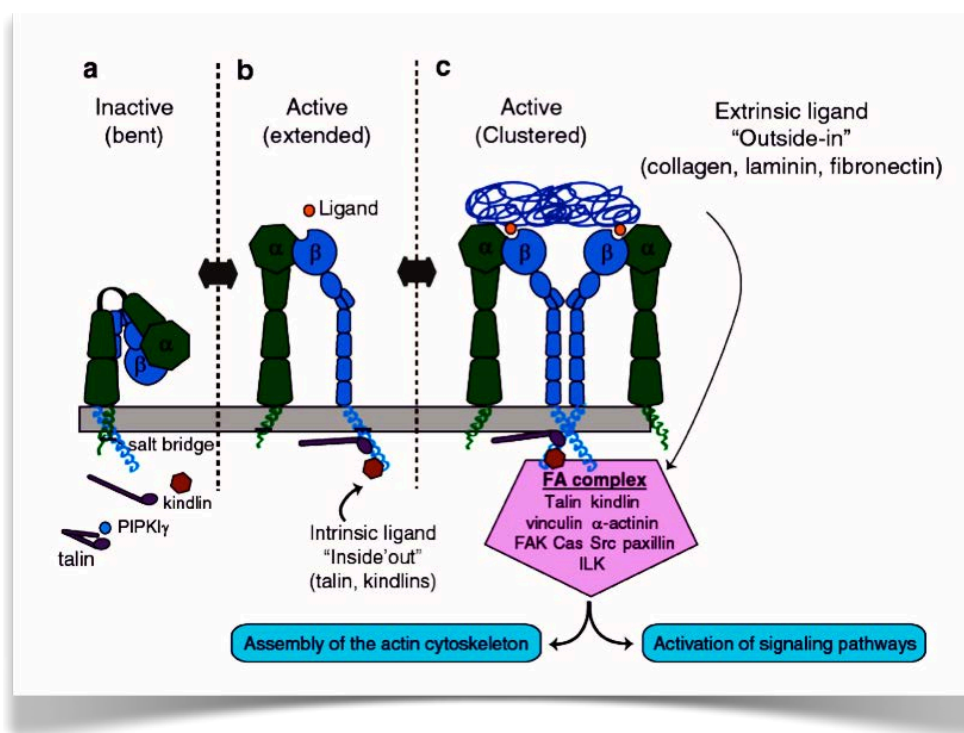


Figure 3.2- Integrin activation cascade (Srichai and Zent 2010).

3.3 Focal adhesion contacts

When integrins are occupied they clusterize and become activated which results in the formation of focal adhesion (FA) complexes. FA is the places where the actual anchorage of cells takes place and where subsequent cellular response is triggered (Damsky and Ilić 2002). The functions

of the FA can be divided into two groups: mechanical and signaling. The association of FA as cell surface sites with the actin cytoskeleton illustrates their mechanical function. FA assures the support for cells movements and allows the cell to remodel the matrix through alteration of the stress in certain locations (Halliday and Tomasek 1995; Geiger et al. 2001). The stress applied, often termed tension or contractility, is generated by the actomyosin cell system, but the talin/vinculin connection plays a major role for the force transmission (Evans and Calderwood 2007). This cellular tension is fundamental for FA contacts maintenance and their formation and stabilization depends highly on the activity of one of the major contractility regulators-Rho. The close relation of FA with mechanical tension exchanged between the cells and environment offers the opportunity to consider these structures as mechanosensors that transmit information about the physical characteristics of the substrate and allow the cell to respond with adequate contractility (Evans and Calderwood 2007; Geiger and Yamada 2011).

The other function of the FA is to register and transmit chemical signals. The clustering of integrins initiates a cascade of specific biochemical events known as integrin signaling. As the cytoplasmic tail of integrins does not have enzymatic activity it depends on the recruitment of adaptor and signaling molecules (Geiger et al. 2001). These include activation of tyrosine kinases such as focal adhesion kinase (FAK) and Src; serine/threonine kinases such as integrin linked kinase (ILK), MAP kinases, jun kinases (JNK), and protein kinase C (PKC), intracellular ions such as protons and calcium, the small GTPase Rho, lipid mediators such as phosphoinositides, diacylglycerol and arachidonic acid metabolites (Geiger et al. 2001; Thiery 2003). A very important and well-studied mechanism in integrin signaling is the FAK-mediated signal transduction. When integrins clusterize they provoke auto-phosphorylation of FAK tyrosine 397 either in an inter- or intra-molecular manner. This phosphorylation leads to the recruitment and activation of the Src family kinases, which lead to phosphorylation of additional sites on FAK. The induced phosphorylation of FAK on tyrosine 925 seems to play a major role in activating the pro-survival Ras/Raf/MEK/MAPK pathway (Geiger et al. 2001; Hanks et al. 2003). This activation is crucial for cell growth and differentiation since it activates MAPK signal-transduction pathway inducing transcriptional regulation of genes. The MAPK pathway give cells the ability to perceive, respond and change in response to their environment (Boudreau and Jones 1999). These signaling events, controlled by FA, offer an important tool for fine assessment of surface biocompatibility (Owen et al. 2005). By testing the activity of the major signal transduction pathways one can evaluate the ability of the new biomaterial to ensure normal cell survival and growth.

3.3.1 Fibrillar adhesions

The next step in the maturation of integrin adhesions, observed particularly in fibroblasts adhering to FN matrix, is the formation of “fibrillar adhesions” (Pankov et al. 2000; Geiger and Yamada 2011). They consist of elongated matrix contacts that are particularly prominent in central regions of cultured fibroblasts. This type of adhesions incorporates the information of a fibrillar FN matrix in the actin cytoskeleton using $\alpha_5\beta_1$ integrins as transmembrane receptors and tensin and praxilin complexed in the cytoplasmic tail of these integrins. They are associated with populations of highly activated $\alpha_5\beta_1$ integrins that together with tensin rapidly move from regions of focal contacts towards the center of the cell body along actin filaments. This movement of integrins applying tensile stretch to fibronectin molecules is a mechanism to induce FN fibrillogenesis (Pankov et al. 2000). The formation of these fibrillar adhesions, the FA complexes, and the consequent matrix reorganization are all force dependent process that highlight the mechanosensitive nature of integrins, from the earliest to the most mature (Zhong et al. 1998; Geiger and Yamada 2011).

3.3.2 Three-dimensional matrix adhesions

The study of cells under conditions that reproduce an *in vivo* environment involves the 3D culture approach. Normally cell-derived or laboratory-produced 3D matrices are used and the big advantage against the 2D cultures is that in 3D system the artificial dorsal-ventral polarization is lost (Cukierman et al. 2001; Cukierman et al. 2002). In these 3D systems fibroblasts form the third type of integrin adhesive structures - 3D matrix adhesions. Something that supports the existence of this type of adhesions in living organisms is that similar types of adhesions were also identified in tissues sections. The 3D matrix adhesions differ from the other two types of adhesions reported here mainly by their extraordinary elongation. The formation of 3D matrix adhesion induces important alterations on cell behavior. Cells cultured on 3D matrices showed increased proliferation, faster migration and altered morphology when compared with cells cultured on 2D surfaces (Cukierman et al. 2001). Whether cells sense artificial materials prepared for example for implantation as a real 3D environment is difficult to answer. However, the existence of different balance between signal transduction pathways in 3D versus 2D environment, together with the specific morphological characteristics of 3D matrix adhesions, may provide a sensitive tool for assessment of the three-dimensionality that allow precise characterization of diverse artificial scaffolds prepared for use in regenerative medicine (Pankov and Momchilova 2010).

3.4 Dynamics of cell adhesion

All the described types of adhesions appear in a specific consequence of time, which allow identification of the *in vitro* evolution or maturation of cell matrix adhesions (Cukierman et al. 2002). The first integrin complexes that are formed at cell substrate contacts are normally named focal complexes. The mechanical forces generated by the intracellular contractile machinery involve the activation of the small GTPase family – Rho, which results in the stabilization and growth of the focal complexes into focal adhesions (Geiger et al. 2001). The maturation process from adhesion sites to focal complexes is accompanied by the recruitment of other plaque proteins like paxilin, vinculin, FAK, and α -actinin building up a strong connection to the actin cytoskeleton (Arnaout et al. 2007). As stated previously, although focal adhesion play an important role in attachment, migration and signaling on ECM substrates, they also play a vital role in the production and organization of newly formed ECM (Pankov et al. 2000). Yamada's group showed that focal adhesion serves as sites for support from which activated $\alpha_5\beta_1$ integrins bound to fibronectin, depart and move centripetally. The centripetal movement of $\alpha_5\beta_1$ integrins bounded to ECM FN fibrils drives the formation of a distinct type of cell-matrix adhesion - the fibrillar adhesions. FN fibrillogenesis is believed to be the result of the tension applied by $\alpha_5\beta_1$ adhesion structures on FN molecules inducing the exposition of cryptic sites for polymerization (Pankov et al. 2000). In fact, the new 3D environment for the cells results from ongoing fibrillogenesis that leads to accumulation of thicker matrix. As result, the cells detach from the surface and become completely embedded in a new 3D environment where the formation of different contacts analogous to those seen in multicellular organisms appears – e.g. 3D-matrix adhesions. This process can be considered as a way of cells to adapt to the flat and rigid environment of *in vivo* conditions, which is one process expected to appear on the surface of a biomaterial after implantation, and transforming flat systems into way of testing the biocompatibility of a biomaterial (Pankov and Momchilova 2010).

Figure 3.3 integrates the main information described in this chapter describing the dynamic cross-talk between cells and ECM: The ECM contributes to the assembly of individual cells into tissues, thus affecting this process at both receptor and cytoskeleton levels; Adhesion-mediated signaling based on cell's capacity to sense the chemical and physical properties of the matrix affects both global cell physiology and the local molecular scaffolding on the adhesion sites. Finally, the molecular interactions within the adhesion site stimulate, in turn, the signaling process, by clustering together the structural and signaling components (Streuli 1999; Hynes 2002; Geiger and Yamada 2011).

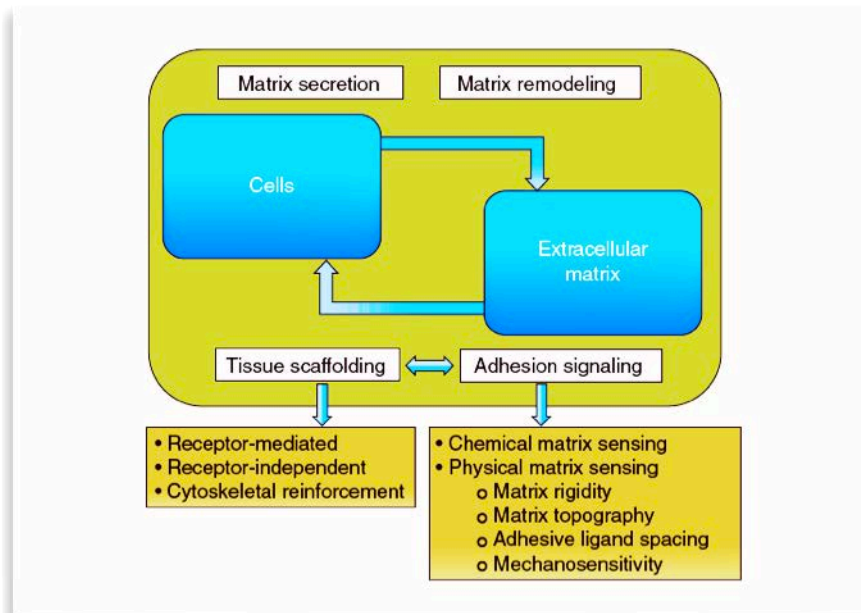


Figure 3.3 - Dynamic cross-talk between cells and ECM (Geiger and Yamada, 2011).

4. Protein behavior at interfaces

4.1 Protein adsorption and biocompatibility

When cells get in contact with a biomaterial, it is rare that they establish direct contact with its surface. Normally the adsorption of proteins from blood or serum is the process that “translates” the composition of the foreign biomaterial surface into a “biological language” (Wilson et al. 2005). Therefore, protein adsorption plays a fundamental role in biocompatibility. This language will determine cell behavior because cells depend on specific proteins for anchorage and extracellular instructions. For this reason, the adsorbed proteins, if correctly presented, can stimulate constructive cell response, favoring wound repair and tissue integration while if proteins are not in a recognizable state this might indicate a foreign material to be removed or isolated (Vogel and Baneyx 2003; Latour 2005).

Protein adsorption is the first step in many biological processes such as transmembrane signaling or in the blood coagulation cascade. On biomedical implants that are in contact with blood stream protein adsorption can lead to thrombosis whereas on artificial tissue scaffolds protein adsorption is the key factor for a proper cellular interaction and/or neovascularization (Vogel and Baneyx 2003). Inflammation cascades or fouling processes are possibly promoted by the adhesion of particles, bacteria or cells to adsorbed proteins. Nonspecific adsorption on sensors surfaces, protein chips, or assay platforms is a serious problem degrading the analytical performance of the device (Hlady and Buijs 1996). All these happens because protein adsorption to solid surfaces can cause a protein to undergo conformational changes that denature epitopes for cell binding receptors, such as integrins, or expose other domains that may provide signals to inflammatory cells, such as macrophages. So it would be very helpful if one can quantitatively predict the orientational and conformational rearrangements that occur due to adsorption to synthetic surfaces and with it control cellular response (Hu et al. 2001; Nakanishi et al. 2001; Gray 2004; Latour 2005; Rabe et al. 2011). Many factors are known to affect protein adsorption and can be divided in external parameters, protein properties and surface properties (Rabe et al. 2011). In this chapter we will review the factors governing the process of protein adsorption particularly the effect of surface properties to serve as base to understand Col IV behavior onto model biomaterial surfaces.

4.2 Effect of external parameters in protein adsorption

The adsorption behavior of a protein is highly influenced by external parameters. Consequently, the conditions under which the protein adsorption experiments are conducted have a decisive influence on protein adsorption behavior. The temperature, pH, ionic strength, and buffer

composition are therefore external parameters, which should be fixed if one wants to mimic true physiological conditions.

4.2.1 Temperature effect on protein adsorption

The amount of adsorbed proteins normally increases at elevated temperatures since it has an effect on both the equilibrium state and the kinetics of protein adsorption. This means that elevated temperatures accelerate diffusivity of proteins towards the sorbent surface resulting in increased adsorption rates. High temperatures induce entropy gain arising from the release of surface adsorbed water molecules, salt ions, and from structural rearrangements inside the protein which are the major driving force of protein adsorption (Hlady and Buijs 1996; Norde 1996).

4.2.2 Effect Ionic strength on protein adsorption

The term ionic strength is related to the concentration of dissolved ions in the solution containing the protein and is another parameter controlling protein adsorption. The Debye length (e.g. the distance over which significant charge separation can occur) correlating with the damping distance of the electric potential of a fixed charge in an electrolyte is determined by the ionic strength. This means that the higher the ionic strength the shorter are the electrostatic interactions between charged entities. As a consequence the adsorption to like-charged substrates is enhanced whereas the adsorption of charged proteins to oppositely charged substrata is hampered. Therefore the adsorption kinetics can be influenced by such a electrostatic effects. The efficient screening of the electric potential of proteins can reduce lateral interactions that are usually of electrostatic nature. This can result in increase packing density, a suspension of cooperative effects, or protein-protein repulsions since increase tendency for protein aggregation result from high ionic strength conditions (Jones and O'Melia 2000; Lubarsky et al. 2005; Rabe et al. 2011).

4.2.3 Effect of pH on protein adsorption

The electrostatic state of proteins is determined by the pH. A protein is a net neutral molecule when the pH equals the isoelectric point (pI) and the number of negative and positive charges is balance. Proteins are negatively charged at high pH conditions when ($\text{pH} > \text{pI}$) and at low pH conditions ($\text{pH} < \text{pI}$) proteins are positively charged. Higher packing densities on the surface are reached at the isoelectric point since electrostatic protein-protein repulsions are minimized. Electrostatic attractions accelerate the protein migration towards the surface therefore adsorption rates are high when protein and substrate bear opposite charges. Nevertheless, the higher adsorption is generally observed at the isoelectric point (Bremer et al. 2004; Lubarsky et al. 2005).

4.2.4 Effect of buffer composition on protein adsorption

Other external factor affecting protein adsorption is the buffer composition. Buffer type as well as buffer concentration can have significant effects on protein adsorption. This sensitivity to buffer type and buffer concentration means that care must be exercised when selecting the buffer conditions for adsorption studies and when evaluating biomedical implants as well as when comparing adsorption data. The behavior of PBS buffer, the most commonly used buffer at physiological pH, is particularly complex in adsorption studies due to the various types of phosphate ions present and the tendency of these ions to adsorb competitively and/or to form complexes either with the proteins or with the surfaces. The “Hofmeister-series” concept describes the fact that salt ions differ by their ability to precipitate proteins from a solution. Kosmotropes are the ions that promote protein precipitation (e.g. SO_4^{2-} , F^- , Mg^{2+} , and Ca^{2+}) and chaotropes ions the ones that decelerate protein precipitation (e.g. ClO_4^- , SCN^- , and NH_4^+). The native conformation of proteins, which influences their adsorption tendency, is correlated with the ability to stabilize (kosmotropic effect) or destabilize (chaotropic effect) protein conformation (Evers et al. 2009; Rabe et al. 2011).

4.2.5 “Vroman” effect

Another important consideration has to be done if the solution in contact with a surface is a mixture of proteins. The protein in highest concentration and with higher diffusivity has the best chance of adsorbing to a surface. This protein will dominate the surface if this protein binds to the surface at a rate that depletes all available surface sites before any other protein approaches. If a protein binds to the surface loosely, it can be easily replaced by other protein that may be present in much lower concentration but may bind to the surface with much higher surface affinity predominantly (e.g. higher molecular weight). This effect is called “Vroman” (Lu et al. 1994; Noh and Vogler 2007) and may play important role when one seek to follow the behavior of a single protein at biomaterials interface.

4.3 Measurement of protein adsorption

To understand protein adsorption to solid surfaces two types of measurements are used (a) the adsorption isotherm and (b) the adsorption kinetics. Although it is considered that protein adsorption is much more complex and is not reversible (as for gases) the Langmuir isotherms have been used to characterize the protein adsorption process. This is complex to approximate because during initial protein-surface contact the adsorption process is partially reversible but once the surface gets saturated with protein almost none of the adsorbed proteins can be removed by the solvent alone. Adsorption kinetics probably is the best way to characterize protein

adsorption since you plot surface concentration of protein with time. Figure 4.1 shows an example of the both types of measurements from a high vs low protein concentration solution adsorbing on hydrophilic vs hydrophobic surfaces (Magnani et al. 2002; Tie et al. 2003; Latour 2005).

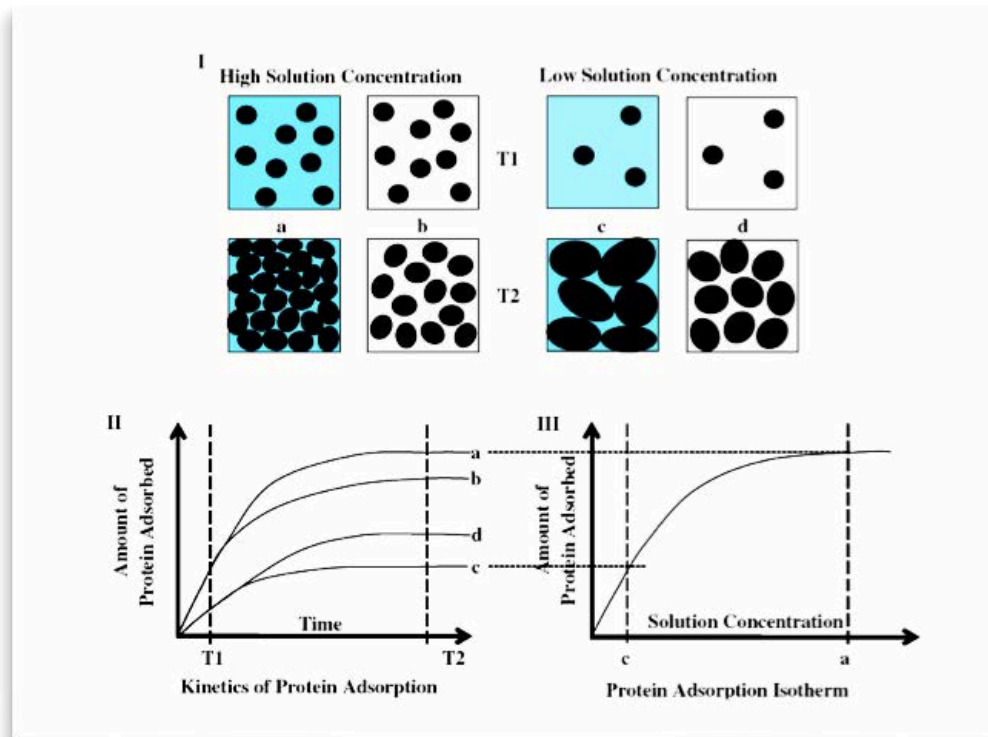


Figure 4.1- Illustration of the final state of a protein layer adsorbed from a single protein solution. (I) Comparison between adsorbed protein layers in high vs. low protein concentration solution on to hydrophobic (a, c) and hydrophilic (b, d) surfaces at different time points (T1 and T2). (II) Plot of the amount of adsorbed protein vs. time for conditions (a)-(d). (III) It results in irreversible adsorption isotherm with reversible Langmuir isotherm-like appearance. Each point on the isotherm plot represents a fully saturated irreversibly adsorbed protein layer (Latour 2005).

Study the adsorption of protein to surfaces requires high accuracy since in some cases the amount of protein per unit of area is really low. Several techniques have been used to measure adsorbed proteins on solid surfaces and are described in Table 1 including their description, principle and information obtained.

Table 1 -Summary of techniques used to study protein adsorption behavior. Adapted from (Nakanishi et al. 2001).

Technique	Principle	Information obtained
Depletion	Decrease in solute concentration after incubation with solid surface.	Amount of adsorbed molecules.
Radiotracer	Decrease in concentration of radioisotope-labelled molecules in solution. Radioactivity in the surface due to radioisotope-labelled molecules adsorbed.	Amount of adsorbed molecules from single- and multi-competent solutions. Amount of irreversibly adsorbed molecules
Quartz crystal microbalance (QCM)	Change in the oscillating frequency of piezoelectric devices upon mass loading	Courses of adsorption and desorption
Enzyme-linked immunosorbent assay (ELISA)	Epitope recognition by primary antibodies	Amount of irreversibly adsorbed molecules
Ellipsometry	Change in the state of polarized light upon reflection	Amount and thickness of adsorbed protein and their changes
Total internal reflection fluorescence (TIRF)	Fluorescence due to surface-adsorbed molecules excited by evanescent field	Amount of fluorophores adsorbed on the surface
Neutron reflection	Reflectivity of neutrons at solid-water interface	Amount and layer thickness of protein adsorbed on the surface
Fourier transform infrared spectroscopy (FTIR)	Change in infrared spectrum of protein on adsorption	Conformation of the protein adsorbed on the surface
Fluorescence spectroscopy	Change in fluorescence spectrum of protein on adsorption	Conformation of protein molecules on the surface
Atomic force microscopy (AFM)	Atomic interaction between surface and scanning probe	Three dimensional image of the surface

5. Engineering of Cell - Biomaterial Interface

5.1 Control of protein adsorption

5.1.1 Effect of intrinsic properties of the proteins on adsorption

The problem of predicting the adsorption behavior of a protein came from the complexity and diversity of their structure. They differ between each other from the basic structure of amino acid sequence to the posterior arrangements. For that reason to classify proteins in respect to their interfacial behavior we have to consider properties like size, structural stability and composition (Andrade et al. 1992). “Hard” proteins are the ones that have little tendency for structural alterations upon adsorption and usually comprise the small and rigid proteins (e.g. α -chymotrypsin, ribonuclease, lysozyme and β -lactoglobulin (β -Lg)) (Norde 1996; Norde 2008). The majority of the abundant plasma proteins (albumin, transferrin, immunoglobulins, etc) are considered intermediate size proteins and are susceptible to undergo conformational reorganization upon adsorption and are denominated as “soft” proteins (Andrade et al. 1992). One way to simplify protein complex structure is to divide their structure into domains exhibiting specific properties like hydrophilic/hydrophobic, polar/non-polar or charged/uncharged. Hard proteins only adsorb to polar surfaces and if are electrostatically attracted more commonly they do not adsorb (Figure 5.1).

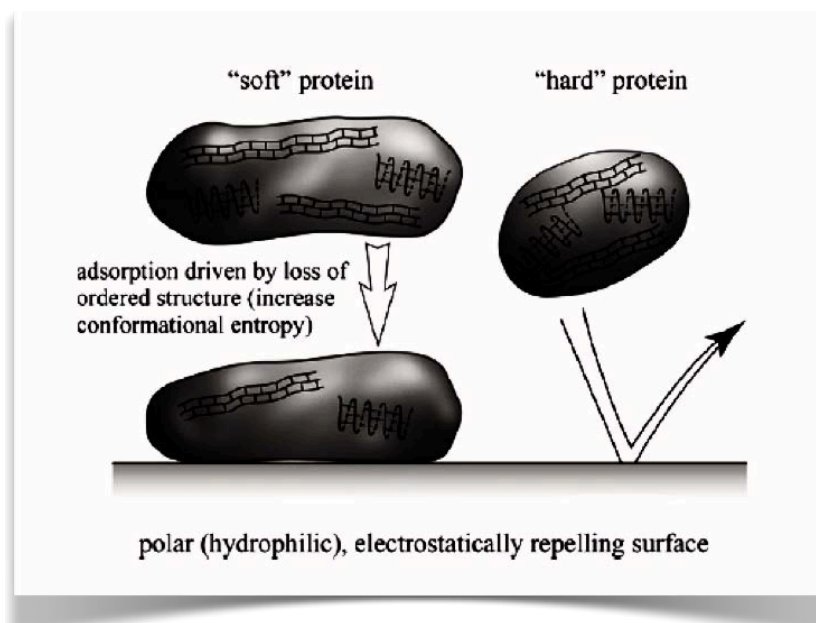


Figure 5.1 – Soft versus hard protein adsorption on hydrophilic surfaces. The loss of ordered (secondary) structure might drive “soft” proteins to adsorb onto hydrophilic and electrostatically repelling surfaces. “Hard” proteins if are electrostatically attracted to polar surfaces do not adsorb (Norde 2008).

Soft proteins are susceptible for structural changes, which can result in the secondary structure reordering with entropy gain that leads them to adsorb at a polar, electrostatically hostile surfaces (Figure 5.1) (Andrade and Hlady 1986).

5.1.2 Effect of surface properties on protein adsorption

Important parameters that have to be considered for the effect of surface properties in protein adsorption include surface energy, polarity, charge, and morphology. Important also is to consider that protein-surface interactions are affected by the protein's properties on one side and by the surface properties on the other side (Hlady and Buijs 1996). The experimental work normally determines the material choice. The more commonly used materials include quartz, mica, glass, metals, or graphite since they are easily modified to obtain suitable model surfaces. One of the more frequently used methods to functionalize surfaces is the silanization of hydroxyl group bearing substrates through chlorosilanes or ethoxysilanes. In this way any of the above materials can easily be modified with a monolayer of desired functionality without changing optical properties of the material like transparency. This method is called self-assembled monolayers (SAMs) and can be used also to modify conducting substrates by exposing alkanethiols to noble metal substrates, normally gold. This technique and the use of these model materials will be further discussed in this chapter. Other materials used to study protein adsorption include polymer coated surfaces, films or membrane filter material, and Langmuir-Blodgett films. All of them enable the easy tune of parameters such as surface energy, charge, and polarity by choosing the appropriate functionality (Anand et al. 2010; Rabe et al. 2011). By using these model surfaces combined with AFM one is able to determine the adhesion energy of proteins varying in tension, polarity, charge and wettability. It's assumed from previous data that proteins tend to adhere more strongly to non-polar than polar, to high surface tension than to low surface tension and to charged then to uncharged. Belfort et al. described that non-polar surfaces destabilize proteins and thereby facilitate conformational reorientations leading to strong inter-protein and protein-surface interactions (Anand et al. 2010). This explains the fact that affinity of proteins to surfaces increases on hydrophobic substrates and decreases on hydrophilic (Andrade and Hlady 1986).

The involvement in directing reactions to surface topography is less clear than differences in surface chemistry and wettability. There is some evidence that proteins adsorb differentially with variations in surface roughness, although relatively scarce. The dominance of surface area effects on rough surfaces cannot be ruled out, so many of these studies do not categorically explain the mechanism and biological effects of roughness differences, particularly in relation to the adsorption characteristics (Wilson et al. 2005). Topographic features may create confined spaces apart from increasing the surface area. It has been speculated that these may interfere with wetting of hydrophobic surfaces, which lead to a localized dilution of the coating solution, or restrict

protein exchange between the surface and solution (Wilson et al. 2005). It has been suggested that topographic effects on protein adsorption relate to an increase in surface energy, but this has not been well substantiated (Von Recum and Van Kooten 1996).

5.1.3 Protein adsorption orientation

When in solution proteins rotate freely but when get closer to a surface they acquire an orientation that will determine the part that is in contact with the surface and the part that is exposed to the bulk solution (Xu et al. 2006). Depending on the amino acid residues composition and in the complex structure of the protein they exhibit different affinities in different regions. These regions can be divided in hydrophilic, hydrophobic, positively or negatively charged. In hydrophilic and hydrophobic surfaces proteins normally expose to the surface the same hydrophilic or hydrophobic patches while when proteins adsorbing positively or negatively charge surfaces they expose oppositely charged regions (Latour 2005; Rabe et al. 2011). If a protein is structurally stable and is attached to a surface through its long axis one can characterize his orientation as “side on” while if protein is attached through its short axis his orientation will be “end-on”. Normally the proteins adsorb in the orientation that favors more the surface-protein interaction resultant from electrostatic attraction. At lower concentrations this repulsion does not have significant effect because distance between proteins is large but since this distance became smaller the initial adsorption orientation becomes less favorable compared to other orientation that minimizes the repulsive forces. As result the proteins change orientation by rotation associated with a loss of binding energy which for one way stabilizes the adsorbed proteins but on the other can increase the desorption rate (Lhoest et al. 1998; Karlsson and Carlsson 2005).

5.1.4 Conformational changes

Since the free energy of a protein when is in contact with a surface does not correspond to the free energy of this protein in solution it is widely accepted that it undergoes conformational changes upon adsorption. The native state of the proteins in solution is not obligatory to be the preferred orientation on a surface since the interaction of protein-to-surface starts to prevail. In this sense it is expected that conformational and/or orientational changes after adsorption affect proteins biological function. Other possible option is that after adsorption the protein suffers from alterations that block their refold into the native structure after desorption. In the other hand the adsorption of proteins to a surface can stabilize their structure and improve their resistance to denaturation when compared to dissolved proteins (Hlady and Buijs 1996; Gray 2004; Rabe et al. 2011).

5.1.5 Protein assembly at solid surface

Once in contact with a surface the protein solution will favor the surface coverage. The formed protein layer can be densely or loosely packed in a monolayer or multilayers (Rabe et al. 2011). Monolayer formation is associated with weak protein-protein interactions or with repulsive forces. This means that monolayers formation is associated with the strength of the electrostatic repulsions between adsorbed-proteins. When $\text{pH} \neq \text{pI}$ and at low ionic strength conditions the protein bears a relatively high net charge consequently proteins assemble into loose layers while when $\text{pH} = \text{pI}$ or in high ionic strength conditions proteins are net neutral and assemble in more densely packed layer (Malmsten 1998; Lubarsky et al. 2005). One factor influencing the protein surface density is the bulk solution concentration since at low concentration the coverage is slow and the conformational changes in protein can take place while at high bulk concentration the surface is rapidly covered and structural changes in proteins are hindered due to the lack of available empty surface (Rabe et al. 2011). If there is no significant protein-protein interaction the proteins will adsorb to empty places but if a protein oriented towards the surface hit another protein it will be rejected to the bulk solution. Normally this results in a surface coverage full of gaps between proteins where no new protein can be accommodated (Andrade 1985; Norde and Anusiem 1992; Latour 2005).

5.1.6 Lateral interactions between adsorbed proteins

The lateral interactions comprise the interaction between proteins, not only with the surface as described above. If buffer solution does not fit the isoelectric point of a protein other proteins from the same species will bear a net charge that will result in high inter protein repulsions. This is the reason for higher packing density of protein when buffer has $\text{pH} = \text{pI}$ (compared to when pH is higher or lower than pI). In this case the monolayer is more likely to be a loose layer. Conversely, if the repulsion forces between charged proteins are shielded by the screening effect of dissolved ions, an increase of the protein packing density may be observed (Rabe et al. 2011). Nevertheless, important is to notice that these effects only enter in scene after a considerable coverage of the surface and when decrease in the distance between adsorbed proteins takes place (Höök et al. 1998; Bremer et al. 2004; Rabe et al. 2011). Of course, lateral interactions may appear in other more specific reasons, coming from the natural structure of the protein, for example like in the network-forming protein such as type IV collagen (Yurchenco and Furthmayr 1984), laminin (Colognato and Yurchenco 2000), or FN (Lhoest et al. 1998), that are separately described.

5.2 Self-assembled monolayers as model biomaterial surfaces

In order to understand the complex process of protein adsorption and the consequent cellular response it is important to use model materials. In that sense SAMs of silanes build on some hydroxyl group bearing substrates, or alkanethiolates on gold surfaces permit the control over the properties of the interface at the molecular scale (Mrksich and Whitesides 1996; Mrksich 2009).

5.2.1 Self-assembled monolayers

When molecules in solution or in vapor phase adsorb they spontaneously organize into a single layer forming a self-assembled monolayer. This may happen only after the contact of functional organic molecules onto a suitable solid substrate. The molecules that assemble are normally composed of three parts (Figure 5.2): the head group (that is responsible for anchoring the molecules onto the substrate); the alkyl chain (that provides stability and ordering of the monolayer due to van der Waals interactions); and the terminal end group (that add the chemical functionality into the monolayer important for the overall properties of the surface) (Ulman 1996; Raynor et al. 2009).

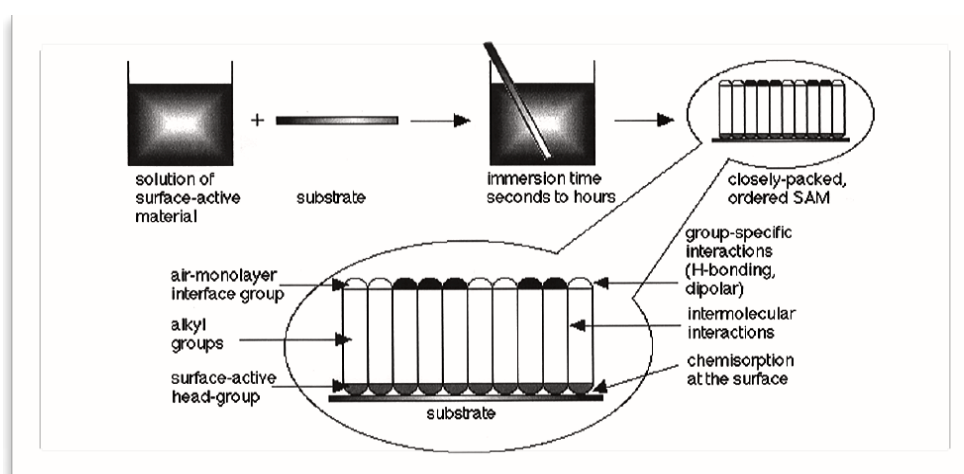


Figure 5.2 – General self assembled monolayers structure and formation. Formation of self assembled monolayers by immersion of a surface-active material into a solution (Ulman 1996).

5.2.2 Silane based self-assembled monolayers

The more commonly used silanes for preparing SAMs are those based on alkylchlorosilanes, alkylalkoxysilanes, and alkylaminosilanes and all require hydroxylated surfaces as substrates for their formation. The hydrolytic bond formation of the siloxane with -OH surface groups forms a cross-link that stabilizes the molecules in the surface (Mrksich and Whitesides 1996; Raynor et al. 2009; Haensch et al. 2010). Thus, different chemical functionalities can be presented by the monolayer. The different chemistries can be obtained essentially by two methods. First is to use

pre-functionalized molecules (e.g. octadecyltrichlorosilane (CH_3) which can be synthesized by different synthetic routes and subsequent self-assembly of these moieties on the surface. The other approach is to chemically modify the monolayer by using a chemical surface reaction. This method enables the introduction of a wide range of terminal end groups on well-defined base monolayers by the application of a large variety of organic reactions (Ulman 1996; Haensch et al. 2010). Silicon oxide, aluminum oxide, quartz, glass, mica, zinc selenide, germanium oxide and gold are materials that have been successfully modified using these monolayers. These surfaces provide the possibility to tailor surface properties like wettability, chemistry, charge, and conductivity in a controlled way since with the modification of the terminal end groups of the monolayer the effective tune of these properties were obtained. The adsorption of these monolayers is irreversible but is a process highly sensitive to water since the presence of water might induce the formation of multilayers. Once formed this monolayers are thermally stable but easily disrupted by UV radiation (Mrksich and Whitesides 1996; Ulman 1996; Raynor et al. 2009; Haensch et al. 2010). One example of silane SAM is presented in figure 5.3B.

5.2.3 Self-assembled monolayers of alkanethiolates on gold

The formation of this SAMs is based on the adsorption of a long-chain alkanethiol [i.e., $\text{HS-CH}_2\text{n-X}$, where $n \geq 10$] from solution (or vapor) to a gold surface. The gold atoms of the surface coordinate with the sulfur atoms of the adsorbate. As for silane SAMs the physicochemical properties of the monolayer are determined by the chemical composition of the terminal group of the adsorbate. The so-called mixed SAMs (Mrksich and Whitesides 1996), can be formed, by exposing the gold surface to a mixture of two alkanethiolates. Once prepared this SAMs are stable for large periods of time (months) in air, or in contact with water, but they are disrupted by temperatures above 70°C or by UV irradiation. An example of thiol SAM structure is presented on figure 5.3A (Whitesides and Gorman 1995; Mrksich and Whitesides 1996; Mrksich 2009; Shekaran and Garcia 2011).

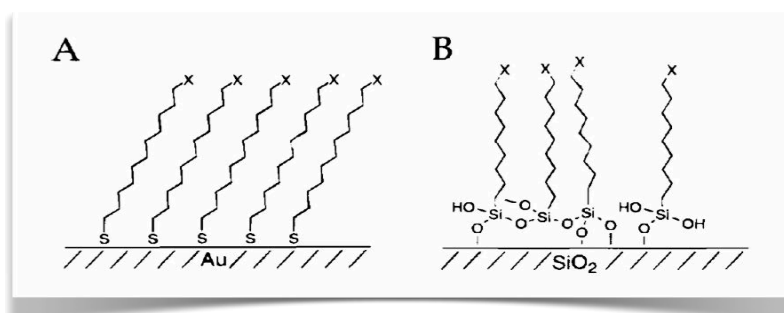


Figure 5.3 -Models for SAMs of alkanethiolates on gold and alkylsiloxanes on hydroxylated surfaces. (A) The thiol groups coordinate to the hollow threefold sites of the gold (1 1 1) surface, and the alkyl chains pack in a quasi-crystalline array. (B) The conformations of alkylsilanes and the details of their bonding to surface hydroxyl groups are less clear; a mixture of possible conformations and geometries is probably involved. The surface properties of both SAMs are controlled by the terminal function of group X.

5.2.4 Bio-specific motifs presented by self-assembled monolayers

The first approach to use SAMs to expose bio-specific motifs appeared with the inert surfaces. The big majority of the work done is on the use of poly(ethylene glycol) that was reported to exclude protein adsorption due to a mechanism dependent on the conformational properties of highly solvated polymer layers. Further work showed selective interaction of proteins with SAMs prepared from oligo(ethylene glycol)-terminated alkanethiols where approximately 1% of the chains presented a covalently attached ligand (Prime and Whitesides 1993; Mrksich 2009). The role of peptide ligands in cell adhesion and migration was also studied using specific protein motifs RGD against a background of tri(ethylene glycol) groups. It was found that fibroblasts cultured in this SAMs were able to attach and spread, develop focal adhesion complexes through clustering of integrins, and organize actin stress filaments. The simple addition of soluble RGD was able to block the adhesion. This work proved the potentiality of monolayers to control ligand-receptor interactions using cells. This monolayers can be used to study the influence of both ligand density and affinity on cell attachment because they are sufficiently structurally ordered (Houseman and Mrksich 2001).

5.3 Control of material surface properties

5.3.1 Most important methods for surfaces characterization

Several experimental techniques are employed to probe the quality and chemical nature of biomaterial surfaces, from local techniques that examine the structure of the SAMs or polymer coatings down to atomic resolution. In this section we will describe mainly the ones used in the experimental part of this thesis.

5.3.2 Contact angle goniometry

Contact angle is generally used to measure the ability of a liquid to spread on a surface. The method is based on measuring the angle between the outline tangent of a drop deposit on a solid and the surface of this solid (Andrade et al. 1979). It is linked to the surface energy and so one can calculate the surface tension and discriminate between polar and apolar interactions (Owens and Wendt 1969). Employing this technique one can obtain three different parameters: (i) the affinity of a liquid to a solid surface (e.g. using water a small angle indicates hydrophilic and a big angle hydrophobic character of the surface); (ii) using different referent liquids one can calculate the surface energy of the surface, discriminating between polar and dispersive components; finally (iii) one can obtain information about the homogeneity of the surface (rugosity, contamination, etc.) by measuring the hysteresis – e.g. the difference between advancing and receding angles (Gao and McCarthy 2006).

5.3.3 X-ray photoelectron spectroscopy

To probe the chemical nature of the surfaces most often is used X-ray photoelectron spectroscopy (XPS). This technique uses incident X-rays to bombard the sample with electrons that are ejected from the core shells of the atoms. The electrons are collected and dispersed in an analyzer, and the binding energies can be calculated by measuring the kinetic energies of the electrons entering the analyzer. Kinetic energies are specific for each element and give also indication on the oxidation states of the elements. This technique also enables measuring the thickness, for example of SAM by comparing ratios of substrate signal before and after SAM formation (Biebuyck et al. 1994; Smith et al. 2004).

5.3.4 Fourier-transform infrared spectroscopy

Other method to analyze the chemical composition and the vibrational frequencies of molecules attached to surfaces (or of bonds within molecules) is the Fourier-transform infrared spectroscopy (FTIR). This technique only detects molecules whose vibrations are perpendicular to the surface. It has been used to characterize the general order of n-alkyl tails of SAMs on gold (Smith et al. 2004), as well as for the determination of the concentration and distribution of lipids and proteins across the vascular wall of internal mammary artery and saphenous vein and the presence of chemical species, such as lipid esters, that could favor atherogenesis (Reno et al. 2003).

5.3.5 Atomic force microscopy

Atomic force microscopy is an instrument with multiple potentialities to characterize surfaces including SAMs. Many permutations were performed in order to obtain much more than merely topographic information (Smith et al. 2004). AFM uses a micrometer-scale cantilever, with a nanometric sharp tip, to apply well-defined forces on a sample (Kasas et al. 1997). The cantilever will deflect to a certain degree depending on the attractive and repulsive forces between the tip and the chemical environment of the sample (Meyer 1992; Radmacher et al. 1992). A laser is pointed at the tip of the cantilever and is reflected to a sensor. In tapping mode, as the tip goes up and down, the laser hits different parts of the sensor. With the information the sensor collects, an image of the surface can be recreated (Figure 5.4). In force mode, by approaching the cantilever towards the sample and monitoring the exerted force, allows acquisition of a curve relating the exerted force to the indentation created (Cappella and Dietler 1999). The forces due to magnetism, friction, surface charge or potential, or capacitance can be also measured by AFM (Kasas et al. 1997). For that many scanning probes that are specific to molecular-scale properties have been developed. One example of mode of operation chosen to characterize SAMs at the nanoscale is the lateral force microscopy that uses tribological differences to distinguish different chemical functionalities on patterned surfaces (Smith et al. 2004). In the present thesis AFM was

used in tapping mode in air to characterize the SAMs and the consequent adsorption of Col IV to the different materials.

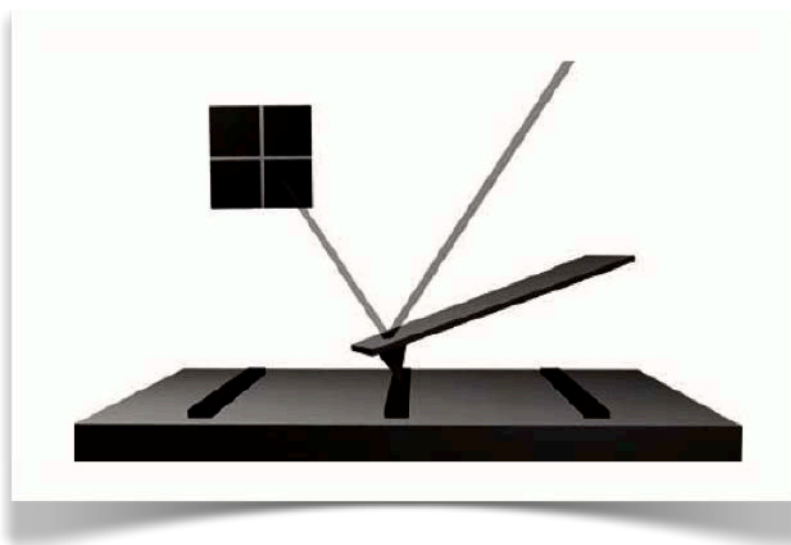


Figure 5.4 - AFM's operation mode. Differences in substratum features are detected by rastering along the surface a sharp tip that resides at the end of a cantilever. The deflection of the AFM tip as function of surface properties is recorded by pointing a laser beam on the top of the cantilever's back and detect the reflection using a position-sensitive photodiode.

5.4 Control of cell behavior-Applying SAMs to study cell-materials interaction

5.4.1 Influence of terminal end groups on cellular responses

Due to the fact that surface functional groups affect protein adsorption and consequent protein-cell interaction substantial research efforts have been placed on studying the influence of SAMs on the cellular response to biomaterials (Wilson et al. 2005; Thevenot et al. 2008). Here we describe some data about the application of different SAMs used in the experimental part of our work, namely: hydrophilic (OH); negatively charged (COOH); positively charged (NH₂); and hydrophobic (CH₃) surfaces.

5.4.2 Hydrophilic (-OH) surface

It was suggested that -OH functionality has low protein affinity, and thus protein repelling properties because of its charge neutrality and hydrophilic nature. Indeed, -OH functionality showed reduced plasma protein adsorption and thus higher blood compatibility (Tidwell et al. 1997). However, high levels of FAK and $\alpha_5\beta_1$ integrin expression leading to increased cell adhesion strength were found when -OH surfaces were coated with fibronectin in comparison to surfaces presenting -CH₃ functional groups (Keselowsky et al. 2003). Higher levels of osteoblasts differentiation and mineralization were also found on -OH surfaces when were compared with other functional groups (Wilson et al. 2005; Thevenot et al. 2008). *In vivo* studies however

showed high levels of inflammatory cells infiltration and development of thickened fibrotic capsule (Kamath et al. 2008).

5.4.3 Negatively charged (-COOH) surface

The -COOH functionality is usually used when one need to exposes a negative charge on the surface. Using this approach it was for example shown that FN and albumin adsorption is lowered when compared with various other model coatings (Tidwell et al. 1997). These functionalities were also associated with enhanced cell grow but a more recent study showed that it depends on the concentration of -COOH groups on the surface; since the concentration of -COOH increases the number of negative charges increases and inhibit cell growth (Ohya et al. 2004). High expression of $\alpha_5\beta_1$ and $\alpha_v\beta_3$ integrins associated with structural and signaling components related to focal adhesions formation were shown when -COOH surfaces were pre-treated with FN (Keselowsky et al. 2004). However, the inhibition of osteoblats differentiation and mineralization was also shown related to $\alpha_v\beta_3$ exposure (Lan et al. 2005). Also, although cell proliferation levels were high, a low level of myoblast differentiation was found on -COOH surfaces again with increased expression of $\alpha_v\beta_3$ integrin (Lan et al. 2005). In vivo studies using -COOH functionalities showed that it attenuates inflammatory responses and reduces fibrotic capsule formation (Kamath et al. 2008).

5.4.5 Positively charged (-NH₂) surface

A positive charge on the biomaterial surface is usually modeled by the inclusion of amine functionality. Using this approach for example a favorable FN and osteopontin conformations after adsorption to positively charge -NH₂ surface were found (Keselowsky et al. 2004). Particularly high density of focal adhesion components was found on FN pre-treated -NH₂ surfaces. Enhanced differentiation and mineralization of osteoblasts and increased endothelial cell growth were also demonstrated (Keselowsky et al. 2004). Fibroblasts on -NH₂ surface showed preferable adhesion, growth, and matrix formation when compared to other surface coatings (Faucheux et al. 2004; Keselowsky et al. 2005). Interestingly, an increased cell spreading on -NH₂ surface with formation of focal adhesion plaques was shown just after 45 minutes of cell culture (Keselowsky et al. 2005). Other study showed low levels of myoblast differentiation combined with the higher level of proliferation on this functionality (Lan et al. 2005). In vivo studies using -NH₂ chemistry indicated that this surface triggers acute inflammatory responses, thick fibrotic capsule formation, and cell infiltration (Kamath et al. 2008).

5.4.6 Hydrophobic (-CH₃) surface

The -CH₃ functionality providing a hydrophobic surface is one of the most commonly used model surface (Keselowsky et al. 2004). It is widely accepted that hydrophobic -CH₃ functionality

promotes protein adsorption but mainly in conformations that are not desirable for cellular interaction (Keselowsky et al. 2004). This was showed by increased FN binding, platelet accumulation and thus poor blood compatibility (Lindblad et al. 1997). The $-\text{CH}_3$ bearing surfaces showed also the highest strength of interaction with fibrinogen (FBG), albumin, and IgG in a study for measuring adhesion strength (Kidoaki and Matsuda 1999). These observations suggest that $-\text{CH}_3$ surfaces do not favor surface interactions with cells because of the magnitude of interaction of bound proteins. It was suggested that these proteins probably will expose sites attracting inflammatory cells (Thevenot et al. 2008). Indeed, high recruitment of inflammatory cells and thick fibrotic capsule formation was shown *in vivo* (Barbosa et al. 2006).

5.4.7 Surfaces with mixed functionalities

With aim to combine the “good properties” of two different functionalities a lot of work have been done in the recent decade. It utilizing mainly mixed SAMs chemistries leading to interesting conclusions. For example, one study using the combination of $-\text{NH}_2$ (positive charge) and $-\text{COOH}$ (negative charge) chemistries in different proportions showed that surface presenting a near neutral charge possesses lowest platelet adhesion (Chuang and Lin 2007). The blood compatibility of biomaterials was therefore related to the possible importance of surface neutrality (Chuang and Lin 2007). Other study with mixing $-\text{OH}$ and $-\text{CH}_3$ functionalities showed decreased fibrinogen adsorption as well as decrease in platelet adhesion and activation with increasing hydrophilicity, attributed to the $-\text{OH}$ chemistry. The decrease in blood platelet adhesion was also reported (Rodrigues et al. 2006). A more recent study using mixed surface functionalities demonstrate higher adhesion of HUVEC to a mixed CH_3/OH SAMs at water contact angle around 40° . Employing other combinations of mixed SAMs such as CH_3/COOH and CH_3/NH_2 , again increased adhesion of HUVEC with increasing the wettability was found (Arima and Iwata 2007). Interestingly, using other cell line of epithelial origin (HeLa) showed again similar maximum of adhesion on CH_3/COOH SAMs with around 50° . Using other mixed SAMs was confirmed a general trend that cell adhesion increased with the increase of surface wettability (Arima and Iwata 2007). The use of mixed SAMs *in vivo* is till now sparsely reported but would be of great value in the biocompatibility studies (Thevenot et al. 2008).

5.4.8 Cellular interaction with surfaces varying in wettability

It is well documented that physicochemical properties of biomaterials surfaces have a great impact on protein adsorption and subsequent adhesion and proliferation of cells (Altankov and Groth 1994; Sipe 2002; Keselowsky et al. 2003). Presumably the most important surface parameter is the wettability characterized by water contact angle (WCA $^\circ$) measurements (Altankov and Groth 1994; Sipe 2002; Wilson et al. 2005; Arima and Iwata 2007) although other

physical parameters might also be critical. Based on Vogler's definition hydrophobic surfaces are those exhibiting water contact angles above 65° (Vogler 1998). The difference in the array of proteins adsorbed to hydrophilic and hydrophobic materials from serum, plasma, or whole blood is one mechanism of enhanced cell response on hydrophilic surfaces (Elwing Hans et al. 1995). The competition for adsorption sites is clearly apparent on hydrophilic surfaces, shown particularly for vitronectin (Fabrizius-Homan and Cooper 1992). In contrast, a marked reduction in cell adhesion is found when fibronectin is adsorbed to hydrophobic surfaces (Grinnell and Feld 1982). The ability of FN to retain its functionality on hydrophilic surfaces is therefore considered as a reason for improved cell responses in these classical studies.

5.4.9 Cellular interaction with surfaces varying in charge

Since virtually all interfaces are charged in aqueous solution, and the fact that cell membranes carry a negative charge, it is close to the mind that electrostatic interactions will play a role in the biological response to implant materials (Lubarsky et al. 2005; Thevenot et al. 2008). However, although interactions between negatively charged cell membranes and charged substrata are significant, many authors point out that these alone are not sufficient to explain the observed differences in adhesion and migration of cells on both positively and negatively charged surfaces. The mode of cell adhesion is distinct for positive and negative charges: cell membranes contact only at distinct points on near-neutral and negatively charged surfaces, while they adhere much closely to positively charged ones (Thevenot et al. 2008).

5.4.10 Cellular interaction with surfaces varying in topography

This topic is out of the scope of our study but we will briefly describe, as it is one of the major concerns in tissue engineering, particularly for the optimization of scaffolds architecture for cell colonization. The role of different protein adsorption for mediating cell responses to the topography is extensively studied (Bowers et al. 1992; Mustafa et al. 2000). Several studies revealed few consistent trends on the effects of surface topography on initial cell adhesion (Wilson et al. 2005), however, differences and inadequacies in characterizing the morphology, as well as magnitude of surface topography, gave rise to complicated interpretation of results. Furthermore, altered surface chemistry and/or physicochemical properties could be the result of used methods to produce surface textures—for example, sandblasting, grinding, and plasma-spraying of titanium (Bowers et al. 1992; Thevenot et al. 2008). The type of cells used also influences the results. The most commonly observed trends are that the differentiation and/or extracellular matrix synthesis increases, with a corresponding reduction in cell proliferation as the roughness and disordering of the surfaces increase (Kieswetter et al. 1996). However, once again, these trends are not absolutely consistent (Kieswetter et al. 1996). Regardless of the mechanism, it seems inevitable that the size, shape, and distribution of surface topographic features will

constrain the mode of cell adhesion and the resultant cell morphology (Thevenot et al. 2008) simply because they mimic to a certain extent the natural cues of the ECM (Altankov et al. 2010).

5.5 Substratum effects on focal adhesion formation and integrin signaling

As described previously one way to access the biocompatibility of a biomaterial is by analyzing the macroscopic cellular responses to material properties (Yamada et al. 2003). Several studies showed that the focal adhesion formation is strongly affected by the surface properties of a biomaterial since completely altered formation of focal adhesion contacts was found on low biocompatible materials (Altankov et al. 2010). In contact with low compatible materials the cells normally present a more rounded morphology suggesting delay cell spreading. At the same time cells are not able to develop focal contacts and present in some cases irregular protrusions (Altankov et al. 1996). Previous work from our group showed altered focal adhesion formation on fibroblasts adhering on hydrophobic octadecylsilane (ODS) surface and normal focal adhesion formation shown by clustering of α_v integrins and high phosphotyrosine expression on hydrophilic glass (Altankov et al. 1996). In the same study co-localization experiments of α_v integrins with phosphotyrosine showed that the cells not only attach better on hydrophilic surfaces but also transmit the proper signals to the cell interior. This results show the importance of studying the initial cell interaction by the formation of focal adhesion complexes since on low biocompatible materials cells do not receive the proper signals and consequently will not interact with the material interface (Altankov et al. 1996).

Other experiments focused on the effect of the surface properties in integrin dynamics showed no big differences in ventral focal adhesion formation but a clear difference on integrin behavior on the dorsal cell surface (Altankov and Groth 1997). A well-pronounced linear arrangement of antibody tagged $\beta 1$ clusters were observed on hydrophilic glass while almost no integrin cluster was found on hydrophobic substrata (Altankov and Groth 1997).

5.6 Control of matrix remodeling

5.6.1 Remodeling of ECM proteins at cell-biomaterial interface

The ECM remodeling is a dynamic process, which consists of two opposite events: assembly and degradation. These processes are mostly active during development and regeneration of tissues, but when miss-regulated, can contribute to diseases such as atherosclerosis, fibrosis, ischemic injury and cancer (Holmbeck et al. 1999; Curino et al. 2005; Heymans et al. 2006; Reisenauer et al. 2007). Previous data from our group showed that cells tend to rearrange adsorbed matrix proteins such as FN, FBG and collagen, at material interface in a fibril like pattern (Altankov and Groth 1996; Altankov and Groth 1997; Tzoneva et al. 2002). Using SAMs as model surfaces it

has been shown that this cellular activity is abundantly dependent on the surface properties of materials, such as wettability, surface chemistry and charge (Altankov et al. 2010). These results point to the possibility that tissue compatibility of a biomaterial may be connected with the allowance of cells to remodel surface associated proteins presumably as an attempt to form their own matrix (Grinnell 1986; Altankov and Groth 1994; Altankov and Groth 1997; Pankov et al. 2000). The remodeling is particularly pronounced for stromal cells like fibroblasts since one of their main functions is to produce ECM proteins. However other cell lines like endothelial cells (Tzoneva et al. 2002), keratinocytes (Altankov et al. 2001), osteoblasts (Gustavsson et al. 2008), and cancer cells (Maneva-Radicheva et al. 2008) also show the ability to organize provisional ECM *in vitro* (Tzoneva et al. 2002; Maneva-Radicheva et al. 2008; Altankov et al. 2010). One can divide the matrix formation activity when studied *in vitro* in two types: early and late matrix formation.

5.6.2 Development of early matrix

As stated above, it was shown that within few hours either fibroblast either endothelial cells both seeded on FN were able to rearrange this protein in a fibril like pattern (Altankov and Groth 1994; Tzoneva et al. 2002). This cellular activity was also shown to be highly dependent on surface properties of materials, such as wettability (Altankov and Groth 1994; Tzoneva et al. 2002), surface chemistry and charge (Gustavsson et al. 2008). Only on highly hydrophilic surfaces WCA = 10° the fibroblasts were able to reorganize FN in a fibril like pattern (Altankov and Groth 1994). This activity was not specific only for FN since other work identified similar differences for adsorbed fibrinogen in contact with endothelial cells (Tzoneva et al. 2002).

5.6.3 Development of late matrix

Once fibroblasts are cultured *in vitro* they synthesize and tend to arrange secreted FN in a specific fibrillar pattern on the materials interface (Lutolf and Hubbell 2005). Important is to notice that the formation of this late FN matrix is altered on low biocompatible hydrophobic materials (Altankov and Groth 1996). Based on previous investigations using different cell models including endothelial cells (Tzoneva et al. 2002), osteoblasts (Gustavsson et al. 2008), keratinocytes (Altankov et al. 2001), and even carcinoma cells (Maneva-Radicheva et al. 2008), one can support the existence of a common cellular mechanism for the provisional ECM formation on biomaterials interface (Altankov et al. 2010). Moreover, as stated above the cells show ability to arrange different matrix proteins, since even Col IV which is not a fibrillar protein was shown to be arranged in a linear like pattern (Maneva-Radicheva et al. 2008) in a process where FN seems to play a leading role because it co-localizes with arranged Col IV molecules (Maneva-Radicheva et al. 2008). Taken together these results point to the possibility that the

allowance of cells to remodel surface associated proteins and to form provisional extracellular matrix may determine to great extent the tissue compatibility of a biomaterial.

5.4.4 Proteolytic remodeling of surface associated ECM

The remodeling of ECM by cells also involves enzymatic degradation carried out by a variety of proteases (such as cathepsins, matrix metalloproteases, serine proteases etc.) before or after the deposition of new matrix (Daley et al. 2008; Place et al. 2009). The degradation of scaffolds by proteolysis can also lead to the loss of their mechanical strength and structure therefore compromising their fate. However, the cellular degradation of a scaffold can be used to generate a material temporal profile in tune with the generation of new tissue (Lutolf and Hubbell 2005; Larsen et al. 2006; Daley et al. 2008; Place et al. 2009). An example, pioneered by Hubbell's group in Switzerland, consists of 3D materials (gels) that are cross-linked by enzyme-degradable peptide sequences, and a combination of cell-mediated degradation and integrin binding is expected to allow the cells to migrate through the gel in a process similar to tissue remodeling (Lutolf et al. 2003). Other example is the incorporation of cleavage sequences into multidomain peptides as the recombinant, crosslinkable elastin-like protein that harbors an adhesion motif (REDV) and an elastase-sensitive sequence. Cleavage of the latter yields a bioactive Val-Gly-Val-Ala-Pro-Gly (VGVAPG) fragment intended to stimulate cell proliferation and improve tissue repair (Girotti et al. 2004). Such functionalization's mimic the complex bioactivity of the ECM, where enzymatic remodeling can result in the liberation of cryptic sites contained within the amino acid sequences of ECM proteins that possess different bioactivity and have direct effect on processes ranging from cell migration to differentiation, proliferation and angiogenesis (Schenk and Quaranta 2003; Girotti et al. 2004). Recent investigations also showed that surface chemistry is an important parameter able to trigger proteolytic routes of cells in an MMP-dependent manner, particularly when FN is adsorbed on planar surfaces (Llopis-Hernández et al. 2011). However, in general such studies dedicated on the degradation of adsorbed proteins on planar surfaces are sparsely reported and further studies in the field are strongly desirable in order to improve synthetic biomaterials design. It represents new tool to direct ECM remodeling at biomaterials interface with all the biological consequences that it can cause.

6. Aim and Specific Objectives

6.1 Aim

With this study, we strive to learn more about the fate of adsorbed Col IV on model biomaterial surfaces, which vary in their wettability, chemistry and charge. We want to know can we control Col IV behavior and the consequent cellular response with cues coming from the materials site that would finally favor the vascular tissue engineering application.

6.2 Specific objectives

- Development of model biomaterial surfaces varying in their wettability, chemistry and charge.
- Study the adsorption kinetic of Col IV on different model surfaces.
- Study the molecular organization of adsorbed protein layer at nanoscale.
- Cellular interaction with adsorbed Col IV on different model surfaces.
 - A. Development of adequate cellular models (primary endothelial cells and fibroblasts);
 - B. Morphological examination of adhering cells (including overall cell morphology, immunofluorescence visualization of focal adhesions, actin cytoskeleton, $\alpha_1\beta_1$ and $\alpha_2\beta_1$ integrins and p-FAK);
 - C. Quantification of cell adhesion and spreading via image analysis;
 - D. Quantitative studies of p-FAK expression by western-blot;
 - E. Quantitative studies on the strength of cellular interaction using flow chamber;
- Remodeling of adsorbed Col IV by living cells on different model surfaces – organization and degradation activity.
 - A. Reorganization of adsorbed Col IV – morphological studies;
 - B. Cellular mechanisms involved in the reorganization of Col IV;
 - C. Degradation of adsorbed Col IV via pericellular proteolysis – morphological evaluation;
 - D. Quantification of degradation activity by measuring of FITC-Col IV release;
 - E. Quantification of MMP2 and MMP9 activity by zymography.
- Studies on the ability of HUVEC to form capillary-like structure on Col IV coated model surfaces.
 - A. Morphological evaluation;
 - B. Quantitative studies on FITC-Col IV degradation during capillary formation.

Chapter 2 – Material and Methods

Model biomaterial surfaces

Hydrophilic glass

To render the hydrophilic surface, glass coverslips (22 x 22 mm, 22 x 40 mm, or rounded with $d = 15$ mm, Fisher Scientific) were cleaned in an ultrasonic bath for 10 minutes (min) in a 1:1 mixture of 2-propanol and tetrahydrofuran. The samples were then exposed to piranha solution (30% (v/v) H_2O_2 and 70% (v/v) H_2SO_4) for 30 min followed by a copious rinsing with milliQ water (18.2 M Ω) and dried.

Hydrophobic surface (CH_3)

The hydrophobic surface was prepared according previously described protocol (Gustavsson et al. 2008) using an organosilane trichloro-(octadecyl)-silane (ODS) (Sigma-Aldrich). Before silanization the glass samples were pre-cleaned as above and then placed in a solution containing 12.5 mL of carbon tetrachloride (CCl_4), 37.5 mL of heptane ($n-C_7H_{16}$) and 220 μ L ODS. The samples were left in this solution for 18 min at room temperature and the excess of silane was washed away with pure heptane. Samples were then heated for one hour at 80 °C.

Positively charged NH_2 surface

The self-assembled monolayers (SAMs) presenting NH_2 groups were prepared according to previously described protocol (Gustavsson et al. 2008). Before functionalization the glass samples were pre-cleaned as above and then immersed for 18 min at room temperature in a solution containing 30 mL methanol, 10 mL of 4% acetic acid and 3-(2-aminoethylamino)propyltrimethoxysilane ($C_8H_{22}N_2O_3Si$, Sigma-Aldrich) to yield a final 1% concentration. Excess of silane was washed away by immersion in excess solvent solution. Samples were air-dried and the heated at 80 °C for one hour.

Negatively charged $COOH$ surface

The SAMs presenting $COOH$ groups were prepared in two steps; first the pre-cleaned glass samples as above were immersed in a 1:3 mixture of CCl_4 and $n-C_7H_{16}$ containing 0.01 M 10-(carbomethoxy)-decyl-dimethylchlorosilane ($C_{14}H_{29}ClO_2Si$, ABCR GmbH&Co) for four hours at 4 °C, which create $COOHCH_3$ functionalities. Samples were then washed in silane-free solvent, heated as above and immersed overnight in a 12 M HCl solution to create $COOH$ surfaces as second step.

Model materials with tailored density of -OH groups

Model materials with tailored density of OH groups were developed and characterized in the Center for Biomaterials and Tissue Engineering at Polytechnic University of Valencia (Professor M. Salmerón-Sánchez group). Briefly, copolymers sheets were obtained by polymerization of a solution of two monomers, ethyl acrylate (EA) (99 % pure, Sigma-Aldrich) and hydroxy ethyl acrylate (HEA) (96 % pure, Sigma-Aldrich), in the proportion as indicated, using 0.1 wt% of benzoin (98 % pure, Scharlau) as photoinitiator and a 2 wt% of ethyleneglycol dimethacrylate (Sigma-Aldrich) as cross-linking agent. The polymerization was carried out up to limiting conversion and against a glass surface seeking to obtain surfaces of controlled and reproducible roughness. Five monomer feed compositions were chosen, given by the weight fraction of HEA in the initial mixture of $X_{OH} = 1; 0.7; 0.5; 0.3; \text{ and } 0$ (it refers to the fraction X of HEA in the copolymer). After polymerization, low molecular mass substances were extracted from the material by boiling in ethanol for twenty-four hours, and then drying in vacuum to a constant weight. Small disks (*10 mm diameter) were cut from the polymerized sheets to be used in the protein adsorption and cell adhesion studies. The samples were sterilized with gamma radiation (25 KGy) before the experiments.

Mixed NH_2/CH_3 self-assembled monolayers

The mixed SAM surfaces were developed and characterized in the Center for Biomaterials and Tissue Engineering as above based on a protocol described elsewhere (Keselowsky et al. 2003) using alkanethiols 1-dodecanethiol ($HS-(CH_2)_{11}-CH_3$) (Sigma-Aldrich) and 12-amino-1-mercaptododecane ($HS-(CH_2)_{12}-NH_2$) deposited on gold (AU).

AU-coated glass coverslips (Fisher Scientific) were prepared by deposition of thin films of Ti (150 Å) followed by Au (150 Å) using a high vacuum evaporator (Polaron E6100) at a deposition rate of 2 Å/s and a chamber base-pressure of $2 \cdot 10^{-6}$ Torr. Glass coverslips were pre-cleaned with 70 % H_2SO_4 and 30 % H_2O_2 at room temperature for one hour, rinsed consequently with deionized H_2O and 95 % ethanol, and dried under a stream of N_2 prior to metal deposition.

Freshly prepared Au-coated surfaces were immersed in alkanethiol solutions (1 mM in absolute ethanol) with different ratios (NH_2/CH_3) and allowed to assemble overnight. SAMs were finally rinsed in 95% ethanol and dried under N_2 .

Characterization of model surfaces

Water contact angle and equilibrium water content

The wettability of surfaces was estimated with water contact angle measurements using sessile drop technique performed on Dataphysics Contact Angle System OCA15. Average values were obtained from at least ten different samples. The equilibrium water content (mass of water absorbed referred to the dry mass of the substrate) of the polymers sheets was also measured under the Dataphysics Contact Angle System.

X-ray photoelectron spectroscopy (XPS)

XPS measurements were performed in a PHI 5500 Multitechnique System (Physical Electronics) using a monochromatic X-ray source and calibrated to the $3d_{5/2}$ line of Ag. The analyzed area was a circle of 0.8 mm diameter, and the selected resolution for the spectra was 23.5 eV of pass energy and $0.1 \text{ eV} \cdot \text{step}^{-1}$. All measurements were made in an ultra high vacuum chamber pressure. We used the XPS elemental sensitivity factors according to the MULTIPAK program for PHI instruments. An automatic XPS signal fitting software has been developed under MATLAB v7.2 (The MathWorks, Inc.) environment to deconvolute the experimental spectra as described elsewhere (García et al. 2009).

Protein adsorption

The adsorption of native Col IV (Abcam) on model surfaces was performed at indicated concentrations in 0.1 M sodium acetate (pH 4.5) for 30 min (cellular studies) or 10 min (AFM studies) at 37 °C.

The adsorption of LAM (Sigma-Aldrich) to model materials with tailored density of -OH groups was performed at indicated concentrations in phosphate-buffered saline (PBS) (pH 7.4) solution in the same conditions as for Col IV. Some samples were coated consecutively, first with Col IV than LAM, with extensive washing with PBS between incubations.

Adsorption of DQTM Collagen type IV (FITC-Col IV, Molecular Probes) where FITC molecules are highly quenched was performed at indicated concentrations in PBS (pH 7.4) as above.

Quantification of Adsorbed FITC-Collagen IV

The adsorption of FITC-Collagen IV at different model surfaces was quantified by NaOH extraction as described before (Gustavsson et al. 2008). Briefly, the model surfaces were cleaned with distilled water in an ultrasonic bath dried and coated for 30 min at 37 °C with FITC-Col IV at concentrations from 5 to 50 $\mu\text{g}/\text{mL}$ dissolved in PBS. It should be noted that according to the manufacturer's manual this protein (collagen type IV from human placenta origin) is conjugated

with FITC in such a conditions that part of its fluorescence is quenched thus increasing significantly the quantum yield upon extraction under denaturing conditions or when is enzymatically cleaved. After coating the samples with different FITC-Col IV concentrations, as indicated, they were rinsed three times with PBS. The adsorbed FITC-Col IV was extracted with 250 μ L of 0.2 M NaOH for two hours at room temperature. In some cases the samples were seeded with cells and then compared with “no-cells” preparations at least in triplicates. The fluorescent intensity of the extracts was measured with a fluorescent spectrophotometer (Horiba-Jobin y Von) at 488 nm (excitation) and 530 nm (emission) and compared to a standard curve based on known concentrations of FITC-Col IV solutions in 0.2 M NaOH.

Atomic force microscopy

We have used the AFM type NanoScope III (Digital Instruments) to follow the Col IV and LAM adsorption profile and the morphology of the adsorbed protein layer operating in the tapping mode in air. Si cantilevers (Veeco) were used with a force constant of 2.8 N/m and a resonance frequency of 75 kHz. The phase signal was set to zero at the resonance frequency of the tip. The tapping frequency was 5-10% lower than the resonance frequency. Drive amplitude was 200 mV and the amplitude set-point A_{sp} was 1.4 V. The ratio between the amplitude set-point and the free amplitude was kept equal to 0.7. AFM images were analyzed using the WSxM software (Nanotec) to observe the topography of non-coated surfaces, as well as, the typical protein distribution on the different substrata. A tailor-made, MATLAB software (The MathWorks, Inc.), was used for volume calculations of the adsorbed protein layer.

Cells

Human Umbilical Vein Endothelial Cells

Human Umbilical Vein Endothelial cells (HUVEC, PromoCell) were culture in endothelial cell growth medium supplemented with SupplementMix (PromoCell) containing 0.4% ECGS/H, 2% fetal calf serum, 1 ng/mL epidermal growth factor, 1 mg/mL hydrocortison, and 1 ng/mL basic fibroblast factor. The medium was exchanged each 3rd day. For the adhesion experiments the cells were detached from around confluent flasks with Trypsin/EDTA (Invitrogen) and the remained trypsin activity was stopped with 100 % Fetal Bovine Serum (FBS) before two times washing with medium without supplements. Finally, the cells were counted and reconstituted in serum-free endothelial cell medium to be seeded on the different modelsurfaces.

Human dermal Fibroblasts

Human Dermal Fribroblast (HF) (PromoCell) were cultured in Dulbecco’s Modified Eagle’s Medium (DMEM) supplemented with 10 % fetal bovine serum (FBS), 1 mM Sodium Pyruvate, 2

mM L-Glutamine, and Penicillin-Streptomycin, all of them purchased from Invitrogen. The growth medium was exchanged each 3rd day. For the experiments the cells were detached from around confluent flasks with Trypsin/EDTA and the remained trypsin activity was stopped with FBS as above. Finally the cells were reconstituted in serum free DMEM.

Initial cellular interaction

Overall Cell Morphology

To study the overall cell morphology we used actin-stained samples. For that purpose, 5×10^4 cells/well were seeded in 24-well Tissue Culture (TC) plates (Costar) containing the samples for two hours in the serum-free medium. Typically, the samples had been pre-coated with Col IV as stated above, at concentration 50 $\mu\text{g}/\text{mL}$ in 0.1 M sodium acetate pH 4.5 for 30 min at 37°C. At the end of incubation, the cells were fixed with 4 % paraformaldehyde (10 min), permeabilized with 0.5 % Triton X-100 for 5 min and saturated with 1 % albumin in PBS (15 min). Actin cytoskeleton was visualized with Alexa Fluor 488 Phalloidin conjugate (Molecular probes) and the nuclei with Hoeschst 34580 (Invitrogen) dissolved in PBS containing 1% albumin. Finally the samples were mounted with Mowiol (Sigma Aldrich) and viewed and photographed on a fluorescent microscope Axio Observer Z1 (Zeiss) at low magnification (10X and 20X, see below). At least three representative images were acquired for each magnification.

Quantification of Cell Adhesion and Spreading

The number of adhering cells and the mean cell surface area were quantified using the image J plug-ins (National Institute of Health). The adhesion was measured by counting the cells nuclei in at least three randomly chosen squares of each sample (photographed at 10 x magnification) using the blue channel of the microscope (viewing the cells nuclei). The average cells area was further measured (μm^2) using the same samples but viewed at 20x magnification in the green channel of the microscope (to visualize cellular actin). The results presented correspond to at least three independent experiments.

Immunofluorescence

Visualization of Focal Adhesion Contacts

For visualization of focal adhesion contacts 5×10^4 cells/well were seeded as described above on Col IV model materials in non-supplemented endothelial cell medium/DMEM. Vinculin was visualized using monoclonal anti-vinculin antibody (Sigma Aldrich) dissolved in PBS - 1 % albumin for 30 min followed by Alexa Fluor 555 goat anti-mouse (Molecular Probes) as secondary antibody. The samples were viewed and photographed in a fluorescent microscope as above, but at higher magnification (63X or 100X). At least three representative images were

acquired for each experimental condition. For most experiments Alexa Fluor 488 Phalloidin conjugate was added to the secondary antibody to visualize actin cytoskeleton together with focal adhesion contacts.

Visualization of Integrins

For the visualization of α_1 and α_2 integrins we used monoclonal anti-human integrin α_1 (Millipore) or α_2 (Abcam) for 30 min followed by Alexa Fluor 555 goat anti-mouse as secondary antibody. Alexa Fluor 488 Phalloidin conjugate was usually added to the secondary antibody as above.

Co-staining for Vinculin and Focal Adhesion Kinase

For some experiments focal adhesion contacts were visualized together with phosphorylated focal adhesion kinase (p-FAK) to learn whether the development of focal adhesions is accompanied with the recruitment of phosphorylated signaling molecules. For this propose we used the same monoclonal anti-vinculin antibody followed by Alexa Fluor 488 goat anti-mouse (Molecular Probes). The p-FAK was viewed using p-FAK specific to tyrosine 925 (Tyr 925) polyclonal antibody (Cell Signaling) dissolved in PBS - 1 % albumin for 30 min, followed by Alexa Fluor 555 goat anti-rabbit (Molecular Probes) as secondary antibody. Preliminary studies with omitting of the corresponding secondary antibodies were performed to confirm no cross-reactivity in the system.

Western-blot analysis

FAK Assay

To analyze the expression of p-FAK by western blot the cells were detached from confluent layer with Trypsin/EDTA after two times washing with endothelial cell medium without supplements. Then 1×10^6 cells were seeded (usually in 1 ml medium) on the model materials (22 x40 mm) coated with 50 $\mu\text{g}/\text{mL}$ Col IV and further cultured for two hours in serum free medium. Cells were lysed in RIPA buffer containing protease and phosphatase inhibitors: (1 % Triton X-100, 1% sodium deoxycholate, 0.1 % SDS, 150 mM NaCl, 50 mM Tris-HCl (pH 7.5), 1 mM PMSF, 10 mg/mL leupeptin, 10 mg/mL aprotinin, 1% NPO_4 , 50 mM NaF, and 200 mM NaVO_4). Total protein was quantified using micro-BCA kit (Pierce). Equal amounts cell lysates were mixed in sample buffer (50 mM Tris-HCl pH 6.8, 100 mM DTT, 2 % SDS, 10 % glycerol, and 0.1 % bromophenol blue) and separated by SDS-Page. After electro-transferring to nitrocellulose membranes (Biorad) they were temporary stained with Ponceau red (Sigma Aldrich) to check the transfer and blocked with 5 % nonfat dry milk in Tris-saline buffer. The membranes were subsequently incubated in the solution of primary polyclonal antibodies against FAK (dilution 1:1000, Cell Signaling), or p-FAK (Tyr 925) (dilution 1:1000, Cell Signaling) overnight at 4 °C.

After extensive washing with TBS-Tween (20 mM Tris-HCL pH 7.6, 137 mM NaCL, 0.1 % Tween-20), and pure TBS, HRP-conjugated anti-rabbit secondary antibody (dilution 1: 3000, Santa Cruz) was added for one more hour. Protein signal was detected using the ECL chemiluminescent system (Amersham). Densitometry analysis, standardized to FAK as control for protein loading, was performed using Image J software (National Institute of Health).

MMP2 assay

To detect the expression of MMP2 in cellular lysates prepared as above primary monoclonal antibody against MMP2 (dilution 1:1000, Santa Cruz) was used. Equal control samples were stained with polyclonal anti-vinculin antibody (dilution 1:1000, Sigma Aldrich). The corresponding HRP-conjugated secondary antibodies were anti-mouse and anti-rabbit (both from Santa Cruz), respectively. Densitometry was standardized to the vinculin content as control for protein loading.

Strength of cell interaction using a parallel flow-chamber

The parallel-flow chamber is well described elsewhere (Owens et al. 1987; Missirlis and Spiliotis 2002) and the flow generated within the chamber can be easily analysed mathematically. In our system we used a Pump (ISMATEC) to provide a fluid steady-state flow along the chamber. The upper plate of the chamber was a 22 x 40 mm glass coverslip, coated with protein (as above) or not (as control), where 1×10^6 human fibroblasts were seeded for 2 hours in serum free DMEM. A solution of 1% PBS (supplemented with 4 mM KCl, 5 mM MgCl₂, and 1 mM CaCl₂) at 37 °C was used to fill the chamber before closing with the sample. The chamber was then placed in an inverted microscope and connected to the pump. An initial phase contrast image of adhering cells (T=0) was taken before exposition to flow. In some cases, fluorescein diacetate (FDA), at final concentration 1 µg/ml was added to the medium to verify cells vitality. After that, the cells were exposed to different flow rates and corresponding images were acquired. The image J software was used to calculate the number of cells at each condition, as above.

Calibration of the flow system

To exert a constant shear stress over the cell culture various parameters of the flow profile were characterized. Wall shear stress (T_w) was calculated from the volumetric flow rate (Q). Briefly, the fluid movement creates a sheer stress at the wall, which may be calculated from equation 1:

$$\tau_w = \Delta P \frac{h}{2L}$$

(1)

where ΔP is the pressure drop (outlet-inlet pressure), $\Delta P = (12L/h^3W)\mu Q$, h is the height, L is the length and W is the width of the chamber, μ is the fluid viscosity and Q is the volumetric flow rate. The assumption is that the wall shear is approximately equal to the shear that is exerted on the cells, as the fibroblast height is two orders of magnitude less than the chamber height. Figure 1 shows the scheme of the chamber used with channel dimensions $L = 2.352$ cm, $W = 1.245$ cm, and $h = 0.035$ cm.

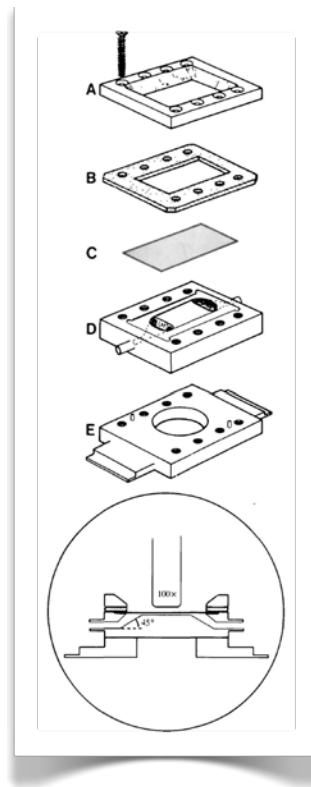


Figure 1 - The parallel flow chamber.

The Reynolds number (Re) must be below the critical value of 2300, to maintain laminar flow inside the chamber. The entrance length (le) that is the necessary distance for the fluid to become steady inside the chamber was also determined to ensure steady flow over the area of interest. Finally, in order to analyse an area where the cells were subjected to a similar shear stress we placed the microscope objective in the middle half of the chamber channel width. To characterize the above described parameters under our conditions we determined the Re number and le as function of the shear stress we wanted to subject the cells. Reynolds number for each flow rate was calculated using the following equation: $Re = (v \cdot \rho \cdot Dh) / \mu$, where v is the linear flow rate, ρ the density of the fluid, Dh is the hydraulic diameter and μ the viscosity. The hydraulic diameter was calculated by the following equation: $Dh = 4 \cdot A / P$, where A is the cross sectional area of the chamber (that is equal to width (W) times height (h)), and P is the perimeter of the chamber. The entrance length was determined with following equation: $le = 0.05 \cdot Dh \cdot Re$.

Visualization of adsorbed Collagen IV

To study the fate of adsorbed Col IV glass cover-slips (22 x 22 mm) were placed in 6-well tissue culture plates and coated with Col IV or FITC-Col IV as above. After three times washing with PBS, 5×10^4 fibroblasts/HUVEC were seeded in serum free medium and cultured for a time as indicated (2, 5 or 24 hours). For longer than 2 hours experiments 10 % serum was added to the medium after one hour of culture in serum free medium.

All samples were fixed with 4% paraformaldehyde (20 min), permeabilized with 0.5% triton X-100 (5 min) and saturated with 1% albumin in PBS (15 min). Immunofluorescence for native Col IV was performed using monoclonal anti-collagen IV antibody (Millipore) followed by Cyth 3-conjugated Affini Pure Goat Anti-Mouse IgG (H+L) (Jackson ImmunoResearch) or Alexa Fluor 488 anti-mouse (Invitrogen) as secondary antibodies.

Samples were viewed and photographed on fluorescent microscope (Nikon Eclipse E800) or Axio Observer Z1 (Zeiss). Some double stained samples were viewed on Laser Scanning Confocal Microscope LSM (Leica TCS-SL).

Preparation of FITC-Labeled Fibronectin

Human plasma fibronectin (FN) (Sigma Aldrich) was dissolved in 0.1 M sodium bicarbonate buffer (pH = 9.0) at 1 mg/mL. Then 10 μ L of fluorescein isothiocyanate (FITC; Sigma Aldrich) dissolved in dimethylsulfoxide to 10 mg/mL was added and left for 2 h at room temperature. The labeled FN was separated from non-conjugated dye on 10 ml Sephadex G-25 (Sigma Aldrich) desalting columns equilibrated with 7 volumes PBS solution. The final protein concentration was estimated by measuring the absorbance at 280 nm, while the degree of FITC-labeling was calculated against the absorbance at 494 nm - see equation 2 below:

$$C_{FN} = \frac{A_{280} - 0.3 A_{494}}{1.2} [mg/ml] \quad (2)$$

where, 0.3 is the correction factor for the absorbance of FITC at 280 nm, and 1.2 is the extinction coefficient of fibronectin (i.e. the absorbance of 1 mg/mL FN at 280 nm). The samples were stored at 4°C.

Co-Localization of Collagen IV with secreted Fibronectin

To study Col IV co-localization with secreted FN cells were cultured in different protocols on Col IV or FITC-Col IV coated samples for 5 or 24 hours as indicated. Native Col IV was visualized

by immunofluorescence using monoclonal anti-Col IV antibody followed by Alexa Fluor 488 anti-mouse as secondary antibody. In this case FN was viewed using polyclonal anti-FN (Sigma Aldrich) followed by Alexa Fluor 555 anti-rabbit (Invitrogen) secondary antibody. In other cases, when cells were cultured on FITC-Col IV, the secreted FN was co-viewed in red using the same polyclonal anti-FN antibody, but followed by Alexa Fluor 555 anti-rabbit secondary antibody.

Co-Localization of Collagen IV with exogenously added Fibronectin

To study co-localization of Col IV with exogenously added soluble FN, Human Plasma Fibronectin (FN, Sigma Aldrich) was added to the medium in different protocols. In the first, the cells were cultured on Col IV coated glass for 5 hours (1st hour in serum free medium, then serum was added). As next step, 100 µg/mL of FN was added to the medium for the last hour of incubation and then both proteins viewed by double immunofluorescence, using monoclonal anti-collagen IV antibody followed by Cyth 3-conjugated AffiniPure Goat Anti-Mouse IgG (H+L) and anti FN rabbit polyclonal antibody (Sigma Aldrich) followed by Alexa Fluor 555 anti-rabbit (Invitrogen) secondary antibody. In second protocol we used FITC-FN for adding to the medium (prepared as described before) and the samples were further stained with monoclonal anti-collagen IV antibody followed by Cyth 3-conjugated AffiniPure Goat Anti-Mouse IgG (H+L) (as above). In third protocol, the glass slides were coated with FITC-Col IV and after 4 hours of culture 100 µg/ml of FN was added to the medium for the last 1 hour of culture. Then FN was stained in red using monoclonal anti-FN (Sigma Aldrich) followed by Cyth 3-conjugated AffiniPure Goat Anti-Mouse IgG (H+L) as secondary antibody.

Co-Localization of secreted FN with exogenously added FITC-Collagen IV

In this protocol the glass slides were coated with serum for 30 minutes and then the cells were seeded in 10% FBS DMEM medium and cultured for 23 hours. After 100 µg/mL of FITC-Col IV was added to the medium for 1 more hour before fixation. Subsequently, the secreted FN was viewed using monoclonal anti-FN antibody as above followed by Cyth 3-conjugated AffiniPure Goat Anti-Mouse IgG (H+L), while FITC - Col IV was viewed directly in the green channel.

Collagen IV degradation

Fluorescent assay

Three different conditions were used to study adsorbed FITC-Col IV: a) direct extraction of adsorbed protein after coating; b) extraction after adding medium for 5 or 24 hours measuring the remaining adsorbed protein (with or without cells), and finally c) measuring the released fluorescent signal after culturing the cells for 5 and 24 hours. As stated above, the adsorbed FITC-Col IV was extracted with 250 µL of 0.2 M NaOH for two hours at room temperature. The fluorescent intensity of the extracts and supernatants were measured with a fluorescent

spectrophotometer (Horiba-Jobin y Von) set to 488 nm (excitation) and 530 nm (emission) and compared to a standard curve based on known concentrations of FITC-Col IV solutions in 0.2 M NaOH.

Zymography

The conditioned medium from 24 hours cultured cells (HUVEC or Fibroblasts) on Col IV coated model materials was used to study the activity of the two major MMPs known to cleave Col IV, namely MMP2, and MMP9. For that purpose, 25 μ L of each supernatant was mixed with 5 μ L of sample buffer (0.04 M Tris-HCL pH 6.8, 4 % SDS, 33 % glycerin, 0.04 % bromophenol blue) and these samples were charged on a Ready Gel Zymogram (Biorad, 15-well) containing 10 % gelatin, and subjected to a gel electrophoresis (SDS-PAGE). The gel was then incubated in 2.5 % Triton X-100 for 30 minutes before overnight incubation with renaturation buffer (1 M Tris-HCL pH 7.5, 5 M NaCl, 1 M CaCl₂, 10 % Triton X-100) at 37 °C. After staining with 0.5 % Coomassie brilliant blue R-250 (in 30 % methanol/10 % acetic acid) and destaining with the same solution without Coomassie, gelatinolytic activity was detected as unstained bands on the blue background of the sample and quantified using a molecular imager gel Doc⁺ (imaging system, Biorad).

In vitro capillary tube formation by HUVEC

HUVEC ability to form capillary-like tubes on different Col IV coated model materials was accessed using basement membrane extract (BME) to overly the samples. First, 5×10^4 cells of HUVEC were seeded on Col IV coated model materials placed in 24 well plates and further cultured for 2 hours in non - supplemented endothelial cell medium. Afterwards the medium was removed and 250 μ L of basement membrane extract BME (AMS Biotechnology) containing 1 % FITC-Col IV at 4°C was added to each sample and incubated for 30 min at 37 °C to form a gel. After that, supplemented endothelial cell medium was added and the cells were further cultured for 5 and 24 hours. Three representative images of each condition were acquired using the phase contrast mode of the microscope Axio Observer Z1 (Zeiss). Parallel experiments without cells were also performed as negative control for spontaneous degradation activity, where the released FITC fluorescence was measured. In other set of experiments, the released FITC was measured after 1mg/mL of collagenase (Sigma Aldrich) treatment as positive control for complete degradation. The supernatants and extracts were centrifuged (1000 g for 10 min) before the fluorescent intensity was measured with a fluorescent spectrophotometer (Horiba-Jobin y Von) set to 488 nm (excitation) and 530 nm (emission) bands.

Chapter 3 - Results

1. Different Assembly of Type IV Collagen on Hydrophilic and Hydrophobic Substrata Alters Endothelial Cells Interaction

1.1 Preface 1

The initial events that take place at biomaterials interface mimic to a certain extent the natural communication of cells with the ECM. This is a cascade of events that are usually initiated by the adsorption of soluble adhesive proteins available in biologic fluids and followed by cell adhesion, spreading and polarization. Apart from the soluble adhesive proteins however, other less soluble ECM proteins like collagen and LAM can also associate with the biomaterial surface eliciting distinct cellular responses. We are particularly interested on the surface behavior of Col IV, the major structural component of the basement membrane (BM). The BM is a specialized form of ECM that provides structural support to tissues and regulates almost all aspects of the cellular behavior. Apart from the rough ECM the BM may be considered as a rather two-dimensional (2D) structure, at least in respect to the cells that reside on it. Nowadays, tissue engineering strives to mimic the 3D organization of ECM with scaffolds that support cellular response and regeneration. However, the development of surfaces that resemble the 2D architecture of BM is also a challenging task as tissue cells often meet such an environment in contact with implanted bioengineering devices (e.g. engineered vascular tissue, bio artificial organs etc.). On the other hand, the behavior of Col IV at biomaterials interface in contact with endothelial cells gains a distinct tissue engineering interest as it can be critical for the successful interaction of implants with this cells – an issue that should be considered if one wants to mimic the natural organization of the vessel wall.

With the aim of mimicking the BM organization at biomaterial interface and considering the vascular tissue engineering application, we studied the Col IV adsorption pattern on model hydrophilic and hydrophobic trichloro(octadecyl)silane (ODS) surfaces known to strongly affect the behavior of other ECM proteins. AFM studies revealed a fine, nearly molecular size network arrangement of Col IV on hydrophilic glass, which turns into a relatively thicker – growing in size – polygonal network on hydrophobic ODS, presumably consisting of molecular aggregates. We further compared the biological activity of these different surface-driven assemblies of Col IV following the interaction with human umbilical vein endothelial cells (HUVEC). We choose primary endothelial cells considering their role in the functional organization of the vascular BM, as well as their involvement in the endothelization of implants and/or their vascularization potential, both events critically important for most tissue engineering applications. We generally found that cells attach less efficiently on hydrophobic ODS, while the fine Col IV network on

hydrophilic substrata support HUVEC interaction involving both α_1 and α_2 integrins clustering in the focal adhesions and concomitant development of actin cytoskeleton. Details of this study are presented in the paper below.

DIFFERENT ASSEMBLY OF TYPE IV COLLAGEN ON HYDROPHILIC AND HYDROPHOBIC SUBSTRATA ALTERS ENDOTHELIAL CELLS INTERACTION

N. Miranda Coelho^{1,2}, C. González-García³, J. A. Planell^{1,2}, M. Salmerón-Sánchez^{3,4,5}, and G. Altankov^{1,4,6*}

¹ Institut de Bioenginyeria de Catalunya, Barcelona, Spain

² Universitat Politècnica de Catalunya (UPC), Barcelona, Spain

³ Center for Biomaterials and Tissue Engineering, Universidad Politécnica de Valencia, 46022 Valencia, Spain

⁴ Networking Research Center on Bioengineering, Biomaterials and Nanomedicine (CIBER-BBN), Valencia, Spain

⁵ Regenerative Medicine Unit, Centro de Investigación Príncipe Felipe, Autopista del Saler 16, 46013 Valencia, Spain

⁶ ICREA (Institució Catalana de Recerca i Estudis Avançats), Barcelona, Spain

Abstract

Considering the structural role of type IV collagen (Col IV) in the assembly of the basement membrane (BM) and the perspective of mimicking its organization for vascular tissue engineering purposes, we studied the adsorption pattern of this protein on model hydrophilic (clean glass) and hydrophobic trichloro(octadecyl)silane (ODS) surfaces known to strongly affect the behavior of other matrix proteins. The amount of fluorescently labeled Col IV was quantified showing saturation of the surface for concentration of the adsorbing solution of about 50 µg/ml, but with approximately twice more adsorbed protein on ODS. AFM studies revealed a fine – nearly single molecular size – network arrangement of Col IV on hydrophilic glass, which turns into a prominent and growing polygonal network consisting of molecular aggregates on hydrophobic ODS. The protein layer forms within minutes in a concentration-dependent manner. We further found that human umbilical vein endothelial cells (HUVEC) attach less efficiently to the aggregated Col IV (on ODS), as judged by the significantly altered cell spreading, focal adhesions formation and the development of actin cytoskeleton. Conversely, the immunofluorescence studies for integrins revealed that the fine Col IV network formed on hydrophilic substrata is better recognized by the cells via both $\alpha 1$ and $\alpha 2$ heterodimers which support cellular interaction, apart from these on hydrophobic ODS where almost no clustering of integrins was observed.

Keywords: Collagen type IV, adsorption, assembly, hydrophilic, hydrophobic, surfaces.

Introduction

The initial cell-biomaterials interaction mimics to a certain extent the natural communication of cells with the extracellular matrix (ECM); it starts with the adsorption of soluble matrix proteins from the surrounding medium followed by cell adhesion, spreading and polarization (Grinnell and Feld, 1982; Griffith and Naughton, 2002; Sipe, 2002). In some cases however, less soluble ECM proteins such as collagens or laminins also associate with the biomaterial surface eliciting distinct cellular responses. In this study we were particularly interested in the behavior of adsorbed type IV collagen (Col IV) – a unique multifunctional matrix protein that plays a crucial role in the organization of the basement membrane (BM). The BM is a highly specialized ECM common to many types of tissues providing spatial organization to the cells and involved in a remarkable number of physiological and pathological processes, such as cell adhesion, migration, development, wound healing and cancer progression (Timpl and Brown, 1996; Charonis *et al.*, 2005; Brown *et al.*, 2006; LeBleu *et al.*, 2007; Khoshnoodi *et al.*, 2008); in addition, it serves as a reservoir for growth factors and enzymes and is responsible for the molecular sieving (Timpl and Brown, 1996). The BM is a fine (approximately 100-300 nm thick) structure that may be considered as two dimensional (2D) in respect to the range of cell size. Nowadays, tissue engineering strives to mimic the three dimensional organization of ECM with scaffolds that support cellular response and regeneration (Daley *et al.*, 2008). However, the development of materials and surfaces that resemble the 2D structure of BM is also a challenging task; moreover, the cells often meet such environments in contact with implanted bioengineered devices. An example is the engineered vascular tissue. To date, blood contacting devices including small diameter vascular grafts, stents, hard valves, etc, suffer from a common defect – the lack of significant endothelial cells ingrowth – presumably caused by the absence of the specialized BM, resulting in an accelerated device failure (Keresztes *et al.*, 2006). In this respect, the molecular assembly of Col IV at different materials interface gains a distinct bioengineering interest (Hudson *et al.*, 1993; Keresztes *et al.*, 2006) as it can be critical for the successful interaction with EC – a fact that should be considered to mimic the natural organization of vessel wall.

*Address for correspondence:

G. Altankov

ICREA – Molecular Dynamics

Feixa Llargà Pàvelo Govern Planta 1 No 1112,

Bellvitge Barcelona Hospitalet de Llobregat

08907 Barcelona, Spain

Telephone Number:

FAX Number:

E-mail: george.altankov@icrea.es

The supramolecular structure of Col IV was extensively studied during the last two decades (Timpl and Brown, 1996; Gelse *et al.*, 2003; White *et al.*, 2004; Charonis *et al.*, 2005; Brown *et al.*, 2006; LeBleu *et al.*, 2007; Khoshnoodi *et al.*, 2008). Once secreted, the triple-helical heterotrimeric molecules of Col IV self-associate to form a 2D network which serves as molecular scaffold for other BM components, such as laminin, perlecan and proteoglycans (Timpl and Brown, 1996; Brown *et al.*, 2006). Detailed *in situ* analysis of high resolution electron micrographs revealed that Col IV molecules self-assemble in the BM forming polygonal networks held together by overlapping and lateral interactions along the triple-helical domain and the N- and C-terminal end-domains (Timpl and Brown, 1996; Charonis *et al.*, 2005).

Like other ECM proteins Col IV is recognized by the cells via integrins – a family of cell surface receptors that provide trans-membrane links between the ECM and the cytoskeleton (Hynes, 2002; White *et al.*, 2004). Out of the 24 integrin heterodimers $\alpha 1\beta 1$, $\alpha 2\beta 1$, $\alpha 10\beta 1$, and $\alpha 11\beta 1$ act as primary receptors for collagens (Vandenberg *et al.*, 1991; Kern *et al.*, 1993; Kapyla *et al.*, 2000; Hynes, 2002; White *et al.*, 2004; Popova *et al.*, 2007), but most abundantly expressed are $\alpha 1\beta 1$ and $\alpha 2\beta 1$ (White *et al.*, 2004; Khoshnoodi *et al.*, 2008). When integrins are occupied they cluster in focal adhesion complexes where specific bidirectional integrin signaling converges with other molecular pathways (Hynes, 2002). Depending on the conformation of adsorbed protein layer, however, different integrin activity may be expected (Grinnell and Feld, 1982; Kapyla *et al.*, 2000; Keresztes *et al.*, 2006; Ludwig *et al.*, 2006).

Despite the extensive research on the biochemistry and physiology of Col IV (Hudson *et al.*, 1993; Gelse *et al.*, 2003; Keresztes *et al.*, 2006) and its involvement in a number of human disorders (Gelse *et al.*, 2003; Charonis *et al.*, 2005), surprisingly little is known about the behavior of Col IV at the biomaterials interface, which in turn, determines the successful cellular interaction.

To learn more about the biological performance of Col IV at the biomaterial interface we followed its adsorption profile and molecular organization of the adsorbed protein layer on model hydrophilic and hydrophobic surfaces known to strongly influence the activity of other proteins (Grinnell and Feld, 1982; Tamada and Ikada, 1994; Altankov *et al.*, 1996; Altankov and Groth, 1996; Altankov *et al.*, 1997; Kowalczyńska *et al.*, 2005). Atomic force microscopic (AFM) studies revealed a fine near molecular size network arrangement of Col IV on hydrophilic glass which turns into a relatively thicker – growing in size – polygonal network on hydrophobic ODS consisting of molecular aggregates. We further compared the biological activity of these surface-induced differently assembled Col IV layers following the interaction with human umbilical vein endothelial cells (HUVEC). We found that cells attach less efficiently on hydrophobic ODS, while the fine Col IV network on hydrophilic substrata support HUVEC interaction involving both $\alpha 1$ and $\alpha 2$ integrins. Details of this study are presented below.

Material and Methods

Preparation of hydrophilic and hydrophobic surfaces

To render the surface hydrophilic, glass coverslips (22x22 mm, Fisher Bioblock, Thermo Fisher Scientific, Waltham, MA, USA) were cleaned in an ultrasonic bath for 10 min in a 1:1 mixture of 2-propanol and tetrahydrofuran. The samples were then exposed to piranha solution (30% (v/v) H_2O_2 and 70% (v/v) H_2SO_4) for 30 min followed by a copious rinsing with milliQ water (18.2 M Ω) and dried.

A hydrophobic surface was prepared according to a previously described protocol (Gustavsson *et al.*, 2008) using an organosilane trichloro-(octadecyl)-silane (ODS) purchased from Sigma (St. Louis, MO, USA) (Cat. No 104817). Before silanization the samples were pre-cleaned as above and then placed in a solution containing 12.5 ml of carbon tetrachloride, 37.5 ml of heptane and 220 μ l ODS. The samples were left in this solution for 18 min at room temperature and the excess of silane was washed away with pure heptane. Samples were then heated for one hour at 80°C.

The wettability of surfaces was estimated with water contact angle measurements using sessile drop technique performed on Dataphysics Contact Angle Systems OCA15. Average values were obtained from at least ten different samples.

Quantification of adsorbed FITC-Collagen IV

The adsorption of FITC-Collagen IV was quantified by NaOH extraction of the protein as described previously (Gustavsson *et al.*, 2008). Briefly, the model surfaces were cleaned with distilled water in an ultrasonic bath. The triplicate samples were dried and coated for 30 min at 37°C with DQTM Collagen type IV (Molecular Probes, Eugene, OR, USA; Cat. No D-12052) from human placenta that was fluorescein isothiocyanate conjugated (FITC-Col IV) and dissolved in phosphate-buffered saline (PBS) at the indicated concentrations. After coating at 37°C the samples were rinsed three times with PBS and dried. The adsorbed FITC-Col IV was extracted with 250 μ l of 0.2M NaOH for 2h at room temperature. The fluorescent intensity of the extracts were measured with a fluorescent spectrophotometer (Horiba-Jobin Yvon, Edison, NJ, USA), set to 488 nm (excitation) and 530 nm (emission) and compared to a standard curve based on known concentrations of FITC-Col IV solutions in 0.2M NaOH.

Atomic force microscopy

We have used the AFM type NanoScope III from Digital Instruments (Santa Barbara, CA, USA) to follow the Col IV adsorption profile and the morphology of the adsorbed protein layer operating in the tapping mode in air. Si cantilevers from Veeco (Manchester, UK) were used with a force constant of 2.8N/m and a resonance frequency of 75 kHz. The phase signal was set to zero at the resonance frequency of the tip. The tapping frequency was 5-10% lower than the resonance frequency. Drive amplitude was 200 mV and the amplitude set-point A_{sp} was 1.4V. The ratio between the amplitude set-point and the free

amplitude was kept equal to 0.7. Several AFM images were analyzed using the WSxM software (Nanotec, Madrid, Spain) to observe the topography of non coated surfaces, as well as, the typical protein distribution on the different substrata.

Cells

Human Umbilical Vein Endothelial Cells (HUVEC) purchased from PromoCell (Heidelberg, Germany; Cat No C-12200) were cultured in Endothelial Cell Growth Medium (PromoCell, Cat No C-22010) supplemented with SupplementMix (PromoCell Cat No C39215) containing 0.4% ECGS/H; 2% Fetal Calf Serum, 1 ng/ml Epidermal Growth Factor, 1 µg/ml hydrocortison and 1 ng/ml basic fibroblast factor. For the experiments the cells were detached from around confluent flasks with Trypsin/EDTA (Invitrogen, Carlsbad, CA, USA) and the remaining trypsin activity was stopped with 100% fetal bovine serum (FBS) before 2 times washing with medium without supplements. Finally the cells were counted and reconstituted in serum free EC medium.

Overall cell morphology

To study the overall cell morphology of adhering HUVEC the cells were stained for actin. For that purpose, 10^5 cells/well were seeded in 6 well TC plates (Costar, Corning, Lowell, MA, USA) containing the samples for 2h in serum free medium. Typically, the samples had been pre-coated with native Col IV (Abcam, Cambridge, UK; Cat. No ab7536,) at a concentration of 50 µg/ml in 0.1M sodium acetate pH 4.5. At the end of incubation, the cells were fixed with 4% paraformaldehyde (10 min) and permeabilized with 0.5% Triton X-1000 for 5 min. Actin cytoskeleton was visualized with 20 µg/ml AlexaFluor 488 phalloidin (Molecular Probes, Eugene, OR; Cat No A12379) in PBS, and finally mounted in Mowiol (Polysciences, Warrington, PA, USA. In some cases phalloidin was added to the secondary antibody solution (e.g., for vinculin staining – see below). The samples were viewed and photographed at 10x objective on a fluorescent microscope (Nikon Eclipse E800; Nikon, Tokyo, Japan) where at least 3 representative images were acquired.

Quantification of cell adhesion and spreading

Morphological parameters such as number of adhering cells and mean cell surface area were evaluated using the Image J plug-ins (NIH, Bethesda, USA; <http://rsb.info.nih.gov/ij/>). The adhesion was measured by counting the cells in 3 randomly chosen images of actin stained samples to obtain the number of cells per cm². Data were collected from at least 3 independent experiments and the average cell area was further measured for each individual image (in µm²), and calculated for each condition.

Statistical analysis was performed with ANOVA software using multiple comparison Fisher's test to determine statistically significant differences between groups ($p < 0.05$). Each data point represents mean \pm standard deviation (SD) for at least three independent experiments.

Immunofluorescence

Visualization of focal adhesion contacts. 1×10^5 cells/well were seeded as described above on native Col IV coated model surfaces for 2h in serum free medium. To visualize focal adhesions fixed and permeabilized samples were saturated with 1% albumin in PBS for 15 min. Vinculin was visualized using monoclonal anti-vinculin antibody (Sigma, Cat No V9131) dissolved in PBS-1% albumin for 30 min followed by Cy3-conjugated Affini-Pure Goat Anti-Mouse IgG (H+L) (Jackson ImmunoResearch, Newmarket, Suffolk, UK, Cat. No 115-165-062) as secondary antibody. The samples were viewed and photographed in a fluorescent microscope Nikon at high magnification (100x). At least 3 representative images were acquired for each experimental condition.

Visualization of $\alpha 1$ and $\alpha 2$ integrins was performed with monoclonal anti-human integrin alpha-1 (Chemicon, Cat No MAB1973; Millipore, Billerica, MA, USA) or alpha-2 (Abcam, No Ab24697) also for 30 min followed by Cy³-conjugated Goat Anti-Mouse IgG (H+L) (Jackson ImmunoResearch, No 115-165-062) as secondary antibody.

Results

Characterization of surfaces

The data presented in Table 1 show a significant increase of water contact angle (WCA⁰) after coating the glass with ODS. Both advancing and receding WCA⁰ were found to increase about 4 times ($p < 0.05$) on ODS confirming the strongly hydrophobic nature of this surface. At the same time an approximately doubled average roughness was measured by AFM on plain ODS in comparison to glass (both substrata non-coated with protein), as shown in Table 2 (left column "Plain"), confirming the homogenous coating of the surface with the silane.

Quantification of adsorbed FITC-Collagen IV

FITC-Col IV adsorption from solutions with different concentration was determined by comparison of extracted fluorescence signals to a standard curve with known FITC-Col IV concentrations (see Methods section). Detectable values were obtained for each concentration (Fig. 1). Both substrata show typical saturation curves at approximate concentrations of 50 µg/ml. ODS surfaces, however, demonstrated significantly higher signal showing about twice more adsorbed protein for each concentration.

Table 1. Values for advancing and receding WCA of model hydrophilic and hydrophobic surfaces.

Surface	Water Contact Angle	
	Advancing	Receding
Hydrophilic	25.4 \pm 7.0	18.6 \pm 8.0
Hydrophobic ODS	103.3 \pm 3.2	96.9 \pm 6.6

The measurements were made on 10 samples in triplicates.

Table 2. Average roughness and height of the model surfaces characterized by AFM

Surface	Non-coated		Col IV-coated	
	Average roughness	Average height	Average roughness	Average height
Hydrophilic	0.79 ± 0.01	2.05 ± 1.80	1.11 ± 0.17	3.93 ± 0.32
Hydrophobic ODS	1.59 ± 0.05	5.38 ± 0.79	4.38 ± 0.33	17.88 ± 2.80

The values were obtained with Roughness analysis tool on the WSX software using at least three scans of 1µm² for each model surface.

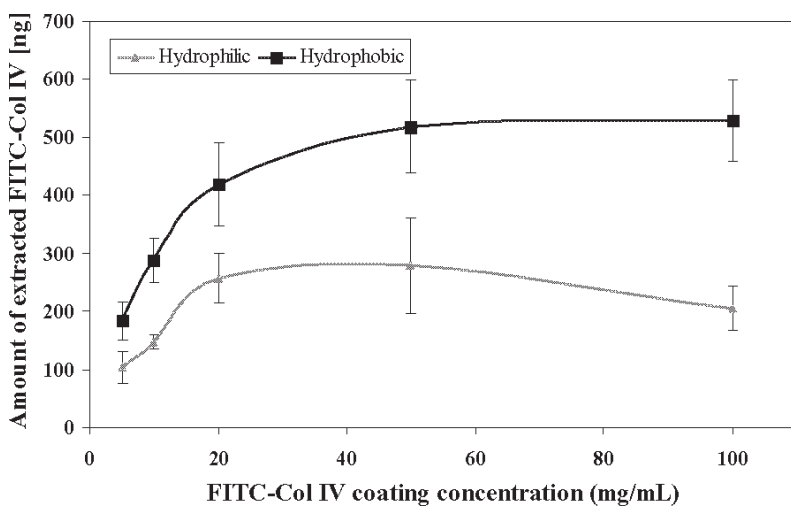


Fig. 1. Adsorption profile of FITC-Col IV on model hydrophilic and hydrophobic ODS surfaces. Triplicate measurements of extracted fluorescence were done for both substrates at different coating concentrations and the values calibrated to a standard curve with known FITC-Col IV concentration.

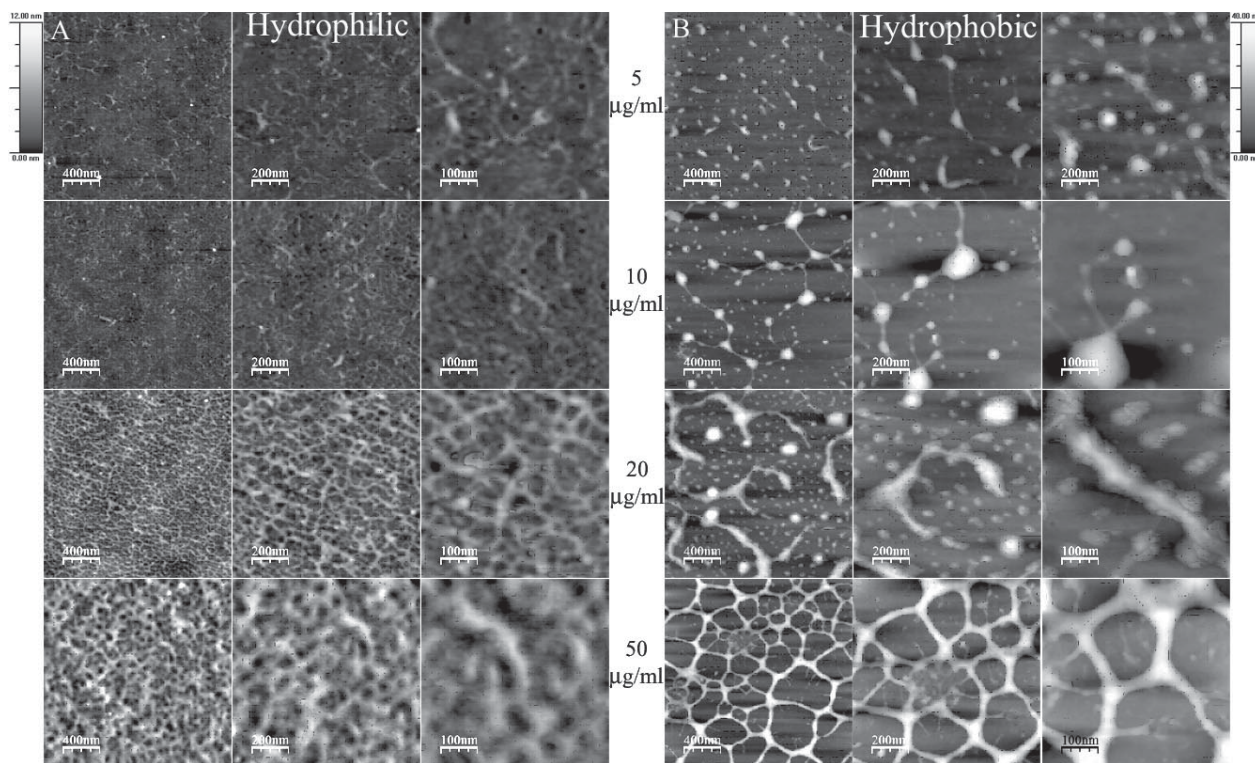


Fig. 2. AFM images of adsorbed native collagen type IV to hydrophilic (A) and hydrophobic (B) surfaces. Adsorption concentration increases from up to down and magnification increases from left to right.

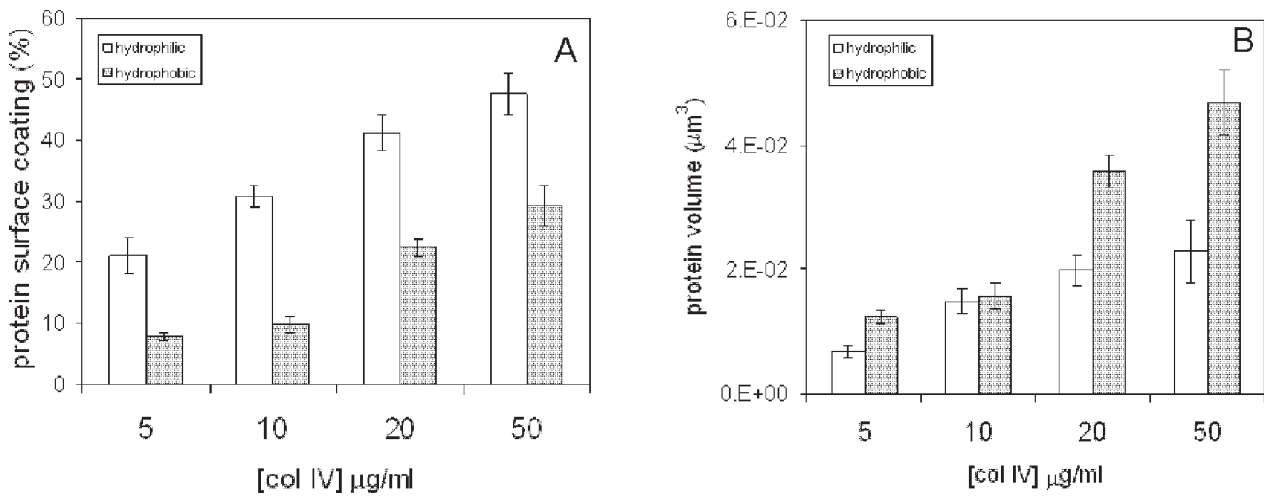


Fig. 3. Fraction of substrate covered by the protein as a function of the concentration of the initial solution (A). Collagen tends to cover larger areas on the hydrophilic than on the hydrophobic substrate. Total volume occupied by the protein on a 2x2 cm² area of the substrate (B). The total volume occupied by the protein on the hydrophobic surface is higher than on the hydrophilic one.

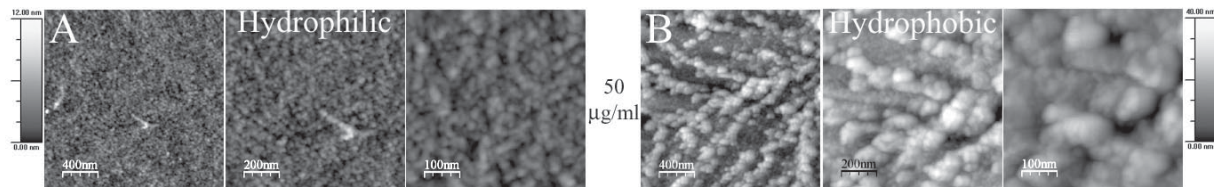


Fig. 4. AFM images of adsorbed native collagen type IV to hydrophilic (A) and hydrophobic (B) surfaces at adsorption concentration was 50 μg/ml for 30 minutes.

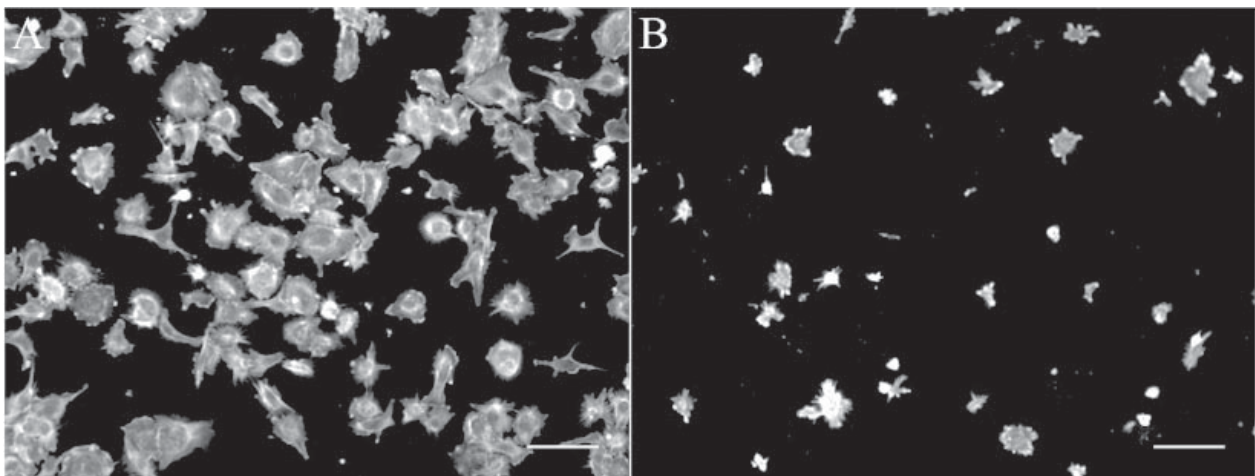


Fig. 5. Overall morphology of HUVEC adhering on native Col IV coated hydrophilic (A) and hydrophobic ODS (B) surfaces. The cells were stained for actin. Bar = 100 μm.

Atomic force microscopy

In the tapping mode of AFM, the cantilever oscillates with the probing tip close to its free resonance frequency at a given amplitude. The interaction between the sample and the probe gives rise to a shift in the probe vibration respective to that measured in a free oscillation, i.e., with the probe far away from the sample. The vertical displacement (height) needed to keep the set amplitude provides information about topography of the system. On the other hand, the measured phase shift may be caused by variation in the viscoelastic properties in different parts (or phases) of the sample, and in this sense it can provide some information about the morphology of the system.

However, differences in phase lag may be caused by geometric features such as edges, and can be a mere reflection of the topography of the system. There are several strategies for programming the apparatus parameters to obtain both accurate surface topographies (height) and morphologies (phase). Recent studies have shown that only when the amplitude of the vibrating cantilever is programmed to be equal to that of the free cantilever, does the height of the topography represent a true surface topography, and that a much harder tapping is necessary to observe maximum phase shift contrast between stiff and soft regions of the material (Rodríguez Hernandez *et al.*, 2007).

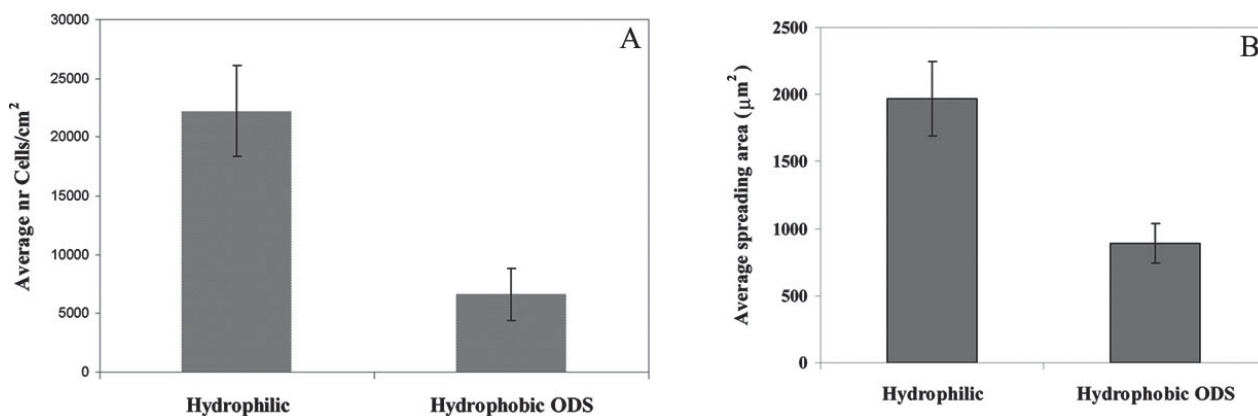


Fig. 6. Quantification of cell adhesion expressed as number of cells per cm² (A) and the average spreading area measured in mm² (B) to hydrophilic and hydrophobic Col IV coated surfaces.

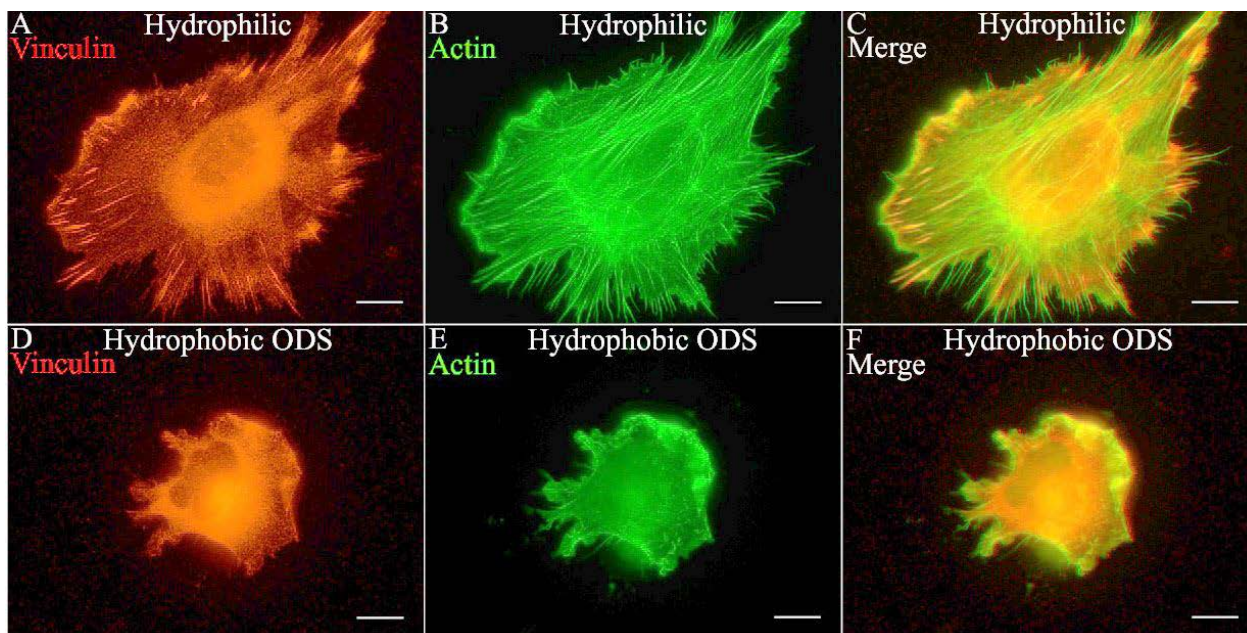


Fig. 7. Development of focal adhesions contacts and actin stress fibers of HUVEC seeded on Col IV coated hydrophilic (A, B, C) and hydrophobic ODS (D, E, F) surfaces. Bar = 10 µm.

Fig. 2 shows the complex AFM images of native Col IV adsorbed for 10 min at acidic conditions (0.1 M Na acetate, pH 4.5) on hydrophilic (Fig. 2A) and hydrophobic ODS (Fig. 2B) model substrates. Overall, the organization of collagen layers changes as function of the concentrations from which the protein is adsorbed increasing as 5, 10, 20 and 50 µg/ml (from top to bottom). At lowest coating concentration of 5 µg/ml, mainly single, isolated features was found on both substrates, representing elongated fibril-like morphology on hydrophilic glass (Fig. 2A) and rather globular clusters on ODS (Fig. 2B). At 10 µg/ml these structures enlarge on the hydrophobic substrate and tend to connect to each other (on both substrata) suggesting the initial formation of intermolecular links, i.e., the establishment of protein-protein contacts through the surface. Further increase of the coating concentrations results in the formation of networks on both surfaces, which again differ significantly in morphology. On hydrophilic glass, AFM revealed formation of a thin protein network with nearly single molecule size (see the gray scale bar) tending to cover the surface. The average height of the

layers quantified using WSxM software was 3.93 ± 0.32 nm (see Table 2 right column entitled “Col IV coated”), which confirms the single molecule arrangement of the network. Conversely, on ODS the thickening of the observed fibril-like structures make rise to a prominent protein network (Fig. 2B, see 20 µg/ml and 50 µg/ml) consisting of well-defined interconnected fibrils arranged in polygonal features with 300-400 nm long arms and about 20 nm thick. More precise WSxM measurements revealed that the average height of the layer amounted to 17.9 ± 2.8 nm (see Table 2, right column), which suggests the formation of supramolecular aggregates.

Considering the fact, that the non-homogenous distribution of the observed features could influence the biological activity of the protein (e.g., the accessibility to the cells) we measured the fraction of substrate covered by protein as a function of the concentration of the adsorbing protein (Fig. 3A). A significantly lower coverage of the surface was found on ODS (approx. 30%) *versus* glass (50%) at all concentrations. Nevertheless, the total volume of the adsorbed protein (Fig. 3B) was also

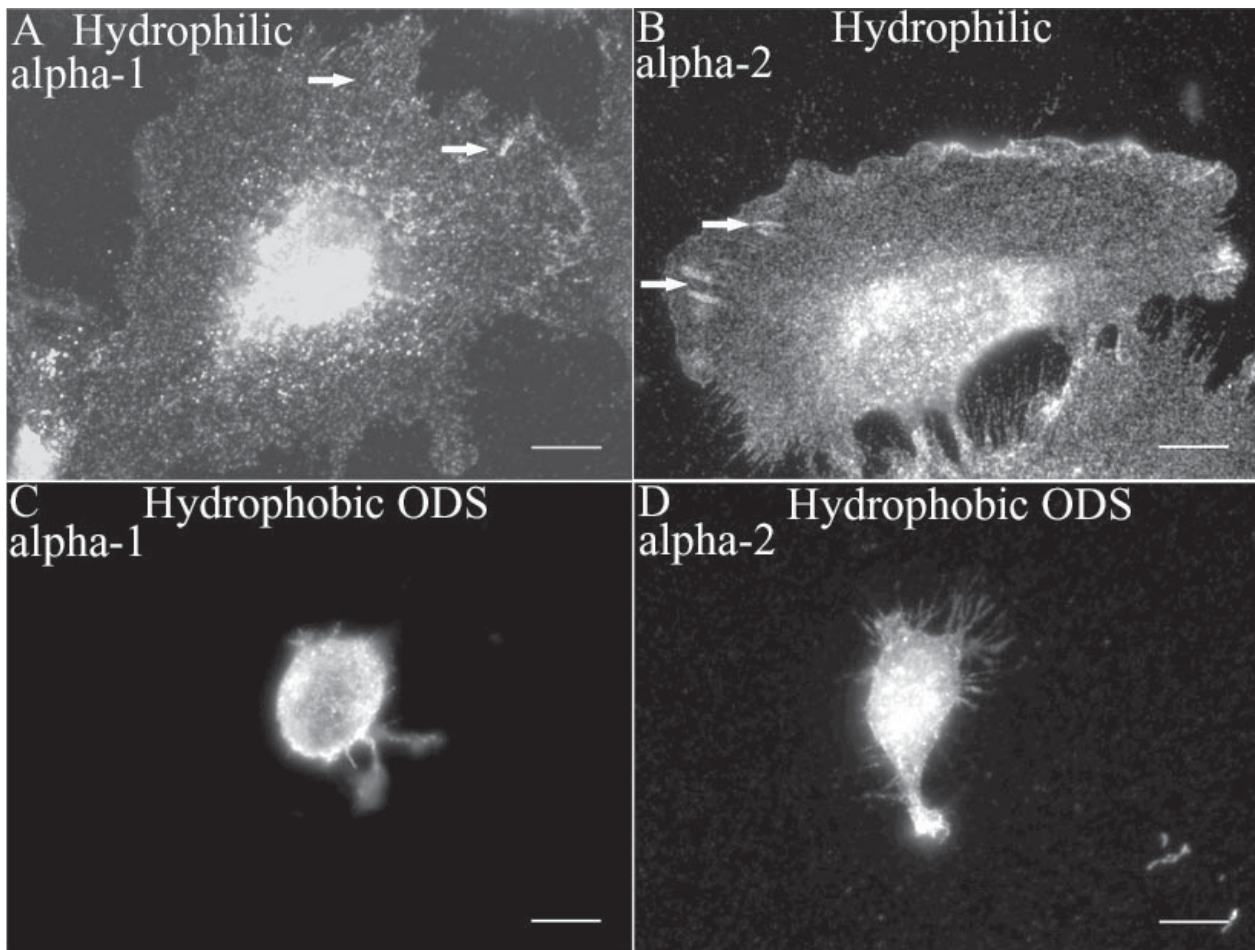


Fig. 8. Expression of alpha 1 (A, C) and alpha 2 (B, D) integrins in HUVEC adhering on hydrophilic (A, B) and hydrophobic ODS (C,D) surfaces coated with Col IV. Bar =10 μ m.

significantly higher on the hydrophobic surface (approximately twice) than on the hydrophilic one, confirming the same trend for different adsorption of Col IV, particularly at near saturation concentrations (Fig. 1).

For the biological studies we have used conditions for Col IV adsorption (e.g., a saturating concentration of 50 μ g/ml for 30 min at pH 4.5), that have been previously established (Maneva-Radicheva *et al.*, 2008; Tuckwell *et al.*, 1994). The organization of the thus deposited protein layer on both hydrophilic and hydrophobic substrata is shown in Fig. 4. Overall, we found more protein bound to the surfaces although the same pattern of deposition was observed on hydrophilic glass (Fig. 4A). Predominantly multilayer-globular aggregates however appeared on hydrophobic ODS (Fig. 4B), obviously because the protein-protein interactions are favored on this surface. This results initially in a network thicker than a single molecule (seen in Fig. 2B, after 10 min), giving rise to globular aggregates growing afterwards on the top (Fig. 4B, after 30 min). Presumably the network is not seen at later times because several superimposed layers of protein are scanned.

Cell adhesion and spreading

The overall morphology of HUVEC adhering on Col IV coated hydrophilic and hydrophobic ODS substrates is shown in Fig. 5 (A and B, respectively). Generally less cell adhesion and delayed cell spreading were observed

on hydrophobic ODS (Fig. 5B); the cells were round and smaller apart from hydrophilic glass where they display a typical flattened morphology (Fig. 5A). Image J software was used to quantify the morphological observations. Fig. 6 shows that both the amount of adhering cells (Fig. 6A) and the cell spreading area (Fig. 6B) differ significantly ($p < 0.05$) between Col IV coated ODS and glass samples. On later approximately 3 times more cells and with about doubled main surface area (in comparison to ODS) are found. On non-coated hydrophilic and hydrophobic surfaces only negligible adhesion and spreading were observed (not shown).

To learn more about the effectiveness of cell adhesion to Col IV the focal contacts were visualised via vinculin together with actin cytoskeleton (Fig. 7). More flattened and elongated cells on glass represented well developed focal adhesion contacts (Fig. 7A) where prominent stress fibres of the actin cytoskeleton often insert (Fig. 7B), better seen on merged images (Fig. 7C). Conversely, on hydrophobic ODS round shaped cells with almost missing focal adhesion complexes (Fig. 7D) and less developed actin cytoskeleton (Figs. 7E and 7F) were typically observed.

Distribution of $\alpha 1$ $\alpha 2$ integrins

To learn which integrins are involved in the adhesion of HUVEC to Col IV we studied the expression and functional organization of both $\alpha 1$ and $\alpha 2$ subunits,

representing the most abundantly expressed collagen receptor heterodimers $\alpha 1\beta 1$ and $\alpha 2\beta 2$ (Hynes, 2002; Khoshnoodi *et al.*, 2008). As shown in Fig. 8 both integrins were found to cluster pronouncedly on hydrophilic substrata (Fig. 8A and B), but $\alpha 2$ (Fig. 8B) tends to localize in the focal adhesion complexes (arrows) while $\alpha 1$ is more diffusely organized (Fig. 8A) in dot-like contacts. Conversely, the almost missing $\alpha 1$ and $\alpha 2$ integrin organization on ODS (Figs. 8C and D, respectively) correlates well with the observed absence of adhesive complexes in HUVEC on the same substratum (Fig. 7D).

Discussion

This study is consistent with the emerging field of tissue engineering aimed at reproducing the functional architecture of BM, and particularly the BM of vascular tissue. More specifically, we investigated the fate of exogenously added type IV collagen on model biomaterial surfaces to learn more about the role of substratum hydrophobicity in its biological performance. We further address the interaction with endothelial cells, considering their important role in the physiology of the vessel wall, aiming to understand their behaviour in contact with foreign materials interfaces. While EC procurement technologies for seeding blood-contacting devices have significantly improved, adhered cells often dedifferentiate or detach which accelerate device failure. We anticipate as a possible reason could be the missing environmental signals from the BM, which in turn, might be reproduced on the biomaterials interface.

Wettability has long been recognized as an important surface parameter for the materials biocompatibility (Grinnell and Feld, 1982; Altankov *et al.*, 1997; Rodriguez Hernandez *et al.*, 2007). In general, hydrophilic surfaces support cellular interaction, fact usually attributed to appropriate conformation of adsorbed adhesive proteins (Grinnell and Feld, 1982; Altankov *et al.*, 1997; Kowalczyńska *et al.*, 2005; Rodriguez Hernandez *et al.*, 2007). However, this is not always straightforward since materials with very high wettability, which bind much water like hydrogels, do not support protein adsorption and cell adhesion (Tamada and Ikada, 1994; Gugutkov *et al.*, 2010). However, gels from natural polymers like collagen, gelatin or fibrin are good substrata for cell attachment (Brown *et al.*, 2006; Daley *et al.*, 2008) and work well also in adsorbed state (Tamada and Ikada, 1994; Ludwig *et al.*, 2006). Conversely, strongly hydrophobic surfaces may support cell adhesion, for example, due to the spontaneous protein network assembly (Gurdak *et al.*, 2006; Rodriguez Hernandez *et al.*, 2007; Gugutkov *et al.*, 2009; Gugutkov *et al.*, 2010). Col IV cannot form gels as it is not fibrillar protein, but it strongly promotes cell adhesion through binding to $\alpha 1\beta 1$ integrin via sequence localized in a spatial vicinity of Asp461 on $\alpha 1(IV)$ chain and Arg461 on $\alpha 2(IV)$ chain (Tuckwell *et al.*, 1994), or via $\alpha 2\beta 1$ integrins which recognize the GFOGER motif in the αI domain (Knight *et al.*, 1998; Zhang *et al.*, 2003). The role of substratum wettability for Col IV assembly

and its subsequent biological recognition is not clear, although some recent studies describe the surface arrangement of fibrillar type I collagen (Dupont-Gillain *et al.*, 2005; Gurdak *et al.*, 2006; Keresztes *et al.*, 2006). Our results show that adsorption of FITC-Col IV is strongly dependent on substratum wettability. It reaches saturation at approximately 50 $\mu\text{g}/\text{ml}$ coating concentration, for both kind of surfaces, although the hydrophobic ODS represents significantly higher adsorption, approximately twice in comparison to glass. Further increase of coating concentration or increasing the coating time lead to the additional formation of molecular aggregates as we found for ODS (Fig. 4) which also increased the extracted fluorescence signal with about 30% at concentration 200 $\mu\text{g}/\text{ml}$ (not shown). This result is not surprising since many proteins represent stronger adsorption to hydrophobic substrata due to the polar interactions (Grinnell and Feld, 1982), although, this is often not in correlation with their biological activity. As labeling of Col IV with FITC could interfere its native configuration, we studied the adsorption pattern of native (acid soluble) Col IV with AFM. The results confirmed the above difference as about twice higher volume of adsorbed protein was found on ODS, but also showed that Col IV tends to arrange in a different pattern: a fine near single molecular network on hydrophilic substrata which turn to much thicker polygonal network arrangements on hydrophobic ODS. This fact suggests that Col IV has different affinity depending on the substratum hydrophobicity. As Col IV molecules arrives to the surface, adsorption takes place on the hydrophilic substrate up to forming a single monolayer of protein that maintains even after long-term adsorption (Fig. 4) suggesting a conformation of the protein with diminished inter-molecular interaction; whereas, on the hydrophobic ODS, once a few molecules are adsorbed on the surface, the newly arriving ones from the solution tend to form multilayer aggregates rather than occupying empty space on the substrate. This points to the possibility that the molecular conformation of the protein is different on each surface, since only ODS favors the formation of multiple protein layers. Moreover, it is suggested that protein-protein contacts are favored on the hydrophobic ODS which results, first in a thicker than molecular size network (Fig. 2) and afterwards – in the long term – giving rise to multilayer-adsorption of the protein in the form of aggregates after the substrate's surface is covered (Fig. 4B).

Type IV collagen molecules are heterotrimers of about 390 nm long composed of three alpha chains existing in six genetically distinct forms. *In vivo* these isoforms organize into a unique network that provides BM specificity (Hudson *et al.*, 1993). Assembly of type IV collagen is initiated by the formation of protomers (Timpl *et al.*, 1985; Siebold *et al.*, 1988) where three alpha chains associate through their non-collagenous domains before folding into a triple helices (Timpl *et al.*, 1985; Hudson *et al.*, 1993). The lateral association of the triple helix, the covalent binding of 7S domains and the association of alpha chains at the NC1 domains are essential for the formation of the protomeric network that serves as a

scaffold for BM constituents. AFM studies revealed spontaneous *in vitro* assembly of Col IV in di- and tetramers upon adsorption to mica (Chen and Hansma, 2000), which suggest a similar assembly of Col IV in our conditions. At least it is the case at the hydrophilic interface, where both globular and linear fibril-like features are visible at low coating concentration (Fig. 2A upper row). But the study also showed that at higher concentration, Col IV molecules assemble in a fine network that tends to cover the surface. The size of these linear structures is in the range of 300–400 nm in length and of about 3–4 nm thick suggesting a single molecule arrangement.

Another novel observation in this study is that on hydrophobic environment Col IV assemble in a completely different way. Depending on the concentration it may represent single globular aggregates, which tend to connect over the substratum as the concentration increases. Thus at coating concentration of 50 µg/ml these aggregates already form a well-established network where globular features disappear on early stages of adsorption. This suggests a non-physiological molecular arrangement. Moreover, the average height of the layer is 17.9 ± 2.8 nm (see Table 2) confirming the formation of supra molecular aggregates which obviously become globular at longer adsorption time (Fig. 4). Interestingly, although the amount of adsorbed protein is about twice as high on hydrophobic ODS, obtained by both extracted fluorescence and AFM approaches, the ratio of the occupied surface area on AFM images is significantly less, i.e. about 30% from the total substratum area is covered in comparison to 50% for glass – a fact again suggesting stronger intermolecular interaction.

An important question is how the observed difference in the organization of self-assembled Col IV layer affects its biological performance. It is well documented that protein adsorption depends on the surface properties which produces great impact on the cellular interaction (Altankov *et al.*, 2000; Keselowsky *et al.*, 2003; Lan *et al.*, 2005). Here we found that significantly increased Col IV adsorption on hydrophobic ODS does not support cellular interaction, a fact observed also for other matrix proteins (Grinnell and Feld, 1982; Tzoneva *et al.*, 2002) and cell systems (Grinnell and Feld, 1982). The initial adhesion of HUVEC was strongly altered on ODS accompanied with delayed cell spreading and nearly absent focal adhesion complexes. This points to the possibility that aggregated conformation of adsorbed Col IV is less recognizable for the cells, which correlates with the altered development of actin cytoskeleton and integrin clustering. That is to say, the different patterns observed by AFM must be linked to the reduced availability of the binding site for both $\alpha 1$ and $\alpha 2$ integrins located most probably approximately 100 nm away from the amino-terminus within cyanogen bromide fragment CB3 (Timpl *et al.*, 1985; Hudson *et al.*, 1993; Khoshnoodi *et al.*, 2008). But even in the case that adsorption of Col IV on hydrophobic substrates took place in a conformation that allowed adequate CB3 exposition its density would not be enough since most of the domains must be hidden due to lateral interactions between chains. This is obviously not the case on hydrophilic substrata

because of the single molecule distribution of adsorbed Col IV layer (Fig. 2A). We found also higher accumulation of $\alpha 1$ and $\alpha 2$ integrins on hydrophilic glass and despite the observation that $\alpha 2$ tend to localize in focal adhesion complexes while $\alpha 1$ is more diffusely organized, this suggests stronger involvement of both $\alpha 1\beta 1$ and $\alpha 1\beta 2$ collagen receptors in EC spreading under these conditions. Although data exist for predominant recognition of Col IV by $\alpha 1\beta 1$ integrin (Gardner *et al.*, 1996) other authors state that Col IV express additionally two binding sites for $\alpha 2$ integrins (Kern *et al.*, 1993) which could well explain the observed agonistic expression of $\alpha 1$ and $\alpha 2$ subunits. But why they organize differently during endothelial cells spreading in hydrophilic environments remains unclear. Nevertheless, both integrins looked inactive on hydrophobic surfaces as no organization was found suggesting very low specific recognition of adsorbed Col IV by HUVEC.

Conclusion

A novel observation in this study is the different substratum-induced assembly of Col IV on hydrophilic and hydrophobic environment, a nearly single molecular network arrangement on hydrophilic glass and prominent polygonal network consisting of molecular aggregates on hydrophobic ODS surface. We further found that endothelial cell attach less efficiently to the aggregated form of Col IV, although twice as much adsorbed protein was observed, while the fine Col IV network on hydrophilic substrata is well recognized by the cells via both $\alpha 1$ and $\alpha 2$ integrins. Thus, the material surface wettability appears to be a powerful tool for tailoring the appropriate arrangement of Col IV on foreign materials interface, particularly applicable in vascular tissue engineering.

References

- Altankov G, Grinnell F, Groth T (1996) Studies on the biocompatibility of materials: fibroblast reorganization of substratum-bound fibronectin on surfaces varying in wettability. *J Biomed Mater Res* **30**: 385-391.
- Altankov G, Groth T (1996) Fibronectin matrix formation by human fibroblasts on surfaces varying in wettability. *J Biomater Sci Polymer Ed* **8**: 299-310.
- Altankov G, Groth T, Krasteva N, Albrecht W, Paul D (1997) Morphological evidence for a different fibronectin receptor organization and function during fibroblast adhesion on hydrophilic and hydrophobic glass substrata. *J Biomater Sci Polymer Ed* **8**: 721-740.
- Altankov G, Thom V, Groth T, Jankova K, Jonsson G, Ulbricht M (2000) Modulating the biocompatibility of polymer surfaces with poly(ethylene glycol): effect of fibronectin. *J Biomed Mater Res* **52**: 219-230.
- Brown B, Lindberg K, Reing J, Stolz DB, Badylak SF (2006) The basement membrane component of biologic scaffolds derived from extracellular matrix. *Tissue Eng* **12**: 519-526.

- Charonis A, Sideraki V, Kaltezioti V, Alberti A, Vlahakos D, Wu K, Tsilibary E (2005) Basement membrane peptides: functional considerations and biomedical applications in autoimmunity. *Curr Med Chem* **12**: 1495-1502.
- Chen CH, Hansma HG (2000) Basement membrane macromolecules: insights from atomic force microscopy. *J Struct Biol* **131**: 44-55.
- Daley WP, Peters SB, Larsen M (2008) Extracellular matrix dynamics in development and regenerative medicine. *J Cell Sci* **121**: 255-264.
- Dupont-Gillain CC, Jacquemart I, Rouxhet PG (2005) Influence of the aggregation state in solution on the supramolecular organization of adsorbed type I collagen layers. *Colloids Surf B Biointerfaces* **43**: 179-186.
- Gardner H, Kreidberg J, Koteliensky V, Jaenisch R (1996) Deletion of integrin $\alpha 1$ by homologous recombination permits normal murine development but gives rise to a specific deficit in cell adhesion. *Dev Biol* **175**: 301-313.
- Gelse K, Poschl E, Aigner T (2003) Collagens – structure, function, and biosynthesis. *Adv Drug Deliv Rev* **55**: 1531-1546.
- Griffith LG, Naughton G (2002) Tissue engineering – current challenges and expanding opportunities. *Science* **295**: 1009-1014.
- Grinnell F, Feld MK (1982) Fibronectin adsorption on hydrophilic and hydrophobic surfaces detected by antibody binding and analyzed during cell adhesion in serum-containing medium. *J Biol Chem* **257**: 4888-4893.
- Gugutkov D, Gonzalez-Garcia C, Rodriguez Hernandez JC, Altankov G, Salmeron-Sanchez M (2009) Biological activity of the substrate-induced fibronectin network: insight into the third dimension through electrospun fibers. *Langmuir* **25**: 10893-10900.
- Gugutkov D, Altankov G, Rodriguez Hernandez JC, Monleon Pradas M, Salmeron Sanchez M (2010) Fibronectin activity on substrates with controlled – OH density. *J Biomed Mater Res A* **92**: 322-331.
- Gurdak E, Rouxhet PG, Dupont-Gillain CC (2006) Factors and mechanisms determining the formation of fibrillar collagen structures in adsorbed phases. *Colloids and surfaces. B, Biointerfaces* **52**: 76-88.
- Gustavsson J, Altankov G, Errachid A, Samitier J, Planell JA, Engel E (2008) Surface modifications of silicon nitride for cellular biosensor applications. *J Mater Sci Mater Med* **19**: 1839-1850.
- Hudson BG, Reeders ST, Tryggvason K (1993) Type IV collagen: structure, gene organization, and role in human diseases. Molecular basis of Goodpasture and Alport syndromes and diffuse leiomyomatosis. *J Biol Chem* **268**: 26033-26036.
- Hynes RO (2002) Integrins: bidirectional, allosteric signaling machines. *Cell* **110**: 673-687.
- Kapyla J, Ivaska J, Riikonen R, Nykvist P, Pentikäinen O, Johnson M, Heino J (2000) Integrin $\alpha 2$ I domain recognizes type I and type IV collagens by different mechanisms. *J Biol Chem* **275**: 3348-3354.
- Keresztes Z, Rouxhet PG, Remacle C, Dupont-Gillain C (2006) Supramolecular assemblies of adsorbed collagen affect the adhesion of endothelial cells. *J Biomed Mater Res A* **76**: 223-233.
- Kern A, Eble J, Golbik R, Kuhn K (1993) Interaction of type IV collagen with the isolated integrins $\alpha 1$ $\beta 1$ and $\alpha 2$ $\beta 1$. *Eur J Biochem* **215**: 151-159.
- Keselowsky BG, Collard DM, Garcia AJ (2003) Surface chemistry modulates fibronectin conformation and directs integrin binding and specificity to control cell adhesion. *J Biomed Mater Res A* **66**: 247-259.
- Khoshnoodi J, Pedchenko V, Hudson BG (2008) Mammalian collagen IV. *Microsc Res Techn* **71**: 357-370.
- Knight CG, Morton LF, Onley DJ, Peachey AR, Messent AJ, Smethurst PA, Tuckwell DS, Farnsdale RW, Barnes MJ (1998) Identification in collagen type I of an integrin $\alpha 2$ $\beta 1$ -binding site containing an essential GER sequence. *J Biol Chem* **273**: 33287-33294.
- Kowalczyńska HM, Nowak-Wyrzykowska M, Kolos R, Dobkowski J, Kaminski J (2005) Fibronectin adsorption and arrangement on copolymer surfaces and their significance in cell adhesion. *J Biomed Mater Res A* **72**: 228-236.
- Lan MA, Gersbach CA, Michael KE, Keselowsky BG, Garcia AJ (2005) Myoblast proliferation and differentiation on fibronectin-coated self assembled monolayers presenting different surface chemistries. *Biomaterials* **26**: 4523-4531.
- LeBleu VS, Macdonald B, Kalluri R (2007) Structure and function of basement membranes. *Exp Biol Med* **232**: 1121-1129.
- Ludwig NS, Yoder C, McConney M, Vargo TG, Kader KN (2006) Directed type IV collagen self-assembly on hydroxylated PTFE. *J Biomed Mater Res A* **78**: 615-619.
- Maneva-Radicheva L, Ebert U, Dimoudis N, Altankov G (2008) Fibroblast remodeling of adsorbed collagen type IV is altered in contact with cancer cells. *Histology Histopathol* **23**: 833-842.
- Popova SN, Lundgren-Akerlund E, Wiig H, Gullberg D (2007) Physiology and pathology of collagen receptors. *Acta Physiol* **190**: 179-187.
- Rodriguez Hernandez JC, Salmeron Sanchez M, Soria JM, Gomez Ribelles JL, Monleon Pradas M (2007) Substrate chemistry-dependent conformations of single laminin molecules on polymer surfaces are revealed by the phase signal of atomic force microscopy. *Biophys J* **93**: 202-207.
- Siebold B, Deutzmann R, Kuhn K (1988) The arrangement of intra- and intermolecular disulfide bonds in the carboxyterminal, non-collagenous aggregation and cross-linking domain of basement-membrane type IV collagen. *Eur J Biochem* **176**: 617-624.
- Sipe JD (2002) Tissue engineering and reparative medicine. *Ann N Y Acad Sci* **961**: 1-9.
- Tamada Y, Ikada Y (1994) Fibroblast growth on polymer surfaces and biosynthesis of collagen. *J Biomed Mater Res* **28**: 783-789.
- Timpl R, Brown JC (1996) Supramolecular assembly of basement membranes. *BioEssays* **18**: 123-132.
- Timpl R, Oberbaumer I, von der Mark H, Bode W, Wick G, Weber S, Engel J (1985) Structure and biology of the globular domain of basement membrane type IV collagen. *Ann N Y Acad Sci* **460**: 58-72.

Tuckwell DS, Ayad S, Grant ME, Takigawa M, Humphries MJ (1994) Conformation dependence of integrin-type II collagen binding. Inability of collagen peptides to support alpha 2 beta 1 binding, and mediation of adhesion to denatured collagen by a novel alpha 5 beta 1-fibronectin bridge. *J Cell Sci* **107**: 993-1005.

Tzoneva R, Groth T, Altankov G, Paul D (2002) Remodeling of fibrinogen by endothelial cells in dependence on fibronectin matrix assembly. Effect of substratum wettability. *J Mater Sci Mater Med* **13**: 1235-1244.

Vandenberg P, Kern A, Ries A, Luckenbill-Edds L, Mann K, Kuhn K (1991) Characterization of a type IV

collagen major cell binding site with affinity to the alpha 1 beta 1 and the alpha 2 beta 1 integrins. *J Cell Biol* **113**: 1475-1483.

White DJ, Puranen S, Johnson MS, Heino J (2004) The collagen receptor subfamily of the integrins. *Int J Biochem Cell Biol* **36**: 1405-1410.

Zhang WM, Kapyla J, Puranen JS, Knight CG, Tiger CF, Pentikainen OT, Johnson MS, Farndale RW, Heino J, Gullberg D (2003) alpha 11 beta 1 integrin recognizes the GFOGER sequence in interstitial collagens. *J Biol Chem* **278**: 7270-7277.

1.3 Supplementary results 1

Atomic force microscopy

Collagen IV

AFM studies were performed using also a low Col IV adsorption concentration (1 $\mu\text{g/mL}$) on the same model hydrophilic (Figure 1 A) and hydrophobic ODS (Figure 1 B) surfaces. At this concentration, mainly single, isolated features, representing elongated fibril-like morphology on hydrophilic glass (A) and globular clusters on ODS (B) were found.

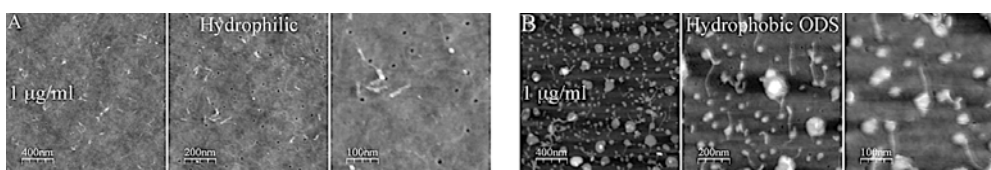


Figure 1 - AFM images of Col IV adsorbed onto hydrophilic (A) and hydrophobic (B) surfaces. Different magnifications (increasing from right to left) are presented. Adsorption concentration is 1 $\mu\text{g/mL}$.

FITC-Collagen IV

AFM studies at two different coating concentrations were also performed to follow the adsorption pattern and the organization of FITC-Col IV layer on the same model surfaces. Figure 2 shows different surface dependent patterns of adsorbed FITC-Col IV resembling network-like structures on hydrophilic glass (A) presumably arranged from single molecules and globular molecular aggregates on hydrophobic ODS (B).

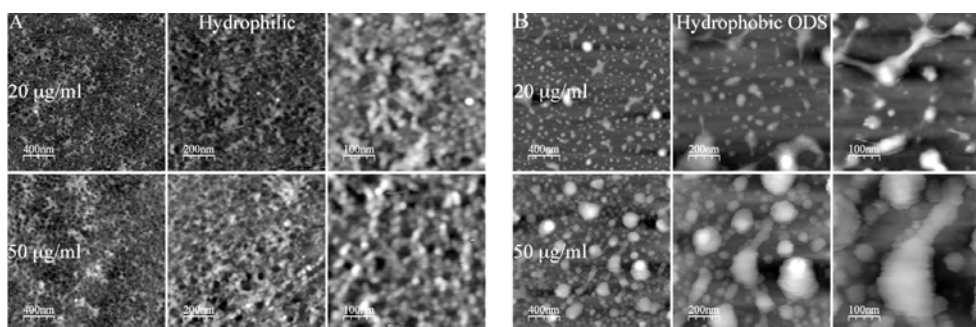


Figure 2 – AFM images of FITC-Col IV adsorbed onto model hydrophilic (glass) and hydrophobic (ODS) surfaces. Two different adsorption concentrations were studied, 20 $\mu\text{g/ml}$ and 50 $\mu\text{g/ml}$ as indicated.

As the coating concentration increases the single molecular arrangements of FITC-Col IV augments on hydrophilic glass (A) while on hydrophobic ODS (B) already bigger molecular aggregates are observed.

2. Arrangement of Type IV Collagen and Laminin on Substrates with Controlled Density of –OH Groups

2.1 Preface 2

Col IV and LAM are the main components of the vascular BM where endothelial cells reside in a rather 2D environment, e.g. in a similar geometry as when adhering to the surface of blood contacting devices, where endothelization is highly desirable. Tailoring the behavior of adsorbed Col IV and LAM on biomaterials interface would provide a powerful tool (from the material site) for maintaining the functional performance of an implant. In the first section we described a distinct phenomenon of material-induced assembly of Col IV on model hydrophilic and hydrophobic substrata. However, except on wettability, the substrata used differ also in their chemistry, which raise some obstacles in the interpretation of results. Here we describe the material-driven arrangements of adsorbed Col IV and LAM in correlation with the biological performance of the adsorbed protein layers formed on model surfaces where fraction of -OH groups vary as an independent parameter. This well defined family of polymer substrates was developed in the Center for Biomaterials and Tissue Engineering at Polytechnic University of Valencia (Professor M. Salmerón-Sánchez group) and successfully used previously for tailoring the adsorption pattern and bioactivity of other ECM proteins, including fibronectin, vitronectin and fibrinogen. In fact, here we extend these studies corroborating them with the substrate behavior of Col IV and LAM as main BM constituents. We tested the biological activity of the adsorbed proteins using again primary endothelial cells.

Our results demonstrate that the adsorption pattern of both Col IV and LAM is strongly dependent on the surface fraction of -OH groups. AFM studies revealed specific substratum-induced assembly of these proteins, from single molecule arrangements to specific networks - the later better pronounced on hydrophobic environment. The initial interaction with endothelial cells surprisingly shows two optima - a hydrophilic ($X_{OH} = 1$) and a hydrophobic one ($X_{OH} = 0.3$) - evaluated by changes in the adhering cells morphology, the quantities of cell adhesion and spreading and the development of focal adhesions and actin cytoskeleton. When both proteins were adsorbed consecutively, a distinct complex morphology of the adsorbed protein layer was observed resulting in a hydrophobic shift in the cellular interaction (to $X_{OH} = 0$). Details of this study are presented in the paper below.

The Supplementary results showed similar trend in the cellular interaction with adsorbed Col IV when higher adsorbing concentration (e.g. saturating) of 50 $\mu\text{g/mL}$ was used. Furthermore we demonstrate that the improved interaction of HUVEC on hydrophilic ($X_{OH} = 1$) and relatively hydrophobic ($X_{OH} = 0.3$) substrates involves the clustering of both α_1 and α_2 integrins.

Arrangement of Type IV Collagen and Laminin on Substrates with Controlled Density of –OH Groups

Nuno Miranda Coelho, (Ph.D. student)^{1,2} Cristina González-García, (Ph.D. student)^{3,4}
Manuel Salmerón-Sánchez, Ph.D.,^{3,4} and George Altankov, M.D., Ph.D.^{1,3,5}

Collagen IV (Col IV) and laminin (Lam) are the main structural components of the basement membrane where they form two overlapping polymeric networks. We studied the adsorption pattern of these proteins on five model surfaces with tailored density of –OH groups obtained by copolymerization of different ratios ethyl acrylate (EA) and hydroxyl EA (HEA): $X_{OH}=0$, $X_{OH}=0.3$, $X_{OH}=0.5$, $X_{OH}=0.7$, and $X_{OH}=1$ (where X refers the ratio of HEA). Atomic force microscopy revealed substratum-specific adsorption patterns of Col IV and Lam, ranging from single molecules deposition on more hydrophilic substrata to the formation of complex networks on hydrophobic ones. Human umbilical endothelial cells were used to study the biological performance of adsorbed proteins, following the overall cell morphology, the quantities for cell adhesion and spreading, and the development of focal adhesion complexes and actin cytoskeleton. Surprisingly, two optima in the cellular interaction were observed—one on the most hydrophilic $X_{OH}=1$ and other on the relatively hydrophobic $X_{OH}=0.3$ substrate—valid for both Col IV and Lam. When the proteins were adsorbed consecutively, a hydrophobic shift to $X_{OH}=0$ substratum was obtained. Collectively, these data suggest that varying with the density of –OH groups one can tailor the conformation and the functional activity of adsorbed basement membrane proteins.

Introduction

TISSUE ENGINEERING STRIVES to replace the damaged tissue with scaffold (colonized or not with cells) that mimics the natural 3D organization of extracellular matrix (ECM).^{1–3} However, the various currently used medical devices such as stents, prosthesis, and metal implants cannot avoid the 2D contact with tissues. Upon implantation they hamper the local organization of ECM and alter the biocompatibility of implant. The initial cellular events that take place at the biomaterials interface mimic to a certain extent their natural interaction with the ECM.^{4–6} Although the cells avoid direct contact with foreign materials, they readily attach to the adsorbed soluble matrix proteins such as fibronectin, vitronectin, fibrinogen, and others,^{3,5} which are uniformly available in the biological fluids. At longer contact with tissues, however, other less soluble ECM proteins such as collagens and Lam may also associate with the biomaterial surface influencing significantly the adjacent cells behavior and function.^{3,7,8} Recently, we are particularly interested on the fate of adsorbed type IV collagen (Col IV) and Lam

considering their important role for the assembly of basement membranes (BM)—a highly specialized ECM common to many types of tissues.⁹ The BM provides underlinement for the organ-specific cells supporting their functional organization.¹⁰ Consequently, the biohybrid organ technologies require construction of modules based on membranes in order to mimic the spatio-temporal organization and permeability of BM.^{3,11} However, despite the extensive studies on the role of BM components in various physiological and pathological conditions—ranging from the early development, wound healing, and angiogenesis,¹² to the atherosclerosis, tissue fibrosis, and cancer^{13,14}—our knowledge on the behavior of Col IV and Lam at biomaterials interfaces is limited. Making use of atomic force microscopy (AFM) we recently described a distinct phenomenon of material-induced assembly of Col IV on model hydrophilic and hydrophobic substrata.¹⁵ We found a spontaneous formation of a fine network on hydrophilic glass and a prominent polygonal network on hydrophobic octadecylsilane (ODS) that alters significantly Col IV activity.¹⁵ However, except on wettability the substrata we used differ in their chemistry,

¹Institut de Bioenginyeria de Catalunya, Barcelona, Spain.

²Universitat Politècnica de Catalunya, Barcelona, Spain.

³CIBER de Bioingeniería, Biomateriales y Nanomedicina (CIBER-BBN), Valencia, Spain.

⁴Center for Biomaterials, Universidad Politècnica de Valencia, Valencia, Spain.

⁵ICREA (Institució Catalana de Recerca i Estudis Avançats), Catalonia, Spain.

which rise obstacles for interpretation of results. Moreover, we did not consider the behavior of the other main BM player—the Lam—particularly in conditions where both proteins are adsorbed. Therefore, here we describe the material-driven arrangements of adsorbed Col IV and Lam on model surfaces¹⁶ where fraction of –OH groups vary as an independent parameter. Using this well-defined family of polymer substrata,¹⁶ we recently described the adsorption pattern of various ECM proteins, including fibronectin,¹⁷ vitronectin,¹⁸ and fibrinogen,¹⁹ showing that it may strongly influence their biological activity.^{16–18} Here we extend these studies corroborating the substrate behavior Col IV and Lam as main BM constituents. To follow their biological performance we choose primary endothelial cells considering their role for the functional organization of vascular BM and their involvement in the neovascularization^{3,11} both events critically important for most tissue engineering applications.^{11,12}

Here we demonstrate that the adsorption patterns of both Col IV and Lam are strongly dependent on the surface fraction of –OH groups. AFM studies revealed specific substratum-induced assembly of these proteins, from single molecule arrangements to the specific networks—the later better pronounced on hydrophobic environment. The initial interaction of endothelial cells surprisingly shows two optima—a hydrophilic ($X_{OH}=1$) and a hydrophobic one ($X_{OH}=0.3$)—evaluated from the changes in adhering cells morphology, the quantities for cell adhesion and spreading, and the development of focal adhesions and actin cytoskeleton. When both proteins were adsorbed consecutively, a distinct complex morphology of the adsorbed protein layer was observed resulting in a hydrophobic shift in the cellular interaction (to $X_{OH}=0$). Details of this study are reported herein.

Materials and Methods

Materials

Copolymer sheets were obtained by polymerization of a solution of both monomers ethyl acrylate (EA) (Aldrich, 99% pure) and hydroxyl EA (HEA) (Aldrich, 96% pure), in the desired proportion, using 0.1 wt% of benzoin (Scharlau, 98% pure) as photoinitiator and a 2 wt% of ethyleneglycol dimethacrylate (Aldrich, 98% pure) as crosslinking agent. The polymerization was carried out up to limiting conversion and against a smooth glass surface seeking to obtain surfaces of controlled and reproducible roughness. Five monomer feed compositions were chosen, given by the weight fraction of HEA in the initial mixture of $X_{OH}=1, 0.7, 0.5, 0.3,$ and 0 (it refers to the fraction X of HEA in the copolymer). After polymerization, low molecular mass substances were extracted from the material by boiling in ethanol for 24 h and then drying *in vacuo* to constant weight.

The equilibrium water content (mass of water absorbed referred to the dry mass of the substrate) and the water contact angle (using a Dataphysics OCA) were measured for the different substrates.

Small disks (~10 mm diameter) were cut from the polymerized sheets to be used in the protein adsorption and cell adhesion studies. The samples were sterilized with gamma radiation (25kGy) before the experiments.

XPS experiments were performed in a PHI 5500 Multi-technique System (from Physical Electronics) with a mono-

chromatic X-ray source and calibrated using the $3d_{5/2}$ line of Ag. The analysed area was a circle of 0.8 mm diameter, and the selected resolution for the spectra was 23.5 eV of pass energy and $0.1 \text{ eV} \cdot \text{step}^{-1}$. All measurements were made in an ultra high vacuum chamber pressure. XPS elemental sensitivity factors according to the MULTIPAK program for PHI instruments were used. An automatic XPS signal fitting software has been developed under MATLAB v7.2 (The MathWorks, Inc.) environment to deconvolute the experimental spectra as described elsewhere.²⁰ The fitting software makes use of an independent Voigt function per peak (which in our case means four Voigt functions to fit the C 1s spectra and three Voigt functions to fit the O 1s peaks).

Protein adsorption

The adsorption concentration for both proteins was 20 $\mu\text{g}/\text{mL}$: in 0.1 M sodium acetate (pH 4.5) for Col IV (Abcam) and in phosphate-buffered saline (PBS) (pH 7.4) for LAM (Sigma). Some samples were coated consecutively, first with Col IV than Lam, with extensive washing with PBS between incubations. The incubation period was of 10 min for AFM studies and 30 min for cellular interaction, both at 37°C. Afterward, the samples were extensively washed with PBS.

AFM

Samples with the adsorbed protein were quickly dried using Nitrogen air flow. AFM was performed in a NanoScope III from Digital Instruments operating in tapping mode in air. Si-cantilevers from Veeco were used with force constant of 2.8 N/m and resonance frequency of 75 kHz. The phase signal was set to zero at a frequency 5%–10% lower than the resonance one. Drive amplitude was 200 mV and the amplitude set-point A_{sp} was 1.4 V. The ratio between the amplitude set-point and the free amplitude A_{sp}/A_0 was kept equal to 0.7. The WSxM software was used to process height AFM images to obtain topographical profile (number of event per given altitude) and a tailor-made MATLAB software (The MathWorks, Inc.) for volume calculations of the adsorbed protein layer. Volume protein calculated following this procedure must be interpreted in a relative way. That is to say, the total real volume of the adsorbed protein must be higher due to the hydration effects. Moreover, our calculated protein volume cannot be directly used to infer protein mass density on each surface. Nevertheless, assuming the drying process will equally modify both Col IV and Lam on every surface, the obtained values provide valuable information to compare the amount of adsorbed protein among surfaces and the influence of their sequential adsorption.

Cells

Human umbilical vein endothelial cells (HUVEC, PromoCell) were cultured in endothelial cell growth medium supplemented with SupplementMix (PromoCell) containing 0.4% ECGS/H, 2% fetal calf serum, 1 ng/mL epidermal growth factor, 1 $\mu\text{g}/\text{mL}$ hydrocortison, and 1 ng/mL basic fibroblast factor. For the adhesion experiments the cells were detached from around confluent flasks with Trypsin/EDTA (Invitrogen) and the remained trypsin activity was stopped with 100% FBS before two times washing with medium without supplements. Finally, the cells were counted and

reconstituted in serum-free endothelial cell medium to be seeded on the different surfaces.

Overall cell morphology

To study the overall cell morphology of HUVEC adhering to different samples, 5×10^4 cells/well were seeded in 24-well TC plates (Costar) containing the samples for 2 h in the serum-free medium. At the end of incubation, the cells were fixed with 4% paraformaldehyde (10 min) and permeabilized with 0.5% Triton X-100 for 5 min. For the overall morphology studies and cell adhesion measurements the actin cytoskeleton was stained with 20 $\mu\text{g}/\text{mL}$ AlexaFluor 488 phalloidin (Molecular Probes) in PBS before the samples were washed and mounted in Mowiol. In some cases phalloidin was added to the secondary antibody solution (for double vinculin/actin staining). The samples were viewed on fluorescent microscope (Nikon Eclipse E800) and at least three representative images were acquired.

Quantification of cell adhesion and spreading

Morphological parameters such as number of adhering cells and mean cell surface area were evaluated using the ImageJ plug-ins (NIH; <http://rsb.info.nih.gov/ij/>). The adhesion was measured by counting the cells in three randomly chosen images of actin-stained samples to obtain the number of cells per cm^2 . Data were collected from at least three independent experiments and the average cell area was further measured for each individual image (in μm^2) and calculated for each condition.

Immunofluorescence

Observation of focal adhesion contacts. About 5×10^4 cells/well were seeded as above for 2 h in serum-free medium. To observe focal adhesions, fixed and permeabilized samples were saturated with 1% albumin in PBS for 15 min. Focal adhesion complexes were observed using monoclonal anti-vinculin antibody (Sigma) dissolved at 1% albumin solution in PBS for 30 min followed by Cy³-conjugated AffiniPure Goat Anti-Mouse IgG (H+L) (Jackson ImmunoResearch) as secondary antibody. The samples were viewed and photographed on a Laser Scanning Confocal Microscope Leica at high magnification where at least three representative images were acquired for each experimental condition.

Statistical analysis. All cellular studies were performed with at least three replicates. Morphological quantification for each surface and each condition was obtained from at least six representative pictures, which were digitally analyzed. Statistics was performed using StatGraphics Plus software employing ANOVA simple and Kruskal-Wallis tests to determine statistically significant differences between groups ($p < 0.05$). Each data point represents mean \pm standard deviation from at least three independent experiments.

Results and Discussion

Col IV and Lam are the main component of the vascular BM^{11,12} where endothelial cells reside in a rather 2D environment, for example, in a similar geometry when adhering to the surface of blood contacting devices where the endothelialization is highly desirable.^{7,11,12} However, while en-

dothelial cells procurement technologies for seeding implants have significantly improve, adhering cells often dedifferentiate and act in a counterproductive manner, accelerating device failure.^{3,4,6} We anticipate that an important factor for this altered endothelialization response might be the missing environmental signals from the natural BM. Thus, tailoring the behavior of adsorbed Col IV and Lam on biomaterials interface would provide a powerful tool (from the materials site) for maintaining the functional performance of implant.

It is well documented that the substratum -OH groups strongly affect both the conformation and biological performance of adsorbed proteins.^{17,19,21,22} Relatively little is known, however, about the intermolecular associations of adsorbed protein molecules, particularly when they tend to assembly within the protein layer. In this study we used a family of model substrates based on the copolymerization of EA and HEA monomers, which have a vinyl backbone chain with the side groups $-\text{COOCH}_2\text{CH}_3$ and $-\text{COOCH}_2\text{CH}_2\text{OH}$, respectively. Their combination gives rise to a random copolymer²² with tailored concentration of -OH groups that determines both the surface energy and the hydrophilicity of the substrate (Table 1).

Topography of the surfaces examined by AFM prior protein adsorption yielded similar roughness parameters regardless the polymer composition. Roughness parameters obtained were $R_a = 18 \pm 4$ nm and $R_{ms} = 22 \pm 4$ nm (R_a is the arithmetic average of the height deviations; R_{ms} is defined as standard deviation of the height values).

The fraction of -OH groups on the surface was assessed by XPS. Table 1 includes the surface HEA molar fraction for each of the copolymers. It is noteworthy that the fraction of hydrophilic units on the surface is similar to the initial ratio of HEA in the feeding mixture of co-monomers. That is to say, most of the hydroxyl groups in the system remain available to interact with the biological media.

Behavior of adsorbed Col IV on surfaces with different -OH content

The network-forming Col IV is a triple helical molecule composed of three alpha chains, which self-assemble by antiparallel interactions and extensive disulfide bounding.¹⁰ In the BM these monomers associate with their C-terminal globular NC1 domains to form dimers or with N-terminals to form tetramers.^{10,23,24} Observations have been made that

TABLE 1. EQUILIBRIUM WATER CONTENT AND WATER CONTACT ANGLE FOR THE DIFFERENT SUBSTRATES WITH INCREASING FRACTION OF -OH GROUPS

X_{OH}	EWC (%)	WCA ($^\circ$)	X_{OH} (XPS)
0	1.7 ± 0.4	89 ± 1	0
0.3	7.6 ± 0.9	80 ± 2	0.25 ± 0.05
0.5	18.2 ± 1.7	67 ± 1	0.45 ± 0.08
0.7	40.6 ± 0.4	55 ± 1	0.68 ± 0.06
1	134 ± 5	45 ± 2	1

The first column represents the fraction of HEA units used in the copolymerization process; the last one is the fraction of HEA units available on the material surface as obtained from XPS analysis.

EWC, equilibrium water content; WCA, water contact angle; HEA, hydroxyethyl acrylate.

Col IV could be linearly organized during early BM assembly,²⁵ suggesting that cells are also involved in the process. While the molecular mechanisms that endow the spatial organization of Col IV in the BM are still debatable, our current results^{15,26} suggest that material surface-associated Col IV may undergo cell-dependent rearrangement, presumably through reversible association with FN fibrils—a fact that brings forth our interest on the molecular arrangement of BM proteins at biomaterials interface.

Structure of Col IV molecule was extensively studied during last decades^{23,24,27} and AFM provide significantly insight.²⁸ AFM is an exceptional tool to explore the conformation and distribution of matrix proteins at the biomaterial interface. Since roughness for most of the biomaterials surfaces is well above the height of protein molecules (5–10 nm)²⁸ direct observations of ECM proteins deposition on commonly used biomaterials are sparsely reported. In previous research we could show that the phase magnitude in tapping mode AFM is a good approach to obtain significant information on protein configuration.²¹ The reason why we have chosen working in air in this study is mainly due to the stability of the system, which continues to be much better in air compared to the scanning in liquid environments. For example, we have found that on hydrophobic materials, images obtained in air are comparable to those acquired in liquid but with much better resolution. By contrast, on very hydrophilic surfaces that moreover adsorbed large amounts of water, the interpretation of the AFM images must be done carefully.

The AFM phase images shown on Figure 1A describe the surface behavior of adsorbed Col IV depending on the fraction of –OH groups, which vary from $X_{OH}=0$ to $X_{OH}=1$. Two general trends might be distinguished: (i) single molecules arrangement (see arrowhead on $X_{OH}=0.5$) characteristic for the intermediate hydrophobic substrata, and (ii) a tendency for molecular assembly in network (see arrow on $X_{OH}=0.7$), which increase with hydrophobicity, leading to the formation of an augmented network structure at $X_{OH}=0$, presumably consisting of molecular aggregates. Elongated fibril-like features were observed also on the most hydrophilic poly EA; equal to $X_{OH}=0$ (PEA) surface presumably representing few laterally associated molecules (arrowhead on $X_{OH}=1$). When Col IV adsorbs on mica it typically forms dimers through intermolecular interactions of two Col IV monomers via the globular NC1 domains.²⁸ Indeed, such globular features connected with long arms can be easily distinguished on intermediate hydrophilic $X_{OH}=0.5$ and $X_{OH}=0.3$ samples (see arrowhead on $X_{OH}=0.5$). Even on mica, however, Col IV dimers display a variety of configurations often forming loops and folds,²⁸ which may explain the appearance of rather complex shapes seen on $X_{OH}=0.7$. The formation of tetramers via interactions of 7S domains is also feasible²⁸ (see arrow on $X_{OH}=0.3$) presumably involved in the formation of networks (upon decrease of –OH content) as single tetramer features were not observed. Nevertheless, the longitudinal sizes of obtained structures vary between 300 and 600 nm (see arrowhead on $X_{OH}=0.5$), which is in the range of individual molecules size of unfolded Col IV monomer ($346+3.8$ nm)²⁸ and dimers might be maximally doubled, for example, around 700 nm, but when are completely unfolded. The Col IV arrangement on $X_{OH}=0.3$ is more subtle. Here the links between individual molecules cause a tendency for network assembly. Since there are no

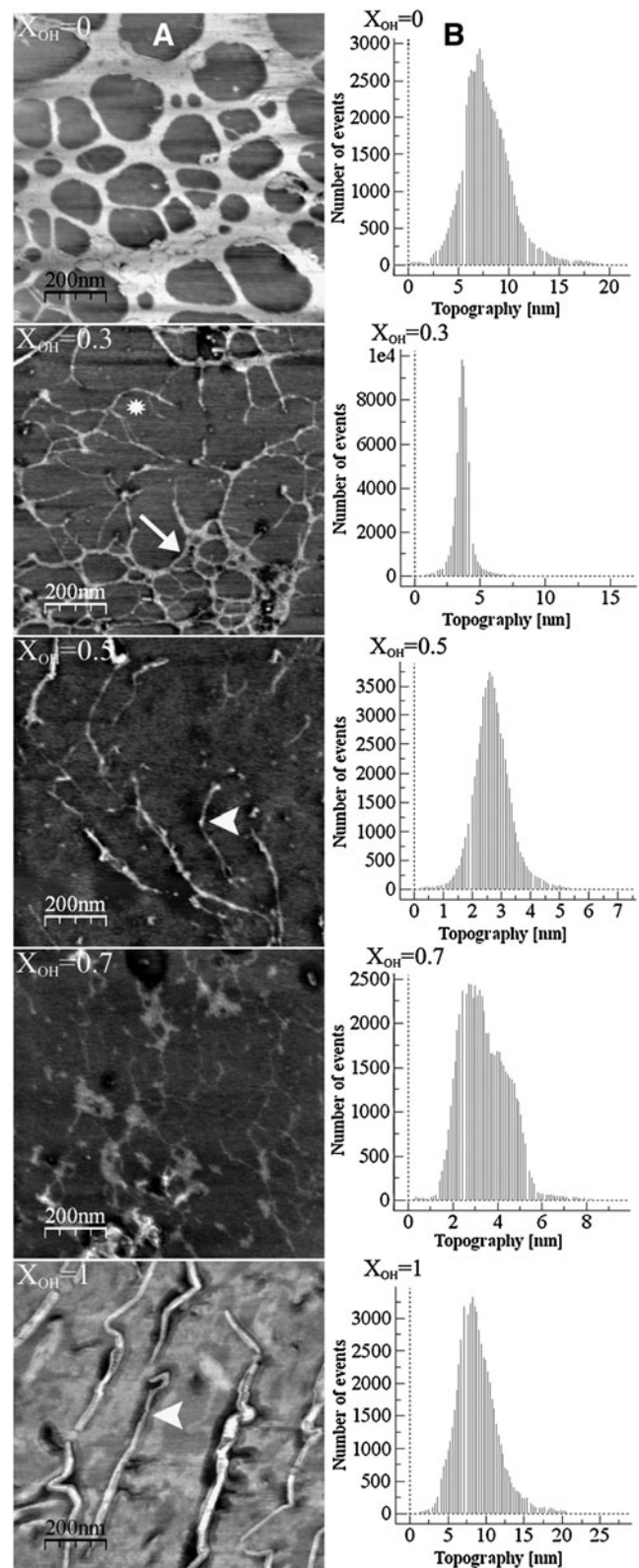


FIG. 1. Phase AFM images of adsorbed Col IV on substrates with increasing fraction of –OH groups (A) following the order: $X_{OH}=0$, $X_{OH}=0.3$, $X_{OH}=0.5$, $X_{OH}=0.7$, $X_{OH}=1$ from the top to the bottom. Corresponding topographic profiles of adsorbed Col IV on the same substrates (B) viewed by AFM software (see Methods section). AFM, atomic force microscopy; Col IV, collagen IV.

overlapping regions, arrangement at single molecules level is very probable. More precise topographical analysis also shows the most homogenous size distribution of the features on this sample (Fig. 1, column B) suggesting formation of complex structure consisting of small repeating units. That is to say, the topography histograms (1B) show a single distribution of molecules within the interval 5–15 nm for most of the samples that even narrows to 2–6 nm for $X_{OH}=0.3$. Indeed, we cannot discard that the formation of structures on this surface is partly a consequence of the drying process, which could lead to lateral reorganization of the adsorbed layer at the air–liquid interface, but this process seems to be favored on very hydrophilic surfaces because of the absence of protein–surface interactions strong enough to prevent protein relaxation during water release.³⁹

As shown in Table 2, the total amount of adsorbed Col IV decreases sharply as the hydrophilicity of the sample increases and then remains in barely constant. Conversely, on pure PEA ($X_{OH}=0$) the process turns to the formation of an augmented network that enhances interactions between molecules, resulting in the formation of a complex protein structure (aggregate) where individual molecules cannot be distinguished any more. This arrangement of Col IV on PEA ($X_{OH}=0$) occurs as on hydrophobic ODS but with different volumetric distribution: multilayer aggregates on ODS versus lateral interactions on $X_{OH}=0$.¹⁵ This fact supports the idea that the concrete underlying chemistry—not only the wettability of the substrate—determines protein adsorption and distribution at the material interface.^{16,17}

Biological response to the adsorbed Col IV

The surface wettability has long been recognized as an important parameter for protein adsorption and cellular interaction.^{5,16,29} In general, hydrophilic surfaces support cell adhesion and spreading, usually attributed to the appropriate conformation of adsorbed matrix proteins.^{5,21,30,31} However, this is not always straightforward since materials with very high wettability, which bind much water-like hydrogels, do not support protein adsorption and cell adhesion.³² Our study shows a very good interaction of HUVEC with the most hydrophilic $X_{OH}=1$ substratum, which is not surprising, as this surface might be considered as moderately wettable where the best cellular interaction is expected.^{32,33} Indeed, the cells look well spread (Fig. 2A, left column) and develop an elongated morphology. The promoted cellular interaction is confirmed by the quantitative measurements for the adhesion (Fig. 2D, left chart) and spreading (Fig. 2D,

right), both optima showing a significant increase over other conditions ($p<0.05$). Surprisingly, however, HUVEC represents a second optimum for cell interaction, that is on the relatively hydrophobic $X_{OH}=0.3$ surface (hydrophobic effect), where adhesion and spreading again significantly ($p<0.05$) improve (Fig. 2A). For comparison, on the same chart are shown the quantities for adhesion and spreading to glass (as a positive control). It can be seen that adhesion, but not spreading, of cell on $X_{OH}=0.3$ is significantly higher, whereas on $X_{OH}=1$ it equal with the control. The spreading area is equal for all $X_{OH}=0.3$, $X_{OH}=1$, and control samples. The overall morphology of cells on the control sample might be seen on Fig. 5C. Further decrease of –OH groups ($X_{OH}=0$ surface) tends to diminish the cellular interaction. HUVEC fail to interact also with the intermediate fractions of $X_{OH}=0.5$ and $X_{OH}=0.7$: overall, the cells tend to round (Fig. 2, row A) and both adhesion and spreading show significantly lower ($p<0.05$) quantities (Fig. 2D), all this confirming the optimum at $X_{OH}=0.3$. Nevertheless, on the $X_{OH}=0$ and partly $X_{OH}=0.3$ surfaces, the cells represent an irregular shape with often appearance of star-like protrusions, rich on actin (see Fig. 2A and C), but normal focal contacts formation (Fig. 2B), which suggest a rather good cellular interaction. To rationalize this cellular behavior in terms of protein adsorption shown on Figure 1, it suggests that supramolecular-sized fibrillar features formed on the $X_{OH}=1$ substrate favor cell adhesion; that is to say, Col IV is adsorbed in such a way that it provides enhanced availability of the binding site (for $\alpha 1$ and $\alpha 2$ integrins) located ~ 100 nm away from the amino-terminus.^{23,24,27} As the hydrophilicity of the substrate diminishes, protein distribution became complicated, from more complex features seen on $X_{OH}=0.7$ (see Fig. 1A), the isolated fibrils are more characteristic for $X_{OH}=0.5$ (Fig. 1A), but why these structures appear worse for the cellular interaction is not clear. Moreover, lateral protein interactions are enhanced on $X_{OH}=0$, which must hidden binding domains resulting in poorer cell interaction.

Assembly of LAM on surfaces with different –OH density

It is proposed that the assembly of BM is initiated by Lam. It self-assembles into heterotrimers that bind to the cell surface via integrin receptors.^{34–36} The structure of Lam molecules has been extensively studied during the recent decades employing electron microscopy and also AFM.^{16,37,38} Consistent with this studies an appearance of cross-shaped molecules with approximate size of 70–100 nm (depending on their conformation) might be expected as the maximal dimensions of the completely extended cruciform Lam molecule is 125 nm long, 72 nm wide, and 2.2 nm thick.³⁷

The phase images on Figure 3A show Lam distribution after adsorption from solution of a high concentration (20 $\mu\text{g}/\text{mL}$). Note, although such concentration is not optimal for AFM imaging, it is the one used for the cellular investigations. We found a clear tendency for protein assembly in networks at almost all ranges of surfaces (Fig. 3, column A). However, these networks vary significantly in their thickness and organization: on substrates with low OH content, these structures are prominent ($X_{OH}=0$ – $X_{OH}=0.5$), whereas a rather subtle protein deposition is characteristic for $X_{OH}=1$ and $X_{OH}=0.3$ surfaces (see Fig. 3, row A). It

TABLE 2. TOTAL VOLUME OCCUPIED BY THE PROTEIN ON A $1 \mu\text{m}^2$ AREA OF THE SUBSTRATE AS CALCULATED FROM AFM DATA AFTER ADSORPTION OF COL IV, LAM, OR COL IV + LAM

X_{OH}	Col IV	Lam	Col IV/Lam
0	6.0 ± 1.1	5.0 ± 1.2	8.0 ± 1.3
0.3	2.1 ± 0.3	3.0 ± 0.9	3.5 ± 1.1
0.5	0.7 ± 0.2	2.5 ± 0.8	3.7 ± 1.2
0.7	1.5 ± 0.2	0.7 ± 0.2	6.0 ± 1.4
1	1.2 ± 0.3	6.0 ± 1.5	4.5 ± 1.3

AFM, atomic force microscopy; Col IV, Collagen IV; Lam, Laminin.

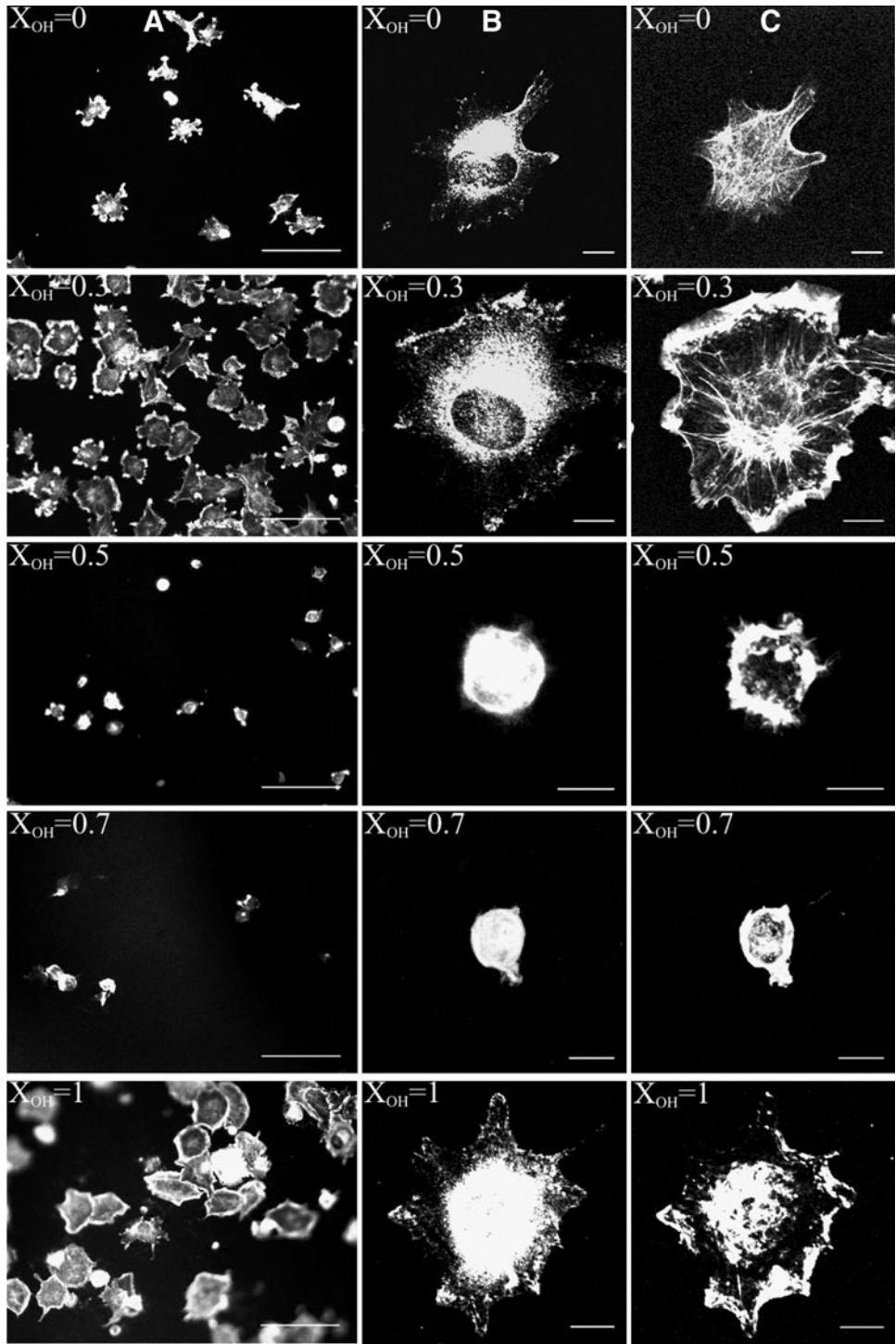
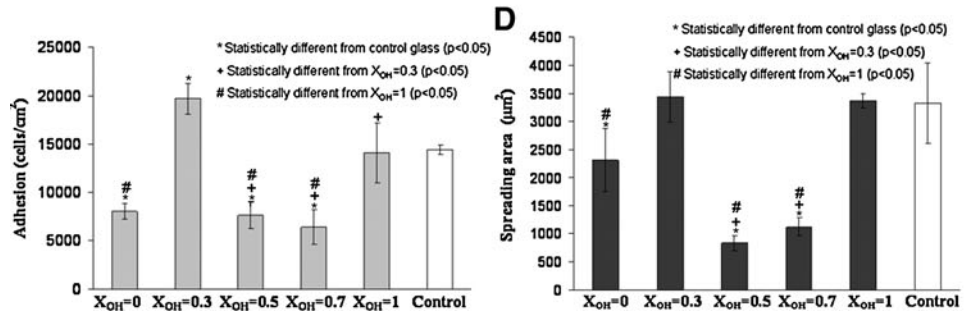


FIG. 2. Overall morphology of HUVEC adhering on Col IV-coated substrates with increasing -OH density (A). Bar 100 μm . The same samples were stained for vinculin (B) and actin (C) to study the formation of focal adhesion contacts and actin cytoskeleton organization, respectively. Bar 10 μm . The quantities for cell adhesion expressed as number of cells per cm^2 (D, left graph) and cell spreading area shown in μm^2 (D, right graph) are compared to the control glass samples (white bars). HUVEC, human umbilical vein endothelial cells.



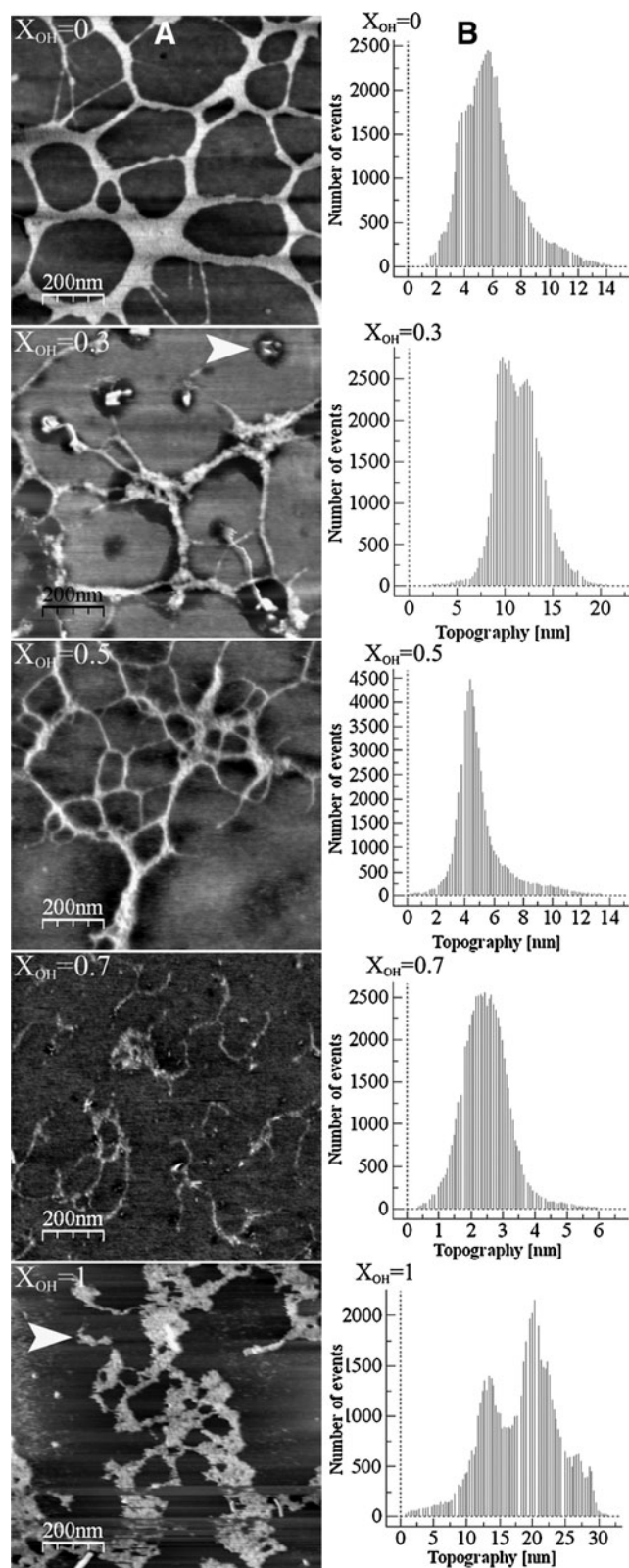


FIG. 3. Phase AFM images of adsorbed Lam on substrates with increasing fraction of -OH groups (A) following the same order as in Figure 1. Corresponding topographic profiles of adsorbed Lam on the same substrates (B) viewed by AFM software. Lam, Laminin.

seems that increasing the fraction of -OH groups tend to diminish the network formation presumably reducing the lateral intermolecular interactions. However, on most hydrophilic $X_{OH}=1$ surface, Lam shows again surprisingly high protein deposition as extrapolated from the calculations for the adsorbed protein volume (Table 2). The same non-monotonic trend in the amount of adsorbed protein was previously found on this family of surfaces using fibronectin.²¹ Note, on the same surface we have previously found globular-like Lam deposition after adsorption from solutions of much lower protein concentration,¹⁶ which stress the importance of the competition between protein-protein versus protein-material interactions to determine the conformation of LAM at the material interface. On a collateral side, swelling of polymer may result in the entrapment of some Lam aggregates within the polymer, which may also explain the biphasic size distribution of features seen on $X_{OH}=1$ substratum only (Fig. 3, column B, bottom). Also, the drying process could lead to lateral reorganization of the adsorbed protein layer at the air-liquid interface, and this process seems to be favored on very hydrophilic surfaces because of the absence of protein-surface interactions strong enough to prevent protein relaxation during water release.³⁹ Nevertheless, independently of the complex arrangements of Lam on our surfaces some cross-shaped structures that resemble single molecules seen on mica³⁷ can be sparsely observed on $X_{OH}=0.3$ and $X_{OH}=1$ surfaces (Fig. 3A, arrowheads), suggesting a protein deposition in a near-natural configuration.

Cellular interaction with LAM

Figure 4A describes the behavior of HUVEC on Lam adsorbed on the same substrates order. Again, two maxima in the cellular interaction were obtained at $X_{OH}=1$ and $X_{OH}=0.3$ surfaces. Overall, the cells look better spread in comparison to Col IV samples (Fig. 2), evident from the well-developed focal adhesion complexes (Fig. 4, column B) and prominent actin stress fibers (Fig. 4, column C). Likewise, the cellular interaction is abolished on $X_{OH}=0.7$ and $X_{OH}=0.5$ samples, which is confirmed from the quantitative measurements of both adhesion (Fig. 4D, left) and spreading (Fig. 4C, right), showing significantly lower values ($p < 0.05$). Interestingly, here both the adhesion and spreading to $X_{OH}=0.3$ and $X_{OH}=1$ override the values of control glass samples (Fig. 4D) although not significantly ($p > 0.05$). The overall morphology of cells on the control Lam-coated sample might be seen on Figure 5D. Again, a tendency for diminished cellular interaction on the most hydrophobic $X_{OH}=0$ surface was found (Fig. 4A).

This family of Lam-coated polymers was used for *in vitro* studies with other cell systems. While better adhesion of Schwann cells was obtained at $X_{OH}=0.8$ (close to the maximum $X_{OH}=0.7$ found with HUVEC), the best performance using neural progenitors was found for $X_{OH}=0.5$, on which HUVEC interact worst.^{40,41} Taken together, it points out the cell type specificity in the interaction with Lam-coated materials.

Spontaneous interaction of HUVEC with bare substrata

AFM images show areas of bare polymer, which raise an important question: do the cells adhere to the plain polymers

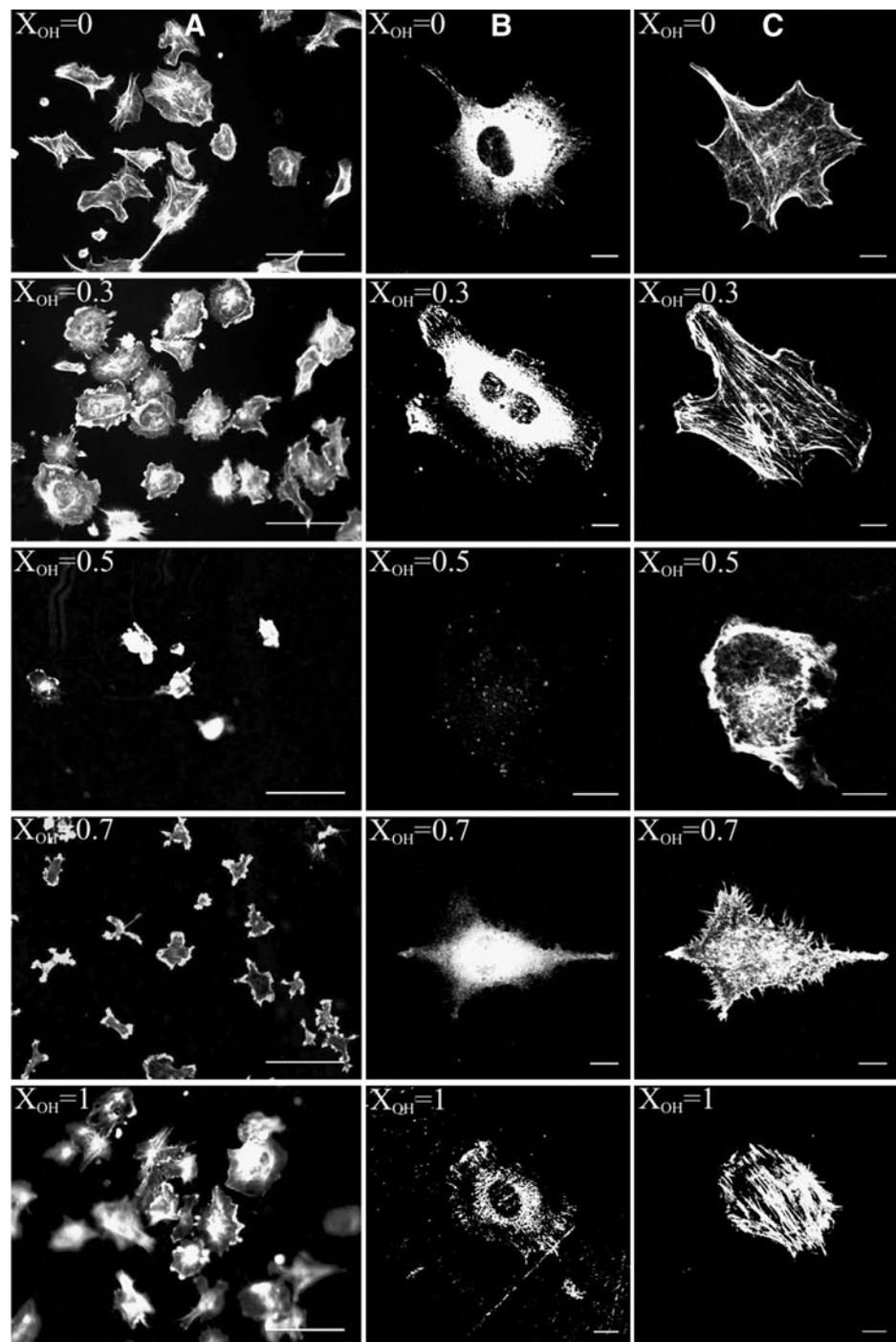
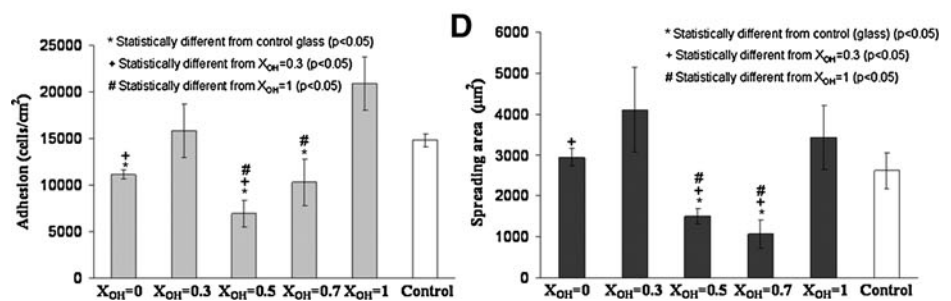


FIG. 4. Overall morphology of HUVEC adhering to Lam-coated substrates with increasing $-OH$ density (A). Bar 100 μm . Cells were stained also for vinculin (B) and actin (C) as in Figure 2. Bar 10 μm . Quantities for cell adhesion (D, left graph) and spreading (D, right graph) are compared to control glass samples (white bars).



and does this adhesion vary with $-OH$ density? To address this we performed separate experiment exploring the cellular interaction with bare surfaces. Figure 5 (column A) clearly demonstrates that the cells attach less efficiently and look shrink on all bare substrata suggesting a nonphysiological attachment, but a surprising tendency for higher attachment

on $X_{OH}=1$ and $X_{OH}=0.3$ was found, further confirmed by the quantitative measures for cell adhesion ($p < 0.05$) (Fig. 5H, upper chart), which suggests that these substrates provide better physical environment for cell attachment even in comparison to the control glass surface. However, it concerns cell adhesion, but not spreading, as the latter was even

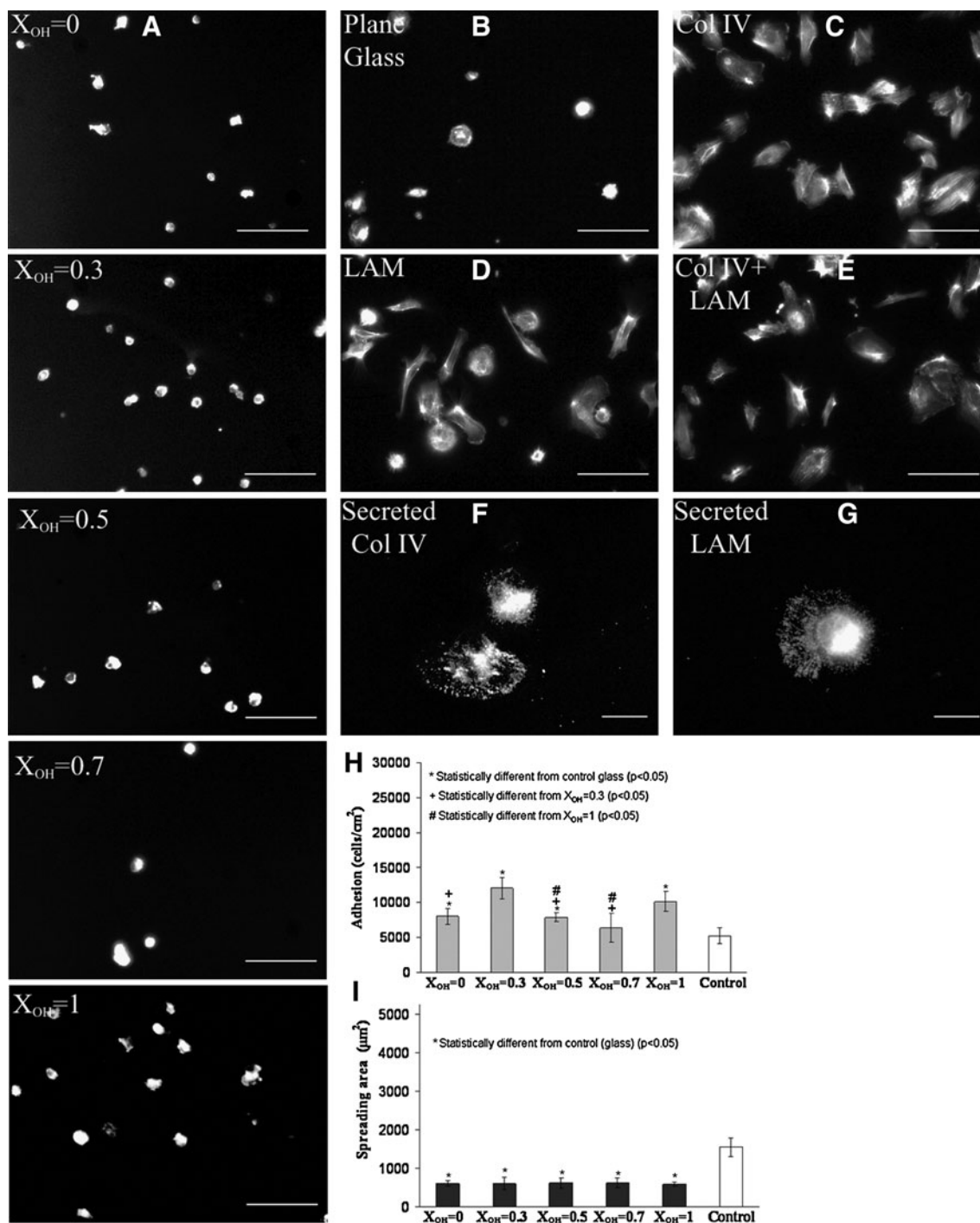


FIG. 5. Overall morphology of HUVEC adhering on plain substrates with increasing OH density (A), and different control samples including plain glass (B), Col IV-coated glass (C), Lam-coated glass (D), and sequential Col IV/Lam-coated glass (E). Bar 100 μm. The last two images demonstrate spontaneous secretion of Col IV (F) and Lam (G) by HUVEC within 2 h of incubation on glass. Bar 20 μm. The charts below represent quantities for cell adhesion (H) and spreading (I) to bare samples compared with glass control (white bars).

lowered versus control glass (Fig. 5H, lower chart), showing that these polymers provide conditions that are not sufficient to support the development of normal cell shape. On the other hand, it seemed unlikely that the cells adhere directly to bare substrates; therefore, the existence of some traces of adhesive proteins in the system might be expected. Presumably, they have to be secreted by HUVEC, as the effect of serum proteins can be excluded after the two times washing step we use for cell harvesting (See Methods section). Indeed, when HUVEC were stained for Col IV and Lam, both proteins were identified on the substratum beneath the cells even after 2h incubation (Fig. 5F and G, respectively). Therefore, the improved spontaneous adhesion of HUVEC on $X_{OH}=1$ and $X_{OH}=0.3$ should be attributed to the constitutive release of Col IV and Lam (and may be other adhesive proteins), which influence the cellular interaction during the adhesion process. It is noteworthy, however, that this behavior of Col IV and Lam differs significantly from other matrix proteins, such as fibronectin¹⁷ and fibrinogen.¹⁹ Although they also tend to assemble on pure PEA ($X_{OH}=0$) the cellular interaction gradually increases as the fraction of OH groups diminishes. Conversely, vitronectin cannot form networks¹⁸ but show the same trend in bioactivity. The very similar biphasic behavior of HUVEC on Col IV and Lam-coated $X_{OH}=0.3$ and $X_{OH}=1$ substrata suggests that the adsorbed proteins acquire a configuration close to the natural one, and interestingly, single molecular-size features were observed for both proteins on $X_{OH}=0.3$ only (see arrow on Fig. 1A and arrowhead on Fig. 3A).

Sequential deposition of Col IV and Lam

The resemblances in the behavior of Col IV and Lam in respect to their assembly and cellular interaction suggest that similar forces might guide their organization in the BM, where they form overlapping polymeric network.^{10,13,24,42} This provoked our interest in a joint Col IV-Lam deposition, which could provide insights on their natural interplay in the BM. Unfortunately, these two proteins possess different solubility (Col IV dissolves in acid, whereas Lam in neutral conditions), which exclude their assembly together. Thus, the only simple solution was to adsorb them consequently, first Col IV and then Lam.

Figure 6A displays the complex phase images obtained after sequential Col IV/Lam adsorption. A tendency for joint network formation was found on most surfaces, except on $X_{OH}=1$, where rather globular protein deposition (resembling the behavior of Lam) was obtained (see Fig. 3, column A). It is still difficult to distinguish Col IV or Lam features, though clearly better network formation is seen on $X_{OH}=0.3$ sample. Sequential adsorption shows that the amount of adsorbed protein (see Table 2) is not just a superposition of these obtained for Col IV and Lam independently. Except for $X_{OH}=1$, it is always above these quantities (Table 2), which is consistent with the possibility that some Lam is additionally deposited on the surface. Interestingly, Lam tend to absorb preferentially on $X_{OH}=0.5$ and $X_{OH}=0.7$ surfaces after Col IV deposition than on the bare polymers (Table 2), suggesting heterotypic intermolecular interaction.

The structure of the protein layer looks different on PEA ($X_{OH}=0$). Here prevails the homogenous "sponge-like" protein deposition interrupted by polygonal empty spaces,

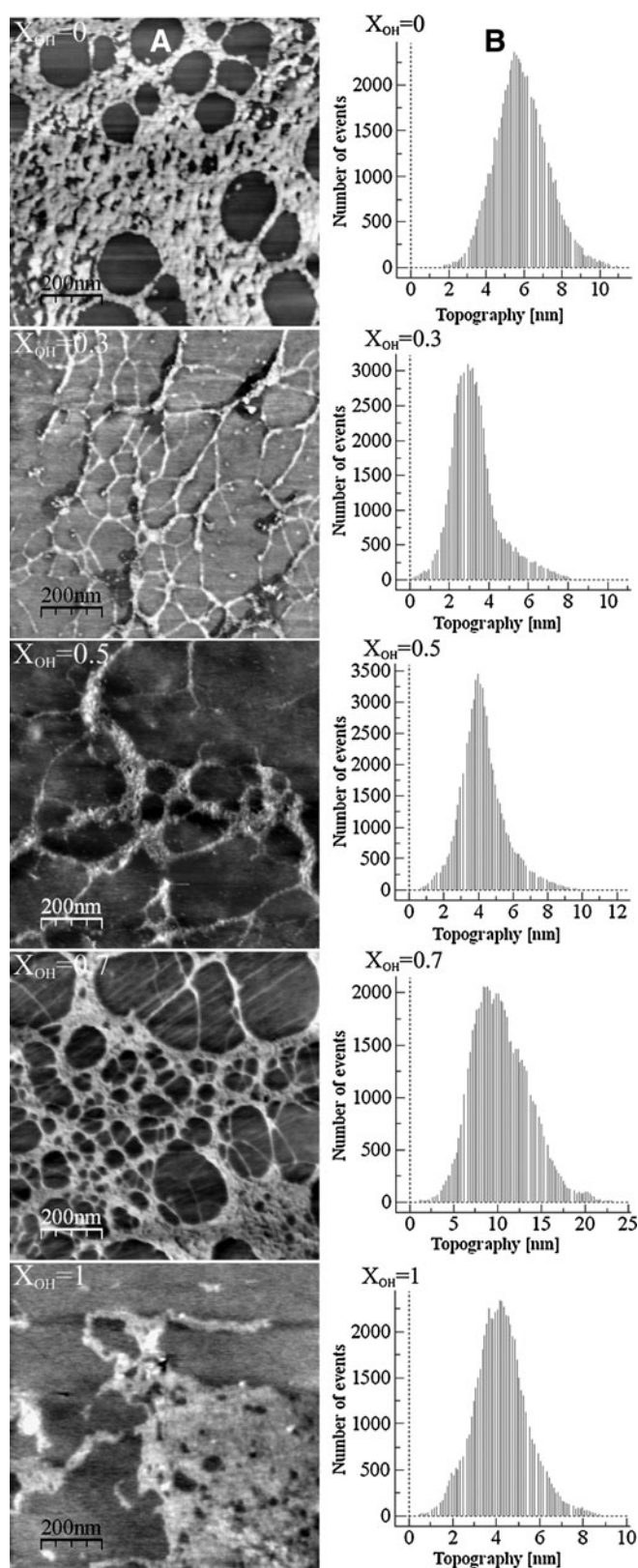


FIG. 6. Phase AFM images of sequentially adsorbed Col IV and Lam on substrates with increasing fraction of -OH groups (A) following the same order as in Figure 1. Corresponding topographic profiles of adsorbed proteins on the same substrates (B) viewed by AFM software.

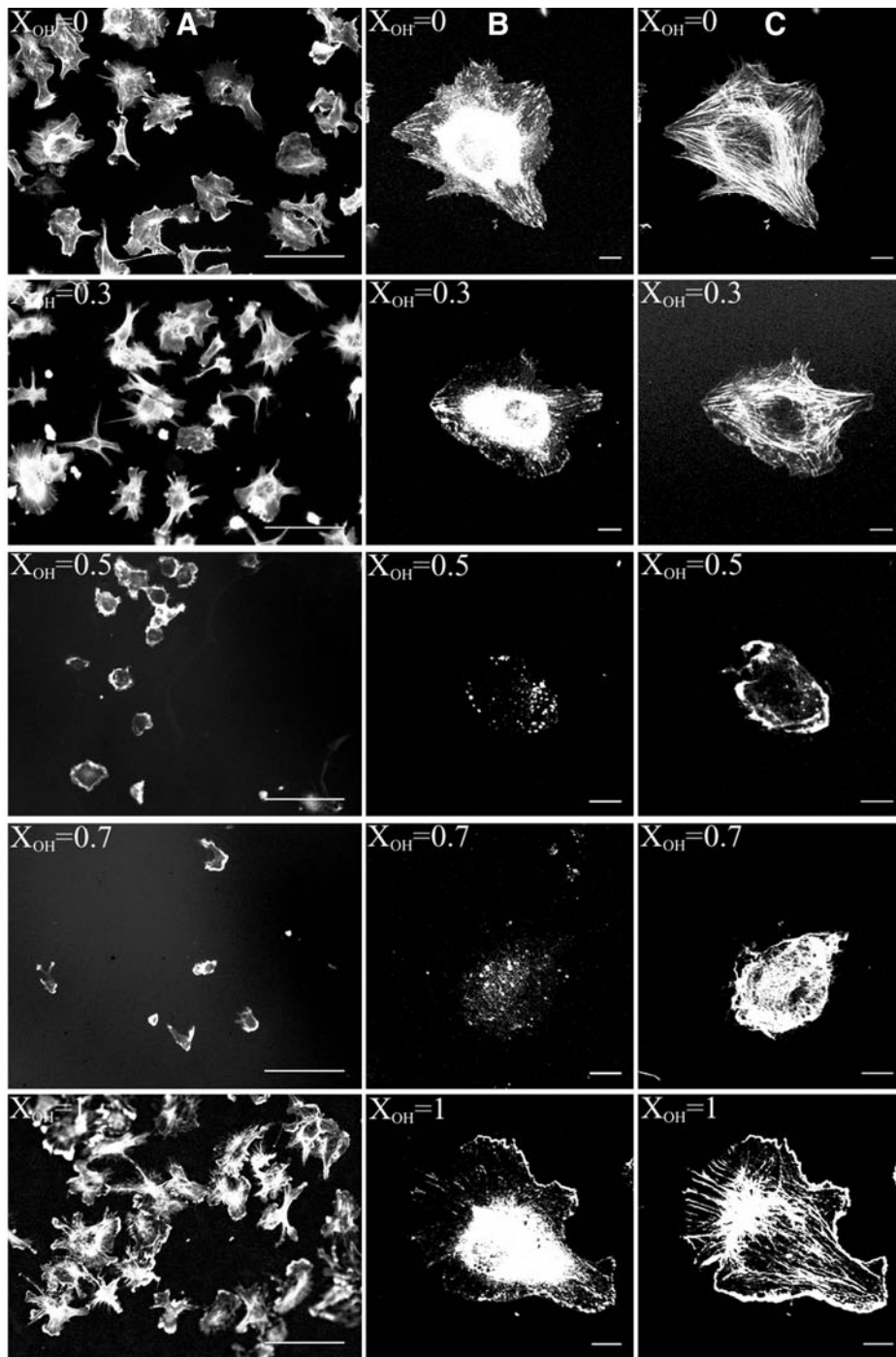
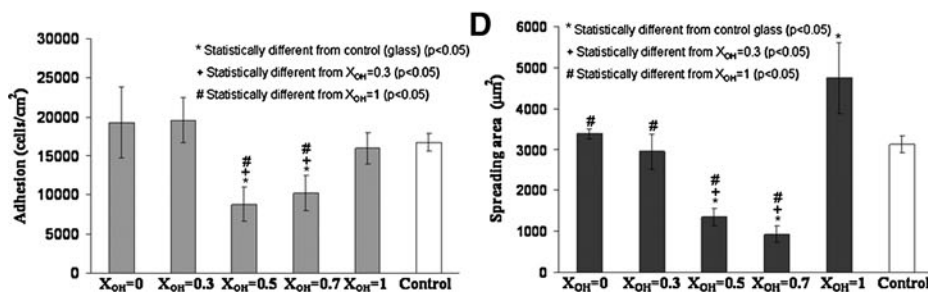


FIG. 7. Overall morphology of HUVEC adhering to sequentially adsorbed Col IV and Lam on substrates with increasing -OH density (A). Bar 100 μm . The cells were stained also for vinculin (B) and actin (C). Bar 10 μm . Quantities for cell adhesion (D, left graph) and spreading (D, right graph) are compared to control glass samples (white bars).



thus resembling the pattern of both Col IV (Fig. 1A) and Lam (Fig. 3A) networks. As Col IV adsorbs first it probably serves as a template for subsequent Lam assembly. The dominating sponge-like structure, however, presumably represents a joint Col IV-Lam network as it is not seen on the single protein series. Interestingly, the morphology of this complex network structure looks similar to those shown on the topographic AFM images of the natural BM underlying the corneal epithelium.⁴³

The above assumption is confirmed by the improved cellular interaction that we obtained on $X_{OH}=0$ surface. As shown on Figure 7A, HUVEC represents the best morphology exactly on this sample demonstrating advanced cell spreading and polarized cell morphology reflecting their active crawling on the substratum. The most extensive formation of focal adhesions (Fig. 7B) and actin stress fibers (Fig. 7C) also confirm the improved cellular interaction. This suggests the appearance of a hydrophobic shift in bioactivity, confirmed also by the quantitative measurements, as cell spreading was significantly higher not only within the group, including control glass (Fig. 7D, right), but also compared to all other single protein series. Note, though the cells are well spread on $X_{OH}=0.3$ (optimum for single Col IV and Lam-coated series), they are often lacking their focal adhesions at cell borders, which points for a lowered strength of interaction with the substratum; that is, these samples start to represent lowered bioactivity when the matrix proteins are jointly assembled. Conversely, the complex Col-Lam network formation obviously supports the cellular interaction on the most hydrophobic $X_{OH}=0$ surface, which provides better environment for the cells presumably because it resembling the natural structure of the BM.⁴³

Conclusion

This work describes the behavior of the main components of the BMs—Col IV and LAM—on well-defined surfaces with tailored density of hydroxyl groups. AFM studies revealed substratum-induced assembly of both proteins from a single-molecule arrangement to the specific networks better pronounced on hydrophobic environment.

The interaction of endothelial cells surprisingly shows two optima, a hydrophilic ($X_{OH}=1$) one and a hydrophobic ($X_{OH}=0.3$) one, revealed from the changes in the adhering cells morphology, the quantities for cell adhesion and spreading, and the development of focal adhesion complexes. When both proteins were applied consequently, distinct complex morphology of the adsorbed protein layer was observed resulting in a “hydrophobic shift” in cellular interaction. In this article, we do not describe the specific conformation of individual molecules as it is difficult to follow with AFM on such rough environment. However, we show that the supramolecular assembly of both Col IV and Lam play an important role, which is the rationale of this work. Although at this time we cannot provide a real model for the functional interplay between proteins and cells, we could show the main players that affect the surface behavior of these matrix proteins: (1) the tendency (not obligatory!) for single molecule deposition on more hydrophilic substrata; (2) the hydrophobic environment provokes the assembly of proteins in networks (including joint Col IV-Lam networks); (3) these networks improve the cellular interaction (with

optimum at $X_{OH}=0.3$), and (4) the very hydrophilic environment may also provoke the cellular interaction, presumably providing better molecular conformation (unfolded) of proteins that is more accessible for integrin receptors. Conversely, we do not state that these findings are universal, as our previous data show that other proteins like fibronectin,^{17,21} vitronectin,¹⁸ and fibrinogen¹⁹ behave differently on the same family of surfaces.

This work opens the door of using similar approaches to study different protein systems involved in cell–biomaterial interaction and BM organization.

Acknowledgments

AFM was performed under the technical guidance of the Microscopy Service at the Universidad Politécnica de Valencia, whose advice is greatly appreciated. The work was supported by the Spanish Ministry of Science and Innovation through project nos. MAT2009-14440-C02-0 and MAT2009-14440-C02-02.

Disclosure Statement

No competing financial interests exist.

References

- Atala, A. Engineering organs. *Curr Opin Biotechnol* **20**, 575, 2009.
- Bueno, E.M., and Glowacki, J. Cell-free and cell-based approaches for bone regeneration. *Nat Rev Rheumatol* **5**, 685, 2009.
- Daley, W.P., Peters, S.B., and Larsen, M. Extracellular matrix dynamics in development and regenerative medicine. *J Cell Sci* **121**, 255, 2008.
- Griffith, L.G., and Naughton, G. Tissue engineering—current challenges and expanding opportunities. *Science* (New York, N.Y.) **295**, 1009, 2002.
- Grinnell, F., and Feld, M.K. Fibronectin adsorption on hydrophilic and hydrophobic surfaces detected by antibody binding and analyzed during cell adhesion in serum-containing medium. *J Biol Chem* **257**, 4888, 1982.
- Sipe, J.D. Tissue engineering and reparative medicine. *Ann NY Acad Sci* **961**, 1, 2002.
- de Mel, A., Jell, G., Stevens, M.M., and Seifalian, A.M. Bio-functionalization of biomaterials for accelerated *in situ* endothelialization: a review. *Biomacromolecules* **9**, 2969, 2008.
- Lutolf, M.P., and Hubbell, J.A. Synthetic biomaterials as instructive extracellular microenvironments for morphogenesis in tissue engineering. *Nat Biotech* **23**, 47, 2005.
- LeBleu, V.S., Macdonald, B., and Kalluri, R. Structure and function of basement membranes. *Exp Biol Med* (Maywood, N.J.) **232**, 1121, 2007.
- Timpl, R., and Brown, J.C. Supramolecular assembly of basement membranes. *Bioessays News Rev Mol Cell Dev Biol* **18**, 123, 1996.
- Rivron, N.C., Liu, J.J., Rouwkema, J., de Boer, J., and van Blijsterswijk, C.A. Engineering vascularised tissues *in vitro*. *Eur Cells Mater* **15**, 27, 2008.
- Sephel, G.C., Kennedy, R., and Kudravi, S. Expression of capillary basement membrane components during sequential phases of wound angiogenesis. *Matrix Biol* **15**, 263, 1996.
- Van Agtmael, T., and Bruckner-Tuderman, L. Basement membranes and human disease. *Cell Tissue Res* **339**, 167, 2010.

14. Potenta, S., Zeisberg, E., and Kalluri, R. The role of endothelial-to-mesenchymal transition in cancer progression. *Br J Cancer* **99**, 1375, 2008.
15. Coelho, N.M., González-García, C., Planell, J.A., Salmerón-Sánchez, M., and Altankov, G. Different assembly of type IV collagen on hydrophilic and hydrophobic substrata alters endothelial cells interaction. *Eur Cells Mater* **19**, 262, 2010.
16. Hernández, J.C.R., Salmerón Sánchez, M., Soria, J.M., Gómez Ribelles, J.L., and Monleón Pradas, M. Substrate chemistry-dependent conformations of single laminin molecules on polymer surfaces are revealed by the phase signal of atomic force microscopy. *Biophys J* **93**, 202, 2007.
17. Gugutkov, D., Altankov, G., Rodríguez Hernandez, J.C., Monleón Pradas, M., and Salmerón Sanchez, M. Fibronectin activity on substrates with controlled—OH density. *J Biomed Mater Res Part A* **92**, 322, 2009.
18. Toromanov, G., González-García, C., Altankov, G., and Salmerón-Sánchez, M. Vitronectin activity on polymer substrates with controlled -OH density. *Polymer* **51**, 2329, 2010.
19. Hernández, J.C.R., Rico, P., Moratal, D., Pradas, M.M., and Salmerón-Sánchez, M. Fibrinogen patterns and activity on substrates with tailored hydroxy density. *Macromol Biosci* **9**, 766, 2009.
20. González-García, C., Ferrus, L.L., Moratal, D., Pradas, M.M., and Sánchez, M.S. Poly(L-lactide) substrates with tailored surface chemistry by plasma copolymerisation of acrylic monomers. *Plasma Processes Polym* **6**, 190, 2009.
21. Rico, P., Rodríguez Hernández, J.C., Moratal, D., Altankov, G., Monleón Pradas, M., and Salmerón-Sánchez, M. Substrate-induced assembly of fibronectin into networks: influence of surface chemistry and effect on osteoblast adhesion. *Tissue Eng Part A* **15**, 3271, 2009.
22. Campillo-Fernández, A.J., Salmerón Sánchez, M., Sabater i Serra, R., Meseguer Dueñas, J.M., Monleón Pradas, M., and Gómez Ribelles, J.L. Water-induced (nano) organization in poly(ethyl acrylate-co-hydroxyethyl acrylate) networks. *Eur Polym J* **44**, 1996, 2008.
23. Hudson, B.G., Reeders, S.T., and Tryggvason, K. Type IV collagen: structure, gene organization, and role in human diseases. Molecular basis of Goodpasture and Alport syndromes and diffuse leiomyomatosis. *J Biol Chem* **268**, 26033, 1993.
24. Khoshnoodi, J., Pedchenko, V., and Hudson, B.G. Mamalian collagen IV. *Microsc Res Tech* **71**, 357, 2008.
25. Fleischmajer, R., Perlish, J.S., Ii, D.E.M., Schechter, A., Murdoch, A.D., Iozzo, R.V., and Yamada, Y. There is binding of collagen IV to beta 1 integrin during early skin basement membrane assembly. *Ann NY Acad Sci* **857**, 212, 1998.
26. Maneva-Radicheva, L., Ebert, U., Dimoudis, N., and Altankov, G. Fibroblast remodeling of adsorbed collagen type IV is altered in contact with cancer cells. *Histol Histopathol* **23**, 833, 2008.
27. Timpl, R., Oberbaumer, I., von der Mark, H., Bode, W., Wick, G., Weber, S., and Engel, J. Structure and biology of the globular domain of basement membrane type IV collagen. *Ann NY Acad Sci* **460**, 58, 1985.
28. Chen, C.H., and Hansma, H.G. Basement membrane macromolecules: insights from atomic force microscopy. *J Struct Biol* **131**, 44, 2000.
29. Altankov, G., and Groth, T. Fibronectin matrix formation by human fibroblasts on surfaces varying in wettability. *J Biomater Sci Polym Ed* **8**, 299, 1997.
30. Altankov, G., Groth, T., Krasteva, N., Albrecht, W., and Paul, D. Morphological evidence for a different fibronectin receptor organization and function during fibroblast adhesion on hydrophilic and hydrophobic glass substrata. *J Biomater Sci Polym Ed* **8**, 721, 1997.
31. Kowalczyńska, H.M., Nowak-Wyrzykowska, M., Kolos, R., Dobkowski, J., and Kaminski, J. Fibronectin adsorption and arrangement on copolymer surfaces and their significance in cell adhesion. *J Biomed Mater Res Part A* **72**, 228, 2005.
32. Tamada, Y., and Ikada, Y. Fibroblast growth on polymer surfaces and biosynthesis of collagen. *J Biomed Mater Res* **28**, 783, 1994.
33. Altankov, G., Grinnell, F., and Groth, T. Studies on the biocompatibility of materials: fibroblast reorganization of substratum-bound fibronectin on surfaces varying in wettability. *J Biomed Mater Res* **30**, 385, 1996.
34. Beck, K., Hunter, I., and Engel, J. Structure and function of laminin: anatomy of a multidomain glycoprotein. *FASEB J* **4**, 148, 1990.
35. Durbeej, M. Laminins. *Cell Tissue Res* **339**, 259, 2010.
36. Tzu, J., and Marinkovich, M.P. Bridging structure with function: structural, regulatory, and developmental role of laminins. *Int J Biochem Cell Biol* **40**, 199, 2008.
37. Chen, C.H., Clegg, D.O., and Hansma, H.G. Structures and dynamic motion of laminin-1 as observed by atomic force microscopy. *Biochemistry* **37**, 8262, 1998.
38. Hansma, H.G. Varieties of imaging with scanning probe microscopes. *Proc Nat Acad Sci USA* **96**, 14678, 1999.
39. Ortega-Vinuesa, J.L., Tengvall, P., and Lundstrom, I. Aggregation of HSA, IgG, and fibrinogen on methylated silicon surfaces. *J Colloid Interface Sci* **207**, 228, 1998.
40. Liesi, P.I., Dahl, D., and Vaheri, A. Neurons cultured from developing rat brain attach and spread preferentially to laminin. *J Neurosci Res* **11**, 241, 1984.
41. Soria, J.M., Ramos, C.M., Bahamonde, O., Cruz, D.M.G., Sánchez, M.S., Esparza, M.A.G., Casas, C., Guzmán, M., Navarro, X., Ribelles, J.L.G., Verdugo, J.M.G., Pradas, M.M., and Barcia, J.A. Influence of the substrate's hydrophilicity on the *in vitro* Schwann cells viability. *J Biomed Mater Res Part A* **83A**, 463, 2007.
42. Charonis, A., Sideraki, V., Kaltezioti, V., Alberti, A., Vlahakos, D., Wu, K., and Tsilibary, E. Basement membrane peptides: functional considerations and biomedical applications in autoimmunity. *Curr Med Chem* **12**, 1495, 2005.
43. Abrams, G.A., Goodman, S.L., Nealey, P.F., Franco, M., and Murphy, C.J. Nanoscale topography of the basement membrane underlying the corneal epithelium of the rhesus macaque. *Cell Tissue Res* **299**, 39, 2000.

Address correspondence to:

George Altankov, M.D., Ph.D.
 Institut de Bioenginyeria de Catalunya
 Feixa Llarga, s/n, Pavelló Govern
 1^o Planta, Pta 1121
 08907 L'Hospitalet de Llobregat
 Barcelona
 Spain

E-mail: george.altankov@icrea.cat; altankov@abv.bg

Received: December 10, 2010

Accepted: May 03, 2011

Online Publication Date: June 16, 2011

2.3 Supplementary results 2

Cell adhesion and spreading

When model materials with tailored density of -OH groups were coated with 50 $\mu\text{g/mL}$ Col IV the same trend on the initial HUVEC interaction was found. HUVEC interact better with Col IV when is adsorbed to the most hydrophilic $X_{\text{OH}} = 1$ substrata (e) and presented another optimum of interaction on relatively hydrophobic $X_{\text{OH}} = 0.3$ substrata (b), followed by $X_{\text{OH}} = 0$, as judged by the elongated and flatten cell morphology with prominent actin stress fibers arranged in the direction of cell polarization (b, e and g, j). Conversely on the other intermediate substrata ($X_{\text{OH}} = 0.5$ and $X_{\text{OH}} = 0.7$) HUVEC presented delayed spreading with rather small actin fibers (a, c, d and h, i). The effectiveness of HUVEC interaction was further evaluated by studying the focal adhesion contacts formation. Again on the two optimums, $X_{\text{OH}} = 1$ and $X_{\text{OH}} = 0.3$, cells presented best-developed focal adhesion contacts (l and o). These morphologic observations were further confirmed by quantitative measurements for adhesion (Figure 1B) and spreading area (Figure 1C) both showing significant increase in $X_{\text{OH}} = 1$ and $X_{\text{OH}} = 0.3$ over the other conditions.

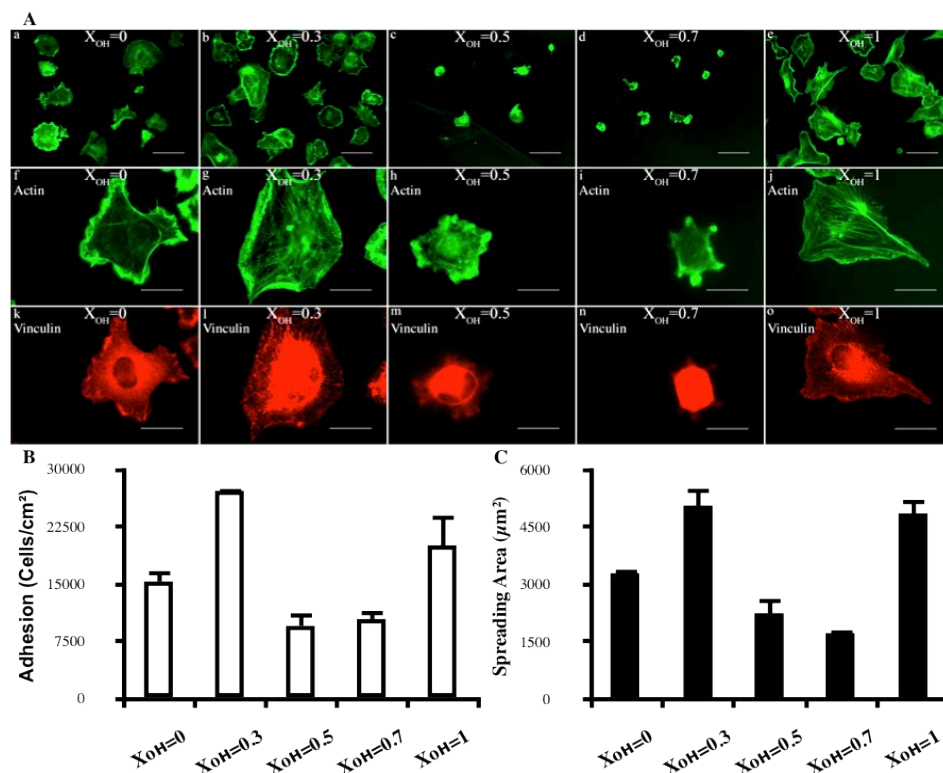


Figure 1 - (A)- Overall morphology (a-e) of HUVEC adhering to Col IV-coated substrates with increasing density of -OH groups. Bar 100 μm . At higher magnification is viewed the actin stress fibers arrangement (f-j) and focal adhesion contacts visualized by vinculin (k-o). Bar = 20 μm . Quantities for cell adhesion expressed as number of cells per cm^2 (B) and cell spreading area shown in μm^2 (C).

Integrin signaling

To learn which integrins were involved in the adhesion process we further studied the organization of $\alpha_1\beta_1$ and $\alpha_2\beta_1$ heterodimers. Figure 2 shows that both integrins are expressed in HUVEC adhering to $X_{OH} = 1$ and $X_{OH} = 0.3$ surfaces (B, E, G, and J). α_1 however represents a rather punctual organization (B, E), also visible on $X_{OH} = 0$ substrata (A), while α_2 show more pronounced clusters resembling focal adhesion contacts (G and J). In contrast on $X_{OH} = 0.5$ and $X_{OH} = 0.7$ surfaces no any integrins organization was found (C, D, H, and I), which correlates with the suppressed development of adhesive complexes on these materials (Figure 1). On more hydrophobic surface, as $X_{OH} = 0$, α_2 expression was similar to α_1 , both presenting a dot like morphology.

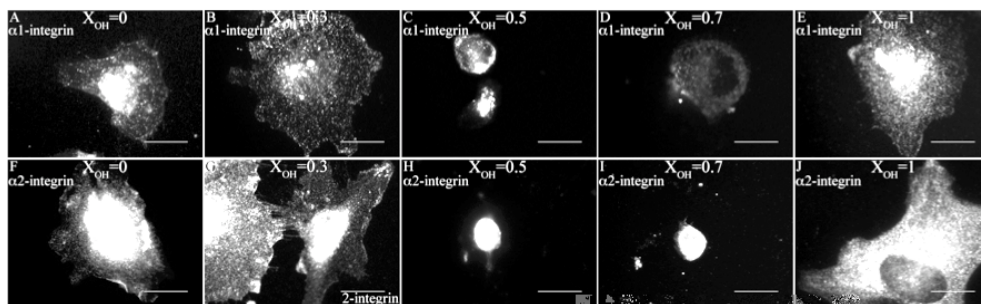


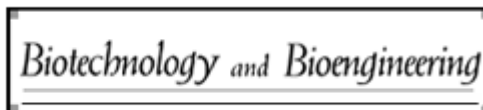
Figure 2 - Expression of alpha 1 (A to E) and alpha 2 (F to J) integrins in HUVEC adhering to the same Col IV coated model surfaces with increasing density of OH groups from left to right. Bar 20 μ m.

3. Arrangement of Type IV Collagen on NH₂ and COOH Functionalized Surfaces

3.1 Preface 3

Molecular engineering of cell-materials interface can be advantageously obtained by *in vitro* reconstruction of supramolecular structures of extracellular matrix (ECM). In this respect collagen is an extremely important molecule because of its abundance in mammalian organisms and its wide variety of specific functional interactions. As stated before we are particularly interested on the surface behavior of Col IV as a unique multifunctional matrix protein involved in the organization of vascular BM. Despite extensive studies on Col IV biochemistry and its involvement in various human disorders, surprisingly little is known about its behavior at biomaterials interface. In Section 1 and 2 we showed that substratum wettability significantly affects Col IV adsorption pattern, and in turn, it alters endothelial cells interaction. Except wettability however, a variety of other surface properties, including chemistry and charge may alter protein adsorption/conformation, and thus influencing the cellular response. Here we describe the behavior of Col IV in contact with two new model surfaces, the self-assembled monolayers (SAMs) exposing positively charged -NH₂ and negatively charged -COOH functionalities, in order to learn more about the effect of substratum chemistry and charge on the biological performance of materials.

AFM studies revealed distinct patterns of Col IV assembly resembling network-like structures on NH₂ and aggregates on COOH substrates suggesting altered protein conformation at later. Col IV on NH₂ surface presented close to single molecular arrangement at low coating concentrations where biologically relevant structures resembling dimers and tetramers can also be seen. As the coating concentration increases the Col IV molecules assemble in linear features. Conversely, on COOH the sponge-like morphology with appearance of rather globular protein aggregates remains almost unaltered with increasing the coating concentration. HUVECs attached less efficiently to Col IV adsorbed on negatively charged COOH surface as judged by altered cell spreading, focal adhesions formation, and actin cytoskeleton development. Immunofluorescence studies further revealed a better Col IV recognition by both α_1 and α_2 integrins on positively charged NH₂ substrata resulting in higher p-FAK recruitment to the focal adhesion complexes. Conversely, on COOH surface no integrin clustering was observed. This study provides a further causal link between the protein conformation and the endothelial cells interaction. It suggests that NH₂ functionalization combined with Col IV pre-adsorption comprises a prospective tool for the engineering of biomimetic interface that might improve the endothelization of implants. Details of this study are presented in the paper below.



Arrangement of Type IV Collagen on $-NH_2$ and $-COOH$ functionalized surfaces

Journal:	<i>Biotechnology and Bioengineering</i>
Manuscript ID:	Draft
Wiley - Manuscript type:	Article
Date Submitted by the Author:	n/a
Complete List of Authors:	Altankov, George; Institució Catalana de Recerca i Estudis Avançats (ICREA), Campus de Ciències de la Salut Bellvitge; Institute for Bioengineering of Catalonia (IBEC), Molecular Dynamics at cell-Biomaterial Interface group Coelho, Nuno; Institute for Bioengineering of Catalonia (IBEC), Molecular Dynamics at cell-Biomaterial Interface group; Universitat Politècnica de Catalunya, IBEC González-García, Cristina; Universidad Politécnica de Valencia, Center for Biomaterials and Tissue Engineering Salmerón Sánchez, Manuel; Universidad Politécnica de Valencia, Center for Biomaterials and Tissue Engineering
Key Words:	Collagen type IV, SAMs, AFM, surface-induced protein assembly, Endothelial cells, Vascular grafts

SCHOLARONE™
Manuscripts

1
2
3 **Arrangement of Type IV Collagen on –NH₂ and –COOH functionalized surfaces**
4
5
6

7
8 Nuno Miranda Coelho^{1,2}, Cristina González-García^{4,5}, Manuel Salmerón-Sánchez^{4,5} and
9

10 George Altankov^{1,3,4*}
11

12
13
14
15 ¹ Institut de Bioenginyeria de Catalunya, Barcelona, Spain
16

17 ² Universitat Politècnica de Catalunya, Barcelona, Spain
18

19 ³ ICREA (Institució Catalana de Recerca i Estudis Avançats), Catalonia, Spain
20

21 ⁴ CIBER de Bioingeniería, Biomateriales y Nanomedicina (CIBER-BBN), Valencia,
22
23 Spain
24

25
26
27 ⁵ Center for Biomaterials and Tissue Engineering, Universidad Politécnica de Valencia,
28
29 46022 Valencia, Spain
30

31 * Corresponding author: George Altankov; e-mail: george.altankov@icrea.cat
32

33
34 Running title: collagen IV assembly depends on substructure charge
35
36
37
38
39
40
41
42
43
44
45
46
47
48
49
50
51
52
53
54
55
56
57
58
59
60

Abstract

Apart from the paradigm that cell-biomaterials interaction depends on the adsorption of soluble adhesive proteins we anticipate that upon distinct conditions other, less soluble ECM proteins such as collagens, also associate with the biomaterials interface and the cellular response they elicit might be of significant bioengineering interest. Making use of Atomic Force Microscopy (AFM) we seek to follow the nanoscale behaviour of adsorbed type IV collagen (Col IV) – a unique multifunctional matrix protein involved in the organization of basement membranes (BM) including vascular one. Likewise we have previously shown that the substratum wettability affects significantly Col IV adsorption pattern which in turn alters endothelial cells interaction. Now we introduce two new model surfaces (SAMs), a positively charged $-NH_2$ and negatively charged $-COOH$ to learn more about the particular effect of these uniformly available bio-functionalities. AFM studies revealed distinct pattern of Col IV assembly resembling different aspects of network-like structure or aggregates suggesting altered protein conformation. The amount of adsorbed FITC labelled Col IV was also quantified showing about twice more protein on NH_2 substrata. We further found that human umbilical vein endothelial cells (HUVEC) attach less efficiently to Col IV adsorbed on negatively charged $-COOH$ surface judged by the altered cell spreading, focal adhesions formation and actin cytoskeleton development. Immunofluorescence studies revealed also better Col IV recognition by both α_1 and α_2 integrins on positively charged $-NH_2$ substrata resulting in higher pFAK recruitment in the focal adhesion complexes, apart from $-COOH$ surface where no integrin clustering was observed. Collectively, these results point to the possibility that combined NH_2 and Col IV functionalization may support endothelialization of cardiovascular implants.

Introduction

To date, blood contacting devices including small diameter vascular grafts, stents, hard valves etc., suffer from a common defect – the lack of significant endothelial cells ingrowth – presumably caused by the absence of specialized basement membrane (BM). It results in restenosis and an accelerated device failure (Baber et al. 2010; de Mel et al. 2008; Dvir et al. 2011). In this context we seek to learn more about the surface behaviour of type IV collagen (Col IV) as this unique multifunctional matrix protein plays a vital role in the organization and functional performance of BM (Charonis et al. 2005; Hudson et al. 1993; Khoshnoodi et al. 2008; Kruegel and Miosge 2010), including the vascular one (Kalluri 2003). We anticipate that understanding how Col IV assembly at biomaterials interface (Coelho NM 2010; Hudson et al. 1993; Keresztes et al. 2006) might provide critical impact if one wants to mimic the natural organization of the vessel wall.

When a foreign material is implanted the rapid adsorption of proteins from the surrounding medium precedes the subsequent cellular interaction (Altankov et al. 1996; Allen et al. 2006; Lee et al. 2006). A variety of surface properties including wettability, chemistry, topography and charge, have been shown to alter protein adsorption/conformation thus influencing the cellular response (Altankov et al. 1996; Allen et al. 2006; Keselowsky et al. 2005; Sherratt et al. 2005; Xu and Siedlecki 2007). Relatively little is known however about the behavior of matrix proteins which are less soluble in the biological fluids, such as collagens, laminins and others that exist in the tissues as natural polymers. At longer contact or under distinct non-physiological conditions these proteins may also associate with the surfaces thus determining the cellular interaction. Employing AFM and other nano indentation techniques recently we have shown that some surface properties such as wettability may strongly affect the

1
2
3 pattern of Col IV adsorption (Coelho NM 2010); we found that even adsorbed from acid
4 conditions it assembly in a nearly single molecular features on hydrophilic substrata
5 (glass) while tend to form prominent polygonal shapes consisting of molecular
6 aggregates on the hydrophobic octadecylsilane surface; likewise, the endothelial cells
7 attach more efficiently to the single molecular arrangements in comparison to the
8 aggregated form of Col IV (Coelho NM 2010). Here we describe the behavior of Col IV
9 in contact with two new model surfaces, the self assemble monolayer's (SAMs)
10 exposing positively charged $-NH_2$ and negatively charged $-COOH$ functionalities, to
11 learn more about the effect of substratum chemistry. Indeed, AFM studies revealed
12 distinct pattern of Col IV assembly resembling different aspects of network-like
13 structure on NH_2 and aggregates on $COOH$ substrata, which were further shown to
14 corroborate with the endothelial cells interaction.

15
16
17 Col IV is recognized by integrins – a family of cell surface receptors that provide trans-
18 membrane links between the ECM and the cytoskeleton (Barczyk et al. 2010; Hynes
19 2002; White et al. 2004). Out of the known 24 integrin heterodimers, $\alpha_1\beta_1$, $\alpha_2\beta_1$, $\alpha_{10}\beta_1$,
20 and $\alpha_{11}\beta_1$ act as primary receptors for collagens(Barczyk et al. 2010; Hynes 2002;
21 Kapyla et al. 2000; Kern et al. 1993; Popova et al. 2007; Vandenberg et al. 1991), but
22 most abundantly expressed are $\alpha_1\beta_1$ and $\alpha_2\beta_1$ integrins (Khoshnoodi et al. 2008; White
23 et al. 2004). Upon occupation integrins clusterize in focal adhesion complexes where
24 their specific bidirectional signalling converges with other signalling pathways (Hynes
25 2002) through a tyrosine phosphorylation dependent mechanism. It involves Focal
26 Adhesion Kinase (FAK) and many other signalling components including Src, Cas, and
27 paxillin (Guan 1997; Michael et al. 2009; Sieg et al. 1999). Depending on the
28 conformation of adsorbed protein however, different cellular interaction (Grinnell and
29
30
31
32
33
34
35
36
37
38
39
40
41
42
43
44
45
46
47
48
49
50
51
52
53
54
55
56
57
58
59
60

1
2
3 Feld 1982) and integrin signalling may be expected (Kapyla et al. 2000; Keresztes et al.
4
5
6 2006; Ludwig et al. 2006).

7
8 We found that human umbilical vein endothelial cell (HUVEC) attach less efficiently on
9
10 negatively charged $-\text{COOH}$ surface, as judged by the altered cell spreading, focal
11
12 adhesions formation and actin cytoskeleton development. Likewise,
13
14 immunofluorescence studies revealed better Col IV recognition on positively charged
15
16 NH_2 substrata involving both α_1 and α_2 integrins and resulting in higher p-FAK
17
18 recruitment. This suggests successful transmission of adhesive signals to the cells
19
20 interior, apart from COOH substrata where almost no integrin clustering was observed.
21
22 Thus, our studies provide a causal link between the protein conformation and the
23
24 endothelial cells interaction. Details of this study are presented below.
25
26
27

28 29 **Material and Methods**

30
31 *Self-assembly monolayers:* Two SAMs were prepared according to previously described
32
33 protocol(Gustavsson et al. 2008). Shortly, round shaped glass coverslips (Fisher
34
35 Bioblock 15 mm diameter) were cleaned in an ultrasonic bath for 10min in a 1:1
36
37 mixture of 2-propanol and tetrahydrofuran. The samples were then exposed to piranha
38
39 solution (30% (v/v) H_2O_2 and 70% (v/v) H_2SO_4) for 30 min followed by a copious
40
41 rinsing with milliQ water (18.2M Ω) and dried. For *NH₂ functionalization* the samples
42
43 were immersed for 18min at room temperature in a solution containing 30ml methanol,
44
45 10ml of 4% acetic acid glacial and 3-(2-aminoethylamino) propyltrimethoxysilane
46
47 ($\text{C}_8\text{H}_{22}\text{N}_2\text{O}_3\text{Si}$, Fluka) to yield a final 1% concentration. Excess of silane was washed by
48
49 immersion in excess solvent solution. Samples were air dried and than heated at 80°C
50
51 for 1h. *COOH functionalization* was performed in two steps, by immersing the samples
52
53 in a 1:3 mixture of CCl_4 and $n\text{-C}_7\text{H}_{16}$ containing 0.01M 10-(carbomethoxy) decyl
54
55 dimethylchlorosilane ($\text{C}_{14}\text{H}_{29}\text{ClO}_2\text{Si}$, ABCR GmbH &Co) for 4h at 4°C, which create
56
57
58
59
60

1
2
3 COOHCH₃ functions. Samples were then washed in silane-free solvent, heated as above
4
5 and immersed overnight in a 12M HCl solution to create COOH surfaces as second
6
7 step.
8
9

10
11 *Water contact angle:* Wettability of -NH₂ and -COOH SAMs was estimated with water
12
13 contact angle measurement using sessile drop technique under Dataphysics Contact
14
15 Angle Systems OCA15. The same measurements were also performed after coating the
16
17 samples with 50µg/ml native Col IV (see below) for 30 min at 37⁰C. Average values
18
19 were obtained from 3 measurements in at least three different samples.
20
21

22
23 *Quantification of adsorbed FITC-Collagen IV:* The adsorption of FITC-Collagen IV
24
25 was quantified by NaOH extraction as described previously(Coelho NM 2010). Briefly,
26
27 the model surfaces were cleaned with distilled water in an ultrasonic bath, dried and
28
29 coated for 30min at 37⁰C with DQTM Collagen type IV (Molecular Probes, Cat. No D-
30
31 12052) at concentrations 5-50 µg/ml dissolved in PBS. This collagen (type IV from
32
33 human placenta origin) is conjugated with FITC (FITC-Col IV) in such a way that part
34
35 of it fluorescence is quenched thus increasing significantly the quantum yield upon
36
37 extraction under denaturing conditions. After coating the samples with different Col IV
38
39 concentrations, as indicated, they were rinsed three times with PBS and dried. The
40
41 adsorbed FITC-Col IV was extracted with 250µl of 0.2M NaOH for 2h at room
42
43 temperature. The fluorescent intensity of the extracts were measured with a fluorescent
44
45 spectrophotometer (Horiba-Jobin y Von, USA) set to 488nm (excitation) and 530nm
46
47 (emission) and compared to a standard curve based on known concentrations of FITC-
48
49 Col IV solutions in 0.2M NaOH.
50
51
52
53

54
55 *Atomic force microscopy:* For AFM measurements -NH₂ and -COOH samples were
56
57 coated with native Col IV (Abcam, Cat. No ab7536, UK) at indicated concentrations 1-
58
59 50µg/ml in 0.1M sodium acetate (pH 4.5) for 10 min and then dried. We have used the
60

1
2
3 AFM NanoScope III from Digital Instruments (Santa Barbara, CA) operating in the
4 tapping mode in air utilising Si cantilever from Veeco (Manchester, UK) with force
5 constant of 2.8N/m and resonance frequency of 75 kHz. The phase signal was set to
6 zero at the resonance frequency of the tip. The tapping frequency was 5-10% lower than
7 the resonance one. Drive amplitude was 200mV and the amplitude set-point A_{sp} was
8 1.4V. The ratio between the amplitude set-point and the free amplitude was kept equal
9 to 0.7. Some AFM images were analyzed using the WSxM software (Nanotec, Spain) to
10 observe the initial topography of non coated surfaces, as well as, the uniform
11 distribution of protein on the different SAMs.
12
13
14
15
16
17
18
19
20
21
22
23

24 *Cells:* Human Umbilical Vein Endothelial Cells (HUVEC) purchased by PromoCell
25 (Cat No C-12200) were cultured in Endothelial Cell Growth Medium (PromoCell, Cat
26 No C- 22010) supplemented with SupplementMix (PromoCell Cat No C39215)
27 containing 0.4% ECGS/H; 2% Fetal Calf Serum, 01ng/ml Epidermal Growth Factor,
28 1 μ g/ml Hydrocortison and 1ng/ml basic fibroblast factor. The growth medium was
29 exchanged at each 3rd day. For the experiments the cells were detached from around
30 confluent flasks with Trypsin/EDTA (Invitrogen) and the remained trypsin activity was
31 stopped with 100% FBS before 2 times washing with pure medium to remove any
32 traces of serum proteins. Finally the cells were reconstituted in serum free EC medium.
33
34
35
36
37
38
39
40
41
42
43
44

45 *Overall Cell morphology:* To study the overall cell morphology we used actin stained
46 samples. For that purpose, 10⁵ cells/well were seeded in 6 well TC plates (Costar)
47 containing the samples for 2h in serum free medium. Typically, the samples had been
48 pre-coated with native Col IV as stated above, at concentration 50 μ g/ml in 0.1M sodium
49 acetate pH 4.5 for 30 min. At the end of adhesion, the cells were fixed with 4%
50 paraformaldehyde (20min) and permeabilized with 0.5% Triton X-1000 for 5min. Actin
51 cytoskeleton was visualized with FITC-phalloidin (Molecular Probes, Cat No A12379)
52
53
54
55
56
57
58
59
60

1
2
3 and the nuclei with Hoechst 34580 (Invitrogen, Cat No H21486) dissolved in PBS
4 containing 1% albumin. Finally the samples were mounted in Mowiol. The samples
5 were viewed and photographed on a fluorescent microscope Axio Observer Z1, (Zeiss,
6 Germany) at different magnification (see below). At least 3 representative images for
7 each magnification were acquired.

8
9
10
11
12
13
14
15 *Quantification of cell adhesion and spreading:* The number of adhering cells and the
16 mean cell surface area were evaluated using the Image J plug-ins (NIH,
17 <http://rsb.info.nih.gov/ij/>, USA). The adhesion was measured by counting the cells
18 nuclei in at least 3 randomly chosen squares of each sample (photographed at 10X
19 magnification) using the blue channel of microscope (viewing the cells nuclei). The
20 average cells area was further measured (in μm^2) using the same samples but viewed at
21 20x magnification in the green channel of microscope (to visualize cellular actin). Three
22 slides were studied for each condition and the results presented correspond to 3
23 independent experiments.

24
25
26
27
28
29
30
31
32
33
34
35
36 *Immunofluorescence:* 10^5 cells/well were seeded for 2h as above. To visualize focal
37 adhesions and phosphorylated focal adhesion kinase (pFAK) the fixed and
38 permeabilized samples were saturated with 1% albumin in PBS for 15min. Vinculin was
39 visualized using monoclonal antibody (Sigma, cat No V9131) dissolved in PBS-1%
40 albumin for 30min followed by AlexaFluor 488 goat anti-mouse (Invitrogen) as
41 secondary antibody. The p-FAK was visualized using pFAK (Tyr925) polyclonal
42 antibody (Cell Signaling cat No 3284) dissolved in PBS-1% albumin for 30min,
43 followed by AlexaFluor 555 goat anti-rabbit (Invitrogen) as secondary antibody. When
44 double or triple staining was used, the preliminary studies with omitting of the
45 corresponding secondary antibodies were performed confirming no cross-reactivity. $\alpha 1$
46 and $\alpha 2$ integrins were viewed with monoclonal anti-human integrin Mabs (Chemicon,
47
48
49
50
51
52
53
54
55
56
57
58
59
60

1
2
3 Cat No MAB1973) and (Abcam, No Ab24697), respectively, followed by AlexaFluor
4
5 555 goat anti-mouse (Invitrogen) as secondary antibody. In some cases FITC phalloidin
6
7 was added to the secondary antibody. The samples were viewed and photographed in a
8
9 fluorescent microscope Axio Observer as above. At least 3 representative images were
10
11 acquired (63X) for each experimental condition.
12
13

14
15 *Statistical analysis* was performed using Stat Graphics Plus software employing
16
17 ANOVA test to determine statistically significant differences between groups ($p < 0.05$).
18
19 Each data point represents mean \pm standard deviation (SD) from at least three
20
21 independent experiments.
22
23

24 25 **Results**

26
27 *Water contact angle measurements:* The data presented in Table 1 show a significant
28
29 increase of water contact angle (WCA $^\circ$) after silanization of the samples confirming the
30
31 homogenous coating with SAMs. NH₂ surfaces show WCA $^\circ$ of $53.2 \pm 6.9^\circ$, which is
32
33 about 30% higher than COOH ($p < 0.05$). However, after coating with Col IV the WCA $^\circ$
34
35 of both surfaces substantially decrease to a relatively hydrophilic value of 24-27 $^\circ$, which
36
37 suggests that the cells will not “sense” significant differences in wettability upon
38
39 contact with above surfaces.
40
41
42

43
44 *Adsorption of Col IV on NH₂ and COOH surfaces:* Commercially available FITC-Col
45
46 IV (monomeric) was used to study its adsorption kinetic to the model surfaces. Adsorbed
47
48 Col IV was determined by comparison of extracted fluorescence signals (using 0.2M
49
50 NaOH) to a standard curve with known FITC-Col IV concentrations as previously
51
52 described (Coelho NM 2010; Gustavsson et al. 2008). Detectable values were obtained
53
54 on both substrata (Fig. 1) showing typical saturation curves with a tendency for
55
56 equilibrium at about 50 $\mu\text{g/ml}$. NH₂ surfaces demonstrated about twice significantly
57
58 higher fluorescent signal for concentrations above 20 $\mu\text{g/ml}$.
59
60

1
2
3
4
5
6
7
8
9
10
11
12
13
14
15
16
17
18
19
20
21
22
23
24
25
26
27
28
29
30
31
32
33
34
35
36
37
38
39
40
41
42
43
44
45
46
47
48
49
50
51
52
53
54
55
56
57
58
59
60

Atomic Force Microscopy: Fig. 2 represents the nanoscale adsorption pattern of Col IV studied with AFM onto NH₂ (A) and COOH (B) surfaces as function of the coating concentrations from which the protein is adsorbed, increasing as 0, 1; 5; 10; 20; and 50 μg/ml (ordered from top to bottom). At lower concentrations as 1 μg/ml multiple features with nearly single molecule size distribution were found which can not be seen on both plain surfaces (0 μg/ml) and this morphology appears to be similar for concentrations up to 10 μg/ml. At concentrations above 20 μg/ml large linear structures appeared on NH₂ surface, presumably consisting of molecular aggregates (Fig. 2A), which correlates with the observed twice higher amount of protein (Fig. 1). Conversely, on COOH surface (Fig. 2D) the sponge-like morphology with appearance of rather globular protein aggregates that remains almost unaltered with increasing the coating concentration is observed. Another evidence for the higher amount of protein on NH₂ surfaces is the considerably greater thickness of the protein layer (see the reference z-scale bar on the right). In fact, as brighter is the image the thicker is the protein layer and this difference is obviously better pronounced at higher coating concentrations (above 20 μg/ml), also used for the biological studies (50 μg/ml).

Cell adhesion and spreading: The overall morphology of HUVEC adhering for 2h on Col IV coated NH₂ and COOH surface is shown on Fig. 3. On COOH cells represent delayed spreading (Fig. 3B) with short actin filaments (Fig. 3D), while on NH₂ they are more flattened (Fig. 2A) with prominent actin stress fibers extending to the direction of cell polarization (Fig. 3C). The quantitative data presented on Fig. 3E and 3F shows a significant increase in both cell adhesion ($p < 0.05$) and cell spreading area ($p < 0.05$), respectively, on NH₂ in comparison to COOH substrata. On non-coated samples only negligible cell spreading was observed with no difference between substrates (not shown).

1
2
3 The difference in the effectiveness of cell adhesion was confirmed by the simultaneous
4 visualization of focal adhesion contacts (red) and the actin cytoskeleton (green) shown
5
6 on Fig. 3. The flattened and elongated cell morphology of HUVEC on NH₂ (Fig. 3C)
7
8 correlates with the well developed focal adhesion contacts, where stress fibres often
9
10 insert (see the arrow in merges at Fig. 3C). Conversely, on COOH surface round shaped
11
12 morphology correlates with less expressed focal adhesion complexes (Fig. 3D).
13
14
15

16
17 *Signalling by integrins:* To learn which integrins are involved in the adhesion process
18
19 we studied the organization of $\alpha 1\beta 1$ and $\alpha 2\beta 1$ heterodimers referred to us as main
20
21 collagen receptors: the first specific for Col IV, and the second recognizing all collagen
22
23 types (Hynes 2002; Khoshnoodi et al. 2008). As shown in Fig. 4 both integrins are
24
25 expressed in HUVEC adhering on Col IV coated NH₂ surface (Fig. 4A and C); $\alpha 1$
26
27 represents a rather linear organization (Fig. 4A) along with actin stress fibres (not
28
29 shown) while $\alpha 2$ show well pronounced clusters resembling focal adhesion contacts
30
31 (Fig. 4C). Conversely, almost missing $\alpha 1$ and $\alpha 2$ integrins organization on COOH was
32
33 found (Fig. 4B and D, respectively), which correlates with the worse development of
34
35 adhesive complexes (Fig. 3D).
36
37
38
39

40
41 To learn whether the development of focal adhesions induced recruitment of
42
43 phosphorylated signalling molecules we co-stain the samples for vinculin and pFAK.
44
45 The data presented on Fig. 5 show a higher level of co-localisation between the well
46
47 developed focal adhesion contacts (viewed by vinculin in green) and pFAK (red) on
48
49 NH₂ substrata resulting in orange in merges (see inset on Fig. 5E). Conversely, Fig. 5 B,
50
51 D and E demonstrates that even some cells are able to make focal contacts (Fig. 5B),
52
53 significantly less p-FAK is recruited on COOH (Fig. 5D), resulting in prevalent green at
54
55 merges (see the enlarged view on Fig. 5F) - an observation suggesting altered
56
57 transmission of signal to the cell interior.
58
59
60

Discussion

Despite the extensive studies on biochemistry of Col IV (Gelse et al. 2003; Hudson et al. 1993; Keresztes et al. 2006) and its involvement in various human disorders (Charonis et al. 2005; Gelse et al. 2003), surprisingly little is known about the behavior of this important matrix protein at biomaterials interface. This study demonstrates a clear dependence of Col IV adsorption pattern on the substratum chemistry and provides a causal link between the protein conformation and the cellular interaction. The NH₂ and COOH functions are abundantly expressed in all biological systems and their influence on the substratum behavior of adsorbed proteins is critical (Lee et al. 2006; Thevenot P Fau - Hu et al. 2008). As the amount of free COOH and NH₂ groups in proteins is equal, the difference in their substratum behavior might be attributed to their intrinsic physical properties. One possibility is that the positively charged NH₂ surfaces possess higher affinity because of the net negative charge of Col IV molecules in acidic conditions. Likewise, the appearance of repulsive forces might be expected on the negatively charged COOH substrata (Lee et al. 2006; Mrksich 2009; Thevenot P Fau - Hu et al. 2008). However, the AFM studies revealed that Col IV molecules do not adsorb stochastically, but rather tend to assemble in networks or aggregates, which points on the involvement of intermolecular forces. In fact, we obtained a specific surface induced assembly of Col IV which tends to augment with increasing the coating concentrations. It confirms our previous study (Coelho NM 2010) showing similar networks of Col IV on hydrophilic vs. aggregates on hydrophobic surfaces. However, this similarity is valid only for the low coating concentrations, as at higher, the volumetric distribution of the protein differs significantly: on NH₂ the Col IV molecules tend to associate in fibril-like features (Fig.2A), while on COOH the aggregated, sponge-like morphology remains. Thus, the increased amount of Col IV on NH₂

1
2
3 substrata should be attributed to the protein-protein interactions, while on COOH the
4
5 substratum interactions are prevalent. That is to say, the specific interaction between the
6
7 chemical groups on the surface (either NH₂ or COOH) and the different domains of the
8
9 Col IV molecule results in altered conformation upon adsorption that facilitates
10
11 intermolecular association of collagen molecules on NH₂ or leads to a favoured
12
13 interaction with COOH surface. This behaviour however is rather particular, if one
14
15 keeps in mind that electrostatic interactions should enhanced the opposite, which
16
17 suggests the existence of specific biological-non/biological interactions with stronger
18
19 probability than just the electrostatic interactions.
20
21
22
23

24
25 On NH₂ surface Col IV molecules tend to organize in large linear structures,
26
27 surprisingly resembling fibbers. It should be noted however that Col VI is not fibrillar
28
29 protein as it typically forms 2D networks in the BM (Shamhart and Meszaros 2010;
30
31 Timpl et al. 1985). Similar linear arrangement of Col IV has been found during early
32
33 BM assembly (Fleischmajer et al. 1998) or deposited by embryonic mouse cells on the
34
35 culture substratum (Chen and Little 1985). Fibroblasts can also remodel Col IV in fibril
36
37 like pattern (Maneva-Radicheva et al. 2008), but it has to be admitted that all these
38
39 arrangements are cell-dependent. The present study provides evidence for the first time
40
41 that Col IV may assembly in linear features spontaneously, provoked by the substratum
42
43 chemistry.
44
45
46
47

48
49 The supramolecular structure of Col IV was extensively studied during the last decades
50
51 (Hudson et al. 1993; Khoshnoodi et al. 2008; Kühn 1995; Timpl et al. 1985). Like many
52
53 other matrix proteins Col IV is secreted as monomeric pro-form (Kalluri 2003; Kühn
54
55 1995; LeBleu et al. 2007). Once secreted the triple-helical heterotrimeric molecules of
56
57 Col IV self-associate to form 2D network which serves as molecular scaffold for other
58
59 BM components (Charonis et al. 2005; Kalluri 2003; Kruegel and Miosge 2010).
60

1
2
3 Detailed *in situ* analysis of high resolution electron micrographs revealed that Col IV
4
5 molecules self-assemble forming polygonal networks held together by overlapping and
6
7 lateral interactions along the triple-helical domain and the N- and C-terminal end-
8
9 domains (Abrams et al. 2000). Thus, Col IV is not soluble in the biological fluids
10
11 (Gelse et al. 2003), but *in vitro* it can be adsorbed to the materials from acid conditions,
12
13 where the triple helical molecules are unfolded and the lateral interactions minimized
14
15 (Timpl et al. 1985). Many studies have shown that the acid soluble collagen is in a
16
17 reversible configuration (Kühn 1995) and once switched to a physiological environment
18
19 (pH 7.4, 37°C and distinct ionic content) polymerize in a highly functional gel-like
20
21 matrix (Sung et al. 2009). An important observation from this and also from our
22
23 previous study (Coelho NM 2010) is that upon adsorption the soluble Col IV tends to
24
25 assembly in a rather 2D network - a configuration similar to those in the BM (Kühn
26
27 1995). Now we provide new insight in the diverse mechanisms for Col IV assembly on
28
29 oppositely charged substrata showing that NH₂ substrata promote networks formation
30
31 that influence positively its biological performance.

32
33
34 The use of primary endothelial cells in this study is not accidentally. Col IV is the main
35
36 component of the vascular BM (Rivron et al. 2008; Sephel et al. 1996), where
37
38 endothelial cells reside in a rather 2D environment, i.e. in geometry similar when
39
40 adhering to blood contacting devices (de Mel et al. 2008; Rivron et al. 2008; Sephel et
41
42 al. 1996). However, while endothelial cells procurement technologies for seeding
43
44 implants have significantly improved, adhering cells often dedifferentiate and act in a
45
46 counterproductive manner, accelerating device failure (Daley et al. 2008; Griffith and
47
48 Naughton 2002; Sipe 2002). We anticipate that a reason might be the missing
49
50 environmental signals from the natural BM. Our data show significantly improved
51
52 interaction of HUVEC on Col IV coated NH₂ surface suggested by the well developed
53
54
55
56
57
58
59
60

1
2
3 focal adhesion complexes and actin cytoskeleton. Conversely, a delayed cell spreading
4
5 was observed on COOH substrata. The reason for this difference is not clear, but it is
6
7 obviously connected with the conformation of adsorbed protein. Presumably the
8
9 aggregated Col IV is less favored for the cells because of screening the recognition
10
11 sequences. The main cellular receptor for collagens is $\alpha 2\beta 1$ integrin (Kapyla et al. 2000;
12
13 Kern et al. 1993; Popova et al. 2007), while $\alpha 1\beta 1$ is Col IV specific (Kapyla et al. 2000;
14
15 Kern et al. 1993; Vandenberg et al. 1991). Our results show that both $\alpha 1$ and $\alpha 2$
16
17 integrins are involved, which correlates with a previous observations (Coelho NM
18
19 2010). On NH_2 surface however $\alpha 2$ integrin form structures, resembling focal
20
21 adhesions, while $\alpha 1$ integrin appears in a rather linear pattern, resembling fibrillar
22
23 adhesions (Cukierman et al. 2001) which corroborates with the previously obtained co-
24
25 localization of substratum arranged Col IV with fibronectin fibrils (Maneva-Radicheva
26
27 et al. 2008). Nevertheless, these patterns of the receptors are missing on COOH
28
29 substrata suggesting lowered recognition of the protein.
30
31
32
33
34

35
36 Upon adsorption on mica Col IV forms dimmers and tetramers (Chen and Hansma
37
38 2000). It is noteworthy that similar features resembling dimmers (see arrow in the
39
40 augmented insets of Fig. 2C) or tetramers (arrowhead) might be distinguished on NH_2
41
42 substrata (at low coating concentrations only), obviously representing configuration that
43
44 is easily recognized by the cells. The spontaneous formation of fibril-like structures at
45
46 higher coating concentrations however should not be underestimated. It is well
47
48 documented that the cells can “read” the geometry of the underlining substrata (Daley et
49
50 al. 2008) which can dramatically change their behavior. Indeed, the better recognition of
51
52 Col IV on NH_2 surface is confirmed by the obvious recruitment of p-FAK in the focal
53
54 adhesion complexes. The focal adhesion kinase (FAK) plays an important role in
55
56 integrin signaling (Barczyk et al. 2010; Groth and Altankov 1996; Michael et al. 2009;
57
58
59
60

1
2
3 Sieg et al. 1999). The activation of FAK by integrin clustering results in
4
5
6
7
8
9
10
11
12
13
14
15
16
17
18
19
20
21
22
23
24
25
26
27
28
29
30
31
32
33
34
35
36
37
38
39
40
41
42
43
44
45
46
47
48
49
50
51
52
53
54
55
56
57
58
59
60

Sieg et al. 1999). The activation of FAK by integrin clustering results in autophosphorylation at tyrosine 397, which is a binding site for Src family kinases. The recruitment of Src kinases result in the phosphorylation of several tyrosine residues (Calalb et al. 1995) which include the one selected by us (Tyr925) reflecting the transmission of signals from the substratum to the cell interior (Calalb et al. 1995; Geiger et al. 2001; Groth and Altankov 1996; Guan 1997). In fact, our results confirm the higher activity of integrin – p-FAK pathway upon Col IV recognition on NH₂ surface. p-FAK co-localizes well with the focal adhesion complexes (see augmented insets on Fig. 5E), confirming an improved transmission of signal. Conversely, on COOH surface the altered integrin clustering correlates with an abrogated expression of p-FAK (see the augmented inset at Fig. 5E) which imply on it lowered biocompatibility. Collectively, these results suggest that NH₂ functionalization combined with Col IV pre-adsorption comprises a prospective tool for the engineering of biomimetic interface that might improve the endothelization of cardiovascular implants.

Acknowledgments

AFM was performed under the technical guidance of the Microscopy Service at the Universidad Politécnica de Valencia, whose advice is greatly appreciated. The work was supported by the Spanish Ministry of Science and Innovation through projects MAT2009-14440-C02-01 and MAT2009-14440-C02-02.

Bibliography

- Abrams GA, Goodman SL, Nealey PF, Franco M, Murphy CJ. 2000. Nanoscale topography of the basement membrane underlying the corneal epithelium of the rhesus macaque. *Cell and Tissue Research* 299(1):39-46.
- Altankov G, Grinnell F, Groth T. 1996. Studies on the biocompatibility of materials: fibroblast reorganization of substratum-bound fibronectin on surfaces varying in wettability. *Journal of Biomedical Materials Research* 30(3):385-391.
- Allen LT, Tosetto M, Miller IS, O'Connor DP, Penney SC, Lynch I, Keenan AK, Pennington SR, Dawson KA, Gallagher WM. 2006. Surface-induced changes in protein adsorption and implications for cellular phenotypic responses to surface interaction. *Biomaterials* 27(16):3096-3108.

- 1
2
3 Baber U, Kini AS, Sharma SK. 2010. Stenting of complex lesions: an overview. *Nat*
4 *Rev Cardiol* 7(9):485-496.
5
6 Barczyk M, Carracedo S, Gullberg D. 2010. Integrins. *Cell and Tissue Research*
7 339(1):269-280.
8 Calalb M, Polte T, Hanks S. 1995. Tyrosine phosphorylation of focal adhesion kinase at
9 sites in the catalytic domain regulates kinase activity: a role for Src family
10 kinases. *Mol. Cell. Biol.* 15(2):954-963.
11 Coelho NM G-GC, Planell JA, Salmerón-Sánchez M, Altankov G 2010. Different
12 assembly of type IV collagen on hydrophilic and hydrophobic substrata alters
13 endothelial cells interaction. *European cells & materials* 19:262-272.
14 Cukierman E, Pankov R, Stevens DR, Yamada KM. 2001. Taking Cell-Matrix
15 Adhesions to the Third Dimension. *Science* 294(5547):1708-1712.
16 Charonis A, Sideraki V, Kaltezioti V, Alberti A, Vlahakos D, Wu K, Tsilibary E. 2005.
17 Basement membrane peptides: functional considerations and biomedical
18 applications in autoimmunity. *Current medicinal chemistry* 12(13):1495-1502.
19 Chen CH, Hansma HG. 2000. Basement membrane macromolecules: insights from
20 atomic force microscopy. *Journal of structural biology* 131(1):44-55.
21 Chen JM, Little CD. 1985. Cells that emerge from embryonic explants produce fibers of
22 type IV collagen. *The Journal of Cell Biology* 101(4):1175-1181.
23 Daley WP, Peters SB, Larsen M. 2008. Extracellular matrix dynamics in development
24 and regenerative medicine. *Journal of cell science* 121(Pt 3):255-264.
25 de Mel A, Jell G, Stevens MM, Seifalian AM. 2008. Biofunctionalization of
26 Biomaterials for Accelerated in Situ Endothelialization: A Review.
27 *Biomacromolecules* 9(11):2969-2979.
28 Dvir T, Timko BP, Kohane DS, Langer R. 2011. Nanotechnological strategies for
29 engineering complex tissues. *Nat Nano* 6(1):13-22.
30 Fleischmajer R, Perlsh JS, Ii DEM, Schechter A, Murdoch AD, Iozzo RV, Yamada Y.
31 1998. There is binding of collagen IV to beta 1 integrin during early skin
32 basement membrane assembly. *Annals of the New York Academy of Sciences*
33 857(MORPHOGENESIS: CELLULAR INTERACTIONS):212-227.
34 Geiger B, Bershadsky A, Pankov R, Yamada KM. 2001. Transmembrane crosstalk
35 between the extracellular matrix and the cytoskeleton. *Nat Rev Mol Cell Biol*
36 2(11):793-805.
37 Gelse K, Poschl E, Aigner T. 2003. Collagens--structure, function, and biosynthesis.
38 *Advanced Drug Delivery Reviews* 55(12):1531-1546.
39 Griffith LG, Naughton G. 2002. Tissue engineering--current challenges and expanding
40 opportunities. *Science (New York, N.Y.)* 295(5557):1009-1014.
41 Grinnell F, Feld MK. 1982. Fibronectin adsorption on hydrophilic and hydrophobic
42 surfaces detected by antibody binding and analyzed during cell adhesion in
43 serum-containing medium. *The Journal of biological chemistry* 257(9):4888-
44 4893.
45 Groth T, Altankov G. 1996. Studies on cell-biomaterial interaction: role of tyrosine
46 phosphorylation during fibroblast spreading on surfaces varying in wettability.
47 *Biomaterials* 17(12):1227-1234.
48 Guan J-L. 1997. Focal adhesion kinase in integrin signaling. *Matrix Biology* 16(4):195-
49 200.
50 Gustavsson J, Altankov G, Errachid A, Samitier J, Planell JA, Engel E. 2008. Surface
51 modifications of silicon nitride for cellular biosensor applications. *Journal of*
52 *materials science. Materials in medicine* 19(4):1839-1850.
53
54
55
56
57
58
59
60

- 1
2
3 Hudson BG, Reeders ST, Tryggvason K. 1993. Type IV collagen: structure, gene
4 organization, and role in human diseases. *Molecular basis of Goodpasture and*
5 *Alport syndromes and diffuse leiomyomatosis. The Journal of biological*
6 *chemistry* 268(35):26033-26036.
- 7
8 Hynes RO. 2002. Integrins: bidirectional, allosteric signaling machines. *Cell*
9 110(6):673-687.
- 10
11 Kalluri R. 2003. Basement membranes: structure, assembly and role in tumour
12 angiogenesis. *Nat Rev Cancer* 3(6):422-433.
- 13
14 Kapyla J, Ivaska J, Riikonen R, Nykvist P, Pentikainen O, Johnson M, Heino J. 2000.
15 Integrin alpha(2)I domain recognizes type I and type IV collagens by different
16 mechanisms. *The Journal of biological chemistry* 275(5):3348-3354.
- 17
18 Keresztes Z, Rouxhet PG, Remacle C, Dupont-Gillain C. 2006. Supramolecular
19 assemblies of adsorbed collagen affect the adhesion of endothelial cells. *Journal*
20 *of biomedical materials research.Part A* 76(2):223-233.
- 21
22 Kern A, Eble J, Golbik R, Kuhn K. 1993. Interaction of type IV collagen with the
23 isolated integrins alpha 1 beta 1 and alpha 2 beta 1. *European journal of*
24 *biochemistry / FEBS* 215(1):151-159.
- 25
26 Keselowsky BG, Collard DM, Garcia AJ. 2005. Integrin binding specificity regulates
27 biomaterial surface chemistry effects on cell differentiation. *Proceedings of the*
28 *National Academy of Sciences of the United States of America* 102(17):5953-
29 5957.
- 30
31 Khoshnoodi J, Pedchenko V, Hudson BG. 2008. Mammalian collagen IV. *Microscopy*
32 *research and technique* 71(5):357-370.
- 33
34 Kruegel J, Miosge N. 2010. Basement membrane components are key players in
35 specialized extracellular matrices. *Cellular and Molecular Life Sciences*
36 67(17):2879-2895.
- 37
38 Kühn K. 1995. Basement membrane (type IV) collagen. *Matrix Biology* 14(6):439-445.
- 39
40 LeBleu VS, Macdonald B, Kalluri R. 2007. Structure and function of basement
41 membranes. *Experimental biology and medicine (Maywood, N.J.)* 232(9):1121-
42 1129.
- 43
44 Lee MH, Ducheyne P, Lynch L, Boettiger D, Composto RJ. 2006. Effect of biomaterial
45 surface properties on fibronectin-[alpha]5[beta]1 integrin interaction and cellular
46 attachment. *Biomaterials* 27(9):1907-1916.
- 47
48 Ludwig NS, Yoder C, McConney M, Vargo TG, Kader KN. 2006. Directed type IV
49 collagen self-assembly on hydroxylated PTFE. *Journal of biomedical materials*
50 *research.Part A* 78(3):615-619.
- 51
52 Maneva-Radicheva L, Ebert U, Dimoudis N, Altankov G. 2008. Fibroblast remodeling
53 of adsorbed collagen type IV is altered in contact with cancer cells. *Histology*
54 *and histopathology* 23(7):833-842.
- 55
56 Michael KE, Dumbauld DW, Burns KL, Hanks SK, Garcia AJ. 2009. Focal Adhesion
57 Kinase Modulates Cell Adhesion Strengthening via Integrin Activation. *Mol.*
58 *Biol. Cell* 20(9):2508-2519.
- 59
60 Mrksich M. 2009. Using self-assembled monolayers to model the extracellular matrix.
Acta Biomaterialia 5(3):832-841.
- Popova SN, Lundgren-Akerlund E, Wiig H, Gullberg D. 2007. Physiology and
pathology of collagen receptors. *Acta physiologica (Oxford, England)*
190(3):179-187.
- Rivron NC, Liu JJ, Rouwkema J, de Boer J, van Blitterswijk CA. 2008. Engineering
vascularised tissues in vitro. *European cells & materials* 15(Journal Article):27-
40.

- 1
2
3 Sephel GC, Kennedy R, Kudravi S. 1996. Expression of capillary basement membrane
4 components during sequential phases of wound angiogenesis. *Matrix Biology*
5 15(4):263-279.
6
7 Shamhart PE, Meszaros JG. 2010. Non-fibrillar collagens: Key mediators of post-
8 infarction cardiac remodeling? *Journal of Molecular and Cellular Cardiology*
9 48(3):530-537.
10
11 Sherratt MJ, Bax DV, Chaudhry SS, Hodson N, Lu JR, Saravanapavan P, Kielty CM.
12 2005. Substrate chemistry influences the morphology and biological function of
13 adsorbed extracellular matrix assemblies. *Biomaterials* 26(34):7192-7206.
14
15 Sieg D, Hauck C, Schlaepfer D. 1999. Required role of focal adhesion kinase (FAK) for
16 integrin-stimulated cell migration. *J Cell Sci* 112(16):2677-2691.
17
18 Sipe JD. 2002. Tissue engineering and reparative medicine. *Annals of the New York*
19 *Academy of Sciences* 961:1-9.
20
21 Sung KE, Su G, Pehlke C, Trier SM, Eliceiri KW, Keely PJ, Friedl A, Beebe DJ. 2009.
22 Control of 3-dimensional collagen matrix polymerization for reproducible
23 human mammary fibroblast cell culture in microfluidic devices. *Biomaterials*
24 30(27):4833-4841.
25
26 Thevenot P, Fau - Hu W, Hu W, Fau - Tang L, Tang L. 2008. Surface Chemistry
27 Influences Implant Biocompatibility. *Current Topics in Medicinal Chemistry*
28 8:270-280.
29
30 Timpl R, Oberbaumer I, von der Mark H, Bode W, Wick G, Weber S, Engel J. 1985.
31 Structure and biology of the globular domain of basement membrane type IV
32 collagen. *Annals of the New York Academy of Sciences* 460:58-72.
33
34 Vandenberg P, Kern A, Ries A, Luckenbill-Edds L, Mann K, Kuhn K. 1991.
35 Characterization of a type IV collagen major cell binding site with affinity to the
36 alpha 1 beta 1 and the alpha 2 beta 1 integrins. *The Journal of cell biology*
37 113(6):1475-1483.
38
39 White DJ, Puranen S, Johnson MS, Heino J. 2004. The collagen receptor subfamily of
40 the integrins. *The international journal of biochemistry & cell biology*
41 36(8):1405-1410.
42
43 Xu L-C, Siedlecki CA. 2007. Effects of surface wettability and contact time on protein
44 adhesion to biomaterial surfaces. *Biomaterials* 28(22):3273-3283.
45
46
47
48
49
50
51
52
53
54
55
56
57
58

59 **Figure's captions**
60

1
2
3 Table 1 - Water contact angles of NH₂ and COOH surfaces before and after coating
4 with Col IV.
5
6

7
8 Figure 1 - Adsorption profile of FITC-Col IV on model NH₂ and COOH SAMs.
9
10 Triplicate measurements were done at different coating concentrations and the main
11 values compared to a standard curve with known FITC-Col IV concentration.
12
13

14
15 Figure 2 - AFM images of adsorbed native collagen type IV to model NH₂ (A) and
16 COOH (B) surfaces. Adsorption concentration increases from up to down and
17 magnification increases from left to right for each panel. Some amplification zones
18 shown on A and B are presented on C and D, respectively.
19
20
21
22
23

24
25 Figure 3 - Overall cell morphology of HUVEC adhering on native Col IV coated NH₂
26 (A,C) and COOH (B,D) surfaces. On the upper panel the cells were viewed for actin
27 and nuclei at low magnification (bar 100µm). The lower panel represents the merged
28 images of focal adhesion contacts (vinculin, red) and actin (green). Bar 20 µm. The
29 results from the quantitative measurement of cell adhesion (E) and spreading (F) are
30 presented on the on the right part of the figure.
31
32
33
34
35
36
37

38
39 Figure 4 - Expression of alpha 1 (A, B) and alpha 2 (C, D) integrins in HUVEC
40 adhering on NH₂ (A, C) and COOH (B,D) samples coated with Col IV. Bar 20 µm.
41
42

43
44 Figure 5 - Recruitment of the signalling molecule p-FAK (C,D-red) in the focal
45 adhesion complexes (A,B-green) in HUVEC seeded on Col IV coated NH₂ (A, C, E)
46 and COOH (B;D, F) samples. The merged images are shown on (E and F) including the
47 enlarged insets of the focal complexes. Bar 20 µm.
48
49
50
51
52
53
54
55
56
57
58
59
60

Surface	Water Contact angle	
	Non Coated	50 mg/ml Col IV
NH ₂	53.2 ± 6.9	24.75 ± 3.5
COOH	34.2 ± 4.5	27.05 ± 3.5

Table 1 - Water contact angles of NH₂ and COOH surfaces before and after coating with Col IV.

Or Peer Review

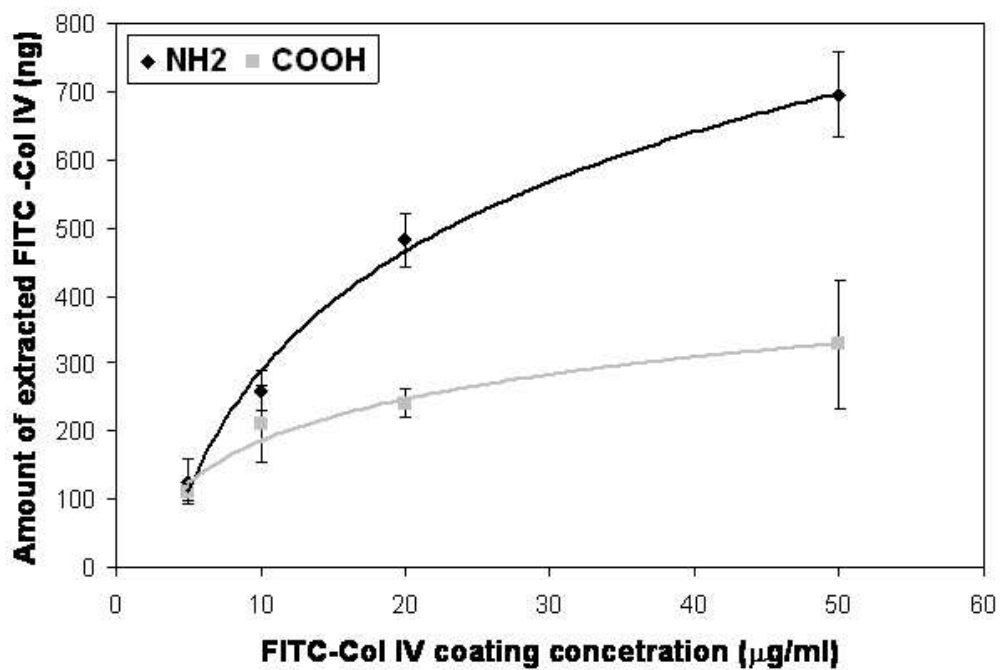
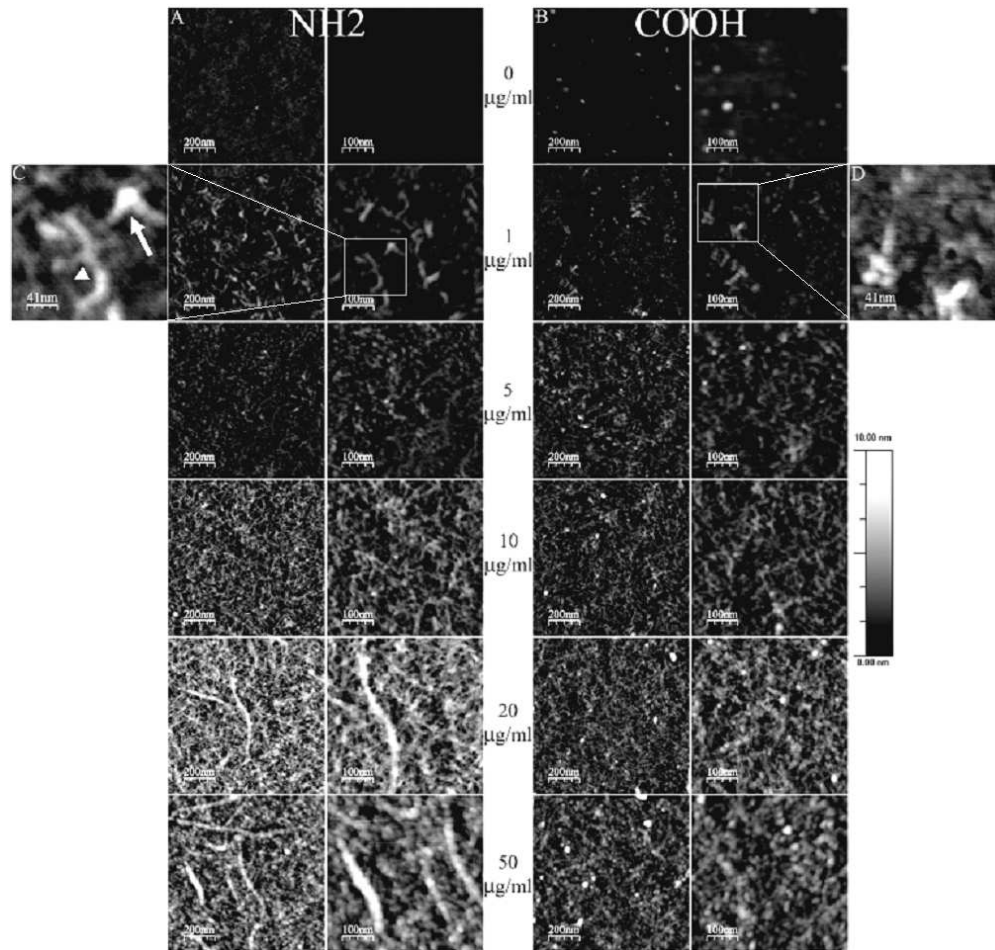


Figure 1 - Adsorption profile of FITC-Col IV on model NH₂ and COOH SAMs. Triplicate measurements were done at different coating concentrations and the main values compared to a standard curve with known FITC-Col IV concentration.



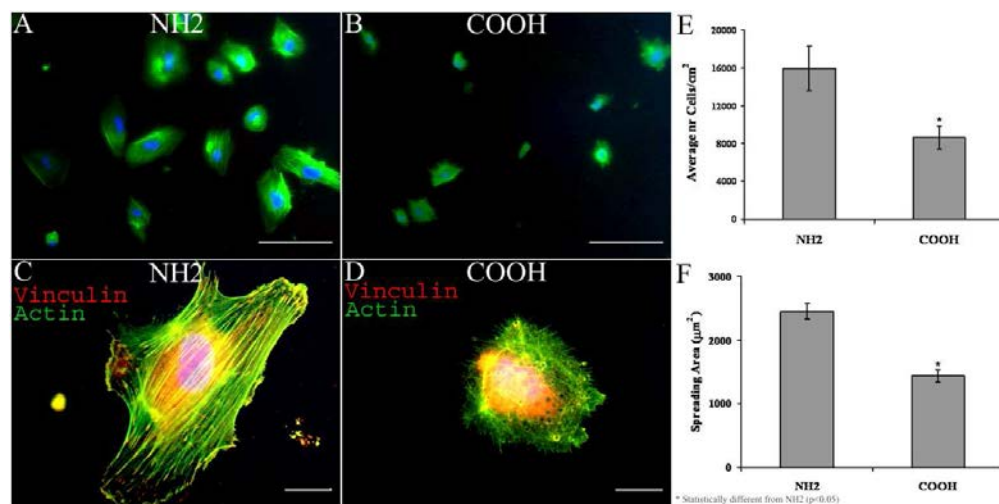
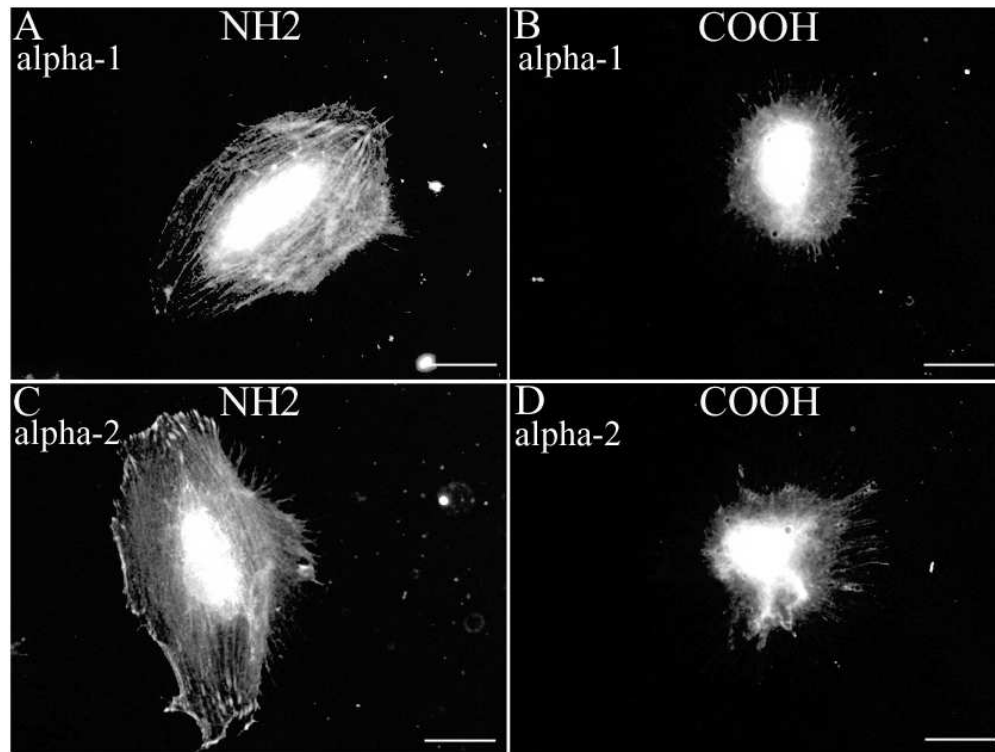


Figure 3 - Overall cell morphology of HUVEC adhering on native Col IV coated NH₂ (A,C) and COOH (B,D) surfaces. On the upper panel the cells were viewed for actin and nuclei at low magnification (bar 100μm). The lower panel represents the merged images of focal adhesion contacts (vinculin, red) and actin (green). Bar 20μm. The results from the quantitative measurement of cell adhesion (E) and spreading (F) are presented on the on the right part of the figure.



32
33
34
35
36
37
38
39
40
41
42
43
44
45
46
47
48
49
50
51
52
53
54
55
56
57
58
59
60

Figure 4 - Expression of alpha 1 (A, B) and alpha 2 (C, D) integrins in HUVEC adhering on NH₂ (A, C) and COOH (B,D) samples coated with Col IV. Bar 20 μ m.

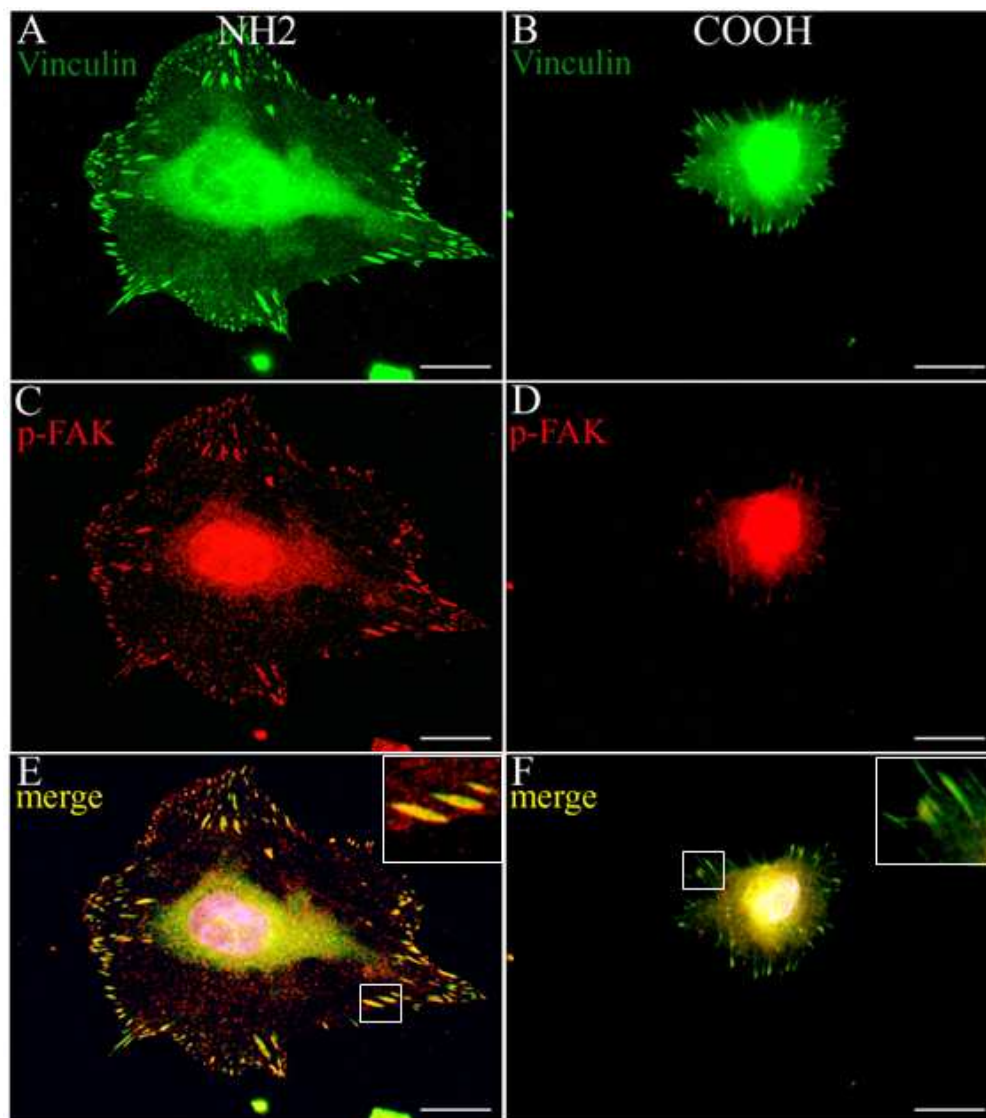


Figure 5 - Recruitment of the signalling molecule p-FAK (C,D-red) in the focal adhesion complexes (A,B-green) in HUVEC seeded on Col IV coated NH₂ (A, C, E) and COOH (B;D, F) samples. The merged images are shown on (E and F) including the enlarged insets of the focal complexes. Bar 20 μ m.

4. Fibroblasts Remodeling of Type IV Collagen at Biomaterials Interface depends on Fibronectin and Substratum Chemistry

4.1 Preface 4

ECM undergo distinct remodeling at cell-biomaterials interface as it mimic to a great extent the natural cell-ECM interactions. In vivo the cells accept distinct mechanical stimuli from the surrounding matrix to strengthen their connections with the cytoskeleton, thus responding to the mechanical properties of the environment. As the stiffness of the surrounding matrix is in the same order of magnitude as cells, they tend to organize this matrix in a way optimal for their functioning (Lutolf and Hubbell 2005; Daley et al. 2008). The cells behave similarly also *in vitro* as they tend to rearrange adsorbed proteins in a fibril-like pattern presumably as an attempt to make their own matrix (Altankov et al. 2010). On the other hand, the cells often degrade adjacent proteins via a process known as pericellular proteolysis (Stamenkovic 2003), which is a way to remove excess ECM from the surface. However, upon implantation of a material these local relations may be hampered, particularly if the material have hydrophobic or too rough surface that support inflammatory cell response. Examples are the over-accumulation of ECM forming fibrous capsule around the implants, or conversely, the failure of an implant because of a gap-formation caused by missing ECM deposition (Moon et al. 1999; Stamenkovic 2003). Therefore, any *in vitro* study providing information about the balance between these processes and their outcome in vivo is strongly desirable.

The intimal part of the vascular BM is the place where endothelial cells reside, but from outside the BM is also in contact with the rough connective tissue where the fibroblasts are the principal cells. Fibroblasts synthesize most ECM constituents, including Col IV and laminin, thus contributing to the formation of BMs, but they are also an important source of ECM-degrading proteases, such as MMPs, which highlights their role in maintaining the ECM homeostasis. The process of degradation is a type of remodeling that strives to remove the excess ECM and some recent investigations, including ours, show that it occurs also at cell-biomaterials interface. Our current data suggest that fibroblasts are able to remodel various surface associated proteins, including VN, FNG and Col IV, however the mechanisms that stay behind these processes needs to be elucidated, moreover it differ between proteins. Indeed, using AFM and other nanoindentation techniques we found different arrangements of Col IV on surfaces varying in wettability, chemistry and charge that resulted in different endothelial cells response. Here we extend this study exploring the activity of fibroblasts to remodel Col IV. We strive to learn how above different surface arrangements of Col IV influence the pattern of it organization, reorganization and degradation by adhering fibroblasts.

Our studies showed that *in vitro* fibroblasts not only interact with adsorbed Col IV, but also tend to remodel it in a morphologically distinct pattern. Two types of cell activities might be clearly distinguished when the substratum associated Col IV is labeled directly or viewed by immunofluorescence: first, a trend for Col IV organization in distinct substratum dependent pattern, and second, of Col IV degradation via pericellular enzymatic cleavage. Our results suggest FN as the driving force for the linear organization of Col IV since these proteins frequently co-localize.

We show that fibroblasts, very similarly to HUVEC, interact better with the single molecular arrangements of Col IV on hydrophilic and NH₂ surfaces and it is altered in contact with the aggregated forms of Col IV on hydrophobic and COOH surfaces. Hydrophilic, COOH and NH₂ surfaces also support fibroblast reorganization of Col IV in fibril-like pattern that co-localized with FN fibrils, while the hydrophobic environment provoke their Col IV degradation activity. These observations are supported by the quantitative measurement of FITC-Col IV release, either directly in the medium, or when is extracted from the substratum. The details of this study are presented below in the form of a manuscript prepared for publication in Matrix Biology.

4.2 Fibroblasts Remodeling of Type IV Collagen at Biomaterials Interface Depends on Fibronectin and Substratum Chemistry

Nuno Miranda Coelho^{a,b} and George Altankov^{a,c}

^aInstitut de Bioenginyeria de Catalunya, Barcelona, Spain

^bUniversitat Politècnica de Catalunya (UPC), Spain

^cInstitució Catalana de Recerca i Estudis Avançats (ICREA), Spain

Abstract

This paper describes the fate of adsorbed type IV collagen (Col IV) - the main structural component of the basement membrane (BM) – in contact with fibroblasts on model biomaterial surfaces, varying in wettability, chemistry and charge. We found that fibroblast not only interact with adsorbed Col IV but also tend to reorganize it in fibril like pattern that is strongly dependent on the surface properties. Following the trend of adsorption - NH₂>CH₃>COOH>OH - the reorganization improves with lowering the amount of adsorbed protein. However, the cells interact better with NH₂ and OH surfaces, e.g. act independently on the amount of adsorbed Col IV - fact confirmed by the quantitative measurements of cell adhesion and spreading and also by the expression of α_1 and α_2 integrins and p-FAK. Conversely, the fibroblasts tend to round on COOH and CH₃ surfaces correlating with the altered development of focal adhesion complexes and actin cytoskeleton as well as with the lowered integrin and p-FAK expression – all characterizing altered function of cell adhesion machinery. We further found that fibroblasts remodel adsorbed Col IV in two ways: by mechanical translocation and via proteolytic degradation. We identify the role of FN for the reorganization process as the linearly arranged Col IV often co-localize with FN fibrils formed either from secreted or exogenously added FN. We found also that this reorganization is better pronounced on hydrophilic OH and positively charged NH₂ surfaces. Conversely, on hydrophobic CH₃ and negatively charged COOH the degradation activity toward FITC labeled Col IV and gelatin (zymography) override the reorganization process, observed morphologically and further proved quantitatively by the significantly increased released fluorescence in the medium. Taken together these results support the idea that fibroblast remodeling of surface associated proteins strongly affect the biological performance of a biomaterial. Moreover, we show that Col IV remodeling may be tailored from the materials site, which favors its tissue engineering application.

Keywords: type IV collagen, surfaces, adsorption, remodeling, reorganization, fibronectin.

1. Introduction

The behavior of cells within tissues is strongly dependent on the extracellular matrix (ECM) - a hierarchically organized structure consisting of fibrillar matrix proteins and proteoglycans (Daley et al., 2008). Initially thought to function as a scaffold that maintain tissue and organ structure, nowadays it become clear that ECM contains various spatiotemporal cues (Aumailley and Gayraud, 1998; Kolahi and Mofrad, 2010) that affects virtually all aspects of cell functioning, including cell growth, survival, shape, migration and differentiation (Aumailley and Gayraud, 1998; Goody and Henry, 2010; Hynes, 2009; Kolahi and Mofrad, 2010). ECM is highly dynamic structure continuously remodeled within tissues since cells build and reshape the surrounding matrix by degrading and reassembling it (Daley et al., 2008). ECM remodeling is an important process, which is critical during development, tissue repair, fibrosis, and tumor progression (Alaaho and Kähäri, 2005; Daley et al., 2008; Larsen et al., 2006; Wynn, 2008). It comprises of synthesis, arrangement and degradation and the balance between these three processes determine the loss or net accumulation of ECM (Shi et al., 2010).

ECM undergo remodeling also in contact with biomaterials (Irvine et al., 2011; Llopis-Hernández et al., 2011; Place et al., 2009) as the molecular events that take place at biomaterials interface mimic to a certain extent the natural interaction of cells with the ECM (Altankov et al., 2010; Ratner and Bryant, 2004; Stevens and George, 2005). Cell-materials interaction starts with the adsorption of proteins from the surrounding medium (Grinnell and Feld, 1982) some of which are recognized by integrins at distinct site of the molecule, such as RGD and others motifs (Altankov et al., 1996; García, 2005; Hynes, 2002). Ligands for cell adhesion might be included also within the structure of the material (Mager et al., 2011; Wheeldon et al., 2011) as exemplified by the biomimetic biomaterials (Huebsch and Mooney, 2009; Langer and Tirrell, 2004; Lutolf and Hubbell, 2005). When integrins bind to their ligand they clusterize in focal adhesion complexes where the specific bidirectional integrin signaling converges with other signaling pathways (García, 2005; Hynes, 2002). It goes through a common tyrosine phosphorylation mechanism (Geiger et al., 2001) that involves focal adhesion kinase (FAK) and other signaling molecules including Src, Cas, and paxillin (Yamada and Geiger, 1997). Depending on the conformation of adsorbed protein, different cellular interaction (Grinnell and Feld, 1982) and integrin signaling may occur (Altankov and Groth, 1996; Keselowsky et al., 2003; Keselowsky et al., 2004) which influence the biocompatibility of materials (Käpylä et al., 2000; Keresztes et al., 2006).

A large and growing body of evidences show that the cells need to accept distinct mechanical stimuli from the surrounding structures to strengthen their connections with the cytoskeleton (Janmey and McCulloch, 2007), thus responding to the mechanical properties of the environment (Geiger et al., 2009; Janmey and McCulloch, 2007). As the stiffness of the surrounding ECM *in*

vivo is in the same order of magnitude as cells, they tend to reorganize this matrix in a way optimal for their functioning (Grinnell, 1986; Hubbell, 2003). However, it may be hampered upon implantation of a material, particularly of these biomaterials that represent hydrophobic or rough surfaces. Examples are the over-accumulation of ECM forming fibrous capsule around the foreign body (Stamenkovic, 2003; Thevenot et al., 2008) or the failure of an implant because of a gap-formation caused by missing ECM deposition from the surrounding tissues (Daley et al., 2008). The formation of soft connective tissue surrounding a dental inset, named peri-implant, is critical for its successful integration (Moon et al., 1999); it forms a biological seal at the gingival site (Moon et al., 1999). Collagen is the major component of this peri-implant tissue and fibroblasts play a crucial role on its formation (Abrahamsson et al., 2002; Moon et al., 1999). After initial ECM deposition however, fibroblasts secrete metalloproteinases (MMPs) that cleave the ECM proteins and if this process of resolution fails it can trigger fibrotic response (Daley et al., 2008; Stamenkovic, 2003).

Our previous studies have shown that cells not only interact but also tend to rearrange the adsorbed proteins, such as fibronectin (FN) (Altankov and Groth, 1994) or fibrinogen (FNG) (Tzoneva et al., 2002) in a linear, fibril-like pattern, presumably as an attempt to form provisional ECM (Altankov and Groth, 1996; Altankov et al., 2010). The biological significance of this phenomena is still not clear, but using model surfaces we could demonstrate that this cellular activity is dependent on the type of cells (Altankov and Groth, 1994; Gustavsson et al., 2008; Maneva-Radicheva et al., 2008; Tzoneva et al., 2002) and on the surface properties of the material (Altankov and Groth, 1994; Gustavsson et al., 2008; Tzoneva et al., 2002). This let us to hypothesize that tissue compatibility of materials depends on the allowance of cells to remodel surface associated proteins and to organize provisional ECM (Altankov et al., 2010). We further anticipate that under specific conditions other, non-soluble ECM proteins like collagens may also associate with the biomaterial interface and the cellular response they elicit is of significant bioengineering interest (Altankov et al., 2010). One such protein is type VI collagen (Col IV) (Coelho et al., 2010; Coelho et al., 2011), which although not fibrillar protein, is actively reorganized by the adhering cells such as stromal fibroblasts (Maneva-Radicheva et al., 2008) in a fibril like pattern. The physiological significance of this phenomena is also not clear, but it undoubtedly represents a cell-dependent process (Maneva-Radicheva et al., 2008). Col IV is recognized by the cells via integrins and from the known 24 integrin heterodimers, $\alpha_1\beta_1$, $\alpha_2\beta_1$, $\alpha_{10}\beta_1$, and $\alpha_{11}\beta_1$ that act as primary receptors for collagens (Barczyk et al., 2010; Hynes, 2002; Käpylä et al., 2000; Kern et al., 1993) $\alpha_1\beta_1$ and $\alpha_2\beta_1$ are the most abundantly expressed (Khoshnoodi et al., 2008; White et al., 2004).

Col IV is the main structural component of the basement membranes (BM) (Khoshnoodi et al., 2008; Kühn, 1995; Timpl and Brown, 1996) - a highly specialized ECM that divide tissues into structural compartments. Thus it play crucial role in various fundamental biological processes, including embryonic development, tissue remodeling, angiogenesis and wound healing (Kalluri, 2003; Khoshnoodi et al., 2008; Yurchenco and Schittny, 1990), and also in various pathological conditions, such as fibrosis, inflammation and cancer (Charonis et al., 2005; Van Aghtmael and Bruckner-Tuderman, 2010; Wynn, 2008). As main component of the BM Col IV is involved in the spatiotemporal organization of internal organs (Kalluri, 2003; Yurchenco, 2011).

The behavior of Col IV at biomaterials interface is an important issue as it encompasses various concerns in tissue engineering, such as material induced fibrosis, endothelization of implants, vascularization within many others (Charonis et al., 2005; Kalluri, 2003; Yurchenco, 2011). Recently, employing atomic force microscopy (AFM) and other nano-indentation techniques we have shown that the surface properties of materials, such as wettability (Coelho et al., 2010) and surface chemistry (Coelho et al., 2011) strongly affect the pattern of Col IV adsorption altering the organization of protein layer. It in turn affects cellular interaction but often in an unpredictable way. It is not clear how it corroborates with the Col IV remodeling activity carried out by the adhering cells, which might be critical for the fate of an implant.

To address this we have employed fibroblasts as model system considering their involvement (as stromal cells) in the synthesis, organization and remodeling of ECM (Griffith and Swartz, 2006), including of type IV collagen (Kalluri and Zeisberg, 2006). We found that fibroblast not only interact with adsorbed Col IV but also reorganize it in fibril like pattern that is strongly dependent on the materials surface properties. Following the trend of adsorption $\text{NH}_2 > \text{CH}_3 > \text{COOH} > \text{OH}$ the reorganization pattern of Col IV tend to improve with lowering the amount of adsorbed protein. However, the cells interact better with NH_2 and OH surfaces (representing the highest and the lowest adsorption respectively), e.g. independently on the amount of adsorbed Col IV, and this was confirmed by the quantitative measurements of cell adhesion and spreading and by the expression of α_1 and α_2 integrins. Conversely, the fibroblasts tend to round on COOH and CH_3 surfaces correlating with the altered development of focal adhesion complexes and actin cytoskeleton as well as with the lowered integrin and p-FAK expression – all characterizing the altered function of cell adhesion machinery. We further found that fibroblats remodel adsorbed Col IV in two ways: by mechanical translocation over the surface and via proteolytic degradation. We identify the role of FN in the reorganization process as the linearly arranged Col IV often co-localize with FN fibrils formed either from secreted or exogenously added FN. We found also that this reorganization is better pronounced on hydrophilic OH and positively charged NH_2 surfaces. Conversely, on hydrophobic CH_3 and negatively charged COOH the degradation activity toward

FITC labeled Col IV coated substrata override the reorganization process, proved morphologically and quantified by the released fluorescence in the medium showing significant increase, which corroborates with the altered cell morphology and abrogated cell adhesion machinery. Taken together these results support the view that fibroblast remodeling of surface associated proteins affects the biological performance of a biomaterial, moreover, Col IV remodeling can be tailored from the materials site, which favors the tissue engineering implication of this phenomenon. Details of this study are reported below.

2. Results

2.1. Fibroblast reorganization of Col IV

Figure 1 (B, F) demonstrates that fibroblasts interact very well with adsorbed Col IV, both native (A) and monomeric FITC-Col IV (E) after 5 h of culture. The cells represent well-developed actin cytoskeleton and prominent stress fibers. On (A, C, D) adsorbed native Col IV is visualized by immunofluorescence, while FITC-Col IV (E, G, H) is viewed directly; (A and E) view samples without cells confirming the homogenous distribution of proteins. Fig. 1 C and G show that fibroblasts not only interact with both collagen types, but also tend to reorganize them in fibril-like pattern. The dark zones at cells borders represent places from where the protein was removed to be arranged. The remodeling of Col IV is well pronounced at 5th hour (C and G) and further augments at 24th hour (D and H). No difference in the pattern of remodeling between native and monomeric Col IV was observed. The impact of pericellular proteolysis is difficult to be distinguished morphologically. To determine proteolytic activity, released fluorescence from FITC-Col IV coated substrata was measured at 5 and 24 h. As seen on Fig.1 J however, only small and non - significant increase of fluorescence (versus spontaneous desorption) was found. A reason could be that either cleaved Col IV remains on the substratum. Nevertheless, spontaneous desorption of FITC-Col IV exist as the fluorescence increase about twice after 24 hours (again with no difference if cells are present or not), which relates to the strength of protein-substratum interaction, but not to proteolysis. However, when adsorbed FITC-Col IV was extracted with NaOH (Figure 1 I) a significant increase of the fluorescent signal was found in the presence of cells (vs. no cells), presumably resulting from the de-quenching of cleaved Col IV by fibroblasts (see Methods section). As NaOH extraction itself do not cause de-quenching of FITC-Col IV (not shown) we concluded that the ratio between signals, with and without cells, might characterize quantitatively the pericellular proteolysis of Col IV.

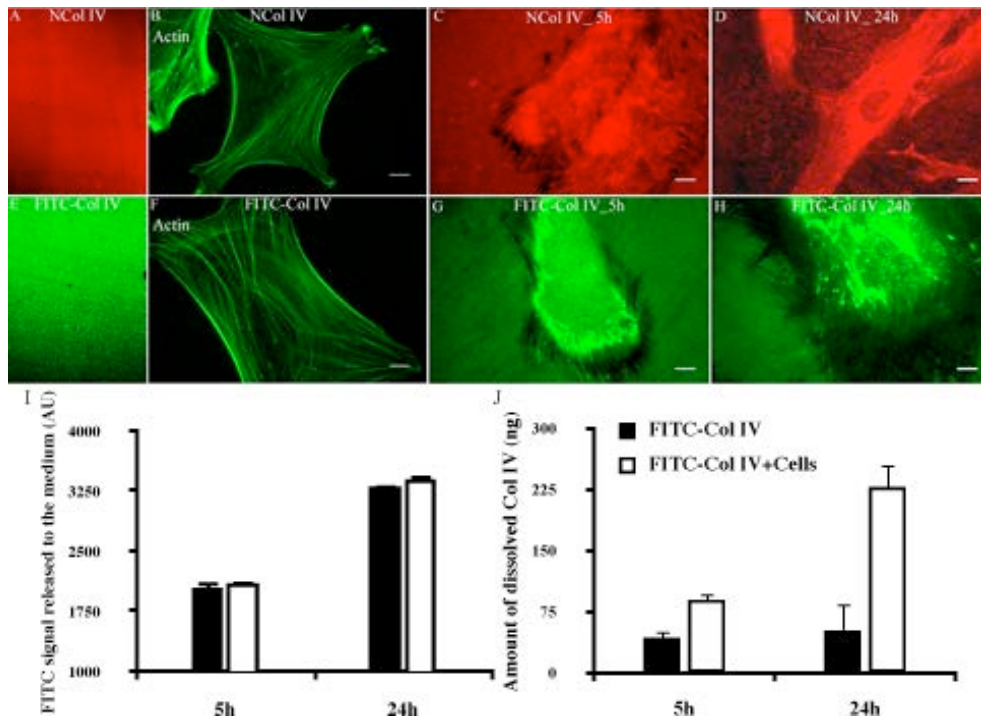


Figure 1 - Human fibroblasts cultured for 5 h (B,C,F,G) or 24 h (D, H) on native (A-C) or FITC-conjugated Col IV (E-G). The immunofluorescent images of plain Col IV (A) and FITC-Col IV (E) coated samples viewed are shown on the left panel. Panel (I) depict the extracted FITC-Col IV signal after 5 or 24 hours, with or without fibroblasts. Panel (J) show the amounts of spontaneously released in the medium FITC-Col IV or after 5 and 24 h of culture. FITC signal is present in relative photometric units as mean \pm SD. Bar = 10 μ m.

2.2. Col IV remodeling is supported by fibronectin

Col IV is not fibrillar protein and therefore its linear arrangement on the substratum cannot be explained with spontaneous assembly (as for FN). Considering however our previous studies (Maneva-Radicheva et al., 2008) showing that Col IV may co-localize with fibronectin (FN), it rises the possibility that the cell-driven process of FN fibrillogenesis could be involved in Col IV reorganization. To prove such possibility we performed a separate experiment where FN and Col IV were “exposed” each other in three different protocols and the results are summarized on Figure 2. The upper panel (Figure 2 A-C) represents native Col IV reorganization by fibroblasts after 5 h of incubation (A) viewed simultaneously with secreted FN via immunofluorescence (B) and both images are merged on (C). Middle panel shows how reorganized Col IV (D) co-localizes with FN fibrils when exogenous FN was added to the medium (E), visualized as above and merged on (F). Finally, on the lower panel FITC-Col IV was added to the medium and viewed (H) together with secreted FN (G), and merged at (I). All three conditions showed high degree of co-localization suggesting involvement of fibroblasts FN matrix formation on Col IV reorganization.

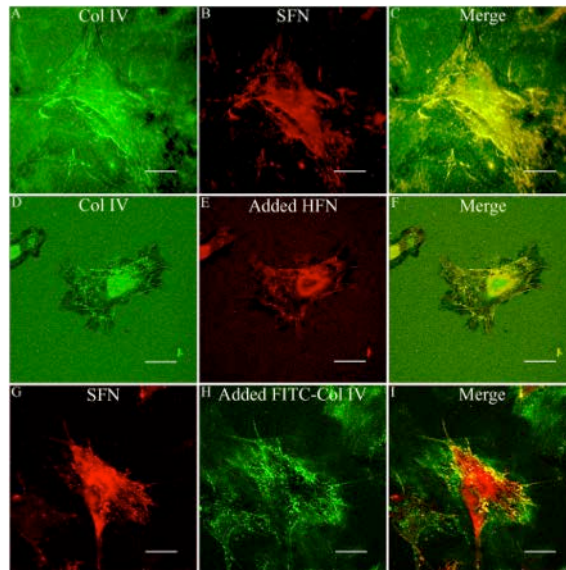


Figure 2 - Co-localization between remodeled Col IV (A, D) and secreted (B) or exogenously added (E) fibronectin in fibroblasts adhering for 5h on Col IV. On the lower panel secreted fibronectin (G) is viewed simultaneously with exogenously added FITC-Col IV (H). The images are merged on the left panel (C, F, I). Bar – 20 μm .

2.3. Model surfaces

To learn whether the surface properties of a material such as charge and wettability, may affect Col IV remodeling, four model surfaces expressing OH (hydrophilic glass), CH₃ (hydrophobic), NH₂ (positively charged) and COOH (negatively charged) were prepared. The data presented in Figure 3 shows a significant change of water contact angles (WCA°) confirming the successful and homogenous coating with SAMs.

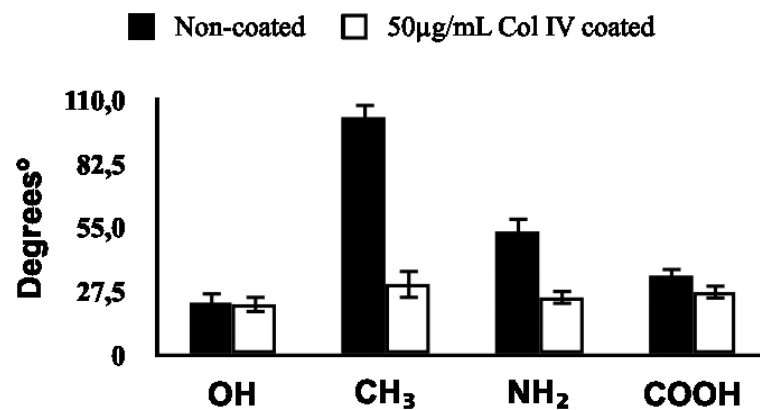


Figure 3- Water contact angles of model surfaces measured before (black bars) and after coating with Col IV (white bars).

The CH₃ surface shows about twice higher WCA° when compared with NH₂ and about triplet value when compared with OH and COOH substrata ($p < 0.05$). However, after coating with Col IV the WCA° of all surfaces decreased substantially and tend to equilibrate at values between 20°

- 35°, which suggest that the cells will not “sense” the difference in wettability upon contact with model surfaces.

2.4. Quantification of adsorbed FITC-Collagen IV

The sensitive FITC-Col IV release assay was applied to study the differences in protein adsorption to the model surfaces. The adsorbed protein was measured by extraction with 0.2M NaOH and compared to a standard curve with known FITC-Col IV concentrations as previously described (Coelho et al., 2010; Coelho et al., 2011). Detectable values of protein were obtained for all substrata at coating concentration of 50 µg/mL (Figure 4 A), the concentration used for the cellular studies, where CH₃ and NH₂ surfaces demonstrated about twice more adsorbed protein compared to OH and COOH.

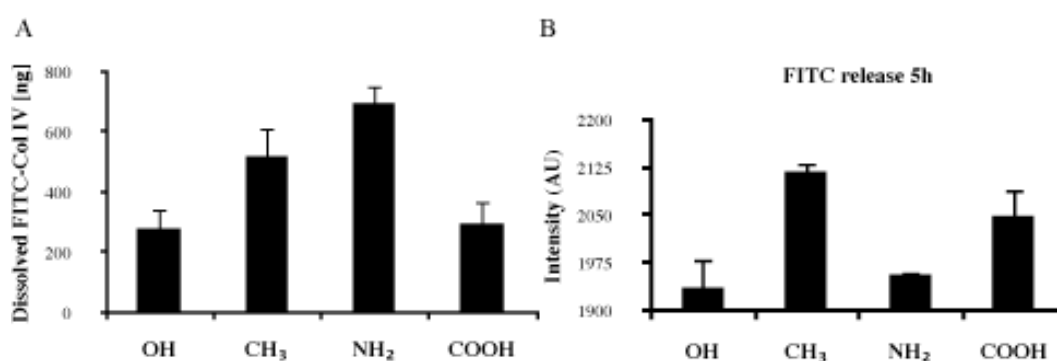


Figure 4- Adsorption and desorption of FITC-Col IV on different model surfaces. A). The amount of adsorbed Col IV was determined by comparison of extracted fluorescence signals (using 0.2M NaOH) to a standard curve with known FITC-Col IV concentrations. B). The release of FITC-Col IV was measured after 5 h of incubation to characterize the spontaneous desorption of protein. Triplicate measurements were performed for each condition. Protein adsorption concentration was 50 µg/ml (see Methods section).

No further increase in the fluorescent signal over this saturation concentration was found (not shown). The spontaneous release of FITC-Col IV in the medium was also measured (B) to characterize indirectly the protein to substratum interaction. Thus, significantly higher rates of desorption were found from CH₃ and COOH substrata in comparison to OH and NH₂ suggesting lowered strength of interaction. However, the quantitative interpretation of these results is embarrassed from the different initial amount of adsorbed protein, which may explain the surprisingly high release from hydrophobic CH₃ shown to strongly bound proteins. Nevertheless, the strongest interaction of Col IV with NH₂ substrata is obvious as it shows highest adsorption (A) and significantly low desorption (B). Conversely, the real desorption from glass (OH) should be much higher if one consider the approximately 3 times lower adsorption in comparison to NH₂ (A) at almost same desorption (B) as from CH₃.

2.5. Cell adhesion and spreading onto model surfaces

The overall morphology of fibroblasts adhering on Col IV coated model surfaces for 2 hours is shown in Figure 5.

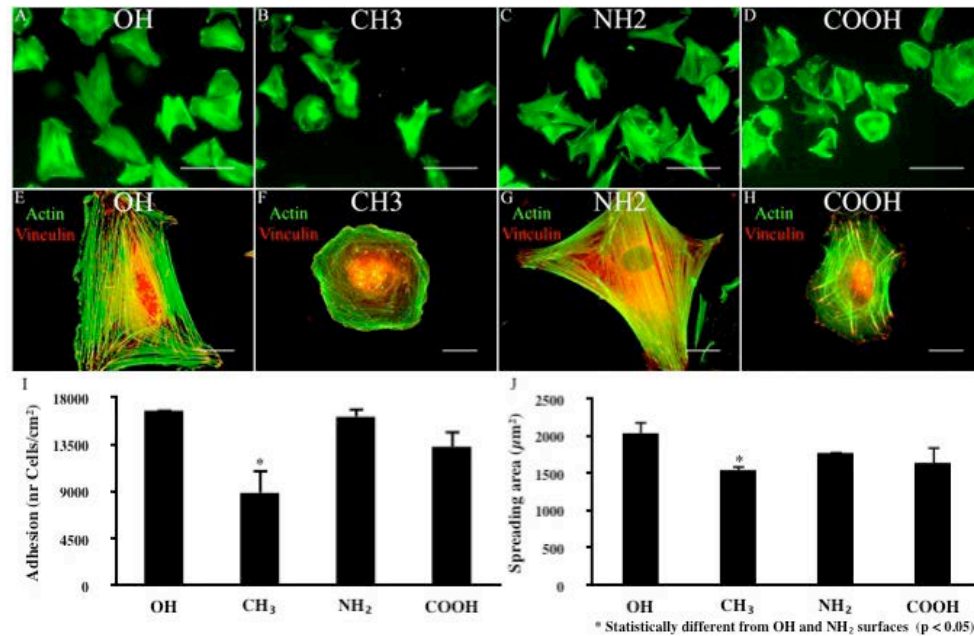


Figure 5 - Overall morphology of human fibroblasts adhering on Col IV coated model materials for 2 h in serum free conditions. Cells were stained simultaneously for actin and vinculin. On (A-D) the cells are viewed for actin at low magnification (Bar 100 µm). The higher magnification on (E-H) depicts the development of focal adhesions contacts and actin stress fibers (Bar 20µm). Below are presented the quantities for cell adhesion (I) and spreading (J).

On OH (A) and NH₂ (C) surfaces the amount of cells was higher and the fibroblasts presented flattened morphology. On COOH (D) and CH₃ cell adhesion was less and the morphology of fibroblasts was non-homogeneous with appearance of round cells suggesting delayed spreading. The quantitative data presented in Figure 5 I and J confirms these morphological observations as a significant increase in both cell adhesion ($p < 0.05$) and spreading area ($p < 0.05$) on OH and NH₂ in comparison to CH₃ substrata was found. On non-coated with Col IV samples only negligible cell spreading was observed with no significant difference between substrates (not shown). The difference in quality of cell adhesion was confirmed by the simultaneous visualization of focal adhesion contacts (red) and the actin cytoskeleton (green) shown in Figure 5: the flattened and elongated cell morphology on OH and NH₂ correlates with the well-developed focal adhesion contacts, where stress fibers often insert (5E and G). Conversely, on CH₃ surface round shaped cell morphology correlates with less expressed focal adhesion complexes (5F). Interestingly, on COOH substrate, although the cells are small they show well-expressed actin stress fibers and focal adhesions (Figure 5H).

2.6. Integrin expression

To learn which integrins are involved in the adhesion process we studied the organization of $\alpha_1\beta_1$ and $\alpha_2\beta_1$ heterodimers, referred to us as main collagen receptors, the first, more specific for Col IV, while second recognizes all collagen types (Hynes, 2002; Khoshnoodi et al., 2008). As shown in Figure 6, both integrins are well expressed in fibroblasts adhering on Col IV coated OH and NH_2 surface (Figure 6A, C and E, G).

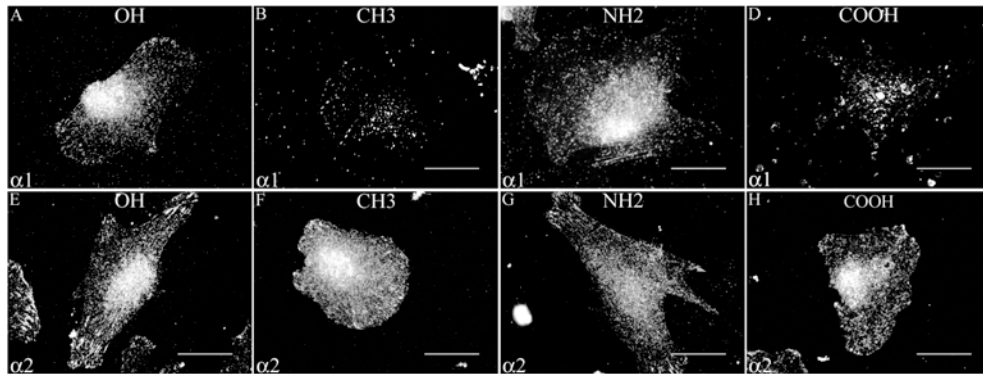


Figure 6- Expression of alpha 1 (A-D) and alpha 2 (E- H) integrins by fibroblasts adhering on Col IV coated model surfaces. Bar 20 μm .

However, α_1 integrin represents a rather linear organization (Figure 6A and C) going along with actin stress fibers (data not shown), while α_2 shows well-pronounced clusters resembling focal adhesion contacts (Figure 5E and G). These data confirm our previous observation with endothelial cells (HUVEC) on the same surfaces (Coelho et al., 2010; Coelho et al., 2011). In contrast, on CH_3 and COOH surfaces almost no α_1 clusters were found (Figure 6B and D, respectively), but α_2 integrins were still expressed and formed clusters resembling small focal adhesions (Figure 6F and H).

2.7. Signaling of integrins

To learn whether the development of focal adhesion complexes induced recruitment of phosphorylated signaling molecules we co-stained the cells for vinculin and p-FAK. The data presented in Figure 7 shows higher degree of co-localization between the well-developed focal adhesion contacts (viewed by vinculin in green) and p-FAK (red) on OH and NH_2 substrata, resulting in orange when merged (Figure 7 I and K). Conversely, on CH_3 and COOH surfaces although some cells are able to make focal contacts (Figure 5 B and D), less p-FAK is recruited (Fig. 7 F and H) as seen on merges (Fig. 7 J and L) - suggesting altered transmission of signal to the cell interior.

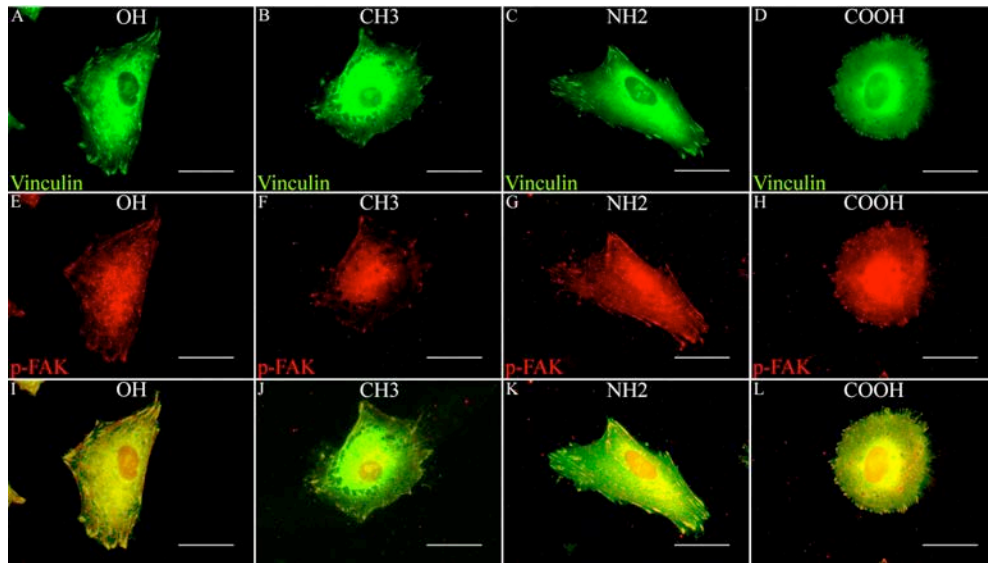


Figure 7 - Recruitment of the signaling molecule p-FAK (E-H-red) in the focal adhesion complexes (A- D-green) of human fibroblasts seeded on Col IV coated model surfaces. The merged images are shown on (I-L). Bar=20 μ m.

2.8. Different remodeling of Col IV on model surfaces

Fibroblasts were seeded for 5 and 24 hours on Col IV coated model OH, CH₃, NH₂, and COOH surfaces to learn whether the differences in the initial cell interaction would affect Col VI remodeling. Hydrophilic glass samples (OH) in this case served as controls and link to the previous investigations. The pattern of Col IV reorganization was studied simultaneously with FN matrix secretion to follow how these processes corroborate with the substratum properties. Figure 8 (upper panel A-D) shows substantial differences in the rearrangement of Col IV, namely, a pronounced linear fibril-like arrangement on OH and NH₂, while an appearance of dark zones of removed protein around cell borders are often found on CH₃ and COOH substrata, which do not corroborate with the amount of rearranged protein, particularly on CH₃ (B). The FN matrix fibrils (middle panel) co-localize well on OH, NH₂ and COOH substrata (E, G, H, respectively) resulting in yellow at merges (I, K and L, respectively), while on CH₃ surface the larger dark zones (B) show very low, rather punctual deposition of FN matrix (F).

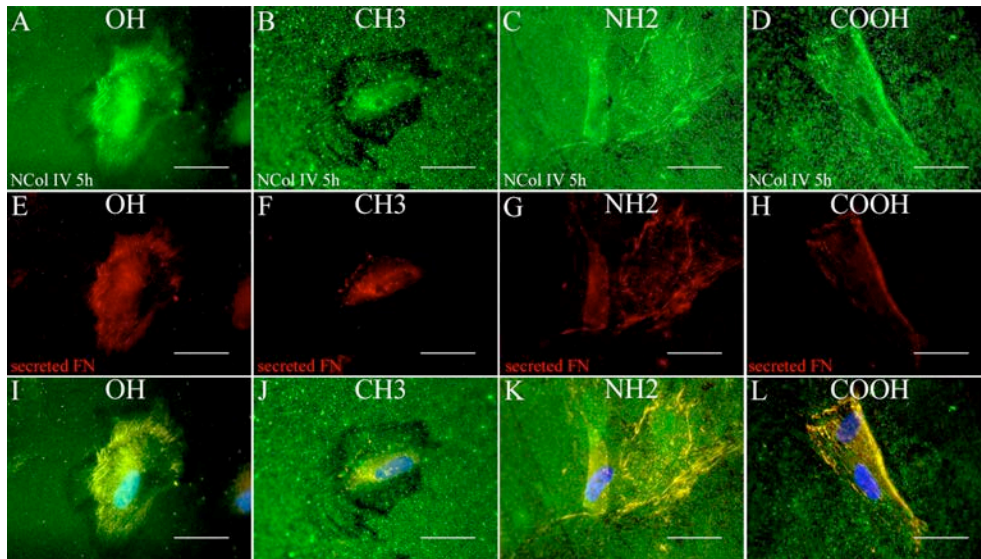


Figure 8 - Fibroblast remodeling of native Col IV on different model surfaces after 5 hours. The cells were stained simultaneously for Col IV and FN. Upper panel represents Col IV (A-D green) co-viewed with FN (E-H red); both images are merged on (I-L). Bar 20 μ m.

After 24h of culture (Figure 9 A-D) the remodeling progress, but followed the same trend of improved reorganization on OH and NH₂ correlating with stronger deposition of FN matrix. FN deposition was particularly strong on NH₂ substrata followed by COOH and OH. Again, the worst reorganization was found on CH₃.

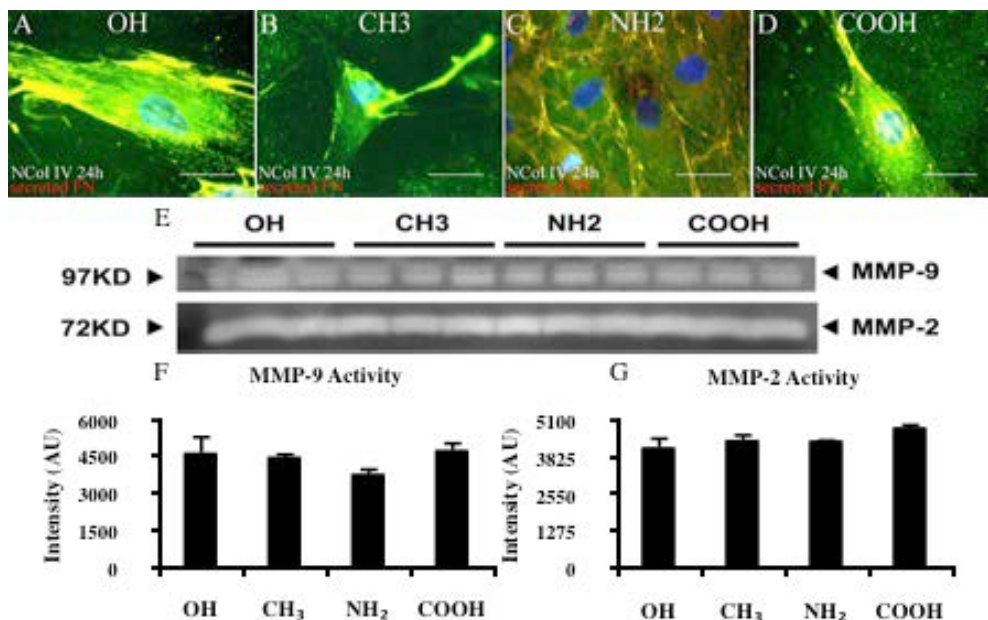


Figure 9 – Fibroblasts remodeling of native Col IV on different model materials after 24 h. The cells were simultaneously stained for Col IV and FN and only merged images are shown (A-D). Middle panel (E) shows the zymography of conditioned medium where Line 1 is MMP9 and Line 2 – MMP2, of 97 and 72 KDa respectively. Lower panel shows the densitometry data for MMP9 (F) and MMP2 (G) activity.

Analyzing the conditioned medium with zymography we could prove the involvement of both MMP9 and MMP2 in Col IV remodeling (Figure 9 E). The densitometry analysis however did not show significant differences in MMP2 activity between model materials, while MMP9 activity was significantly depressed on NH₂ substrata.

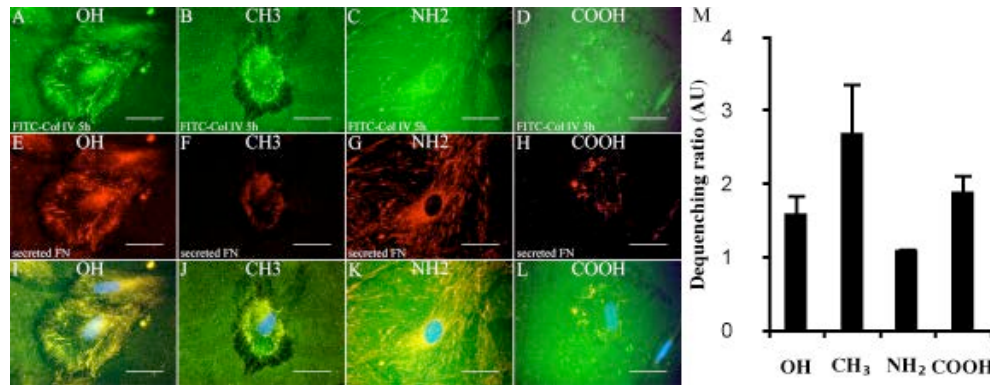


Figure 10– Fibroblasts remodeling of FITC-Col IV on different model surfaces for 5 h (A-D). The cells are simultaneously stained for FN. Upper panel represent FITC-Col IV reorganization (A-D) on the different substrata, which is co-viewed with secreted FN (E-H); both imaged are merged on (I-L). Bar 20 mm. (M) The graph on right represents the quantitative difference in the de-quenching rate of FITC-Col IV caused by the proteolytic activity of cells (see text).

Similar were the morphological observations with FITC-Col IV. As shown on Figure 9 (A-L) the cells easily arrange Col IV on OH and NH₂, followed by COOH and CH₃ substrata. Although the arrangement followed the same trend, an advantage of this system is that it can be used for the quantification of fibroblast degradation activity leading to de-quenching of FITC Col IV (Figure 1G). Considering however, the differences in the initial amount of adsorbed protein, only the ratios between the extracted fluorescent signal with cells and without cells were compared. The graph on Figure 9 M depict the calculated de-quenching ratios for the different model surfaces showing significantly higher fibroblast Col VI degradation on CH₃ followed by COOH and OH surfaces. The lowest degradation of Col VI was measured on NH₂ surface.

3. Discussion

Cell-biomaterials interaction depends on the surface associated ECM proteins deposited and frequently remodeled by the adhering cells (Chen et al., 2008; Mager et al., 2011). Over or less deposition of ECM in tissues strongly affects the fate of implant (Daley et al., 2008) and because it often progress in an unpredictable way, any *in vitro* studies providing information about the balance of these processes are strongly desirable (Daley et al., 2008; Hubbell, 2003). This study demonstrates that human fibroblasts not only interact well with adsorbed Col IV *in vitro*, but also tend to remodel it in a morphologically distinct pattern. Two types of cell activities might be

foreseen: first, Col IV reorganization, and second, the degradation of this protein via enzymatic cleavage. In agreement with previous investigation (Maneva-Radicheva et al., 2008) we show that fibroblasts are able to mechanically reorganize adsorbed Col IV in fibril-like pattern that frequently co-localize with FN matrix fibrils (Altankov and Groth, 1996; Grinnell, 1986). An important question is whether this process of spatial reorganization is physiologically relevant, as fibroblasts in 2D cultures often behave differently from their normal 3D environment *in vivo* (Beningo et al., 2004). Col IV is a non-fibrillar matrix protein typically observed in the basement membranes (BM), where it assembles in a sheet-like structure providing the major structural support for epithelial cells (Kalluri, 2003; Khoshnoodi et al., 2008; Kühn, 1995; Yurchenco, 2011). The way of its spatial arrangement in the BM is not clear. It is widely accepted that it self-assembles by anti parallel interactions and extensive disulfide bonding of four molecules to form 7S domain (Kalluri, 2003; Khoshnoodi et al., 2008). Further lateral interaction of its C-terminal globular domains create the network that forms the BM (together with laminin and other linkage proteins) (Khoshnoodi et al., 2008; Vanacore et al., 2004). From this angle the fibroblast rearrangement of adsorbed Col IV does not look physiologically relevant, but it clearly represents a cell-dependent process. It is noteworthy however, that similar linear organization of Col IV has been observed during early basement membrane assembly in an *in vitro* 3D skin culture model (Fleischmajer et al., 1998), shown to be also a cell-driven process (Fleischmajer et al., 1998). In addition, our previous investigations on Col IV remodeling in contact with cancer cells also demonstrate the involvement of $\alpha_2\beta_1$ integrins in the process (Maneva-Radicheva et al., 2008).

Notwithstanding debates on the role of cells, our data suggest that the driving force for Col IV reorganization is the association with FN fibrils. In fact, such mechanism is demonstrated before for fibrillar collagens type I and III (Kadler et al., 2008; Velling et al., 2002), and also for adsorbed fibrinogen (Tzoneva et al., 2002), but we are the first connecting this mechanism with Col IV. Indeed, our double staining experiments clearly show a high degree of co-localization between FN and Col IV confirming involvement of FN in the reorganization. The co-localization however is not obligatory, suggesting also an independent translocation of the protein onto the cell surface presumably dependent on integrins (Sottile and Hocking, 2002). FN is synthesized by many adherent cells, including stromal fibroblasts, which assemble it into a fibrillar network (Wierzbicka-Patynowski and Schwarzbauer, 2003). During its assembly, FN undergoes conformational changes that expose FN-binding sites and promote intermolecular interactions important for the fibril formation (Mao and Schwarzbauer, 2005). The earlier work of Dzamba et al (Dzamba et al., 1993) show that FN binding site in fibrillar type I collagen may regulate FN fibril formation in fibroblasts. Sottile and Hocking (Sottile and Hocking, 2002) also show that FN polymerization into the ECM is required for the deposition of type I collagen. In fact, the association between these two ECM proteins is not surprising, as FN molecule has at least two

binding sites for collagens (Larsen et al., 2006; Mao and Schwarzbauer, 2005) and corresponding binding sites for FN have been identified on the collagen molecule (Sottile and Hocking, 2002; Velling et al., 2002; Zoppi et al., 2004). Furthermore, Chernousov *et al.* (Chernousov et al., 1998) reported that Schwann cells use directly a Col IV-dependent mechanism for FN fibril assembly. Consistent with this are our results showing that fluorescently labeled FN and Col IV (monomeric) frequently co-localize, either when pre-adsorbed or exogenously added in the medium (Figure 2). Hence, in contrast to the earlier belief that collagen polymerization occurs via self-assembly (Kalluri, 2003) our data showed that the preformed FN matrix is essential for Col IV network formation and presumably the specific integrin binding supports this process. It corroborates also by the previously observed coextensive (linear) assembly of Col IV along the actin cytoskeleton (Maneva-Radicheva et al., 2008) - an organization typical for FN matrix fibrils (Christopher et al., 1997; Clark et al., 2005; Wu et al., 1995), as well as, for the substratum reorganized FN (Altankov and Groth, 1996; Grinnell, 1986). On the other hand, it looks that Col IV reorganization does not require the native configuration of protein as it is equal and even supported when partly denatured (monomeric) Col IV have been used. This, together with the fact that denatured collagen possess higher affinity for FN (Ingham et al., 1988) suggests that the transient association with FN fibrils is more important for Col IV reorganization than its specific recognition by integrins.

A novel observation of this study is that fibroblast reorganization of Col IV is dependent on the material surface properties: it is strongly supported on hydrophilic glass, followed by positively charged NH₂ and negatively charged COOH substratum. Finally, it is abrogated on hydrophobic CH₃ surface. The pattern of Col IV reorganization also is different: on hydrophilic glass and partly on COOH the dark zones, from where the protein is removed to be reorganized, are clearly visible, while on NH₂ surface the reorganization goes along with FN fibrils and no zones of removal were observed. Following the trend of adsorption - NH₂>CH₃>COOH>OH - the reorganization improves with lowering the amount of adsorbed protein. However, the cells interact better with NH₂ and OH surfaces, e.g. they act independently on the amount of adsorbed Col IV. This was confirmed by the quantitative measurements of cell adhesion and spreading and also by the expression of a₁ and a₂ integrins and p-FAK – all characterizing the proper function of cell adhesion machinery. Conversely, the fibroblasts tend to round on COOH and CH₃ surfaces correlating with the altered development of focal adhesion complexes. Presumably, these differences are a consequence of the different strength of protein to substratum interaction, as NH₂ represents about twice higher adsorption of Col IV and less desorption after 24 h in comparison to OH and COOH surfaces. Conversely, on CH₃ despite high protein adsorption, a predominant removal, but not reorganization of both Col IV and FN is observed, which raise the

possibility for their proteolytic cleavage by the cells. Indeed, when released fluorescence signal from FITC-Col IV was measured, a significantly higher amount of cleaved protein was observed on CH₃, followed by COOH and OH surface. It seems that when cells face the aggregated forms Col IV characteristic for this protein in hydrophobic environment (Coelho et al., 2010; Coelho et al., 2011) they trigger their proteolytic activity, presumably as an attempt to remove it. Interestingly, on NH₂ substrata although highest amount of protein adsorbs, almost no proteolytic degradation was observed, which correlates with the absence of Col IV aggregates on this substrata (Coelho et al., 2011). With further culturing all these processes progress, but keeping the same trend.

Taken together these results support our view that the ability of cells to remodel surface associated proteins strongly affects the biological performance of a biomaterial. They also show that the appropriate chemical functionalization (NH₂, OH), combined with Col IV pre-adsorption, comprises a prospective biomimetic modification that might improve endothelization of cardiovascular implants.

4. Experimental procedures

4.1. Model surfaces

To render the surface hydrophilic (Coelho et al., 2010) glass coverslips (22x22 mm, Fisher Bioblock) were cleaned in an ultrasonic bath for 10min in a 1:1 mixture of 2-propanol and tetrahydrofuran. The samples were then exposed to piranha solution (30% (v/v) H₂O₂ and 70% (v/v) H₂SO₄) for 30 min followed by a copious rinsing with milli Q water (18.2MΩ) and dried.

Self-assembled monolayers: The hydrophobic CH₃ surfaces were prepared as previously described (Coelho et al., 2010; Gustavsson et al., 2008) using an organosilanetrichloro(octadecyl)silane (ODS) purchased from Sigma (Cat. No 104817). Briefly, the cleaned as above samples were placed in a solution containing 12.5 ml of carbon tetrachloride, 37.5 ml of heptane and 220 μl ODS. The samples were left in this solution for 18 min at room temperature and the excess of silane was washed away with pure heptane. Samples were then heated for one hour at 80°C.

For NH₂ functionalization pre-cleaned as above samples were immersed for 18 min at room temperature in a solution containing 30 ml methanol, 10ml 4% acetic acid glacial and 3-(2-aminoethylamino) propyltrimethoxysilane (C₈H₂₂N₂O₃Si, Fluka) to yield a final 1% concentration. Excess of silane was washed by immersion in an excess of solvent solution. Finally, the samples were air dried and heated at 80°C for 1h.

COOH functionalization was performed in two steps, by immersing the pre-cleaned samples in a 1:3 mixture of CCl_4 and $n\text{-C}_7\text{H}_{16}$ containing 0.01M 10-(carbomethoxy) decyldimethylchlorosilane ($\text{C}_{14}\text{H}_{29}\text{ClO}_2\text{Si}$, ABCR GmbH & Co) for 4h at 4°C , which create COOHCH_3 functions. Samples were then washed in silane-free solvent, heated as above and immersed overnight in a 12M HCl solution to create COOH surfaces as second step.

4.2. Water contact angle measurement

The wettability of OH; CH_3 ; NH_2 and COOH SAMs was measured with water contact angles using sessile drop technique performed on Dataphysics Contact Angle Systems OCA15. The same measurements were performed for all surfaces after coating with 50 $\mu\text{g/ml}$ Col IV (Abcam, Cat. No ab7536, UK) in 0.1M sodium acetate, pH 4.5 for 30 min at 37°C . Average values were obtained from 3 measurements of at least three different SAMs.

Statistical analysis was performed using Stat Graphics Plus software employing ANOVA test to determine statistically significant differences between groups ($p < 0.05$). Each data point represents mean \pm standard deviation (SD) from at least three independent experiments.

4.3. Cells

Human Dermal Fibroblast purchased by PromoCell (Cat No C-12302) were cultured in Dulbecco's Modified Eagle's Medium (DMEM) supplemented with 10% fetal bovine serum (FBS), 1mM Sodium Pyruvate, 2mM L-Glutamine, and Penicillin-Streptomycin, all of them purchased from Invitrogen. The growth medium was exchanged each 3rd day. For the experiments the cells were detached from around confluent flasks with Trypsin/EDTA (Invitrogen) and the remained trypsin activity was stopped with FBS before 2 times washing with pure medium to remove any traces of serum proteins. Finally, the cells were reconstituted in serum free DMEM.

4.4. Overall Cell Morphology

10^5 cells/well were seeded in 6 well TC plates (Costar) containing the samples for 2 h in serum free medium. Typically, the samples were pre-coated with native Col IV as stated above for WCA measurements, at concentration 50 $\mu\text{g/ml}$, in 0.1M sodium acetate, pH 4.5 for 30 min. At the end of incubation, the cells were fixed with 4% paraformaldehyde (20 min) and permeabilized with 0.5% Triton X-100 for 5 min. To study the overall cell morphology we viewed simultaneously the actin cytoskeleton with FITC-phalloidin (Molecular Probes, Cat No A12379) and the nuclei with Hoechst 34580 (Invitrogen, Cat No H21486) stained for 30 min dissolved in PBS containing 1% albumin. Finally, the samples were mounted in Mowiol, viewed and photographed on a

fluorescent microscope Axio Observer Z1, (Zeiss, Germany). At least 3 representative images for each magnification were acquired.

4.5. Quantification of cell adhesion and spreading

The number of adhering cells and the mean cell surface area were quantified using Image J plugins (NIH, USA). The adhesion was measured by counting the cells nuclei in at least 3 randomly chosen squares from the images acquired for each sample (photographed at 10X magnification) using the blue channel of microscope (viewing the cells nuclei). The average cells area was further measured (in μm^2) on the same samples but viewed at 20x magnification in the green channel of microscope (to visualize cellular actin). Three samples were studied for each condition and the results presented are from 3 independent experiments.

4.6. Integrin Signaling

10^5 cells/well were seeded for 2h as above. α_1 and α_2 integrins were viewed with monoclonal anti-human integrin antibodies (Chemicon, Cat No MAB1973) and (Abcam, Cat No Ab24697) followed by AlexaFluor 555 goat anti-mouse (Invitrogen) as secondary antibody. In some cases FITC-phalloidin was added to the secondary antibody. The samples were viewed and photographed in a fluorescent microscope Axio Observer as above. At least 3 representative images were acquired (63X) for each experimental condition.

To visualize simultaneously the focal adhesions and phosphorylated focal adhesion kinase (p-FAK) the fixed and permeabilized samples were saturated with 1% albumin in PBS for 15min. Vinculin was visualized using monoclonal antibody (Sigma, cat No V9131) dissolved in PBS-1% albumin for 30min followed by AlexaFluor 488 goat anti-mouse (Invitrogen) secondary antibody. The p-FAK was visualized using p-FAK (Tyr925) polyclonal antibody (Cell Signaling Cat No 3284) dissolved in PBS-1% albumin for 30min, followed by AlexaFluor 555 goat anti-rabbit (Invitrogen) secondary antibody. For all double (or triple) staining protocols used, the preliminary studies with omitting of first or the corresponding secondary antibodies were performed confirming no cross-reactivity.

4.7. Collagen IV remodeling

To study the fate of adsorbed Collagen IV glass cover-slips (22x22 mm) were placed in 6-well tissue culture plates and coated with Col IV as above. After three times washing with PBS, 5×10^4 fibroblasts were seeded in serum free medium and cultured for a time as indicated (2, 5 or 24 hours). For 5 and 24 hours incubations 10% serum was added to the medium after one hour of culture in serum free medium.

At the end of incubations all samples were fixed with 4% paraformaldehyde (20 min) permeabilized with 0.5% triton X-100 (5min) and saturated with 1% albumin in PBS. The samples were processed for immunofluorescence using monoclonal anti-collagen IV antibody (Millipore, Cat. No. MAB1910) followed by Cyth 3-conjugated Affini Pure Goat Anti-Mouse IgG (H+L) (Jackson ImmunoResearch, Cat. No 115-165-062) or Alexafluor 488 anti-mouse (Invitrogen Cat. No. A11001) secondary antibodies, as specified below.

Most samples were viewed and photographed on fluorescent microscope (Nikon Eclipse E800) and only some double stained ones were viewed on Spectral Laser Scanning Confocal Microscope LSM (Leica TCS-SL).

4.8. Quantification of adsorbed FITC-Collagen IV

The adsorption of FITC-Collagen IV was quantified by NaOH extraction as described previously (Coelho et al., 2010). Briefly, the model surfaces were cleaned with distilled water in an ultrasonic bath dried and coated for 30 minutes at 37 °C with FITC Collagen type IV (Molecular Probes, Cat. No D- 12052) at concentrations 50 µg/ml dissolved in PBS. This collagen (type IV from human placenta origin) is conjugated with FITC (FITC-Col IV) in such a way that part of its fluorescence is quenched thus increasing significantly the quantum yield upon extraction under denaturing conditions.

Three different conditions were used to study adsorbed FITC-Col IV: a) direct extraction of adsorbed protein after coating; b) add medium for 5 and for 24h and then extract remaining adsorbed protein (keeping exactly the same condition as with cells) and C) culture cells for 5 and 24h measure fluorescent signal released to the supernatant and extract the remaining adsorbed protein. The adsorbed FITC-Col IV was extracted with 250 µl of 0.2 M NaOH for 2 h at room temperature. The fluorescent intensity of the extracts and supernatants were measured with a fluorescent spectrophotometer (Horiba-Jobin y Von, USA) set to 488 nm (excitation) and 530 nm (emission) and compared to a standard curve based on known concentrations of FITC-Col IV solutions in 0.2M NaOH.

4.9. Co-localization of collagen IV with fibronectin

To study co-localization of remodeled Col IV with secreted FN the cells were cultured in native Col IV coated glass for 5 or 24 hours as indicated in serum free DMEM for the first hour then 10% serum was added to the medium. Col IV was viewed by indirect immunofluorescence using monoclonal anti-Col IV antibody (Millipore, Cat. No. MAB1910) followed by Alexafluor 488 anti-mouse (Invitrogen Cat. No. A11001) as secondary antibody. Secreted FN was viewed by polyclonal anti-FN (Sigma, Cat. No. F3648) followed by Alexafluor 555 anti-rabbit (Invitrogen,

Cat. No. A21428) as secondary antibody. In other experimental set up the cells were cultured on FITC-Col IV and viewed directly while the secreted FN was viewed as above.

To study co-localization of Col IV with exogenously added FN, the cells were cultured for 4 hour on native Col IV substrata in the presence of 10% serum. After 100 µg/ml of Human Plasma Fibronectin (Sigma, Cat. No F2006) was added to the medium for 1 h before fixation. To view native collagen and FN, the same combination of monoclonal anti-collagen IV and polyclonal anti FN antibodies were used.

Another antibody was used to view FN in the second experimental set up, when slides were coated with FITC-Col IV. Exogenously added FN was viewed in these series using monoclonal anti-FN (Sigma, Cat. No F7387) followed by Cy3-conjugated AffiniPure Goat Anti-Mouse IgG (H+L).

Co-localization of secreted FN with exogenously added FITC-Col IV. In these experiments the glass slides were coated with serum for 30 minutes and cells were seeded and cultured for 23 hours in the presence of 10% serum. After that 100 µg/ml FITC-Col IV was added to the medium for 1 hour before fixation and saturation in 1% albumin (see below). Secreted FN was viewed as above using monoclonal anti-FN antibody followed with Cy³-conjugated Goat Anti-Mouse IgG.

All samples were fixed with 4% paraformaldehyde (20 min) permeabilized with 0.5% triton X-100 (5min) and saturated with 1% albumin in PBS for 15 min before staining. All samples were viewed and photographed on a fluorescent microscope Axio Observer Z1, (Zeiss, Germany) at different magnification. At least 3 representative images for each magnification were acquired.

4.9. Zymography

The conditioned medium from fibroblasts cultured for 24 hours on model materials was used to study the activity of the two major MMPs (MMP2 and MMP9) known to cleave Col IV. For that purpose, 25 µL of each supernatant was mixed with 5 µL of sample buffer (0.04 M Tris-HCL pH 6.8, 4 % SDS, 33 % glycerin, 0.04 % bromophenol blue) and these samples were charged on a Ready Gel Zymogram (Biorad, 15-well) containing 10 %, gelatin, and subjected to a gel electrophoresis (SDS-PAGE). The gel was then incubated in 2.5 % Triton X-100 for 30 minutes before overnight incubation with renaturation buffer (1 M Tris-HCL pH 7.5, 5 M NaCl, 1 M CaCl₂, 10 % Triton X-100) at 37 °C. After staining with 0.5 % Coomassie brilliant blue R-250 (in 30 % methanol/10 % acetic acid) and destaining with the same solution without Coomassie, gelatinolytic activity was detected as unstained bands on the blue background of the sample and quantified using a molecular imager gel Doc⁺ (imaging system, Biorad).

Acknowledgements

The current work was supported by: the Spanish Ministry of Science and Innovation, through projects MAT2009-14440-C02-0 and MAT2009-14440-C02-02.

References

- Abrahamsson, I., Zitzmann, N.U., Berglundh, T., Linder, E., Wennerberg, A., Lindhe, J., 2002. The mucosal attachment to titanium implants with different surface characteristics: an experimental study in dogs. *Journal of Clinical Periodontology* 29, 448-455.
- Ala-aho, R., Kähäri, V.-M., 2005. Collagenases in cancer. *Biochimie* 87, 273-286.
- Altankov, G., Grinnell, F., Groth, T., 1996. Studies on the biocompatibility of materials: fibroblast reorganization of substratum-bound fibronectin on surfaces varying in wettability. *J Biomed Mater Res* 30, 385-391.
- Altankov, G., Groth, T., 1994. Reorganization of substratum-bound fibronectin on hydrophilic and hydrophobic materials is related to biocompatibility. *Journal of Materials Science: Materials in Medicine* 5, 732-737.
- Altankov, G., Groth, T., 1996. Fibronectin matrix formation and the biocompatibility of materials. *Journal of Materials Science: Materials in Medicine* 7, 425-429.
- Altankov, G., Groth, T., Engel, E., Gustavsson, J., Pegueroles, M., Aparicio, C., Gil, F.J., Ginebra, M.-P., Planell, J.A., 2010. Development of Provisional Extracellular Matrix on Biomaterials Interface: Lessons from In Vitro Cell Culture *Advances in Regenerative Medicine: Role of Nanotechnology, and Engineering Principles*, in: Shastri, V.P., Altankov, G., Lendlein, A. (Eds.). Springer Netherlands, pp. 19-43.
- Aumailley, M., Gayraud, B., 1998. Structure and biological activity of the extracellular matrix. *J Mol Med (Berl)* 76, 253-265.
- Barczyk, M., Carracedo, S., Gullberg, D., 2010. Integrins. *Cell Tissue Res* 339, 269-280.
- Beningo, K.A., Dembo, M., Wang, Y.-l., 2004. Responses of fibroblasts to anchorage of dorsal extracellular matrix receptors. *Proceedings of the National Academy of Sciences* 101, 18024-18029.
- Charonis, A., Sideraki, V., Kaltezioti, V., Alberti, A., Vlahakos, D., Wu, K., Tsilibary, E., 2005. Basement membrane peptides: functional considerations and biomedical applications in autoimmunity. *Curr Med Chem* 12, 1495-1502.
- Chen, H., Yuan, L., Song, W., Wu, Z., Li, D., 2008. Biocompatible polymer materials: Role of protein–surface interactions. *Progress in Polymer Science* 33, 1059-1087.
- Chernousov, M.A., Stahl, R.C., Carey, D.J., 1998. Schwann cells use a novel collagen-dependent mechanism for fibronectin fibril assembly. *Journal of Cell Science* 111, 2763-2777.

Christopher, R.A., Kowalczyk, A.P., McKeown-Longo, P.J., 1997. Localization of fibronectin matrix assembly sites on fibroblasts and endothelial cells. *Journal of Cell Science* 110, 569-581.

Clark, K., Pankov, R., Travis, M.A., Askari, J.A., Mould, A.P., Craig, S.E., Newham, P., Yamada, K.M., Humphries, M.J., 2005. A specific $\alpha 5\beta 1$ -integrin conformation promotes directional integrin translocation and fibronectin matrix formation. *Journal of Cell Science* 118, 291-300.

Coelho, N.M., Gonzalez-Garcia, C., Planell, J.A., Salmeron-Sanchez, M., Altankov, G., 2010. Different assembly of type IV collagen on hydrophilic and hydrophobic substrata alters endothelial cells interaction. *Eur Cell Mater* 19, 262-272.

Coelho, N.M., Gonzalez-Garcia, C., Salmeron-Sanchez, M., Altankov, G., 2011. Arrangement of type IV collagen on NH₂ and COOH functionalized surfaces. *Biotechnol Bioeng* 108, 3009-3018.

Daley, W.P., Peters, S.B., Larsen, M., 2008. Extracellular matrix dynamics in development and regenerative medicine. *J Cell Sci* 121, 255-264.

Dzamba, B.J., Wu, H., Jaenisch, R., Peters, D.M., 1993. Fibronectin binding site in type I collagen regulates fibronectin fibril formation. *The Journal of Cell Biology* 121, 1165-1172.

Fleischmajer, R., Perlsh, J.S., Macdonald, D.E., Schechter, A., Murdoch, A.D., Iozzo, R.V., Yamada, Y., 1998. There Is Binding of Collagen IV to $\beta 1$ Integrin during Early Skin Basement Membrane Assembly. *Annals of the New York Academy of Sciences* 857, 212-227.

García, A.J., 2005. Get a grip: integrins in cell–biomaterial interactions. *Biomaterials* 26, 7525-7529.

Geiger, B., Bershadsky, A., Pankov, R., Yamada, K.M., 2001. Transmembrane crosstalk between the extracellular matrix and the cytoskeleton. *Nat Rev Mol Cell Biol* 2, 793-805.

Geiger, B., Spatz, J.P., Bershadsky, A.D., 2009. Environmental sensing through focal adhesions. *Nat Rev Mol Cell Biol* 10, 21-33.

Goody, M.F., Henry, C.A., 2010. Dynamic interactions between cells and their extracellular matrix mediate embryonic development. *Molecular Reproduction and Development* 77, 475-488.

Griffith, L.G., Swartz, M.A., 2006. Capturing complex 3D tissue physiology in vitro. *Nat Rev Mol Cell Biol* 7, 211-224.

Grinnell, F., 1986. Focal adhesion sites and the removal of substratum-bound fibronectin. *The Journal of Cell Biology* 103, 2697-2706.

Grinnell, F., Feld, M.K., 1982. Fibronectin adsorption on hydrophilic and hydrophobic surfaces detected by antibody binding and analyzed during cell adhesion in serum-containing medium. *Journal of Biological Chemistry* 257, 4888-4893.

Gustavsson, J., Altankov, G., Errachid, A., Samitier, J., Planell, J., Engel, E., 2008. Surface modifications of silicon nitride for cellular biosensor applications. *Journal of Materials Science: Materials in Medicine* 19, 1839-1850.

- Hubbell, J.A., 2003. Materials as morphogenetic guides in tissue engineering. *Current Opinion in Biotechnology* 14, 551-558.
- Huebsch, N., Mooney, D.J., 2009. Inspiration and application in the evolution of biomaterials. *Nature* 462, 426-432.
- Hynes, R.O., 2002. Integrins: Bidirectional, Allosteric Signaling Machines. *Cell* 110, 673-687.
- Hynes, R.O., 2009. The Extracellular Matrix: Not Just Pretty Fibrils. *Science* 326, 1216-1219.
- Ingham, K.C., Brew, S.A., Isaacs, B.S., 1988. Interaction of fibronectin and its gelatin-binding domains with fluorescent-labeled chains of type I collagen. *Journal of Biological Chemistry* 263, 4624-4628.
- Irvine, S.M., Cayzer, J., Todd, E.M., Lun, S., Floden, E.W., Negron, L., Fisher, J.N., Dempsey, S.G., Alexander, A., Hill, M.C., O'Rourke, A., Gunningham, S.P., Knight, C., Davis, P.F., Ward, B.R., May, B.C.H., 2011. Quantification of in vitro and in vivo angiogenesis stimulated by ovine forestomach matrix biomaterial. *Biomaterials* 32, 6351-6361.
- Janmey, P.A., McCulloch, C.A., 2007. Cell Mechanics: Integrating Cell Responses to Mechanical Stimuli. *Annual Review of Biomedical Engineering* 9, 1-34.
- Kadler, K.E., Hill, A., Canty-Laird, E.G., 2008. Collagen fibrillogenesis: fibronectin, integrins, and minor collagens as organizers and nucleators. *Current Opinion in Cell Biology* 20, 495-501.
- Kalluri, R., 2003. Basement membranes: structure, assembly and role in tumour angiogenesis. *Nat Rev Cancer* 3, 422-433.
- Kalluri, R., Zeisberg, M., 2006. Fibroblasts in cancer. *Nat Rev Cancer* 6, 392-401.
- Käpylä, J., Ivaska, J., Riikonen, R., Nykvist, P., Pentikäinen, O., Johnson, M., Heino, J., 2000. Integrin $\alpha 2 I$ Domain Recognizes Type I and Type IV Collagens by Different Mechanisms. *Journal of Biological Chemistry* 275, 3348-3354.
- Keresztes, Z., Rouxhet, P.G., Remacle, C., Dupont-Gillain, C., 2006. Supramolecular assemblies of adsorbed collagen affect the adhesion of endothelial cells. *Journal of Biomedical Materials Research Part A* 76A, 223-233.
- Kern, A., Eble, J., Golbik, R., KÜHn, K., 1993. Interaction of type IV collagen with the isolated integrins $\alpha 1 \beta 1$ and $\alpha 2 \beta 1$. *European Journal of Biochemistry* 215, 151-159.
- Keselowsky, B.G., Collard, D.M., García, A.J., 2003. Surface chemistry modulates fibronectin conformation and directs integrin binding and specificity to control cell adhesion. *Journal of Biomedical Materials Research Part A* 66A, 247-259.
- Keselowsky, B.G., Collard, D.M., García, A.J., 2004. Surface chemistry modulates focal adhesion composition and signaling through changes in integrin binding. *Biomaterials* 25, 5947-5954.
- Khoshnoodi, J., Pedchenko, V., Hudson, B.G., 2008. Mammalian collagen IV. *Microscopy Research and Technique* 71, 357-370.

- Kolahi, K.S., Mofrad, M.R., 2010. Mechanotransduction: a major regulator of homeostasis and development. *Wiley Interdiscip Rev Syst Biol Med* 2, 625-639.
- Kühn, K., 1995. Basement membrane (type IV) collagen. *Matrix Biology* 14, 439-445.
- Langer, R., Tirrell, D.A., 2004. Designing materials for biology and medicine. *Nature* 428, 487-492.
- Larsen, M., Artym, V.V., Green, J.A., Yamada, K.M., 2006. The matrix reorganized: extracellular matrix remodeling and integrin signaling. *Current Opinion in Cell Biology* 18, 463-471.
- Llopis-Hernández, V., Rico, P., Ballester-Beltrán, J., Moratal, D., Salmerón-Sánchez, M., 2011. Role of Surface Chemistry in Protein Remodeling at the Cell-Material Interface. *PLoS One* 6, e19610.
- Lutolf, M.P., Hubbell, J.A., 2005. Synthetic biomaterials as instructive extracellular microenvironments for morphogenesis in tissue engineering. *Nat Biotech* 23, 47-55.
- Mager, M.D., LaPointe, V., Stevens, M.M., 2011. Exploring and exploiting chemistry at the cell surface. *Nat Chem* 3, 582-589.
- Maneva-Radicheva, L., Ebert, U., Dimoudis, N., Altankov, G., 2008. Fibroblast remodeling of adsorbed collagen type IV is altered in contact with cancer cells. *Histol Histopathol* 23, 833-842.
- Mao, Y., Schwarzbauer, J.E., 2005. Fibronectin fibrillogenesis, a cell-mediated matrix assembly process. *Matrix Biology* 24, 389-399.
- Moon, I.S., Berglundh, T., Abrahamsson, I., Linder, E., Lindhe, J., 1999. The barrier between the keratinized mucosa and the dental implant. *Journal of Clinical Periodontology* 26, 658-663.
- Place, E.S., Evans, N.D., Stevens, M.M., 2009. Complexity in biomaterials for tissue engineering. *Nat Mater* 8, 457-470.
- Ratner, B.D., Bryant, S.J., 2004. BIOMATERIALS: Where We Have Been and Where We are Going. *Annual Review of Biomedical Engineering* 6, 41-75.
- Shi, F., Harman, J., Fujiwara, K., Sottile, J., 2010. Collagen I matrix turnover is regulated by fibronectin polymerization. *American Journal of Physiology - Cell Physiology* 298, C1265-C1275.
- Sottile, J., Hocking, D.C., 2002. Fibronectin Polymerization Regulates the Composition and Stability of Extracellular Matrix Fibrils and Cell-Matrix Adhesions. *Molecular Biology of the Cell* 13, 3546-3559.
- Stamenkovic, I., 2003. Extracellular matrix remodelling: the role of matrix metalloproteinases. *The Journal of Pathology* 200, 448-464.
- Stevens, M.M., George, J.H., 2005. Exploring and Engineering the Cell Surface Interface. *Science* 310, 1135-1138.
- Thevenot, P., Hu, W., Tang, L., 2008. Surface chemistry influences implant biocompatibility. *Curr Top Med Chem* 8, 270-280.

- Timpl, R., Brown, J.C., 1996. Supramolecular assembly of basement membranes. *Bioessays* 18, 123-132.
- Tzoneva, R., Groth, T., Altankov, G., Paul, D., 2002. Remodeling of fibrinogen by endothelial cells in dependence on fibronectin matrix assembly. Effect of substratum wettability. *Journal of Materials Science: Materials in Medicine* 13, 1235-1244.
- Van Agtmael, T., Bruckner-Tuderman, L., 2010. Basement membranes and human disease. *Cell and Tissue Research* 339, 167-188.
- Vanacore, R.M., Shanmugasundararaj, S., Friedman, D.B., Bondar, O., Hudson, B.G., Sundaramoorthy, M., 2004. The $\alpha 1. \alpha 2$ Network of Collagen IV. *Journal of Biological Chemistry* 279, 44723-44730.
- Velling, T., Risteli, J., Wennerberg, K., Mosher, D.F., Johansson, S., 2002. Polymerization of Type I and III Collagens Is Dependent On Fibronectin and Enhanced By Integrins $\alpha 1 \beta 1$ and $\alpha 2 \beta 1$. *Journal of Biological Chemistry* 277, 37377-37381.
- Wheeldon, I., Farhadi, A., Bick, A.G., Jabbari, E., Khademhosseini, A., 2011. Nanoscale tissue engineering: spatial control over cell-materials interactions. *Nanotechnology* 22, 212001.
- White, D.J., Puranen, S., Johnson, M.S., Heino, J., 2004. The collagen receptor subfamily of the integrins. *The International Journal of Biochemistry & Cell Biology* 36, 1405-1410.
- Wierzbicka-Patynowski, I., Schwarzbauer, J.E., 2003. The ins and outs of fibronectin matrix assembly. *Journal of Cell Science* 116, 3269-3276.
- Wu, C., Keivenst, V.M., O'Toole, T.E., McDonald, J.A., Ginsberg, M.H., 1995. Integrin activation and cytoskeletal interaction are essential for the assembly of a fibronectin matrix. *Cell* 83, 715-724.
- Wynn, T.A., 2008. Cellular and molecular mechanisms of fibrosis. *The Journal of Pathology* 214, 199-210.
- Yamada, K.M., Geiger, B., 1997. Molecular interactions in cell adhesion complexes. *Current Opinion in Cell Biology* 9, 76-85.
- Yurchenco, P., Schittny, J., 1990. Molecular architecture of basement membranes. *The FASEB Journal* 4, 1577-1590.
- Yurchenco, P.D., 2011. *Basement Membranes: Cell Scaffoldings and Signaling Platforms*. Cold Spring Harbor Perspectives in Biology 3.
- Zoppi, N., Gardella, R., De Paepe, A., Barlati, S., Colombi, M., 2004. Human Fibroblasts with Mutations in COL5A1 and COL3A1 Genes Do Not Organize Collagens and Fibronectin in the Extracellular Matrix, Down-regulate $\alpha 2 \beta 1$ Integrin, and Recruit $\alpha \nu \beta 3$ Instead of $\alpha 5 \beta 1$ Integrin. *Journal of Biological Chemistry* 279, 18157-18168.

IMPORTANT : Aquest article va ser publicat a la revista

IMPORTANTE: Este artículo apareció en la revista

IMPORTANT: This article was published in

Biomaterials Science

www.rsc.org/biomaterialsscience

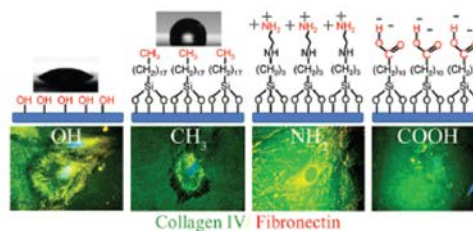
<http://pubs.rsc.org/en/content/articlelanding/BM/2013/c3bm00163f#!divAbstract>

494

Fibroblasts remodeling of type IV collagen at a biomaterials interface

Nuno Miranda Coelho, Manuel Salmerón-Sánchez and George Altankov*

Fibroblasts remodeling of type IV collagen at a biomaterials interface depends on fibronectin and substratum chemistry.



DOI: 10.109/C3BM00163F

4.3 Supplementary Results 3

Measurement of Cell Adhesion Strength via Flow Chamber

Though the flow chamber was not used systematically in our studies, we performed a number of preliminary experiments aiming at calibration of the system, which is presented below.

Calibration of the flow system

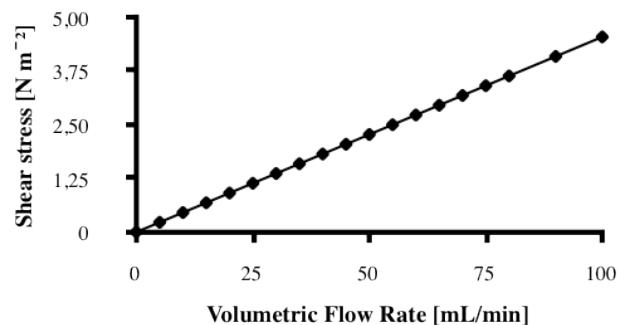


Figure 1 - Relation between the volumetric flow and the shear stress applied in the wall of the chamber.

Figure 1 shows the relation between the volumetric flow rate and the resultant shear stress applied at the chamber wall calculated as described in materials and methods section.

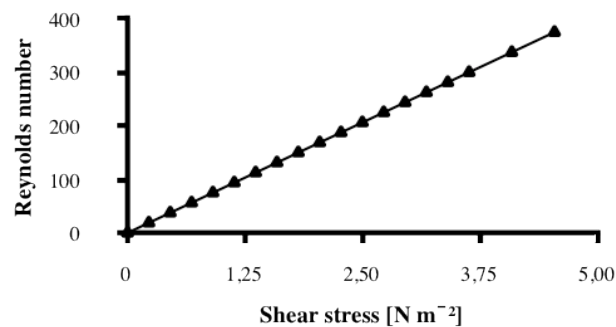


Figure 2- Reynolds number as function of the wall shear stress.

As explained in the Methods section to exert a constant shear stress over the cell culture various parameters of the flow profile were considered. First, the Reynolds (Re) number has to be below the critical value of 2300 in order to maintain laminar flow (Owens et al., 1987). To determine if our system provides laminarity we plotted the shear stress as function of the Re number. As shown on Figure 3 all shear stress values used in the *in vitro* experiments gave values of Re number below 400 showing that our system maintain laminarity (Figure 2). Other important parameter is the entrance length (l_e) because the measurement should be taken at distances bigger than l_e to ensure steady flow over the area of interest (White, 2003). Figure 3 shows the result

determining the l_e at several shear stress values measured up to the maximum value used in our experiments. We defined as l_e 1.2 cm, a value slightly above the value obtained for our maximal shear stress.

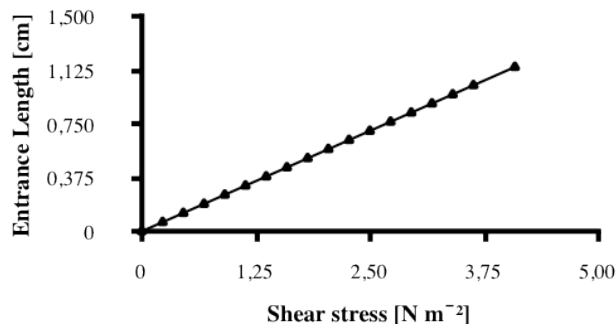


Figure 3- Entrance length as function of the wall shear stress.

After calibration of the flow we defined six points (0.2, 0.5, 0.9, 1.8, 3.6, and 4.5 Nm^{-2}) of flow rate to be used in the experiments.

Fibroblast Adhesion Strength to Col IV on hydrophilic and hydrophobic surfaces

Human fibroblasts were harvested from about confluent flasks and left to attach from a suspension with concentration of 1×10^6 cells/ml in serum free medium to the glass cover of the chamber. The chamber was incubated for 2 h at 37°C in an inverted position. The cover glass slides of the chamber were rendered hydrophilic or hydrophobic by pretreatment with Piranha or ODS solutions, respectively, before coating with $50 \mu\text{g/ml}$ Col IV (See Methods section). After adhesion the chamber was connected to the pump (strictly avoiding air bubbles) and subjected to different flow rates. Each shear stress was applied for two minutes before acquiring an image of the adhering cells (e.g. remained on the substratum). Then the flow was changed gradually to the next point up to 4.5Nm^{-2} .

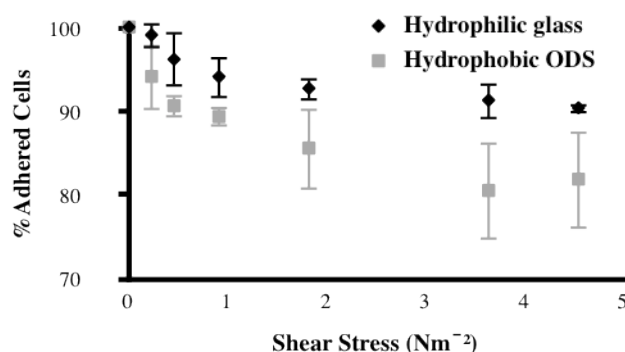


Figure 4 - Detachment of human fibroblast from hydrophilic glass and hydrophobic ODS as function of the shear stress applied (n=5).

The results show a clear trend for higher detachment of fibroblasts when adhering to Col IV coated hydrophobic ODS than to the hydrophilic glass substrata and the difference was significant for values above then 2 Nm⁻².

These differences in cell adhesion strength however, were difficult to be followed on other model materials, because of the high variability between experiments. This was the main reason we decided to stop using this method for characterizing the initial cell-biomaterial interaction. The other limitation was the necessity of using only transparent materials.

5. Remodeling of Type IV Collagen by Endothelial Cells

5.1 Preface 5

As stated in the results Section 4 the remodeling of ECM is an important process that involves ECM synthesis, organization and degradation accomplished mainly by stromal fibroblasts. However, endothelial cells are also involved in modifying ECM. The remodeling of vascular BM is a fundamental process during angiogenesis carried out in response to growth factors and MMPs secretion that promote not only the proliferation and migration of vascular endothelial cells, but also their organization. During angiogenesis the proteolysis accomplished by secreted MMPs can produce specific fragments with different biological activity that regulate tissue architecture through effect on the ECM (Stamenkovic 2003). As stated before, remodeling occurs also at biomaterials surface and at this level it can affect the vascularization of an implant, which in turn is a prerequisite for its successful integration in the tissues. Here we provide insights on the HUVEC ability to remodel adsorbed Col IV in contact with model biomaterial surfaces and show that varying with their wettability, chemistry or charge we can obtain control on this process.

We compared the initial interaction of HUVEC with Col IV and their remodeling potential. Western-blot analysis of p-FAK expression was further performed to confirm the morphological observations. To quantify the proteolytic cleavage we prepared cellular extracts in order to detect early expression of MMP2 and we found significantly higher values when HUVEC were cultured on the aggregated form of Col IV, e.g. on hydrophobic substrata. Zymography of the conditioned medium however showed the involvement of both MMP2 and MMP9 in Col IV remodeling.

We further studied the ability of HUVEC to form capillary-like tubes on Col IV coated model materials overlaid by basement membrane extract (BME) – containing 1% FITC-Col IV. After 24h of culture HUVEC changed their phenotype and start to form tube-like structures. Important is to notice that in agreement with the supported initial interaction these structures were better developed on OH and NH₂ surfaces. The experiments aimed to quantify the degradation activity of HUVEC also showed higher values on OH surfaces where the best capillary-like structures were found.

Finally, considering the involvement of FN in Col IV remodeling (see the results in Section 4) and knowing that NH₂ surfaces support FN fibrillogenesis while CH₃ abrogate it, we create an order of model surfaces - mixed SAMs - expressing different partial ratios of these functions to learn more about the possibilities to control the fate of Col IV at cell-biomaterial interface, in this case, via modifying FN matrix formation. These model material surfaces were produced and

characterized in the Center for Biomaterials and Tissue Engineering at Polytechnic University of Valencia (Professor M. Salmerón-Sánchez group).

We found higher amounts of FITC-Col IV on pure NH_2 (100%) and CH_3 (100%) SAMs suggesting different adsorption mechanisms. We also found that NH_2 provoke Col IV organization while hydrophobic CH_3 – its degradation. On this model we confirmed the involvement of both MMP2 and MMP9 in Col IV remodeling via zymography. Higher MMPs values were found again on 100% CH_3 confirmed by the quantitative studies using FITC-Col IV release. Details of these studies are presented below as supplementary material.

5.2 Supplementary Results 4

Signaling of endothelial cells on Col IV

To learn whether the development of focal adhesion contacts on Col IV induces the recruitment of phosphorylated signaling molecules we co-stained the samples for vinculin and p-FAK. The data shown in Figure 1A shows a higher level of expression and co-localization between the well developed focal adhesion contacts (viewed by vinculin in green) and p-FAK (red) on OH (a and e) and NH₂ (c and g) surfaces resulting in orange when merged (i and k). Conversely, on CH₃ and COOH surfaces, although some cells were able to make focal contacts (b and d), a significantly less p-FAK is recruited (f and h), resulting in prevalent green in merges (j and l). These observations suggest successful transmission of signals to the cell interior on OH and NH₂ surfaces and altered transmission on CH₃ and COOH surfaces.

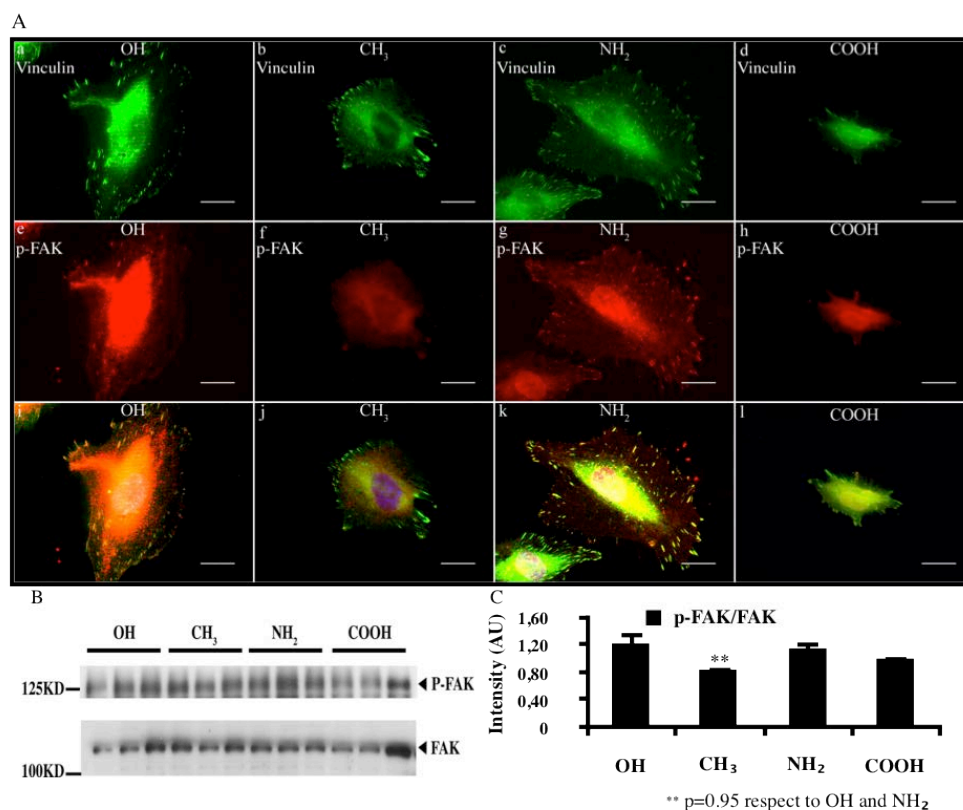


Figure 1 - (A) Recruitment of the signaling molecule p-FAK (e to h and i to l- in red) in the focal adhesion complexes (a to d and i to l- in green) in HUVEC seeded on Col IV coated OH, CH₃, NH₂, and COOH surfaces. Bar 20 μm. (B) Western-blot of cellular extracts of HUVEC adhering to the same Col IV coated model surfaces for 2h. Detection of p-FAK, and FAK expression. (C) Densitometry analysis of p-FAK expression, standardized to FAK as control for protein loading.

In order to confirm these morphologic observations we perform western blot analysis of HUVEC (cellular extracts) after two hours adhesion on Col IV coated model OH, CH₃, NH₂, and COOH surfaces. The results are shown on Figure 1B. The p-FAK expression is standardized to FAK as control for protein loading (Figure 1 C). We found higher values of p-FAK expression on OH and

NH₂ surfaces and this difference was significant ($p > 0.05$) when both surfaces were compared with CH₃ surface. The expression of p-FAK on COOH surface is lower, but the difference is not significant ($p > 0.05$). Collectively, these observations confirm the morphological data suggesting that HUVEC interact better with Col IV on OH and NH₂ surfaces.

In order to learn if the different adsorption/conformation of Col IV on the different materials induces different degradation activity of HUVEC we measured the MMP2 activity (comprising the major MMPs class known to degrade Col IV) of extracts prepared as for previous studies of p-FAK expression. Figure 2 shows the western-blot (A) and the corresponding densitometry analysis for MMP-2 expression normalized to the amount of cellular vinculin (B) as control for protein loading.

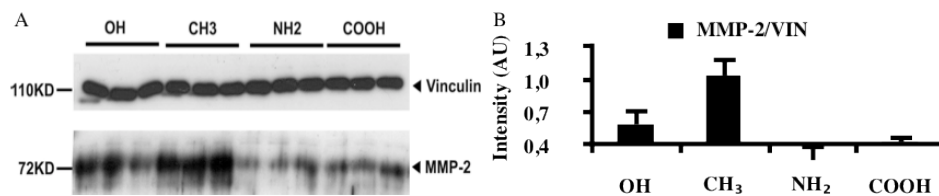


Figure 2 - (A) Western-blot of cellular extracts prepared from HUVEC adhering to Col IV coated model surfaces for 2h. Detection of MMP2 and vinculin expression (B) Densitometry analysis of MMP2 expression is normalized to vinculin as control for protein loading.

Significantly higher ($p < 0.05$) expression of MMP2 was found on CH₃ (Figure 2B) surface when compared to all other Col IV coated surfaces. The next was OH surface with still significantly higher activity than NH₂, followed by COOH surface. These observations suggest that endothelial cells possess significantly higher degradation activity to Col IV on CH₃ and OH surfaces.

Morphological observations of Collagen IV remodeling by endothelial cells

HUVECs were seeded for 5h or 24h on the Col IV coated model surfaces in the presence of serum (see Methods section) and consequently the Col IV reorganization and FN secretion were viewed simultaneously. The results are presented on Figure 3. A typical organization of secreted FN in fibrils that co-localize almost completely with substratum arranged Col IV in linear pattern was found on OH substrata (A and E), resulting in yellow when merged (I) after 5h of culture. Conversely, on CH₃ surface the less Col IV arrangement was combined with appearance of dark zones where Col IV is removed (Figure 3 B), further corroborating with lowered deposition of FN fibrils (Figure 3 F). On NH₂ the arrangement of Col IV was represented with shorter streaks that co-localize also well with secreted FN matrix, but note, the FN fibrils formation was substantially supported by this substrate (Figure 1 C, G, and K). Finally, on COOH again lowered rearrangement of both Col IV and FN was observed (Figure 3 D, H, and L respectively).

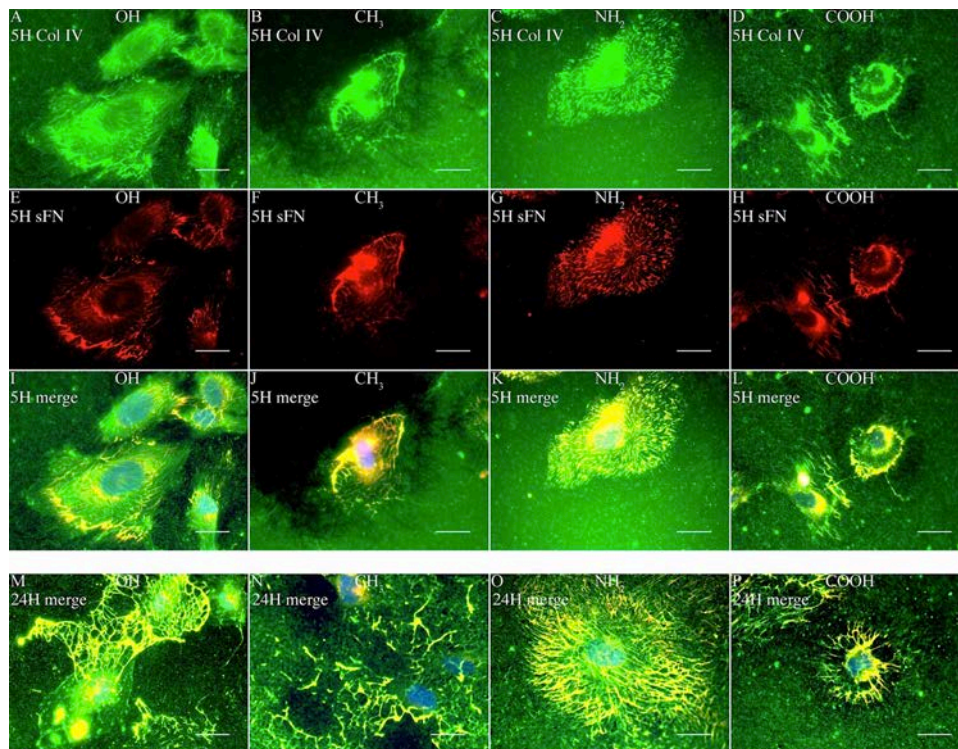


Figure 3 - HUVEC remodeling of adsorbed Col IV on different model surfaces after 5 h (A-D) and 24 h (M-P) corroborated with FN secretion, 5 h (E-H-red) and 24 h. Bar = 20 μ m.

The same trend was observed after 24 h (see Figure 3 M to P; only merges are presented) with increased dark zones on CH₃ (N), much ticker FN fibrils on OH (Figure 3 M) and particularly augmented FN fibrils deposition on NH₂ (Figure 3 O). The lowest cellular activity was again obtained on COOH surface (Figure 3 P).

Zymography

The conditioned medium collected after 24h of HUVEC cultured on Col IV coated model surfaces was used for zymography analysis to study the activity of MMP2 and MMP9 - the two major MMPs known to degrade Col IV. Figure 4 represents that in all conditions HUVEC secrete MMP2 and MMP9, but only MMP-9 seems to be secreted in both inactive and active forms (representing two bands). The densitometry analysis for MMP9 (Figure 4B) showed significantly higher values on CH₃ and COOH, versus OH and NH₂ surfaces, while MMP2 showed higher values for OH and COOH. Collectively, these observations support the morphological data, where the dark zones formed by HUVEC (consisting presumably of degraded Col IV) were visible mainly on CH₃ and COOH surfaces, followed by OH and NH₂ (Figure 3 A, B, D and M, N, P).

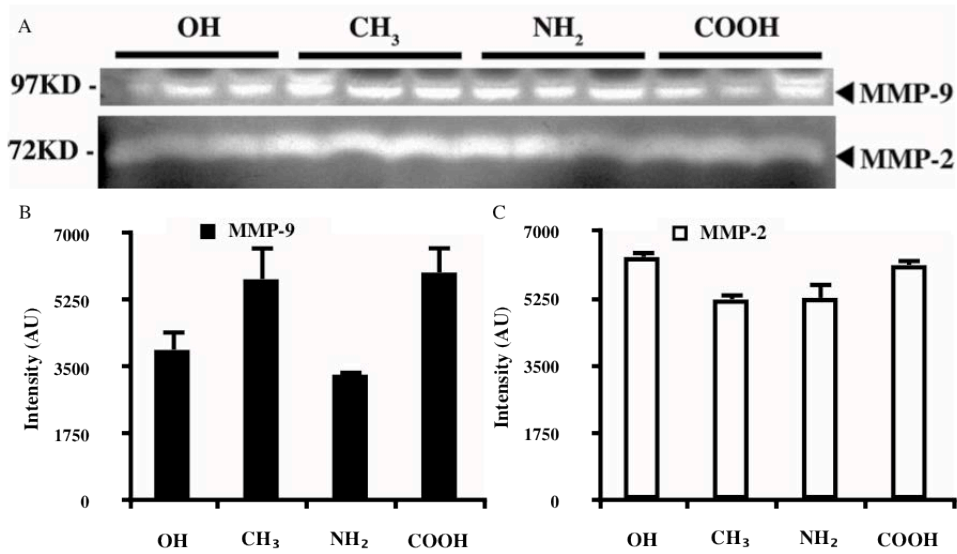


Figure 4 - Zymography of the conditioned medium of HUVEC cultured for 24 h on Col IV coated model materials. Line 1 MMP9 and Line 2 MMP2, 97 and 72 KDa respectively. (B) Densitometry for MMP9 and (C) for MMP2 activity.

Morphological data using the FITC labeled Col IV also confirms the general trend of differences between surfaces (Figure 5). They also confirm the observation that rearranged Col IV co-localizes with FN fibrils, although much higher secretion of FN matrix was observed on NH₂ surface. All this suggested that FITC-Col IV might be used for further quantification of the differences in degradation activity of HUVEC toward Col IV.

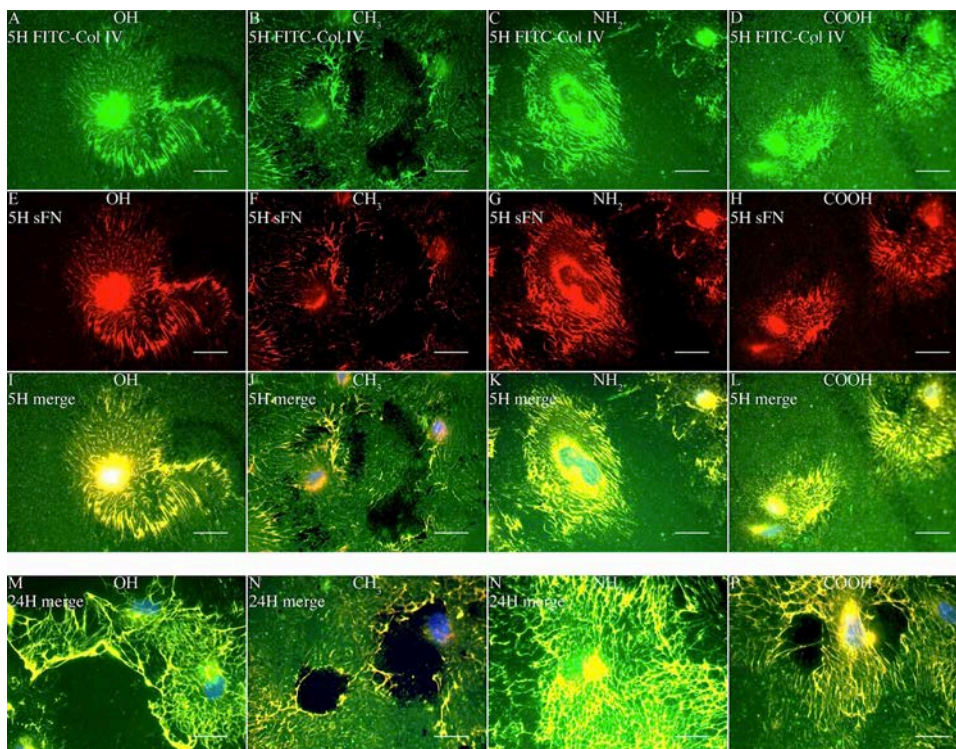


Figure 5 - FITC-Col IV remodeling by HUVEC on different model surfaces for 5 (A-D) and 24 (M-P) hours. FN secretion is also viewed by immunofluorescence after 5h (E-H-red) and 24h (M-P-red) of culture. Bar = 20 μ m.

Indeed, the quantitative studies of FITC release to the supernatant revealed significantly higher values on CH₃ and COOH surfaces in comparison to OH and NH₂ model surfaces after 5h of HUVEC culture (Figure 6A). These results are in agreement with morphological observations where dark zones were mainly visible on CH₃ (Figure 5B) and COOH (Figure D). However, after 24 h of culture this difference was abolished, particularly on OH surface and only NH₂ surface shows still significantly lowered value of FITC release suggesting low proteolysis.

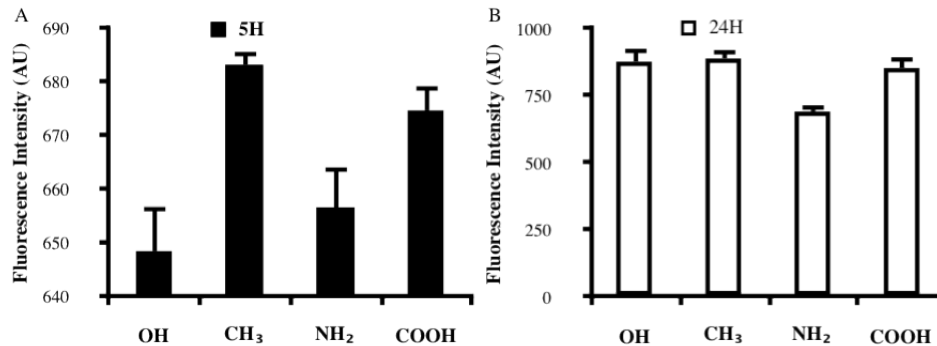


Figure 6 - Release of FITC in the supernatant after culturing HUVEC on FITC-Col IV coated model surfaces or 5 (A) and 24 (B) hours. Released fluorescent signal correlates with the proteolytic activity of the cells.

Formation of capillary-like structures

In this study we were interested to learn if the differences in the initial cell interaction would promote different capillary-like tubes formation. For that purpose the cells were seeded on Col IV coated model surfaces for two hours in serum free medium and then BME-containing 1% FITC-Col IV was overlay at each sample. The morphological response of cells was studied after 5 and 24 hours of culture. In agreement with our observations on early cellular interaction, the amount of cells on Col IV coated OH and NH₂ surfaces (Figure 7A a, c) were higher than on CH₃ and COOH (Figure 7A b, d) after 5h of culture. After 24h of culture however, in all cases HUVEC change their phenotype and start to form tube-like structures (Figure 7A e-h). Nevertheless, it is important to notice that still correlating with the difference in the initial cell adhesion, the formation of these structures looks pronounced on OH surface (Figure 7A e) followed by NH₂ surface (Figure 7A g), while on CH₃ (Figure 7A f) and COOH surfaces (Figure 7A h) the formation seemed to be delayed.

Figures 7B and C show our attempt to quantify the degradation activity of HUVEC via inclusion of FITC labeled Col IV included the BME. Figure 7B shows the amount of released FITC signal to the medium after 24h. However, no big difference between the materials was found, except between the positive (collagenase treated gels) and negative (pure medium) control samples (see Methods section). Conversely, when the remaining FITC-Col IV in the gel was extracted after 24h of incubation (Figure 7C) we found significantly higher value on OH samples in comparison

to other three samples. On the other hand, all materials showed significantly higher signal than the negative control (pure medium) confirming the existing cellular activity. These results points to the possibility that although degraded by HUVEC FITC-Col IV may stay entrapped in the gel and not dissolve in the conditioned medium.

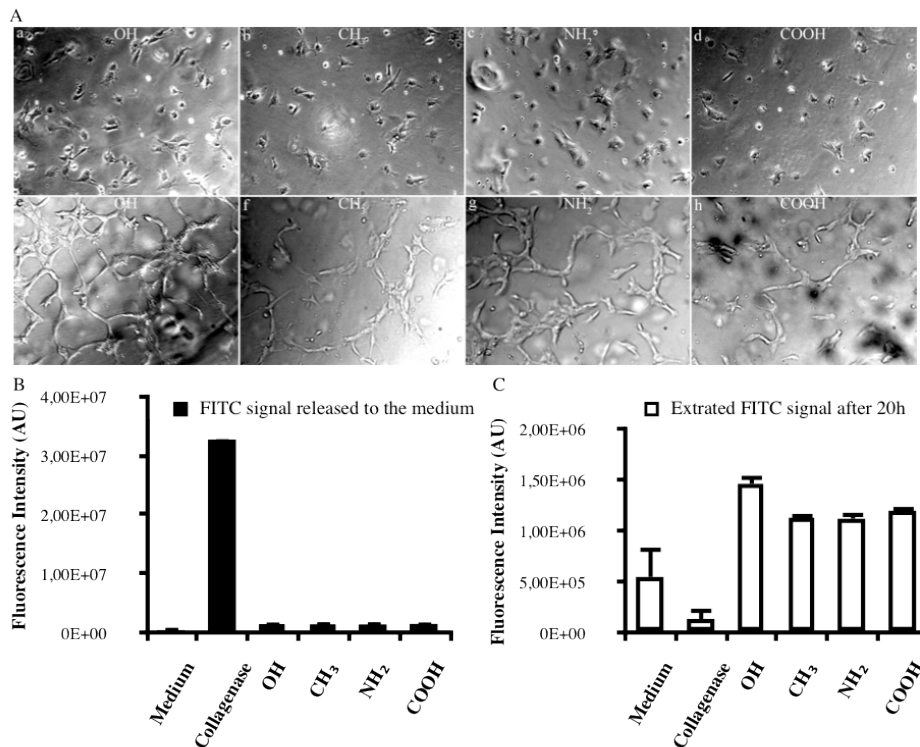


Figure 7 - (A) HUVEC were cultured on Col IV coated model materials for 2h and then the samples were overlaid with BME-2%FITC-Col IV and further cultured for 5 (a-d upper panel) and 24 (e-h lower panel) hours. (B) The cellular proteolytic activity quantified by measuring intensity of the released FITC fluorescence in the medium after 24h of culture. (C) Remaining FITC signal in the gel measured after extraction with 1mg/ml collagenase.

Studies on model surfaces with mixed SAMs

Studies provided above have shown that NH₂ and CH₃ surfaces adsorb more Col IV, but provide completely different conditions for cellular interaction and FN matrix assembly. CH₃ is strongly hydrophobic and suppress FN matrix organization while NH₂ is moderately hydrophilic, but support FN matrix assembly. Considering the involvement of FN in Col IV remodeling we decided to create an order of model surfaces – mixed SAMs - expressing different partial ratios of these functionalities to learn more about the possibilities to control the fate of Col IV at cell-biomaterial interface.

Adsorption of FITC-Col IV on mixed SAMs

FITC-Col IV was again used to study protein adsorption profile onto model mixed SAMs. The amount of adsorbed Col IV was determined by comparison of extracted fluorescence signals

(using 0.2 M NaOH) to a standard curve with known FITC-Col IV concentrations as described above and detectable values were obtained on surfaces (Figure 8) using the adsorption concentration of 50 $\mu\text{g/ml}$.

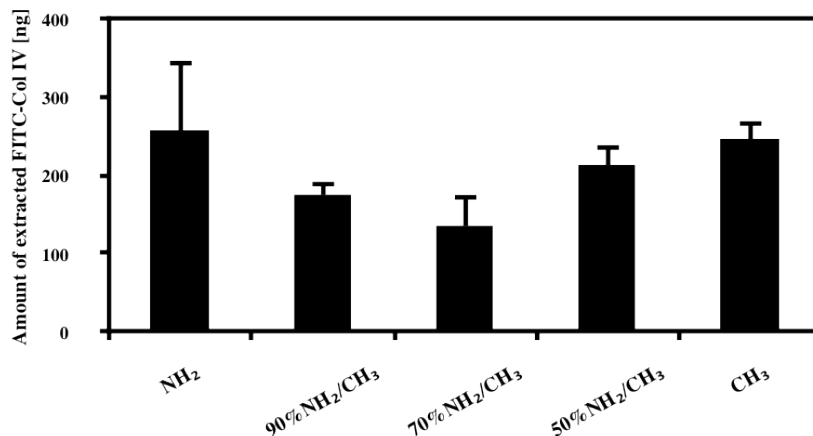


Figure 8 - FITC-Col IV adsorption on model mixed SAMs presenting different portions of NH₂ and CH₃ chemistries as follow: 100% NH₂ (NH₂); 90% NH₂ 10% CH₃ (90% NH₂/CH₃); 70% NH₂ 30% CH₃ (70% NH₂/CH₃); 50% NH₂ 50% CH₃ (50% NH₂/CH₃); 100% CH₃ (CH₃). Triplicate measurements were made using 50 $\mu\text{g/ml}$ coating concentration and compared with standard curve with known FITC-Col IV concentration.

The model surfaces that supported FITC-Col IV adsorption were the NH₂, 50% NH₂/CH₃, and CH₃, all showing no significant differences between each other, but adsorbing a significantly higher amount of protein when compared with the other two mixed SAMs (90% and 70% nNH₂/CH₃).

Cell adhesion and spreading to mixed SAMs

Figure 9A shows the overall morphology of HUVEC adhering for two hours on plane (a-e) and Col IV coated (f-j) model surfaces of mixed SAMs. On plane surfaces, the significantly low amount of adhered HUVECs correlates with the rounded cell morphology (a-e). Improved cell morphology was particularly pronounced on Col IV coated NH₂, 90% NH₂/CH₃, 70% NH₂/CH₃ SAMs (f, g, and h respectively), while on 50% NH₂/CH₃ and CH₃ SAMs, less cells with rather rounded morphology were observed (i and j). The quantitative data for adhesion (Figure 9B) and spreading (Figure 9C) confirm these morphological observations showing a significantly higher amount of cells adhered to Col IV coated SAMs (B) and the number of adhering cells diminished with increasing the percentage of CH₃ groups (Figure 9B-black bars). Cell spreading followed the same trend (Figure 9C).

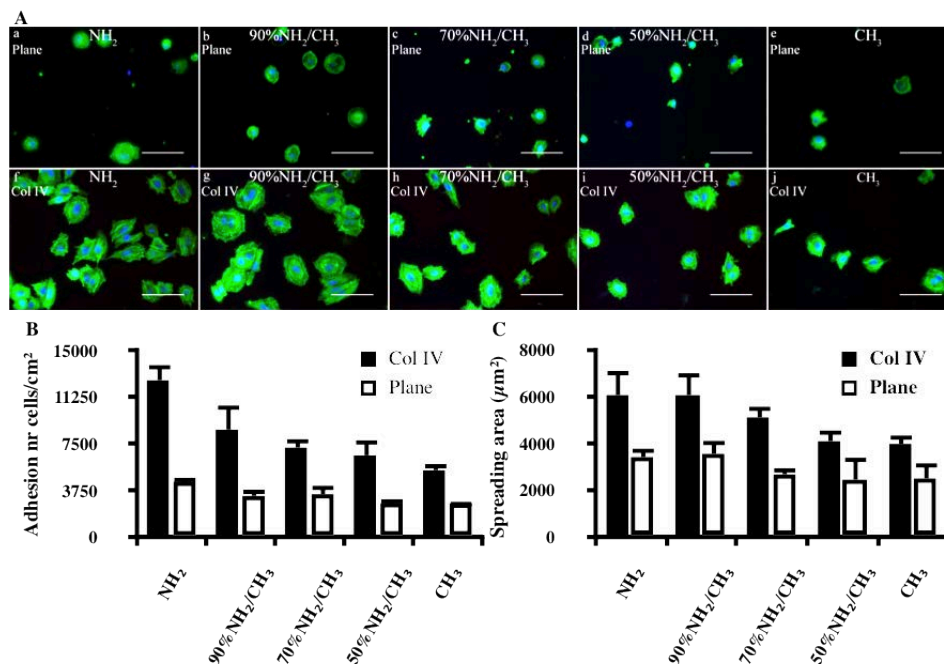


Figure 9 - (A) Overall morphology of HUVEC adhering to plane (a-e) and Col IV coated (f-j) mixed SAMs. The cells are stained for actin and nucleus after 2 h of culture. Bar =100μm. (B) Represents the quantities for cell adhesion expressed as number of cells per cm² and (C) spreading in μm² for both plane (white bars) and Col IV coated (black bars) samples.

Development of focal adhesion complex

To learn more about the effectiveness of cell adhesion to adsorbed Col IV on mixed SAMs the focal adhesion contacts were visualized via vinculin together with actin cytoskeleton. As shown on Figure 10), the more flattened and elongated cells on NH₂ and 90% to 70% NH₂/CH₃ SAMs represented also well developed focal adhesion contacts (F and G) where prominent actin stress fibers often inserts (A and B), as seen on merged images (K and L). On the other SAMs although decreasing in NH₂ content, the cells still develop focal adhesion contacts, but diminishing in size (H-J) correlating with the less organized actin better seen in merged images (N, O).

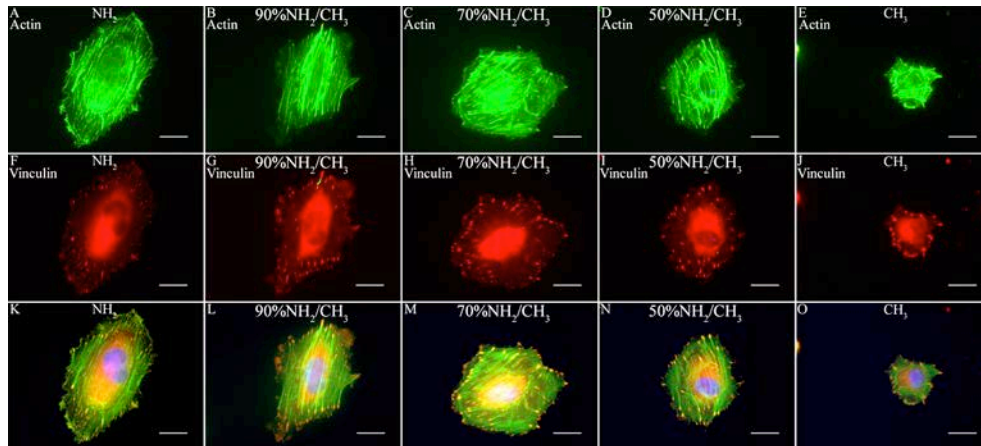


Figure 10 - Development of focal adhesion contacts (F-J vinculin in red) and actin cytoskeleton (A-E) viewed by FITC phalloidin in green, of HUVEC seeded on Col IV coated mixed SAMs for 2h. The images are merged on the lower panel (K-O). Bar = 20 μm .

To learn which integrins were involved in the adhesion we studied the expression and organization of α_1 and α_2 integrin subunits. As shown in Figure 11 both integrins are well expressed (A-E and F-J) although diminish as the percentage of CH_3 groups increase (A-E and F-J) becoming worst on CH_3 (E, J). However, α_1 represents a rather linear organization well seen on most SAMs (A - C) and going along with actin stress fibers (data not shown), while α_2 shows well pronounced clusters resembling focal adhesion contacts (F- J), which diminish with increasing the percentage of CH_3 groups (F-J), thus correlating with the smaller adhesive complexes (see Figure 10).

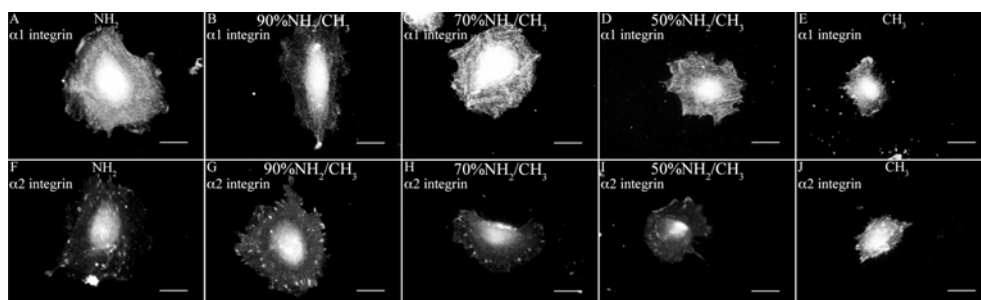


Figure 11 - Expression of alpha 1 (A to E) and alpha 2 (F to J) integrins in HUVEC adhering on the same mixed SAMs coated with Col IV. Bar 20 μm .

Morphological evidence for Collagen IV remodeling on mixed SAMs

HUVEC were seeded for 5h or 24h on Col IV coated mixed SAMs and both Col IV reorganization and FN secretion were viewed separately or superimposed. Figure 12 shows the typical organization of FN fibrils at 5th hour (F-G) that co-localize almost completely with linearly arranged Col IV (A-E). Merged images are presented on (K-O). Reorganization generally diminishes as the percentage of CH_3 groups increase, but interestingly on 70% NH_2/CH_3 we found

peculiar optimum of Col IV arrangement that correlates with maximal FN fibrils assembly. Conversely, the worst Col IV arrangement on CH₃ surface (E) corroborates with the lowered deposition of FN fibrils (J) where dark zones of Col IV removal (E) were also observed.

The same trend was observed after 24 hours, shown on Figure 3 (P–T) where only merged images are presented. Note the increased dark zones on CH₃ (T), suggesting higher Col IV removal, and the augmented FN fibrils deposition on 70%NH₂/CH₃ SAM (P–N).

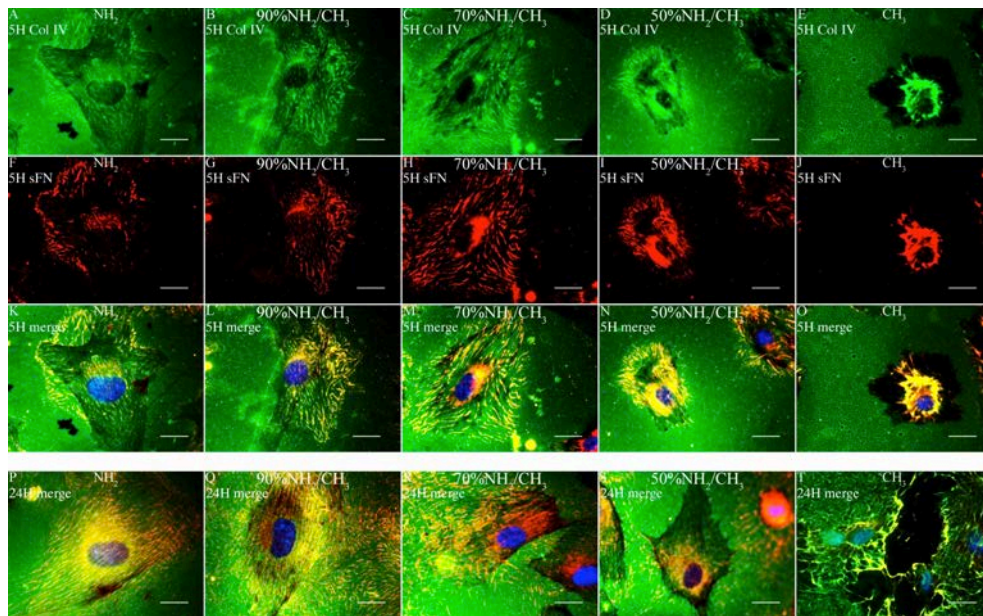


Figure 12 - Remodeling of adsorbed native Col IV by HUVEC on different mixed SAMs for 5 (A–E) and 24 (P–T) hours viewed simultaneously with secreted FN at 5 (F–J) and 24 hours (P–T, only merged images are shown). Bar = 20 μ m.

Zymography

By analogy with previous studies, the conditioned medium of HUVEC adhering on Col IV mixed SAMs was collected after 24h of incubation and used for zymography analysis to follow the activity of MMP2 and MMP9. Zymograms presented on Figure 13 show that HUVEC secrete MMP2 and MMP9 in all conditions, but only MMP-9 seems to be secreted in both inactive and active forms (two bands) while MMP2 was found only in inactive form (one band). The densitometry for MMP9 (Figure 13B) showed significantly higher levels for pure CH₃ and 50%NH₂/CH₃. This observation is partly in agreement with the morphological data where dark zones (presumably of degraded Col IV) were clearly visible on CH₃ after 5h and 24h of culture (Figure 13S and T). For the other surfaces however this correlation is not so clear, but interestingly, the lowest MMP-9 (also MMP-2) was found on 70%NH₂/CH₃ surface where the highest Col IV and FN matrix organization was found (Figure 12). The densitometry for MMP2 (Figure 13B) showed small differences, but again, the only significantly lowered expression was found on 70%NH₂/CH₃ surface.

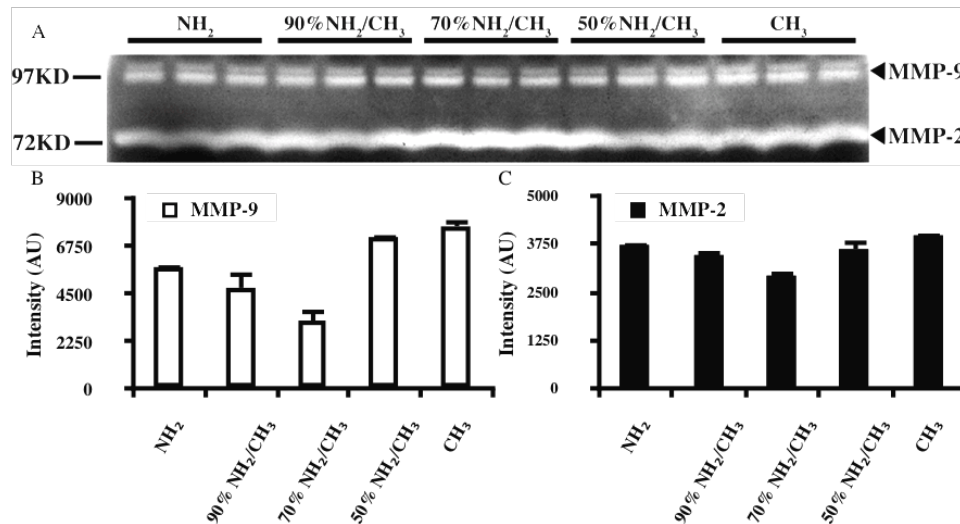


Figure 13 - (A) Zymography of the conditioned medium of HUVEC cultured for 24 h on Col IV coated mixed SAMs. Upper line represents MMP-9 and the lower MMP-2, presenting 97 and 72 KDa, respectively. (B) Shows the densitometry values for MMP-9 and (C) for MMP-2 activity.

Remodeling of FITC-Col IV on mixed SAMs

Morphological data obtained with FITC-Col IV coated samples are shown on Figure 14. They confirm the general trend that rearranged Col IV co-localize with secreted FN fibrils. However, the optimum for Col IV remodeling at 70%NH₂/CH₃ is missing. Instead, a much higher secretion of FN matrix was observed on 70%NH₂/CH₃, 90%NH₂/CH₃ and pure NH₂ SAMs that augment after 24 h (P-R). Conversely, appearance of dark zones of FITC-Col IV removal on both 50%NH₂/CH₃ (D, J, N) and pure CH₃ (E, J, O) surfaces was a typical observation after 5 h and better pronounced after 24 h of incubation.

FITC-Col IV release from mixed SAMs

Studies on FITC-Col IV release in the supernatant revealed significantly higher values on CH₃, followed by 50%NH₂/CH₃ after 5h (Figure 15A), which is in agreement with the morphological observations where dark zones of Col IV removal were mainly visible.

At 24th hour (Figure 15B) however, these differences were abolished, presumably because of the spontaneous desorption of protein in the medium. Nevertheless, the highest and significant FITC-Col IV release ($p < 0.05$) was found on CH₃ surface.

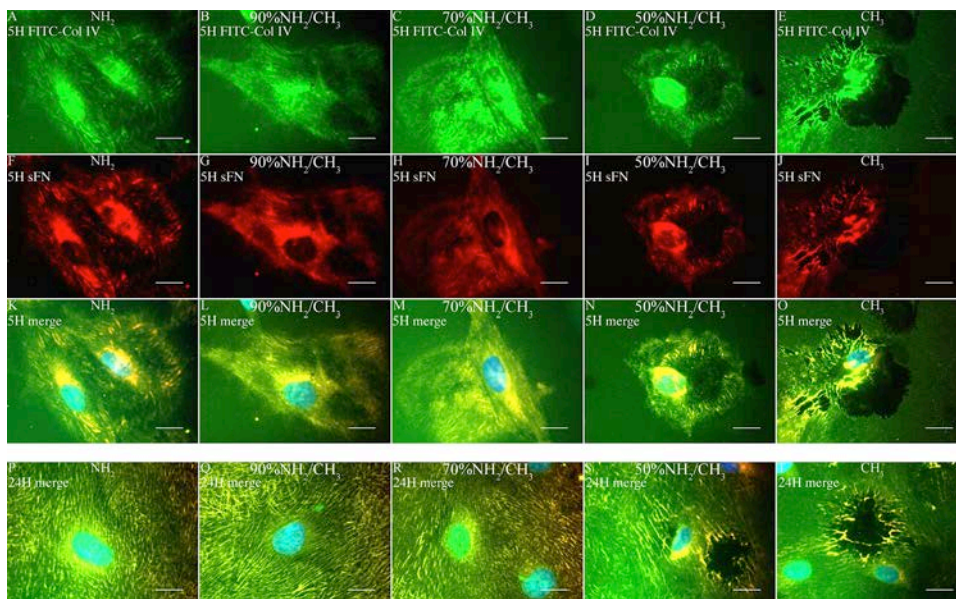


Figure 14 - HUVEC remodeling of adsorbed FITC-Col IV on different model surfaces of mixed SAMs after 5 (A-E) and 24 (P-T) hours. Corresponding FN secretion viewed at 5 (F-J) and 24 h (P-T, only merges). Bar = 20 μm .

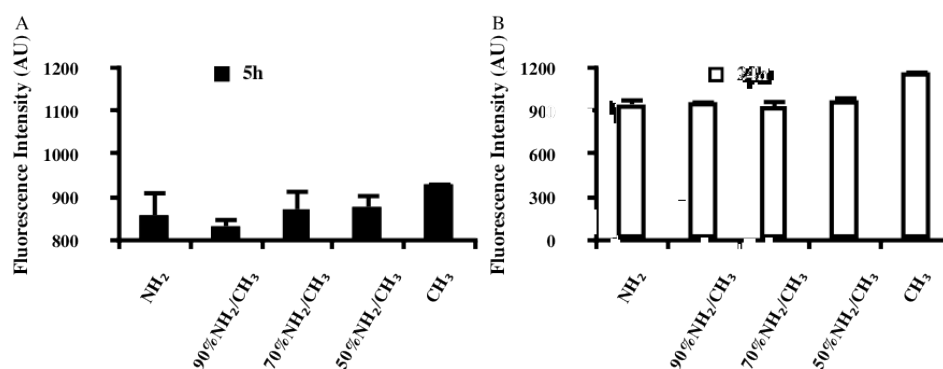


Figure 15 - FITC-Col IV in the supernatants of HUVEC cultured for 5 (A) and 24 (B) hours on FITC-Col IV coated mixed SAMs. The released fluorescent signal is supposed to correlate with the proteolytic activity of cells.

Chapter 4 -Discussion

It has been a long time since ligand-receptor theory was formulated which left us two important messages: first, the cells never interact with foreign materials directly, but with the adsorbed protein layer; and second, once cells recognize the protein, a cascade of biological events take place, which mimic their natural interaction with the ECM (Grinnell and Feld 1982; Griffith and Naughton 2002; Ratner and Bryant 2004; Lutolf and Hubbell 2005; Place et al. 2009). Cells interact with the surrounding microenvironment via transmembrane receptors – integrins - that bind to specific motifs on the matrix proteins, mostly fibronectin and vitronectin, which are uniformly available in the biological fluids (Griffith and Naughton 2002; Hynes 2002; Daley et al. 2008). *In vivo* however they recognize much more matrix proteins of collagenous and non-collagenous origin. Upon binding to ECM proteins integrins clusterize and transmit distinct stimuli to the cell interior, and as biological consequence, the cells spread and polarize (Gumbiner 1996; Hynes 2002; Yamada et al. 2003). But they do this only *in vitro*, while *in vivo* these interactions are much more complex and dynamic (Cukierman et al. 2001; Griffith and Swartz 2006; Altankov et al. 2010). Therefore the main strategy to design a scaffold or a biomaterial with tissue engineering application includes the use of such synthetic or natural materials that are able to interact with the biological environment to a level that allows the cells to participate actively in the pathways of tissue morphogenesis (Griffith and Naughton 2002; Lutolf and Hubbell 2005; Atala 2009; Place et al. 2009).

The natural materials provide appropriate biochemical signaling, but generally do not allow modification of the scaffold properties such as mechanics, nanostructure, and degradation rate, apart from the fact that being animal-derived they may elicit an immune response (Lutolf and Hubbell 2005; Place et al. 2009; Shekaran and Garcia 2011). These limitations have led to extensive research that focuses on engineering specific properties into synthetic materials that are able to mimic the natural ECM while avoiding the problems that arise with the use of materials harvested from animal sources (Mooney and Langer 2000; Lutolf and Hubbell 2005; Place et al. 2009; Sengupta and Heilshorn 2010; Dvir et al. 2011).

One ECM characteristic that inspired several researchers is its fibrillar architecture (Lutolf and Hubbell 2005). In this sense polymer processing technologies such as electrospinning and others like supramolecular protein self-assembly (Zhang 2003) allowed the formation of fibrillar matrices that lay down to nanometric scale (Oberpenning et al. 1999; Zhang 2003; Lutolf and Hubbell 2005; Place et al. 2009). Other key ECM property is its hydrogel character, so it is not surprising that synthetic hydrogels had found increasingly important roles in biology and medicine. Furthermore, within such matrices is possible to incorporate a number of biological

characteristics, including cell adhesion ligands, proteolytic sequences and additives providing relevant elasticity (Langer and Tirrell 2004; Lutolf and Hubbell 2005; Huebsch and Mooney 2009; Place et al. 2009; Phelps et al. 2010; Mager et al. 2011). ECM modulates tissue dynamics through its ability to locally bind, store, and release soluble bioactive molecules such as growth factors, and to direct them to the right place at the right time (Vogel and Baneyx 2003; Ratner and Bryant 2004; Lutolf and Hubbell 2005). It concerns the spatiotemporal organization of ECM. The main strategies of designing such synthetic matrices for temporal growth factors presentation focus on the control of their local concentration and on the sequential delivery of proteolytically activated bioactive molecules (Lutolf and Hubbell 2005; Place et al. 2009; Phelps et al. 2010).

All these applications raise an important issue, connected with the dimensionality of cell biomaterials interaction. Nowadays, tissue engineering strives to mimic the 3D organization of the ECM with scaffolds that are able to support tissue specific cellular responses, including the local regeneration and/or repair (Griffith and Naughton 2002; Hubbell 2003; Griffith and Swartz 2006; Atala 2009). However, various currently used medical devices such as stents, prosthesis, and metal implants cannot avoid the 2D contact with tissues. Upon implantation they hamper the local organization of ECM and alter the biocompatibility of implant. The basement membrane (BM) - a highly specialized type of ECM common to many types of tissues (Kalluri 2003; Yurchenco 2011) - also provides conditions for 2D cellular interaction. Apart from the fact that it determines the spatiotemporal organization of the organ specific (epithelial, endothelial) cells, BM is involved in a remarkable number of physiological and pathological processes, including cell adhesion, migration, embryonic development, wound healing and cancer progression (Paulsson 1992; Kalluri 2003; Van Aghtmael and Bruckner-Tuderman 2010; Yurchenco 2011). In addition, it serves as reservoir for growth factors and enzymes and is responsible for the filtration and molecular sieving of physiological fluids (Paulsson 1992; Kalluri 2003; LeBleu et al. 2007; Van Aghtmael and Bruckner-Tuderman 2010; Yurchenco 2011). As stated above, the BM is a fine (approximately 100-300 nm thick) structure that may be considered as 2D, at least to the range of a cell size. In this respect the *in vitro* surface behavior of Col IV - the major structural component of the BM - resemble at least to some extent the fate of this protein *in vivo*. Moreover, the cells often meet such 2D environments when are in contact with implanted bioengineering devices. An example is the engineered vascular tissue, which is the main target of our interest. To date, blood-contacting devices including small diameter vascular grafts, stents, hard valves, etc., suffer from a common defect - the lack of sufficient endothelial cells ingrowth. As stated in two of the presented papers above, we anticipate that it is presumably caused by the absence of specialized BM resulting in an accelerated device failure (de Mel et al. 2008; Baber et al. 2010; Hibino et al. 2010). Therefore, the development of materials and surfaces that support or reproduce closely the structure of Col IV in the BM is a challenging task.

In general, when a foreign material is implanted the rapid adsorption of proteins from the surrounding medium precedes the subsequent cellular interaction. Therefore, a variety of surface properties, including wettability, chemistry, topography and charge affect the cellular interaction, as have been shown they alter not only protein adsorption, but also its conformation (Wilson et al. 2005; Barbosa et al. 2006; Arima and Iwata 2007; Thevenot et al. 2008). Apart from the soluble proteins however, relatively little is known about the behavior of the other matrix proteins that are less soluble in biological fluids. Such are the collagen, laminins, elastin and many others that exist within tissues as natural polymers (Hubbell 2003; Daley et al. 2008). At longer contact with tissues or under some non-physiological conditions (acid environment) these proteins may also associate with the biomaterial surfaces, and in that way to influence significantly the cellular interaction. In this context we are particularly interested on the surface behavior of Col IV as this unique multifunctional matrix protein plays a vital role in the organization of vascular BM (Kalluri 2003; Kruegel and Miosge 2010). We anticipate that understanding how Col IV assembles at biomaterials interface might provide critical insights if one wants to mimic the natural organization of the vessel wall.

Nowadays technologies enabled investigations on the fate of surface associated proteins at single molecular level, providing a possibility to learn more about their behavior in the nanometric scale. In this sense, the AFM and other nano-indentation techniques are exceptional tools to explore the conformation, distribution and organization of ECM proteins at biomaterials interface. However, since roughness for most of the biomaterials is well above the height of proteins (5-10 nm) (Fingerman and Fingerman 1975) direct observations of ECM components on commonly used biomaterials are sparsely reported. Using the AFM in tapping mode we could overcome some of these limitations (Hernández et al. 2007) and this led us to novel and even a bit surprising observations. We found that Col IV does not adsorb stochastically, but rather tends to self-assemble in distinct patterns depending on the surface properties of the material. In this respect our studies were among the first highlighting the importance of the material surface properties for the fate of various ECM components at biointerfaces.

Selection of model materials

It is well documented that the surface properties of biomaterials have a great impact on protein adsorption and subsequent cellular interaction, thus determining the biocompatibility of a biomaterial (Grinnell and Feld 1982; Altankov and Groth 1997; Keselowsky et al. 2003; Keselowsky et al. 2004; Keselowsky et al. 2005). Among others, the wettability of a material has long been recognized as very important parameter affecting significantly both protein adsorption and cellular interaction. Therefore, not accidentally we choose hydrophilic glass, as a well-established model surface from many previous investigations in the group. In general, hydrophilic

glass support cellular interaction although adsorbs less proteins, a fact usually attributed to the appropriate conformation of adsorbed adhesive components (Grinnell and Feld 1982; Altankov and Groth 1997; Keselowsky et al. 2003). However this is not always straightforward since materials with very high wettability, which bind much water like hydrogels, do not support protein adsorption and cell adhesion (Tamada and Ikada 1994; Gugutkov et al. 2010). Conversely, hydrophobic surfaces are normally associated with high protein adsorption, but in fact, it do not corroborates with an improved cellular response. Such surface is the octadecylsilane (ODS) coated substrate (SAM) that is also extensively studied before (Groth and Altankov 1996; Altankov et al. 1997; Krasteva et al. 2001; Ishizaki et al. 2010).

Several studies reported also for the difference in the dynamic behavior of matrix proteins at biomaterials interface, resulting in varying ability of cells to reorganize them on surfaces varying in wettability. It includes several serum proteins, such as FN (Grinnell and Feld 1982; Altankov and Groth 1997), FBG (Hernández et al. 2009) and VN (Toromanov et al. 2010), but also of other less soluble ones, like collagens I (Storesund and Helle 1975) and laminin (Hernández et al. 2007). These studies highlight the role of protein-substratum interaction in supporting (as do hydrophilic surfaces) or abrogating (hydrophobic ones) the ability of cells to organize their own fibril-like matrix on the biomaterials interface – a process that presumably affects their biocompatibility (Altankov and Groth 1994; Altankov et al. 1996; Altankov et al. 2010). Nevertheless, in some circumstances hydrophobic surfaces may also support cellular interaction, due to the spontaneous protein network assembly (Gurdak et al. 2006; Hernández et al. 2007; Gugutkov et al. 2009; Gugutkov et al. 2010), which do not corroborates with cell reorganization activity.

When we started our investigations, the surface behavior of Col IV was only sparsely studied and poorly understood. Initially, we were interested on the adsorption profile and the molecular organization of the adsorbed Col IV layer, as well as, how it affects the biological performance on model hydrophilic and hydrophobic surfaces known to strongly influence the activity of other proteins. Indeed, as we showed in Section 1 (Coelho et al. 2010) we found a clear relationship between the organization of the protein layer and the subsequent cellular interaction. However, except on wettability the above model materials (glass and ODS) differed also in their chemistry, a fact that raised obstacles in the interpretation of results. Therefore, in the subsequent studies we introduced a new family of polymer substrates, where the fraction of –OH groups varies as an independent parameter without changing the chemistry. This family of polymers (developed by Prof. Salmeron-Sanchez group) is based on the copolymerization of ethyl acrylate (EA) and polyethyl acrylate (PEA) in different ratios that gives rise to a random copolymer with tailor concentration of OH groups. This well defined family of polymer substrata was recently used to

follow the adsorption pattern of other ECM proteins, including fibronectin (Gugutkov et al. 2009; Gugutkov et al. 2010), vitronectin (Toromanov et al. 2010) and fibrinogen (Hernández et al. 2009), showing that it also affect their biologic activity. With our studies we wanted widen these investigations following the behavior of Col IV and LAM aiming to understand the intermolecular associations when both assembly at differently wetttable biomaterials.

To further follow the effect of substratum chemistry and charge we introduced two new model surfaces (SAMs) expressing NH₂ and COOH functions, which are abundantly expressed in all biological systems, moreover possess opposite charge (NH₂ is positive and COOH is negative). During these studies however, we realized a new fact, that NH₂ also support FN matrix synthesis, while CH₃ strongly suppress it. As Col IV remodeling is dependent on FN we introduced a new system - mixed SAMs - expressing varying partial ratios of CH₃ and NH₂ functions to explore the novel possibility of obtaining control on Col IV behavior via modifying the FN assembly.

Collagen IV adsorption and assembly on model surfaces

Our data show that the adsorption of Col IV is strongly dependent on the material surface properties. Using FITC-Col IV we found that the hydrophobic CH₃ represented significant higher adsorption, approximately doubled in comparison to hydrophilic OH and COOH surfaces. In respect to the literature in this field, one can consider that this result is not surprising since other proteins also represent stronger adsorption on hydrophobic substrata, presumably due to the polar interactions (Grinnell and Feld 1982), although this do not correlate with their biological activity. Interestingly, the slightly hydrophilic NH₂ surface (WCA° ≈ 50) showed the highest amount of Col IV adsorption, more than hydrophobic CH₃, resulting in the following sequence from higher to lower adsorption: NH₂>CH₃>COOH>OH. It is noteworthy the similar order was found when FN was adsorbed to SAMs of alkanethiols on gold expressing the same chemistry and close wettability (Keselowsky et al. 2003).

One can support that the different adsorption pattern of Col IV on NH₂ and COOH results from the different surface charge. However, the isoelectric point (pI) of collagen is reported to be at pH 9.3 (Li et al. 2009), that is to say, it should be positively charged under neutral (PBS at pH 7.4) or acidic conditions (sodium acetate pH 4.5). Consequently, appearance of repulsive forces against the positively charged NH₂ might be expected, which is against the observed higher Col IV adsorption on this substratum. Conversely on the negatively charged COOH electrostatic attraction should be expected (Lee et al. 2006; Thevenot et al. 2008; Mrksich 2009), which obviously is not the case, as significantly less protein is observed. An alternative explanation for these controversial observations might be the effect of the ionic strength e.g. the concentration of dissolved ions in the solution containing the protein. It is well documented that the higher the

ionic strength the shorter are electrostatic interactions between charged entities. As consequence the adsorption to same charged substrates is enhanced whereas the adsorption of charged proteins to oppositely charged substrata is hampered (Rabe et al. 2011). Another interesting observation was those with mixed NH_2/CH_3 SAMs model where two picks of adsorption were found: the first pick is on the most hydrophobic SAM (100% CH_3) and the second, on the positively charged SAMs (100% NH_2). This suggests that different mechanisms of adsorption are involved and the mixture of chemistries may disturb the “normal” trend of protein deposition (the negative correlation with surface wettability is endorsed) leading to unpredicted result.

Our AFM studies led to another interesting observation. They revealed that Col IV do not adsorbs stochastically, but tend to make distinct patterns, resembling different aspects of network-like structure or aggregates. We further found that Col IV adsorption pattern is strongly dependent on material surface properties suggesting different lateral interactions between the protein molecules. It is interesting to note that the surface assembly of Col IV on strongly hydrophilic (OH) and moderately hydrophobic NH_2 surfaces presented very similar and close to single molecular arrangement, particularly at lower concentrations where structures resembling dimers and tetramers may be distinguished. As the coating concentration increases the Col IV molecules start to assemble in network containing nearly molecular size features on OH, while forming much larger linear structures on NH_2 . Conversely, on CH_3 and COOH the sponge-like morphology with appearance of rather globular protein aggregates correlates with the altered biological activity. At higher concentrations these structures remains almost unaltered on COOH while show prominent network consisting of molecular aggregates on CH_3 with not clear biological consequence.

There are no observations endorsing the substratum dependent Col IV assembly in the literature, though the supramolecular structure of Col IV was extensively studies during the last decades (Yurchenco and Furthmayr 1984; Timpl et al. 1985; Hudson et al. 1993; Khoshnoodi et al. 2008). It is well documented that Col IV molecules are heterotrimers of about 390 nm long composed of a combination of three alpha chains from the six genetically distinct forms that exist (Yurchenco and Furthmayr 1984; Kühn 1995; Khoshnoodi et al. 2008). Like many other matrix proteins Col IV is secreted as a monomeric pro-form. The assembly of Col IV is initiated by the formation of protomers where three alpha chains associate through their non-collagenous domains before folding into triple helix. The lateral association of the triple helix, the covalent binding of 7S domains and the association of alpha chains at the NC1 domains are essential for the formation of the protomeric 2D network that serves as scaffold for the BM (Yurchenco 1990; Timpl and Brown 1996; Kalluri 2003; Khoshnoodi et al. 2008). Col IV is not soluble in biological fluids (Gelse et al. 2003), but *in vitro* it can be adsorbed to the materials from acid conditions, where the triple helical molecules are unfolded and the lateral interactions minimized (Timpl et al. 1985).

Several studies have shown that acid-soluble collagens are in a reversible configuration (Kühn 1995) and once switched to a physiological environment (pH 7.4, 37 °C and distinct ionic content) they polymerizes in a highly functional gel-like matrix (Sung et al. 2009).

An important observation of our studies was that upon adsorption soluble Col IV tends to assemble in a rather 2D network – a configuration similar to those in the BM (Kühn 1995). Thus, we provide new insight to the diverse mechanisms for Col IV assembly on substrata varying in wettability and chemistry showing different assembly of Col IV depending on material surface properties that in turn influence its biological performance. AFM studies revealed a spontaneous *in vitro* assembly of Col IV molecules in di- and tetramers upon adsorption to mica (Fingerman and Fingerman 1975), which suggest similar assembly of Col IV on biomaterials interfaces, at least it is the case on the OH and NH₂ surfaces, where both di- and tetramers are visible at low coating concentrations.

The surface behavior of Col IV on substrates with tailor density of –OH groups further confirmed our general observations, but also showed some unexpected effects. We observed: (i) a single molecule arrangement on intermediate hydrophobic substrata, and (ii) a tendency for molecular assembly in network, which increase with hydrophobicity. It leads to the formation of an augmented network at $X_{OH} = 0$, presumably consisting of molecular aggregates, while elongated fibril-like features were observed on the most hydrophilic $X_{OH} = 1$. These two trends suggest the possible involvement of both polar and non-polar adsorption mechanisms, which is out of the scope of this study, but presumably may explain the two optimums in the cellular interaction, one hydrophilic ($X_{OH} = 1$) and one hydrophobic at $X_{OH} = 0.3$ (see below).

Another interesting observation from this study was that LAM also tends to make networks in the same as Col IV conditions. A clear tendency for LAM assembly in networks at almost all range of surfaces was found. However, these networks vary significantly in their thickness and organization: they were prominent on $X_{OH} = 0$ and $X_{OH} = 0.5$ surfaces and rather subtle on $X_{OH} = 1$ and $X_{OH} = 0.3$. It seems that increasing the fraction of –OH groups tend to diminish the network formation presumably reducing the lateral interactions. However, on most hydrophilic $X_{OH} = 1$ surface, LAM shows again surprisingly high protein deposition as extrapolated from the calculations for protein volume (Coelho et al. 2011). Interestingly, the same non-monotonic trend of adsorption was previously found on this family of surfaces with fibronectin (Gugutkov et al. 2009). Note, on the same surface Hernandez *et al.* have previously found globular-like LAM deposition after adsorption from solutions of much lower protein concentration (Hernández et al. 2007), which stress on the importance of competition between protein-protein versus protein-material interactions to determine the conformation of LAM at the material interface.

Nevertheless, independently of the complex arrangements of LAM some cross-shaped structures that resemble single molecules (Chen et al. 1998) can be sparsely observed on $X_{OH} = 0.3$ and $X_{OH} = 1$ surfaces, suggesting the deposition of protein in a near natural configuration. Note, on this same surfaces the optimal cellular interaction, with also two maximums as for Col IV, is observed. The resemblances in the behavior of Col IV and LAM in respect to their assembly and cellular interaction suggest that similar forces might guide their organization in the BM, were they form an overlapping polymeric network (Timpl and Brown 1996; Kalluri 2003; Khoshnoodi et al. 2008; Van Agtmael and Bruckner-Tuderman 2010). This provoked our interest in a joint Col IV-LAM deposition, which could provide insights on their natural interplay in the BM. Unfortunately these two proteins possess different solubility (Col IV dissolves in acid, whereas LAM in neutral conditions), which exclude their assembly together. Thus, the only simple solution was to adsorb them consequently, first Col IV and then LAM. As a result, a tendency for joint network formation was found on most surfaces except for the most hydrophilic $X_{OH}=1$, where a rather globular deposition (resembling the behavior of LAM on this substratum) was obtained. It is interesting to mention that the consequent pre-adsorption favored the LAM adsorption pattern especially on intermediate substrates. As Col IV adsorbs first it probably serves as a template for subsequent LAM assembly, but the dominating sponge-like structure presumably representing a joint Col-LAM network cannot be seen on single protein series. It is noteworthy that this complex network structure looks similar to those seen on the topographic AFM images of the natural BM underlying the corneal epithelium (Abrams et al. 2000).

Cellular interaction

To understand the impact of the different Col IV arrangements on the cellular interaction we used primary endothelial cells (HUVEC). To choose these cells we considered that Col IV is the main structural component of the vascular BM (Sephel et al. 1996; Kalluri 2003; Rivron et al. 2008) where endothelial cells reside. On the other hand, when endothelial cells attach to flat and smooth surfaces they encounter a similar geometry to those when interact with blood contacting devices, where endothelization is highly desirable (Sephel et al. 1996; de Mel et al. 2008; Van Agtmael and Bruckner-Tuderman 2010). In general, the endothelization of implants is a main concern in tissue engineering. However, while endothelial cells procurement technologies for seeding implants have been significantly improved, adhering cells often dedifferentiate and act in a counterproductive manner, accelerating device failure (Griffith and Naughton 2002; Sipe 2002; Daley et al. 2008; de Mel et al. 2008). As stated in two of the papers above, we anticipate that a reason for this failure might be the missing environmental signals from the natural BM and this was the second issue we wanted to address in this work.

In general, we found that HUVEC interact better with the single molecular arrangements of Col IV and conversely, show altered attachment to protein aggregated morphology and its derivatives. The improved cell adhesion, focal contacts formation and actin cytoskeleton development correlates with the pronounced integrin clustering and p-FAK recruitment, confirming a favored interaction of HUVEC with NH₂ and OH surfaces, and also the proper transmission of signals to the cell interior. Conversely, the coarse network of Col IV aggregates on hydrophobic CH₃ and negatively charged COOH surfaces correlates with the altered interaction of HUVEC, resulting in down regulation of all cell adhesive machinery. Presumably, the aggregated Col IV molecules are less favorable for cells because of screening of their recognition sequences such as RGD and GDFGER motifs (Vandenberg et al. 1991; Kern et al. 1993). The main cellular receptor for collagens is $\alpha_2\beta_1$ integrin (Kern et al. 1993; Käpylä et al. 2000; Popova et al. 2007), but $\alpha_1\beta_1$ is considered as more specific for Col IV (Vandenberg et al. 1991; Kern et al. 1993; Käpylä et al. 2000). That is to say, the aggregated pattern of Col IV observed by AFM must be linked to the reduced availability of the binding site for both α_1 and α_2 integrins located approximately 100 nm away from the amino-terminus within its CB3 fragment (Timpl et al. 1985; Hudson et al. 1993; Khoshnoodi et al. 2008). But even in the case that adsorption of Col IV on CH₃ and COOH surfaces is in conformation that allowed adequate CB3 exposition, its density would not be enough since most of the domains must be hidden due to lateral interaction between proteins that are favored instead of protein surface interaction (Coelho et al. 2010; Coelho et al. 2011). Conversely, the single molecular arrangement of Col IV induced different integrin clustering since α_2 integrins formed clear focal adhesions, while α_1 integrins appeared in a rather linear pattern, resembling fibrillar adhesions (Cukierman et al. 2001). It corroborates well also with the confirmed for all materials co-localization of substratum arranged Col IV with FN fibrils (Maneva-Radicheva et al. 2008).

As stated above, the interaction of HUVEC with Col IV and LAM on substrates with controlled density of –OH groups showed surprisingly two optima, a hydrophilic one ($X_{OH} = 1$) and a hydrophobic ($X_{OH} = 0.3$), revealed from changes in the adhering cells morphology, the quantities for cell adhesion and spreading and the development of focal adhesion complexes. However, when both proteins were applied consequently leading to the distinct complex morphology of the adsorbed protein layer, a “hydrophobic shift” in cellular interaction was observed, confirmed also at higher coating concentrations (50 $\mu\text{g/ml}$) in the supplementary results. These observations suggest a synergistic behavior of these two BM components, resulting in a similar HUVEC response even when both proteins are adsorbed separately. One possible explanation for this hydrophobic shift is that the strength of the LAM-Col IV binding overrides the protein-substratum interaction resulting in a favored cell-binding configuration of both molecules.

Remodeling of Col IV

ECM is a highly dynamic structure since cells continuously build and reshape it (Daley et al. 2008). ECM remodeling is an important process that is critical during development, tissue repair, fibrosis, and tumor progression (Ala-aho and Kähäri 2005; Larsen et al. 2006; Daley et al. 2008; Wynn 2008). It comprises synthesis, arrangement and degradation and the balance between these processes determine the loss or net accumulation of ECM (Shi et al. 2010). ECM undergoes distinct remodeling also at cell-biomaterials interface (Place et al. 2009; Irvine et al. 2011; Llopis-Hernández et al. 2011). A large and growing body of evidences show that the cells need to accept distinct mechanical stimuli from the surrounding structures to strengthen their connections with the cytoskeleton (Janmey and McCulloch 2007), thus, responding to the mechanical properties of the environment (Janmey and McCulloch 2007; Geiger et al. 2009). As the stiffness of the surrounding matrix *in vivo* is in the same order of magnitude as cells, they tend to reorganize this matrix in a way optimal for their functioning (Grinnell 1986; Hubbell 2003). However, these relations may be hampered upon implantation of a material, particularly if it represents rough or too hydrophobic surface. Examples are the over-accumulation of ECM forming fibrous capsule around the most implants (Stamenkovic 2003; Thevenot et al. 2008) or the failure of an implant because of the gap-formation caused by missing ECM deposition from the surrounding tissues (Daley et al. 2008). The formation of soft connective tissue surrounding the implant, named peri-implant, is critical for its successful integration (Moon et al. 1999). It forms for example the biological seal of dental implants at the gingival site (Moon et al. 1999). Collagens are the major component of this peri-implant tissue and fibroblasts play a crucial role for its formation and remodeling (Moon et al. 1999; Abrahamsson et al. 2002). Therefore, in our general studies we explored the fibroblast cell model although in later investigations we show that endothelial cells also provoke Col IV remodeling at biomaterials interface.

On the other hand, after initial ECM deposition (consisting mainly of collagen), fibroblasts secrete MMPs and other enzymes that cleave the ECM proteins and if this process of resolution fails it can trigger fibrotic cell response (Stamenkovic 2003; Daley et al. 2008). We anticipate that the good cellular interaction with adsorbed proteins is not sufficient to determine the success of an implant. Cells should be allowed to remodel the surface associated proteins (Tzoneva et al. 2002; Daley et al. 2008; Altankov et al. 2010; Llopis-Hernández et al. 2011), which requires that proteins are loosely bound to the surface, so that that cell can easily organize them in a matrix-like structure (Altankov and Groth 1994; Altankov et al. 2010). In the time we start our studies there were limited studies on the substratum behavior of Col IV.

As stated before, in fact the balance between matrix organization and its degradation is of critical importance since over/or less deposition of ECM strongly affects the implant fate (Daley, Peters

et al. 2008). Therefore, these processes need to be studied simultaneously and explored in a way that help to understand and obtain a control on their ballance. As the matrix remodelling often progress in an unpredictable way, any *in vitro* study providing information about it outcome is strongly desirable (Sipe 2002; Hubbell 2003; Daley et al. 2008). In fact, this was a rationale that provoked our studies with model material surfaces; we wanted to learn if we can obtain a control on Col IV remodeling with “tools” from the materials site.

The vascular BM is the place where endothelial cells reside but this specialized structure contact also the surrounding connective tissues where fibroblasts are the principal cells able to synthesize and arrange BM constituents (Kalluri and Zeisberg 2006). They are also an important source of ECM-degrading proteases such as MMPs, which highlights their crucial role in maintaining the ECM homeostasis (Simian et al. 2001; Kalluri and Zeisberg 2006) and the matrix turnover during tissue repair (Tomasek et al. 2002). Thus fibroblasts are the main mediators of scar formation and tissue fibrosis (Hu et al. 2001; Kalluri and Zeisberg 2006; Wynn 2008) and this was the second reason to explore them as model cell system.

Recent investigation showed that fibroblasts are able to remodel surface associated Col IV and that the pattern of this remodeling is altered in contact with cancer cells (Maneva-Radicheva et al. 2008). These studies however, did not clarify the physiological relevance of this process. Thus, with an aim to maximally reproduce the functional architecture of the vascular BM we widen our knowledge in the field following the fibroblasts Col IV remodeling at engineered substratum properties.

Our *in vitro* studies revealed that fibroblasts not only interact with adsorbed Col IV, but also tend to remodel it in a morphologically distinct pattern. Two types of cell activities were foreseen: first, a trend for linear, fibril-like organization, and second, a tendency for degradation of substratum associated protein via enzymatic cleavage. Thus, in agreement with previous investigations (Maneva-Radicheva et al. 2008) we show that fibroblasts are able to mechanically translocate adsorbed Col IV in fibril-like pattern that frequently co-localizes with FN matrix fibrils. An important question was whether this spatial reorganization of Col IV by the cells is physiologically relevant, as fibroblasts in 2D cultures often behave differently from their normal 3D environment (Beningo et al. 2004). Col IV is not a fibrillar protein and assembles in a sheet-like structure in the BMs, also in the vascular BM where it provide the major structural and mechanical support for endothelial cells (Kühn 1995; Kalluri 2003; Khoshnoodi et al. 2008; Yurchenco 2011). From this angle, the observed linear rearrangement of adsorbed Col IV by both fibroblasts and endothelial cells does not look physiologically relevant, but it obviously represents a cell-dependent process. It is noteworthy that similar linear organization of Col IV was observed

during early BM assembly in an *in vitro* 3D skin culture model (Fleischmajer et al. 1998), representing also a cell driven process. In conjunction with the previous investigations on Col IV remodeling by cancer cells (Maneva-Radicheva et al. 2008) in our study we demonstrate the partial involvement of α_1 and α_2 integrins in the process. On the other hand, our results suggest that the main driving force for the substratum Col IV reorganization is the association with FN fibrils. Such a mechanism for co-assembly is not new in the literature and is demonstrated for example during the arrangement of fibrillar proteins, like collagens type I and III (Velling et al. 2002; Kadler et al. 2008) and also for adsorbed fibrinogen by endothelial cells (Tzoneva et al. 2002), but we are the first showing that it works for non-fibrillar Col IV.

FN is synthesized by many adherent cells, including stromal fibroblasts but also endothelial cells, which assemble it into a fibrillar network (Wierzbicka-Patynowski and Schwarzbauer 2003). During its assembly, FN undergoes conformational changes that expose FN-binding sites and promote intermolecular interactions important for fibril formation (Mao and Schwarzbauer 2005). It was shown that FN binding site in fibrillar Col I may regulate FN fibril formation by fibroblasts (Dzamba et al. 1993). Sottile and Hocking also showed that FN polymerization into the ECM is required for the collagen type I deposition, furthermore Chernousov *et al.* reported that Shawann cells use directly a Col IV-dependent mechanism for FN fibril assembly. Actually the association of these two ECM proteins is not surprising, as FN molecule has at least two binding sites for collagens (Mao and Schwarzbauer 2005; Larsen et al. 2006) and corresponding binding sites for FN have been identified on the collagen molecule (Sottile and Hocking 2002; Velling et al. 2002; Zoppi et al. 2004). Consistent with this are our results showing that FITC-FN and Col IV frequently co-localize each other either when are pre-adsorbed and reorganized by fibroblasts, or when are exogenously added in the medium. Hence, in contrast to the earlier belief that collagen polymerization occurs mainly via self-assembly (Kalluri 2003) our data showed that a preformed FN matrix is essential for collagen network formation and presumably the specific integrin binding of adsorbed collagen supports this process. On the other hand, it looks that Col IV reorganization does not require native configuration of the protein as it runs well and is even supported when partly denatured (monomeric) Col IV have been used for coating the substrates. Indeed, our double staining experiments clearly show a high degree of co-localization between FN and Col IV in various model conditions. The co-localization however is not obligatory since there are zones of absent overlapping, suggesting also an independent translocation of the protein onto the cell surface presumably dependent on α_1 and α_2 integrins.

Another very important observation from this work was that the pattern of Col IV remodeling mediated by both fibroblasts and endothelial cells is strongly dependent on the material surface properties. Following the trend of the initial cellular interaction they were able to mechanically

translocate Col IV on hydrophilic and NH₂ surfaces where it represents rather single molecular arrangement. However, on hydrophobic surface, the dark zones (from where the adsorbed protein is removed) are often visible around cell periphery suggesting direct enzymatic cleavage of the protein. Conversely, on NH₂ substrata, although the highest amount of protein adsorbs, almost no zones of protein removal were observed. Interestingly, although on COOH surfaces the Col IV is aggregated fibroblasts were able to reorganize it in a similar pattern as on hydrophilic surfaces, which might be explained with the loose interaction of the protein with substratum.

Degradation of adsorbed Col IV

The prominent network of molecular aggregates observed on hydrophobic surfaces, obviously block the ability of cells to rearrange Col IV, but it is also accompanied with appearance of dark zones around cells suggesting local protein removal. This raises the possibility for an enzymatic cleavage of the adsorbed protein by the cell. To check this opportunity we developed a new fluorimetric approach measuring the released fluorescence from adsorbed FITC-Col IV. Indeed, when the released fluorescence signal was measured, a significantly higher amount of cleaved protein was observed on CH₃, followed by COOH and OH suggesting increase in the degradation activity of cells. The lowest proteolysis was measured on NH₂ for both fibroblasts and endothelial cells.

The vascular BM undergoes continuous remodeling and endothelial cells are also involved and this process, particularly during angiogenesis (Kalluri 2003). It involves synthesis and degradation in response to growth factors and MMPs, also promote the proliferation and migration of vascular endothelial cells (Kalluri 2003; de Mel et al. 2008; Arnaoutova et al. 2009). During angiogenesis the proteolysis can induce specific substrate-cleavage of fragments with different biological activity that may regulate tissue architecture both directly and indirectly (Page-McCaw et al. 2007). MMPs secreted by vascular cells cleave ECM proteins that can change the cellular behavior because generate fragments, which have different biological activities from their precursors. An example is the exposure of cryptic sites on Col IV molecules that promote endothelial cell migration (Kalluri 2003). The degradation of ECM molecules can also result in the release of ECM-bound growth factors, including insulin growth factors and fibroblast growth factors (Egeblad and Werb, 2002; Page-McCaw *et al.*, 2007). How this relates to the fate of Col IV at biomaterials interface was not clear.

We found that HUVEC as fibroblasts are able to remodel surface associated Col IV similarly and the pattern of this remodeling is again strongly dependent on the material surface properties. On hydrophilic glass and NH₂ endothelial cells reorganize adsorbed Col IV in fibril like pattern depending on FN fibrillogenesis and this process is again abolish on hydrophobic CH₃, exchanged

by a prevalent pericellular proteolysis (appearance of dark zones without protein arrangement). Some novel observations come from using the mixed SAMs expressing different ratios of NH₂ versus CH₃ functions. These studies were performed recently and are still not arranged for publication, but they further support the observed tendency of triggering degradation activity from the aggregated forms of Col IV. In addition, this model system allowed us to identify new phenomena, namely the supported FN secretion on NH₂ surfaces. The mechanism of this process is still not clear (which actually delay the publication), but we speculate that it might be connected with the strongest substratum interaction of the protein layer and once the cells cannot remodel it on NH₂ they start to secrete FN in order to favor provisional matrix organization. Why the pericellular degradation activity is not triggered (as on CH₃) however, is not clear.

In order to further prove that the different adsorption/conformation of Col IV may induces HUVECs degradation activity we analyzed the expression of MMP2 and MMP9 - both essential in the remodeling of the BM during angiogenesis (Egeblad and Werb 2002; Monaco et al. 2006; Page-McCaw et al. 2007). Indeed, the zymography confirmed that the remodeling of surface associated Col IV involves both MMP2 and MMP9. A tendency of higher secretion of these MMPs on hydrophobic environment, followed by COOH and OH surfaces, was observed. The lowest activity was found on NH₂. The differences however were significant only for MMP-9 where both active and inactive forms were easily identified.

When released fluorescent signal from adsorbed FITC-Col IV was measured to quantify the HUVEC degradation activity on the different surfaces, we confirmed the same trend of higher FITC release on hydrophobic CH₃, followed by COOH, OH and NH₂ surfaces. This confirmed the higher tendency for degradation of Col IV when is in aggregated form, presumably because the strong protein-protein interactions hide the recognition sequences for cell integrins. We speculate that once Col IV cannot be recognized this triggers the cellular proteolytic machinery to remove it. It cannot be excluded also that via degrading of aggregated Col IV HUVEC may attempt to find new binding sites.

Collectively these results show that materials do not induce any specific effect on endothelial cells ability to remodel Col I but are rather dependent on the protein to substratum interaction that constrain the lateral intermolecular associations.

Neovascularization

The *in vitro* formation of capillary-like tubes by endothelial cells is a powerful method to screen the factors that promote or inhibit angiogenesis (Arnaoutova et al. 2009). Initially cells attach to a given matrix, then migrate toward each other, align and form tubes. These processes are accompanied by concomitant remodeling of surrounding matrix, but also by protein synthesis,

including proteases (Arnaoutova et al. 2009). Therefore, we decided to test our system for both tube formation and pericellular proteolysis by culturing the cells for 2 h on Col IV coated model surfaces and then adding basement membrane extract containing FITC-Col IV for the next 24 hours. Our results (still unpublished) showed that after 24 h of culture HUVEC changed their phenotype and start to form tube-like structures on all model materials. No visible de-quenching activity of FITC-Col IV was observed morphologically. It is important to notice however, that correlating with the initial cell adhesion the formation of capillary-like structures were more pronounced on OH surface followed by NH₂, while on CH₃ and COOH surfaces the process seemed to be delayed. It was partly confirmed quantitatively when FITC-Col IV was extracted from the samples showing significantly higher fluorescence on OH substratum presumably caused by the proteolytic de-quenching.

Collectively evaluated, this is the first systematic study on the behavior of Col IV at cell-biomaterial interface providing major insights on the role of material surface properties. We described for the first time phenomena of material-driven assembly of Col IV established in nano scale, which strongly alters the cellular interaction and functionality. Finally, we provide different surface modifications able to tailor the fate of Col IV, which outline their great potential for tissue engineering application.

Chapter 5 – Conclusion

- We have successfully developed and characterized model biomaterials surfaces varying in wettability, chemistry and charge, further complemented with two complex systems of mixed SAMs and PEA/PHEA co-polymer providing controlled variations with density of CH₃, NH₂ and OH functions.
- The adsorption kinetics of FITC-Col IV showed saturation at concentrations of about - 50 µg/mL - for all surfaces. Maximal adsorption was found on NH₂ decreasing monotonically in the order NH₂>CH₃>COOH>OH.
- AFM studies revealed that Col IV does not adsorb stochastically but tend to self-assembly in a specific substratum-dependent pattern, ranging from fine meshwork formed from single molecules on OH and NH₂ to the complex networks consisting of molecular aggregates on CH₃ and COOH surfaces.
- Single and complex LAM/Col IV networks were observed on substrates with tailored density of OH groups. A natural trend for single molecular arrangements on strongly hydrophilic and moderately hydrophobic surfaces shift to a tendency for aggregation at intermediate hydrophobic surfaces.
- Human umbilical vein endothelial cells (HUVEC) and fibroblasts were used to study the cellular response.
 - It was developed a system for morphological evaluation of cell-materials interaction based on the estimation of overall cell morphology and the focal adhesion complex formation (including reorganizations in actin cytoskeleton, p-FAK, α_1 and α_2 integrins).
 - It was developed an approach for quantitative estimation of cellular interaction, including cell adhesion, cell adhesion strength using flow chamber and cell spreading.
 - It was found that primary endothelial cells and fibroblasts interact better with the fine single molecular arrangements of Col IV on OH and NH₂ surfaces.
 - Cellular interaction with aggregated Col IV networks is suppressed on hydrophobic CH₃ and negatively charged COOH surfaces.
 - Cellular interaction with Col IV is nearly independent on the amount of adsorbed protein.

- Studies with tailored surface expression of -OH functions revealed two maximums in endothelial cells interaction with Col IV, LAM and complex Col IV/LAM networks – a hydrophilic and a hydrophobic ones.
 - Fibroblasts showed higher strength of interaction with Col IV on hydrophilic versus hydrophobic surface.
- Both endothelial cells and fibroblasts tend to remodel adsorbed Col IV in two ways: via mechanical reorganization and via enzymatic degradation.
- Cells reorganize adsorbed Col IV in fibril-like pattern along with FN matrix fibrils.
 - Col IV degradation activity of both endothelial cells and fibroblasts involves MMP-2 and MMP-9.
 - Substratum remodeling of Col IV is strongly dependent on the materials surface properties.
 - Cells reorganize Col IV better when it is arranged in single molecular features or meshwork characteristic for hydrophilic and positively charged NH₂ surfaces.
 - Aggregated forms of Col IV on hydrophobic CH₃ and negatively charged COOH surfaces provoke pericellular proteolysis. It is evident from the quantitative measurements of FITC-Col IV release and zymography.
- Hydrophilic surfaces support the development of capillary-like tubes by endothelial cells, which corroborates with the increased pericellular degradation activity revealed by FITC-Col IV release.

References

- Abecassis, J., R. Millon-Collard, et al. (1987). "Adhesion of human breast cancer cell line MCF-7 to human vascular endothelial cells in culture. Enhancement by activated platelets." Int J Cancer **40**(4): 525-531.
- Abrahamsson, I., N. U. Zitzmann, et al. (2002). "The mucosal attachment to titanium implants with different surface characteristics: an experimental study in dogs." Journal of Clinical Periodontology **29**(5): 448-455.
- Abrams, G. A., S. L. Goodman, et al. (2000). "Nanoscale topography of the basement membrane underlying the corneal epithelium of the rhesus macaque." Cell Tissue Res **299**(1): 39-46.
- Ala-aho, R. and V.-M. Kähäri (2005). "Collagenases in cancer." Biochimie **87**(3-4): 273-286.
- Alberts, B., A. Johnson, et al. (2002). Molecular Biology of the Cell. New York, Garland Science.
- Altankov, G. and T. Groth (1994). "Reorganization of substratum-bound fibronectin on hydrophilic and hydrophobic materials is related to biocompatibility." Journal of Materials Science: Materials in Medicine **5**(9-10): 732-737.
- Altankov, G., F. Grinnell, et al. (1996). "Studies on the biocompatibility of materials: fibroblast reorganization of substratum-bound fibronectin on surfaces varying in wettability." J Biomed Mater Res **30**(3): 385-391.
- Altankov, G. and T. Groth (1996). "Fibronectin matrix formation and the biocompatibility of materials." Journal of Materials Science: Materials in Medicine **7**(7): 425-429.
- Altankov, G. and T. Groth (1997). "Fibronectin matrix formation by human fibroblasts on surfaces varying in wettability." Journal of Biomaterials Science, Polymer Edition **8**: 299-310.
- Altankov, G., T. Groth, et al. (1997). "Morphological evidence for a different fibronectin receptor organization and function during fibroblast adhesion on hydrophilic and hydrophobic glass substrata." Journal of Biomaterials Science, Polymer Edition **8**(9): 721-740.
- Altankov, G., J. Hecht, et al. (2001). "Serum-free cultured keratinocytes fail to organize fibronectin matrix and possess different distribution of beta-1 integrins." Exp Dermatol **10**(2): 80-89.
- Altankov, G., T. Groth, et al. (2010). Development of Provisional Extracellular Matrix on Biomaterials Interface: Lessons from In Vitro Cell Culture. Advances in Regenerative Medicine: Role of Nanotechnology, and Engineering Principles. V. P. Shastri, G. Altankov and A. Lendlein, Springer Netherlands: 19-43.
- Anand, G., S. Sharma, et al. (2010). "Conformational transitions of adsorbed proteins on surfaces of varying polarity." Langmuir **26**(13): 10803-10811.
- Anderson, J. M. (2001). "Biological responses To materials." Annual Review of Materials Research **31**(1): 81-110.

- Anderson, D. G., J. A. Burdick, et al. (2004). "Smart Biomaterials." Science **305**(5692): 1923-1924.
- Andrade, J., S. Ma, et al. (1979). "Contact angles at the solid—water interface." Journal of Colloid and Interface Science **72**(3): 488-494.
- Andrade, J. D. (1985). Principles of protein adsorption. Surface and interfacial aspects of biomedical polymers.
- Andrade, J. and V. Hlady (1986). "Protein adsorption and materials biocompatibility: A tutorial review and suggested hypotheses. Biopolymers/Non-Exclusion HPLC." **79**: 1-63.
- Andrade, J. D., V. Hlady, et al. (1992). "Adsorption of complex proteins at interfaces." Pure and applied chemistry **64**: 1777-1781.
- Aplin, A. E., A. Howe, et al. (1998). "Signal transduction and signal modulation by cell adhesion receptors: the role of integrins, cadherins, immunoglobulin-cell adhesion molecules, and selectins." Pharmacol Rev **50**(2): 197-263.
- Arima, Y. and H. Iwata (2007). "Effect of wettability and surface functional groups on protein adsorption and cell adhesion using well-defined mixed self-assembled monolayers." Biomaterials **28**(20): 3074-3082.
- Arnaut, M. A., S. L. Goodman, et al. (2007). "Structure and mechanics of integrin-based cell adhesion." Curr Opin Cell Biol **19**(5): 495-507.
- Arnautova, I., J. George, et al. (2009). "The endothelial cell tube formation assay on basement membrane turns 20: state of the science and the art." Angiogenesis **12**(3): 267-274.
- Atala, A. (2004). "Tissue engineering and regenerative medicine: concepts for clinical application." Rejuvenation Res **7**(1): 15-31.
- Atala, A. (2009). "Engineering organs." Curr Opin Biotechnol **20**(5): 575-592.
- Aumailley, M. and R. Timpl (1986). "Attachment of cells to basement membrane collagen type IV." J Cell Biol **103**(4): 1569-1575.
- Aumailley, M. and B. Gayraud (1998). "Structure and biological activity of the extracellular matrix." J Mol Med (Berl) **76**(3-4): 253-265.
- Baber, U., A. S. Kini, et al. (2010). "Stenting of complex lesions: an overview." Nat Rev Cardiol **7**(9): 485-496.
- Barbosa, J. N., P. Madureira, et al. (2006). "The influence of functional groups of self-assembled monolayers on fibrous capsule formation and cell recruitment." J Biomed Mater Res A **76**(4): 737-743.
- Barczyk, M., S. Carracedo, et al. (2010). "Integrins." Cell Tissue Res **339**(1): 269-280.
- Belkin, A. M. and M. A. Stepp (2000). "Integrins as receptors for laminins." Microscopy Research and Technique **51**(3): 280-301.

- Beningo, K. A., M. Dembo, et al. (2004). "Responses of fibroblasts to anchorage of dorsal extracellular matrix receptors." Proc Natl Acad Sci U S A **101**(52): 18024-18029.
- Berk, B. C., K. Fujiwara, et al. (2007). "ECM remodeling in hypertensive heart disease." J Clin Invest **117**(3): 568-575.
- Biebuyck, H. A., C. D. Bain, et al. (1994). "Comparison of Organic Monolayers on Polycrystalline Gold Spontaneously Assembled from Solutions Containing Dialkyl Disulfides or Alkanethiols." Langmuir **10**(6): 1825-1831.
- Black, J. (2006). Biological performance of materials : fundamentals of biocompatibility. Boca Raton, CRC Taylor & Francis.
- Boudreau, N. J. and P. L. Jones (1999). "Extracellular matrix and integrin signalling: the shape of things to come." Biochem J **339** (Pt 3)(3): 481-488.
- Bowers, K. T., J. C. Keller, et al. (1992). "Optimization of surface micromorphology for enhanced osteoblast responses in vitro." Int J Oral Maxillofac Implants **7**(3): 302-310.
- Bredin, C. G., K. G. Sundqvist, et al. (1998). "Integrin dependent migration of lung cancer cells to extracellular matrix components." Eur Respir J **11**(2): 400-407.
- Bremer, M. G. E. G., J. Duval, et al. (2004). "Electrostatic interactions between immunoglobulin (IgG) molecules and a charged sorbent." Colloids and Surfaces A: Physicochemical and Engineering Aspects **250**(1-3): 29-42.
- Buck, M. R., D. G. Karustis, et al. (1992). "Degradation of extracellular-matrix proteins by human cathepsin B from normal and tumour tissues." Biochem J **282** (Pt 1): 273-278.
- Cappella, B. and G. Dietler (1999). "Force-distance curves by atomic force microscopy." Surface Science Reports **34**(1-3): 1-104.
- Charonis, A., V. Sideraki, et al. (2005). "Basement membrane peptides: functional considerations and biomedical applications in autoimmunity." Curr Med Chem **12**(13): 1495-1502.
- Chelberg, M. K., E. C. Tsilibary, et al. (1989). "Type IV collagen-mediated melanoma cell adhesion and migration: involvement of multiple, distinct domains of the collagen molecule." Cancer Res **49**(17): 4796-4802.
- Chen, C. H., D. O. Clegg, et al. (1998). "Structures and Dynamic Motion of Laminin-1 As Observed by Atomic Force Microscopy." Biochemistry **37**(22): 8262-8267.
- Chen, H., L. Yuan, et al. (2008). "Biocompatible polymer materials: Role of protein–surface interactions." Progress in Polymer Science **33**(11): 1059-1087.
- Cheng, Y. F. and R. H. Kramer (1989). "Human microvascular endothelial cells express integrin-related complexes that mediate adhesion to the extracellular matrix." J Cell Physiol **139**(2): 275-286.
- Chernousov, M. A., R. C. Stahl, et al. (1998). "Schwann cells use a novel collagen-dependent mechanism for fibronectin fibril assembly." Journal of Cell Science **111**(18): 2763-2777.

- Christopher, R. A., A. P. Kowalczyk, et al. (1997). "Localization of fibronectin matrix assembly sites on fibroblasts and endothelial cells." Journal of Cell Science **110**(5): 569-581.
- Chuang, W. H. and J. C. Lin (2007). "Surface characterization and platelet adhesion studies for the mixed self-assembled monolayers with amine and carboxylic acid terminated functionalities." J Biomed Mater Res A **82**(4): 820-830.
- Ciccione, W. J., 2nd, C. Motz, et al. (2001). "Bioabsorbable implants in orthopaedics: new developments and clinical applications." J Am Acad Orthop Surg **9**(5): 280-288.
- Clark, K., R. Pankov, et al. (2005). "A specific $\alpha 5\beta 1$ -integrin conformation promotes directional integrin translocation and fibronectin matrix formation." Journal of Cell Science **118**(2): 291-300.
- Coelho, N. M., C. Gonzalez-Garcia, et al. (2010). "Different assembly of type IV collagen on hydrophilic and hydrophobic substrata alters endothelial cells interaction." Eur Cell Mater **19**: 262-272.
- Coelho, N. M., C. González-García, et al. (2011). "Arrangement of type IV collagen on NH₂ and COOH functionalized surfaces." Biotechnology and Bioengineering **108**(12): 3009-3018.
- Coelho, N. M., C. Gonzalez-Garcia, et al. (2011). "Arrangement of type IV collagen and laminin on substrates with controlled density of -OH groups." Tissue Eng Part A **17**(17-18): 2245-2257.
- Cohen, D. E. and D. Melton (2011). "Turning straw into gold: directing cell fate for regenerative medicine." Nat Rev Genet **12**(4): 243-252.
- Colognato, H. and P. D. Yurchenco (2000). "Form and function: the laminin family of heterotrimers." Dev Dyn **218**(2): 213-234.
- Cukierman, E., R. Pankov, et al. (2001). "Taking cell-matrix adhesions to the third dimension." Science **294**(5547): 1708-1712.
- Cukierman, E., R. Pankov, et al. (2002). "Cell interactions with three-dimensional matrices." Curr Opin Cell Biol **14**(5): 633-639.
- Curino, A. C., L. H. Engelholm, et al. (2005). "Intracellular collagen degradation mediated by uPARAP/Endo180 is a major pathway of extracellular matrix turnover during malignancy." J Cell Biol **169**(6): 977-985.
- Currie, L. J., J. R. Sharpe, et al. (2001). "The use of fibrin glue in skin grafts and tissue-engineered skin replacements: a review." Plast Reconstr Surg **108**(6): 1713-1726.
- Daley, W. P., S. B. Peters, et al. (2008). "Extracellular matrix dynamics in development and regenerative medicine." J Cell Sci **121**(Pt 3): 255-264.
- Damsky, C. H. and D. Ilić (2002). "Integrin signaling: it's where the action is." Current Opinion in Cell Biology **14**(5): 594-602.

- Danen, E. H. and A. Sonnenberg (2003). "Integrins in regulation of tissue development and function." *J Pathol* **201**(4): 632-641.
- de Mel, A., G. Jell, et al. (2008). "Biofunctionalization of biomaterials for accelerated in situ endothelialization: a review." *Biomacromolecules* **9**(11): 2969-2979.
- Donato, R., E. A. Miljan, et al. (2007). "Differential development of neuronal physiological responsiveness in two human neural stem cell lines." *BMC Neurosci* **8**: 36.
- DuFort, C. C., M. J. Paszek, et al. (2011). "Balancing forces: architectural control of mechanotransduction." *Nat Rev Mol Cell Biol* **12**(5): 308-319.
- Durbeej, M. (2010). "Laminins." *Cell Tissue Res* **339**(1): 259-268.
- Dutta, R. C. and A. K. Dutta (2010). "Comprehension of ECM-cell dynamics: a prerequisite for tissue regeneration." *Biotechnol Adv* **28**(6): 764-769.
- Dvir, T., B. P. Timko, et al. (2011). "Nanotechnological strategies for engineering complex tissues." *Nat Nanotechnol* **6**(1): 13-22.
- Dzamba, B. J., H. Wu, et al. (1993). "Fibronectin binding site in type I collagen regulates fibronectin fibril formation." *J Cell Biol* **121**(5): 1165-1172.
- Egeblad, M. and Z. Werb (2002). "New functions for the matrix metalloproteinases in cancer progression." *Nat Rev Cancer* **2**(3): 161-174.
- Elices, M. J., L. A. Urry, et al. (1991). "Receptor functions for the integrin VLA-3: fibronectin, collagen, and laminin binding are differentially influenced by Arg-Gly-Asp peptide and by divalent cations." *J Cell Biol* **112**(1): 169-181.
- Elwing Hans, B., L. Li, et al. (1995). Protein Displacement Phenomena in Blood Plasma and Serum Studied by the Wettability Gradient Method and the Lens-on-Surface Method. *Proteins at Interfaces II*, American Chemical Society. **602**: 138-149.
- Evans, E. A. and D. A. Calderwood (2007). "Forces and bond dynamics in cell adhesion." *Science* **316**(5828): 1148-1153.
- Evers, F., R. Steitz, et al. (2009). "Analysis of Hofmeister effects on the density profile of protein adsorbates: a neutron reflectivity study." *J Phys Chem B* **113**(25): 8462-8465.
- Fabrizius-Homan, D. J. and S. L. Cooper (1992). "A comparison of the adsorption of three adhesive proteins to biomaterial surfaces." *Journal of Biomaterials Science, Polymer Edition* **3**(1): 27-47.
- Faucheux, N., R. Schweiss, et al. (2004). "Self-assembled monolayers with different terminating groups as model substrates for cell adhesion studies." *Biomaterials* **25**(14): 2721-2730.
- Fingerman, M. and S. W. Fingerman (1975). "The effects of 5-hydroxytryptamine depletors and monoamine oxidase inhibitors on color changes of the fiddler crab, *Uca pugilator*: further evidence in support of the hypothesis that 5-hydroxytryptamine controls the release of red pigment-dispersing hormone." *Comp Biochem Physiol C* **52**(1): 55-59.

- Fleischmajer, R., J. S. Perlish, et al. (1998). "There Is Binding of Collagen IV to β 1 Integrin during Early Skin Basement Membrane Assembly." Annals of the New York Academy of Sciences **857**(1): 212-227.
- Furth, M. E., A. Atala, et al. (2007). "Smart biomaterials design for tissue engineering and regenerative medicine." Biomaterials **28**(34): 5068-5073.
- Gao, L. and T. J. McCarthy (2006). "Contact angle hysteresis explained." Langmuir **22**(14): 6234-6237.
- García, A. J. (2005). "Get a grip: integrins in cell–biomaterial interactions." Biomaterials **26**(36): 7525-7529.
- García, C. G., L. L. Ferrus, et al. (2009). "Poly(L-lactide) Substrates with Tailored Surface Chemistry by Plasma Copolymerisation of Acrylic Monomers." Plasma Processes and Polymers **6**(3): 190-198.
- Gardner, H., J. Kreidberg, et al. (1996). "Deletion of integrin alpha 1 by homologous recombination permits normal murine development but gives rise to a specific deficit in cell adhesion." Dev Biol **175**(2): 301-313.
- Geiger, B., A. Bershadsky, et al. (2001). "Transmembrane crosstalk between the extracellular matrix--cytoskeleton crosstalk." Nat Rev Mol Cell Biol **2**(11): 793-805.
- Geiger, B., J. P. Spatz, et al. (2009). "Environmental sensing through focal adhesions." Nat Rev Mol Cell Biol **10**(1): 21-33.
- Geiger, B. and K. M. Yamada (2011). "Molecular architecture and function of matrix adhesions." Cold Spring Harb Perspect Biol **3**(5).
- Gelse, K., E. Poschl, et al. (2003). "Collagens--structure, function, and biosynthesis." Advanced Drug Delivery Reviews **55**(12): 1531-1546.
- Giannelli, G., J. Falk-Marzillier, et al. (1997). "Induction of cell migration by matrix metalloprotease-2 cleavage of laminin-5." Science **277**(5323): 225-228.
- Girotti, A., J. Reguera, et al. (2004). "Design and bioproduction of a recombinant multi(bio)functional elastin-like protein polymer containing cell adhesion sequences for tissue engineering purposes." J Mater Sci Mater Med **15**(4): 479-484.
- Goody, M. F. and C. A. Henry (2010). "Dynamic interactions between cells and their extracellular matrix mediate embryonic development." Molecular Reproduction and Development **77**(6): 475-488.
- Gray, J. J. (2004). "The interaction of proteins with solid surfaces." Current Opinion in Structural Biology **14**(1): 110-115.
- Greenwood, H. L., P. A. Singer, et al. (2006). "Regenerative Medicine and the Developing World." PLoS Med **3**(9): e381.

- Griffith, L. G. and G. Naughton (2002). "Tissue engineering--current challenges and expanding opportunities." Science (New York, N.Y.) **295**(5557): 1009-1014.
- Griffith, L. G. and M. A. Swartz (2006). "Capturing complex 3D tissue physiology in vitro." Nat Rev Mol Cell Biol **7**(3): 211-224.
- Grinnell, F. and M. K. Feld (1982). "Fibronectin adsorption on hydrophilic and hydrophobic surfaces detected by antibody binding and analyzed during cell adhesion in serum-containing medium." Journal of Biological Chemistry **257**(9): 4888-4893.
- Grinnell, F. (1986). "Focal adhesion sites and the removal of substratum-bound fibronectin." The Journal of Cell Biology **103**(6): 2697-2706.
- Groth, T. and G. Altankov (1996). "Studies on cell-biomaterial interaction: role of tyrosine phosphorylation during fibroblast spreading on surfaces varying in wettability." Biomaterials **17**(12): 1227-1234.
- Gugutkov, D., G. Altankov, et al. (2010). "Fibronectin activity on substrates with controlled --OH density." J Biomed Mater Res A **92**(1): 322-331.
- Gugutkov, D., C. Gonzalez-Garcia, et al. (2009). "Biological activity of the substrate-induced fibronectin network: insight into the third dimension through electrospun fibers." Langmuir : the ACS journal of surfaces and colloids **25**(18): 10893-10900.
- Gumbiner, B. M. (1996). "Cell Adhesion: The Molecular Basis of Tissue Architecture and Morphogenesis." Cell **84**(3): 345-357.
- Gurdak, E., P. G. Rouxhet, et al. (2006). "Factors and mechanisms determining the formation of fibrillar collagen structures in adsorbed phases." Colloids and surfaces.B, Biointerfaces **52**(1): 76-88.
- Gustavsson, J., G. Altankov, et al. (2008). "Surface modifications of silicon nitride for cellular biosensor applications." Journal of Materials Science: Materials in Medicine **19**(4): 1839-1850.
- Haensch, C., S. Hoepfner, et al. (2010). "Chemical modification of self-assembled silane based monolayers by surface reactions." Chemical Society Reviews **39**(6): 2323-2334.
- Halliday, N. L. and J. J. Tomasek (1995). "Mechanical Properties of the Extracellular Matrix Influence Fibronectin Fibril Assembly in Vitro." Experimental Cell Research **217**(1): 109-117.
- Hanks, S. K., L. Ryzhova, et al. (2003). "Focal adhesion kinase signaling activities and their implications in the control of cell survival and motility." Front Biosci **8**: d982-996.
- Hench, L. (1980). "Biomaterials." Science **208**(4446): 826-831.
- Hench, L. L. and O. Andersson (1993). Bioactive glasses. An Introduction to Bioceramics. L. L. Hench and J. Wilson, World Scientific: 41-62.

- Hench, L. L. and J. M. Polak (2002). "Third-generation biomedical materials." Science **295**(5557): 1014-1017.
- Hench, L. L. and I. Thompson (2010). "Twenty-first century challenges for biomaterials." Journal of The Royal Society Interface **7**(Suppl 4): S379-S391.
- Herbst, T. J., J. B. McCarthy, et al. (1988). "Differential effects of laminin, intact type IV collagen, and specific domains of type IV collagen on endothelial cell adhesion and migration." The Journal of Cell Biology **106**(4): 1365-1373.
- Hernández, J. C. R., M. Salmerón Sánchez, et al. (2007). "Substrate Chemistry-Dependent Conformations of Single Laminin Molecules on Polymer Surfaces are Revealed by the Phase Signal of Atomic Force Microscopy." Biophysical Journal **93**(1): 202-207.
- Hernández, J. C. R., P. Rico, et al. (2009). "Fibrinogen Patterns and Activity on Substrates with Tailored Hydroxy Density." Macromolecular Bioscience **9**(8): 766-775.
- Heymans, S., M. Pauschinger, et al. (2006). "Inhibition of Urokinase-Type Plasminogen Activator or Matrix Metalloproteinases Prevents Cardiac Injury and Dysfunction During Viral Myocarditis." Circulation **114**(6): 565-573.
- Hibino, N., E. McGillicuddy, et al. (2010). "Late-term results of tissue-engineered vascular grafts in humans." The Journal of Thoracic and Cardiovascular Surgery **139**(2): 431-436.e432.
- Hlady, V. and J. Buijs (1996). "Protein adsorption on solid surfaces." Current Opinion in Biotechnology **7**(1): 72-77.
- Holmbeck, K., P. Bianco, et al. (1999). "MT1-MMP-Deficient Mice Develop Dwarfism, Osteopenia, Arthritis, and Connective Tissue Disease due to Inadequate Collagen Turnover." Cell **99**(1): 81-92.
- Höök, F., M. Rodahl, et al. (1998). "Structural changes in hemoglobin during adsorption to solid surfaces: Effects of pH, ionic strength, and ligand binding." Proceedings of the National Academy of Sciences **95**(21): 12271-12276.
- Houseman, B. T. and M. Mrksich (2001). "The microenvironment of immobilized Arg-Gly-Asp peptides is an important determinant of cell adhesion." Biomaterials **22**(9): 943-955.
- Hu, W.-J., J. W. Eaton, et al. (2001). "Molecular basis of biomaterial-mediated foreign body reactions." Blood **98**(4): 1231-1238.
- Huang, Y.-C. and Y.-Y. Huang (2006). "Biomaterials and Strategies for Nerve Regeneration." Artificial Organs **30**(7): 514-522.
- Hubbell, J. A. (1995). "Biomaterials in tissue engineering." Biotechnology (N Y) **13**(6): 565-576.
- Hubbell, J. A. (2003). "Materials as morphogenetic guides in tissue engineering." Current Opinion in Biotechnology **14**(5): 551-558.

- Hudson, B. G., S. T. Reeders, et al. (1993). "Type IV collagen: structure, gene organization, and role in human diseases. Molecular basis of Goodpasture and Alport syndromes and diffuse leiomyomatosis." The Journal of biological chemistry **268**(35): 26033-26036.
- Huebsch, N. and D. J. Mooney (2009). "Inspiration and application in the evolution of biomaterials." Nature **462**(7272): 426-432.
- Hunt, J. A. (2004). Foreign body response. . Encyclopedia of Biomaterials and Biomedical Engineering. New York, Marcel Dekker: 641–648.
- Hynes, R. O. (2002). "Integrins: Bidirectional, Allosteric Signaling Machines." Cell **110**(6): 673-687.
- Hynes, R. O. (2009). "The Extracellular Matrix: Not Just Pretty Fibrils." Science **326**(5957): 1216-1219.
- Ingham, K. C., S. A. Brew, et al. (1988). "Interaction of fibronectin and its gelatin-binding domains with fluorescent-labeled chains of type I collagen." Journal of Biological Chemistry **263**(10): 4624-4628.
- Irvine, S. M., J. Cayzer, et al. (2011). "Quantification of in vitro and in vivo angiogenesis stimulated by ovine forestomach matrix biomaterial." Biomaterials **32**(27): 6351-6361.
- Ishizaki, T., N. Saito, et al. (2010). "Correlation of Cell Adhesive Behaviors on Superhydrophobic, Superhydrophilic, and Micropatterned Superhydrophobic/Superhydrophilic Surfaces to Their Surface Chemistry." Langmuir **26**(11): 8147-8154.
- Janmey, P. A. and C. A. McCulloch (2007). "Cell Mechanics: Integrating Cell Responses to Mechanical Stimuli." Annual Review of Biomedical Engineering **9**(1): 1-34.
- Jones, K. L. and C. R. O'Melia (2000). "Protein and humic acid adsorption onto hydrophilic membrane surfaces: effects of pH and ionic strength." Journal of Membrane Science **165**(1): 31-46.
- Kadler, K. E., A. Hill, et al. (2008). "Collagen fibrillogenesis: fibronectin, integrins, and minor collagens as organizers and nucleators." Current Opinion in Cell Biology **20**(5): 495-501.
- Kaido, T., M. Yebra, et al. (2004). "Regulation of Human β -Cell Adhesion, Motility, and Insulin Secretion by Collagen IV and Its Receptor $\alpha 1\beta 1$." Journal of Biological Chemistry **279**(51): 53762-53769.
- Kalluri, R. (2003). "Basement membranes: structure, assembly and role in tumour angiogenesis." Nat Rev Cancer **3**(6): 422-433.
- Kalluri, R. and M. Zeisberg (2006). "Fibroblasts in cancer." Nat Rev Cancer **6**(5): 392-401.
- Kamath, S., D. Bhattacharyya, et al. (2008). "Surface chemistry influences implant-mediated host tissue responses." Journal of Biomedical Materials Research Part A **86A**(3): 617-626.

- Käpylä, J., J. Ivaska, et al. (2000). "Integrin $\alpha 2 I$ Domain Recognizes Type I and Type IV Collagens by Different Mechanisms." Journal of Biological Chemistry **275**(5): 3348-3354.
- Karlsson, M. and U. Carlsson (2005). "Protein Adsorption Orientation in the Light of Fluorescent Probes: Mapping of the Interaction between Site-Directly Labeled Human Carbonic Anhydrase II and Silica Nanoparticles." Biophysical Journal **88**(5): 3536-3544.
- Kasas, S., N. H. Thomson, et al. (1997). "Biological applications of the AFM: From single molecules to organs." International Journal of Imaging Systems and Technology **8**(2): 151-161.
- Keely, P. J., A. M. Fong, et al. (1995). "Alteration of collagen-dependent adhesion, motility, and morphogenesis by the expression of antisense alpha 2 integrin mRNA in mammary cells." Journal of Cell Science **108**(2): 595-607.
- Keresztes, Z., P. G. Rouxhet, et al. (2006). "Supramolecular assemblies of adsorbed collagen affect the adhesion of endothelial cells." Journal of Biomedical Materials Research Part A **76A**(2): 223-233.
- Kern, A., J. Eble, et al. (1993). "Interaction of type IV collagen with the isolated integrins $\alpha 1 \beta 1$ and $\alpha 2 \beta 1$." European Journal of Biochemistry **215**(1): 151-159.
- Keselowsky, B. G., D. M. Collard, et al. (2003). "Surface chemistry modulates fibronectin conformation and directs integrin binding and specificity to control cell adhesion." Journal of Biomedical Materials Research Part A **66A**(2): 247-259.
- Keselowsky, B. G., D. M. Collard, et al. (2004). "Surface chemistry modulates focal adhesion composition and signaling through changes in integrin binding." Biomaterials **25**(28): 5947-5954.
- Keselowsky, B. G., D. M. Collard, et al. (2005). "Integrin binding specificity regulates biomaterial surface chemistry effects on cell differentiation." Proceedings of the National Academy of Sciences of the United States of America **102**(17): 5953-5957.
- Khoshnoodi, J., V. Pedchenko, et al. (2008). "Mammalian collagen IV." Microscopy Research and Technique **71**(5): 357-370.
- Kidoaki, S. and T. Matsuda (1999). "Adhesion Forces of the Blood Plasma Proteins on Self-Assembled Monolayer Surfaces of Alkanethiolates with Different Functional Groups Measured by an Atomic Force Microscope." Langmuir **15**(22): 7639-7646.
- Kieswetter, K., Z. Schwartz, et al. (1996). "Surface roughness modulates the local production of growth factors and cytokines by osteoblast-like MG-63 cells." J Biomed Mater Res **32**(1): 55-63.

- Knight, C. G., L. F. Morton, et al. (1998). "Identification in collagen type I of an integrin alpha2 beta1-binding site containing an essential GER sequence." The Journal of biological chemistry **273**(50): 33287-33294.
- Kolahi, K. S. and M. R. Mofrad (2010). "Mechanotransduction: a major regulator of homeostasis and development." Wiley Interdiscip Rev Syst Biol Med **2**(6): 625-639.
- Krasteva, N., T. H. Groth, et al. (2001). "The role of surface wettability on hepatocyte adhesive interactions and function." J Biomater Sci Polym Ed **12**(6): 613-627.
- Kruegel, J. and N. Miosge (2010). "Basement membrane components are key players in specialized extracellular matrices." Cellular and Molecular Life Sciences **67**(17): 2879-2895.
- Kühn, K. (1995). "Basement membrane (type IV) collagen." Matrix Biology **14**(6): 439-445.
- Lan, M. A., C. A. Gersbach, et al. (2005). "Myoblast proliferation and differentiation on fibronectin-coated self assembled monolayers presenting different surface chemistries." Biomaterials **26**(22): 4523-4531.
- Langer, R. and J. Vacanti (1993). "Tissue engineering." Science **260**(5110): 920-926.
- Langer, R. and D. A. Tirrell (2004). "Designing materials for biology and medicine." Nature **428**(6982): 487-492.
- Larsen, M., V. V. Artym, et al. (2006). "The matrix reorganized: extracellular matrix remodeling and integrin signaling." Current Opinion in Cell Biology **18**(5): 463-471.
- Latour, R. A. (2005). Biomaterials: protein-surface interactions. Encyclopedia of Biomaterials and Biomedical Engineering. New York, Marcel Dekker: 1-15.
- LeBleu, V. S., B. Macdonald, et al. (2007). "Structure and function of basement membranes." Experimental biology and medicine (Maywood, N.J.) **232**(9): 1121-1129.
- Lee, M. H., P. Ducheyne, et al. (2006). "Effect of biomaterial surface properties on fibronectin-[alpha]5[beta]1 integrin interaction and cellular attachment." Biomaterials **27**(9): 1907-1916.
- Leitinger, B. and E. Hohenester (2007). "Mammalian collagen receptors." Matrix Biology **26**(3): 146-155.
- Lhoest, J. B., E. Detrait, et al. (1998). "Fibronectin adsorption, conformation, and orientation on polystyrene substrates studied by radiolabeling, XPS, and ToF SIMS." Journal of Biomedical Materials Research **41**(1): 95-103.
- Li, Y., A. Asadi, et al. (2009). "pH effects on collagen fibrillogenesis in vitro: Electrostatic interactions and phosphate binding." Materials Science and Engineering: C **29**(5): 1643-1649.
- Lindblad, M., M. Lestelius, et al. (1997). "Cell and soft tissue interactions with methyl- and hydroxyl-terminated alkane thiols on gold surfaces." Biomaterials **18**(15): 1059-1068.

- Llopis-Hernández, V., P. Rico, et al. (2011). "Role of Surface Chemistry in Protein Remodeling at the Cell-Material Interface." PLoS One **6**(5): e19610.
- Lu, C. F., A. Nadarajah, et al. (1994). "A Comprehensive Model of Multiprotein Adsorption on Surfaces." Journal of Colloid and Interface Science **168**(1): 152-161.
- Lubarsky, G. V., M. M. Browne, et al. (2005). "The influence of electrostatic forces on protein adsorption." Colloids and Surfaces B: Biointerfaces **44**(1): 56-63.
- Lutolf, M. P., J. L. Lauer-Fields, et al. (2003). "Synthetic matrix metalloproteinase-sensitive hydrogels for the conduction of tissue regeneration: Engineering cell-invasion characteristics." Proceedings of the National Academy of Sciences **100**(9): 5413-5418.
- Lutolf, M. P. and J. A. Hubbell (2005). "Synthetic biomaterials as instructive extracellular microenvironments for morphogenesis in tissue engineering." Nat Biotech **23**(1): 47-55.
- Mager, M. D., V. LaPointe, et al. (2011). "Exploring and exploiting chemistry at the cell surface." Nat Chem **3**(8): 582-589.
- Magnani, A., G. Peluso, et al. (2002). "Protein Adsorption and Cellular/Tissue Interactions." 669-689.
- Malmsten, M. (1998). "Formation of Adsorbed Protein Layers." Journal of Colloid and Interface Science **207**(2): 186-199.
- Maneva-Radicheva, L., U. Ebert, et al. (2008). "Fibroblast remodeling of adsorbed collagen type IV is altered in contact with cancer cells." Histol Histopathol **23**(7): 833-842.
- Mao, Y. and J. E. Schwarzbauer (2005). "Fibronectin fibrillogenesis, a cell-mediated matrix assembly process." Matrix Biology **24**(6): 389-399.
- Mason, C. and P. Dunnill (2007). "A brief definition of regenerative medicine." Regenerative Medicine **3**(1): 1-5.
- Mecham, R. (1991). "Receptors for laminin on mammalian cells." The FASEB Journal **5**(11): 2538-2546.
- Meyer, E. (1992). "Atomic force microscopy." Progress in Surface Science **41**(1): 3-49.
- Miner, J. H. and P. D. Yurchenco (2004). "LAMININ FUNCTIONS IN TISSUE MORPHOGENESIS." Annual Review of Cell and Developmental Biology **20**(1): 255-284.
- Missirlis, Y. F. and A. D. Spiliotis (2002). "Assessment of techniques used in calculating cell-material interactions." Biomol Eng **19**(2-6): 287-294.
- Monaco, S., V. Sparano, et al. (2006). "Enzymatic processing of collagen IV by MMP-2 (gelatinase A) affects neutrophil migration and it is modulated by extracatalytic domains." Protein Sci **15**(12): 2805-2815.
- Moon, I. S., T. Berglundh, et al. (1999). "The barrier between the keratinized mucosa and the dental implant." Journal of Clinical Periodontology **26**(10): 658-663.

- Mooney, D. and R. Langer (2000). Engineering Biomaterials for Tissue Engineering: The 10–100 Micron Size Scale. The Biomedical Engineering Handbook. J. Bronzino, CRC Press LLC.
- Mrksich, M. and G. M. Whitesides (1996). "Using self-assembled monolayers to understand the interactions of man-made surfaces with proteins and cells." Annu Rev Biophys Biomol Struct **25**: 55-78.
- Mrksich, M. (2009). "Using self-assembled monolayers to model the extracellular matrix." Acta Biomaterialia **5**(3): 832-841.
- Murray, J. C., G. Stengl, et al. (1979). "Epidermal cells adhere preferentially to type IV (basement membrane) collagen." The Journal of Cell Biology **80**(1): 197-202.
- Mustafa, K., J. Wroblewski, et al. (2000). "Effects of titanium surfaces blasted with TiO₂ particles on the initial attachment of cells derived from human mandibular bone." Clinical Oral Implants Research **11**(2): 116-128.
- Nakanishi, K., T. Sakiyama, et al. (2001). "On the adsorption of proteins on solid surfaces, a common but very complicated phenomenon." Journal of Bioscience and Bioengineering **91**(3): 233-244.
- Nishiuchi, R., O. Murayama, et al. (2003). "Characterization of the Ligand-Binding Specificities of Integrin $\alpha 3\beta 1$ and $\alpha 6\beta 1$ Using a Panel of Purified Laminin Isoforms Containing Distinct α Chains." Journal of Biochemistry **134**(4): 497-504.
- Noh, H. and E. A. Vogler (2007). "Volumetric interpretation of protein adsorption: Competition from mixtures and the Vroman effect." Biomaterials **28**(3): 405-422.
- Norde, W. and A. C. I. Anusiem (1992). "Adsorption, desorption and re-adsorption of proteins on solid surfaces." Colloids and Surfaces **66**(1): 73-80.
- Norde, W. (1996). "Driving forces for protein adsorption at solid surfaces." Macromolecular Symposia **103**(1): 5-18.
- Norde, W. (2008). "My voyage of discovery to proteins in flatland ...and beyond." Colloids and Surfaces B: Biointerfaces **61**(1): 1-9.
- Oberpenning, F., J. Meng, et al. (1999). "De novo reconstitution of a functional mammalian urinary bladder by tissue engineering." Nat Biotechnol **17**(2): 149-155.
- Ohya, Y., H. Matsunami, et al. (2004). "Cell growth on the porous sponges prepared from poly(depsipeptide-co-lactide) having various functional groups." Journal of Biomaterials Science, Polymer Edition **15**(1): 111-123.
- Owen, G. R., D. O. Meredith, et al. (2005). "Focal adhesion quantification - a new assay of material biocompatibility? Review." Eur Cell Mater **9**: 85-96; discussion 85-96.
- Owens, D. K. and R. C. Wendt (1969). "Estimation of the surface free energy of polymers." Journal of Applied Polymer Science **13**(8): 1741-1747.

- Owens, N. F., D. Gingell, et al. (1987). "Inhibition of cell adhesion by a synthetic polymer adsorbed to glass shown under defined hydrodynamic stress." *J Cell Sci* **87** (Pt 5): 667-675.
- Page-McCaw, A., A. J. Ewald, et al. (2007). "Matrix metalloproteinases and the regulation of tissue remodelling." *Nat Rev Mol Cell Biol* **8**(3): 221-233.
- Pankov, R., E. Cukierman, et al. (2000). "Integrin dynamics and matrix assembly: tensin-dependent translocation of alpha(5)beta(1) integrins promotes early fibronectin fibrillogenesis." *J Cell Biol* **148**(5): 1075-1090.
- Pankov, R. and A. Momchilova (2010). "Cell Adhesions and Signaling: A Tool for Biocompatibility Assessment". *Advances in Regenerative Medicine: Role of Nanotechnology, and Engineering Principles.* 1-17.
- Patino, M. G., M. E. Neiders, et al. (2002). "Collagen as an implantable material in medicine and dentistry." *J Oral Implantol* **28**(5): 220-225.
- Paulsson, M. (1992). "Basement membrane proteins: structure, assembly, and cellular interactions." *Crit Rev Biochem Mol Biol* **27**(1-2): 93-127.
- Pedchenko, V., R. Zent, et al. (2004). "Alpha(v)beta3 and alpha(v)beta5 integrins bind both the proximal RGD site and non-RGD motifs within noncollagenous (NC1) domain of the alpha3 chain of type IV collagen: implication for the mechanism of endothelia cell adhesion." *J Biol Chem* **279**(4): 2772-2780.
- Perris, R. and D. Perissinotto (2000). "Role of the extracellular matrix during neural crest cell migration." *Mech Dev* **95**(1-2): 3-21.
- Phelps, E. A., N. Landazuri, et al. (2010). "Bioartificial matrices for therapeutic vascularization." *Proc Natl Acad Sci U S A* **107**(8): 3323-3328.
- Place, E. S., N. D. Evans, et al. (2009). "Complexity in biomaterials for tissue engineering." *Nat Mater* **8**(6): 457-470.
- Planell, J. A., M. Navarro, et al. (2010). "Materials Surface Effects on Biological Interactions". *Advances in Regenerative Medicine: Role of Nanotechnology, and Engineering Principles.* 233-252.
- Popova, S. N., E. Lundgren-Akerlund, et al. (2007). "Physiology and pathology of collagen receptors." *Acta physiologica (Oxford, England)* **190**(3): 179-187.
- Prime, K. L. and G. M. Whitesides (1993). "Adsorption of proteins onto surfaces containing end-attached oligo(ethylene oxide): a model system using self-assembled monolayers." *Journal of the American Chemical Society* **115**(23): 10714-10721.
- Rabe, M., D. Verdes, et al. (2011). "Understanding protein adsorption phenomena at solid surfaces." *Advances in Colloid and Interface Science* **162**(1-2): 87-106.

- Radmacher, M., R. W. Tillamnn, et al. (1992). "From molecules to cells: imaging soft samples with the atomic force microscope." Science **257**(5078): 1900-1905.
- Ratner, B. D. and S. J. Bryant (2004). "Biomaterials: where we have been and where we are going." Annu Rev Biomed Eng **6**: 41-75.
- Raynor, J. E., J. R. Capadona, et al. (2009). "Polymer brushes and self-assembled monolayers: Versatile platforms to control cell adhesion to biomaterials (Review)." Biointerphases **4**(2): FA3-16.
- Reisenauer, A., O. Eickelberg, et al. (2007). "Increased carcinogenic potential of myeloid tumor cells induced by aberrant TGF-beta1-signaling and upregulation of cathepsin B." Biol Chem **388**(6): 639-650.
- Remes, A. and D. F. Williams (1992). "Immune response in biocompatibility." Biomaterials **13**(11): 731-743.
- Reno, F., M. Sabbatini, et al. (2003). "Fourier transform infrared spectroscopy application to vascular biology: comparative analysis of human internal mammary artery and saphenous vein wall." Cells Tissues Organs **175**(4): 186-191.
- Rivron, N. C., J. J. Liu, et al. (2008). "Engineering vascularised tissues in vitro." European cells & materials **15**(Journal Article): 27-40.
- Rodrigues, S. N., I. C. Goncalves, et al. (2006). "Fibrinogen adsorption, platelet adhesion and activation on mixed hydroxyl-/methyl-terminated self-assembled monolayers." Biomaterials **27**(31): 5357-5367.
- Rubin, K., M. Hook, et al. (1981). "Substrate adhesion of rat hepatocytes: mechanism of attachment to collagen substrates." Cell **24**(2): 463-470.
- Santoro, S. A. (1986). "Identification of a 160,000 dalton platelet membrane protein that mediates the initial divalent cation-dependent adhesion of platelets to collagen." Cell **46**(6): 913-920.
- Schenk, S. and V. Quaranta (2003). "Tales from the crypt[ic] sites of the extracellular matrix." Trends Cell Biol **13**(7): 366-375.
- Sechler, J. L. and J. E. Schwarzbauer (1998). "Control of cell cycle progression by fibronectin matrix architecture." J Biol Chem **273**(40): 25533-25536.
- Sengupta, D. and S. C. Heilshorn (2010). "Protein-engineered biomaterials: highly tunable tissue engineering scaffolds." Tissue Eng Part B Rev **16**(3): 285-293.
- Sephel, G. C., R. Kennedy, et al. (1996). "Expression of capillary basement membrane components during sequential phases of wound angiogenesis." Matrix Biology **15**(4): 263-279.
- Setty, S., Y. Kim, et al. (1998). "Interactions of type IV collagen and its domains with human mesangial cells." J Biol Chem **273**(20): 12244-12249.

- Shekaran, A. and A. J. Garcia (2011). "Extracellular matrix-mimetic adhesive biomaterials for bone repair." J Biomed Mater Res A **96**(1): 261-272.
- Shi, F., J. Harman, et al. (2010). "Collagen I matrix turnover is regulated by fibronectin polymerization." Am J Physiol Cell Physiol **298**(5): C1265-1275.
- Simian, M., Y. Hirai, et al. (2001). "The interplay of matrix metalloproteinases, morphogens and growth factors is necessary for branching of mammary epithelial cells." Development **128**(16): 3117-3131.
- Sipe, J. D. (2002). "Tissue engineering and reparative medicine." Annals of the New York Academy of Sciences **961**: 1-9.
- Smith, R. K., P. A. Lewis, et al. (2004). "Patterning self-assembled monolayers." Progress in Surface Science **75**(1-2): 1-68.
- Sottile, J. and D. C. Hocking (2002). "Fibronectin Polymerization Regulates the Composition and Stability of Extracellular Matrix Fibrils and Cell-Matrix Adhesions." Molecular Biology of the Cell **13**(10): 3546-3559.
- Srichai, M. B. and R. Zent (2010). Integrin Structure and Function. Cell-Extracellular Matrix Interactions in Cancer, Springer New York.
- Stamenkovic, I. (2003). "Extracellular matrix remodelling: the role of matrix metalloproteinases." The Journal of Pathology **200**(4): 448-464.
- Stevens, M. M. and J. H. George (2005). "Exploring and Engineering the Cell Surface Interface." Science **310**(5751): 1135-1138.
- Storesund, A. and K. B. Helle (1975). "Practolol, caffeine and calcium in the regulation of mechanical activity of the cardiac ventricle in *Myxine glutinosa* (L.)." Comp Biochem Physiol C **52**(1): 17-22.
- Streuli, C. (1999). "Extracellular matrix remodelling and cellular differentiation." Curr Opin Cell Biol **11**(5): 634-640.
- Sung, K. E., G. Su, et al. (2009). "Control of 3-dimensional collagen matrix polymerization for reproducible human mammary fibroblast cell culture in microfluidic devices." Biomaterials **30**(27): 4833-4841.
- Takada, Y., X. Ye, et al. (2007). "The integrins." Genome Biol **8**(5): 215.
- Tamada, Y. and Y. Ikada (1994). "Fibroblast growth on polymer surfaces and biosynthesis of collagen." Journal of Biomedical Materials Research **28**(7): 783-789.
- Tang, L., T. A. Jennings, et al. (1998). "Mast cells mediate acute inflammatory responses to implanted biomaterials." Proc Natl Acad Sci U S A **95**(15): 8841-8846.
- Tang, L. and J. W. Eaton (1999). "Natural responses to unnatural materials: A molecular mechanism for foreign body reactions." Mol Med **5**(6): 351-358.

- Taniguchi, Y., H. Ido, et al. (2009). "The C-terminal region of laminin beta chains modulates the integrin binding affinities of laminins." *J Biol Chem* **284**(12): 7820-7831.
- Testaz, S. and J. L. Duband (2001). "Central role of the alpha4beta1 integrin in the coordination of avian truncal neural crest cell adhesion, migration, and survival." *Dev Dyn* **222**(2): 127-140.
- Thevenot, P., W. Hu, et al. (2008). "Surface chemistry influences implant biocompatibility." *Curr Top Med Chem* **8**(4): 270-280.
- Thiery, J. P. (2003). "Cell adhesion in development: a complex signaling network." *Curr Opin Genet Dev* **13**(4): 365-371.
- Tidwell, C. D., S. I. Ertel, et al. (1997). "Endothelial Cell Growth and Protein Adsorption on Terminally Functionalized, Self-Assembled Monolayers of Alkanethiolates on Gold." *Langmuir* **13**(13): 3404-3413.
- Tie, Y., C. Calonder, et al. (2003). "Protein adsorption: Kinetics and history dependence." *Journal of Colloid and Interface Science* **268**(1): 1-11.
- Tiger, C.-F., F. Fougousse, et al. (2001). " α 11 β 1 Integrin Is a Receptor for Interstitial Collagens Involved in Cell Migration and Collagen Reorganization on Mesenchymal Nonmuscle Cells." *Developmental biology* **237**(1): 116-129.
- Timpl, R., I. Oberbaumer, et al. (1985). "Structure and biology of the globular domain of basement membrane type IV collagen." *Annals of the New York Academy of Sciences* **460**: 58-72.
- Timpl, R. and J. C. Brown (1996). "Supramolecular assembly of basement membranes." *Bioessays* **18**(2): 123-132.
- Tomasek, J. J., G. Gabbiani, et al. (2002). "Myofibroblasts and mechano-regulation of connective tissue remodelling." *Nat Rev Mol Cell Biol* **3**(5): 349-363.
- Toromanov, G., C. González-García, et al. (2010). "Vitronectin activity on polymer substrates with controlled -OH density." *Polymer* **51**(11): 2329-2336.
- Tsilibary, E. C. and A. S. Charonis (1986). "The role of the main noncollagenous domain (NC1) in type IV collagen self-assembly." *J Cell Biol* **103**(6 Pt 1): 2467-2473.
- Tuckwell, D. S., S. Ayad, et al. (1994). "Conformation dependence of integrin-type II collagen binding. Inability of collagen peptides to support alpha 2 beta 1 binding, and mediation of adhesion to denatured collagen by a novel alpha 5 beta 1-fibronectin bridge." *Journal of cell science* **107** (Pt 4)(Pt 4): 993-1005.
- Tulla, M., O. T. Pentikainen, et al. (2001). "Selective binding of collagen subtypes by integrin alpha 1I, alpha 2I, and alpha 10I domains." *J Biol Chem* **276**(51): 48206-48212.

- Tzoneva, R., T. Groth, et al. (2002). "Remodeling of fibrinogen by endothelial cells in dependence on fibronectin matrix assembly. Effect of substratum wettability." Journal of Materials Science: Materials in Medicine **13**(12): 1235-1244.
- Tzu, J. and M. P. Marinkovich (2008). "Bridging structure with function: Structural, regulatory, and developmental role of laminins." The International Journal of Biochemistry & Cell Biology **40**(2): 199-214.
- Ulman, A. (1996). "Formation and Structure of Self-Assembled Monolayers." Chem Rev **96**(4): 1533-1554.
- Van Agtmael, T. and L. Bruckner-Tuderman (2010). "Basement membranes and human disease." Cell and Tissue Research **339**(1): 167-188.
- Vanacore, R. M., S. Shanmugasundararaj, et al. (2004). "The $\alpha 1.\alpha 2$ Network of Collagen IV." Journal of Biological Chemistry **279**(43): 44723-44730.
- Vandenberg, P., A. Kern, et al. (1991). "Characterization of a type IV collagen major cell binding site with affinity to the alpha 1 beta 1 and the alpha 2 beta 1 integrins." The Journal of Cell Biology **113**(6): 1475-1483.
- Velling, T., J. Risteli, et al. (2002). "Polymerization of Type I and III Collagens Is Dependent On Fibronectin and Enhanced By Integrins $\alpha 11\beta 1$ and $\alpha 2\beta 1$." Journal of Biological Chemistry **277**(40): 37377-37381.
- Vogel, V. and G. Baneyx (2003). "The tissue engineering puzzle: a molecular perspective." Annu Rev Biomed Eng **5**: 441-463.
- Vogler, E. A. (1998). "Structure and reactivity of water at biomaterial surfaces." Adv Colloid Interface Sci **74**: 69-117.
- Von Recum, A. F. and T. G. Van Kooten (1996). "The influence of micro-topography on cellular response and the implications for silicone implants." Journal of Biomaterials Science, Polymer Edition **7**(2): 181-198.
- Weathington, N. M., A. H. van Houwelingen, et al. (2006). "A novel peptide CXCR ligand derived from extracellular matrix degradation during airway inflammation." Nat Med **12**(3): 317-323.
- Wehrle-Haller, B. and B. A. Imhof (2003). "Integrin-dependent pathologies." J Pathol **200**(4): 481-487.
- Wheeldon, I., A. Farhadi, et al. (2011). "Nanoscale tissue engineering: spatial control over cell-materials interactions." Nanotechnology **22**(21): 212001.
- White, D. J., S. Puranen, et al. (2004). "The collagen receptor subfamily of the integrins." The International Journal of Biochemistry & Cell Biology **36**(8): 1405-1410.
- Whitesides, G. M. and C. B. Gorman (1995). Self-assembled monolayers: Models for organic surface chemistry. . Handbook of Surface Imaging and Visualization.

- Wierzbicka-Patynowski, I. and J. E. Schwarzbauer (2003). "The ins and outs of fibronectin matrix assembly." Journal of Cell Science **116**(16): 3269-3276.
- Williams, D. F. (2008). "On the mechanisms of biocompatibility." Biomaterials **29**(20): 2941-2953.
- Williams, D. F. (2009). "On the nature of biomaterials." Biomaterials **30**(30): 5897-5909.
- Wilson, C. J., R. E. Clegg, et al. (2005). "Mediation of biomaterial-cell interactions by adsorbed proteins: a review." Tissue Eng **11**(1-2): 1-18.
- Wu, C., V. M. Keivenst, et al. (1995). "Integrin activation and cytoskeletal interaction are essential for the assembly of a fibronectin matrix." Cell **83**(5): 715-724.
- Wynn, T. A. (2008). "Cellular and molecular mechanisms of fibrosis." The Journal of Pathology **214**(2): 199-210.
- Xu, H., X. Zhao, et al. (2006). "Orientation of a Monoclonal Antibody Adsorbed at the Solid/Solution Interface: A Combined Study Using Atomic Force Microscopy and Neutron Reflectivity." Langmuir **22**(14): 6313-6320.
- Yamada, K. M. and B. Geiger (1997). "Molecular interactions in cell adhesion complexes." Current Opinion in Cell Biology **9**(1): 76-85.
- Yamada, K. M., R. Pankov, et al. (2003). "Dimensions and dynamics in integrin function." Braz J Med Biol Res **36**(8): 959-966.
- Yannas, I. V. (2001). "Tissue and organ regeneration in adults." from <http://public.eblib.com/EBLPublic/PublicView.do?ptiID=231364>.
- Yu, J., M. A. Vodyanik, et al. (2007). "Induced Pluripotent Stem Cell Lines Derived from Human Somatic Cells." Science **318**(5858): 1917-1920.
- Yu, L. M. Y., N. D. Leipzig, et al. (2008). "Promoting neuron adhesion and growth." Materials Today **11**(5): 36-43.
- Yurchenco, P. D. and H. Furthmayr (1984). "Self-assembly of basement membrane collagen." Biochemistry **23**(8): 1839-1850.
- Yurchenco, P. D., E. C. Tsilibary, et al. (1986). "Models for the self-assembly of basement membrane." J Histochem Cytochem **34**(1): 93-102.
- Yurchenco, P. D. and G. C. Ruben (1987). "Basement membrane structure in situ: evidence for lateral associations in the type IV collagen network." J Cell Biol **105**(6 Pt 1): 2559-2568.
- Yurchenco, P. and J. Schittny (1990). "Molecular architecture of basement membranes." The FASEB Journal **4**(6): 1577-1590.
- Yurchenco, P. D. (1990). "Assembly of Basement Membranes." Annals of the New York Academy of Sciences **580**(1): 195-213.
- Yurchenco, P. D. (2011). "Basement Membranes: Cell Scaffoldings and Signaling Platforms." Cold Spring Harbor Perspectives in Biology **3**(2).

- Zhang, S. (2003). "Fabrication of novel biomaterials through molecular self-assembly." Nat Biotechnol **21**(10): 1171-1178.
- Zhong, C., M. Chrzanowska-Wodnicka, et al. (1998). "Rho-mediated contractility exposes a cryptic site in fibronectin and induces fibronectin matrix assembly." J Cell Biol **141**(2): 539-551.
- Zoppi, N., R. Gardella, et al. (2004). "Human Fibroblasts with Mutations in COL5A1 and COL3A1 Genes Do Not Organize Collagens and Fibronectin in the Extracellular Matrix, Down-regulate $\alpha 2\beta 1$ Integrin, and Recruit $\alpha v\beta 3$ Instead of $\alpha 5\beta 1$ Integrin." Journal of Biological Chemistry **279**(18): 18157-18168.